Imperial College London

Faculty of Medicine

Department of Surgery & Cancer

Section of Cancer

DAPK2 is a Novel Modulator of TRAIL-Induced Apoptosis and It Regulates Oxidative Stress in Cancer Cells by Preserving Mitochondrial Function

---

By

Christoph Richard Schlegel

A thesis submitted for the degree Doctor of Philosophy

Primary supervisor: Dr. Ana P. Costa-Pereira

Second supervisor: Prof. Michael J. Seckl

Statement of Originality

Unless stated below or indicated in the text, I declare that the present thesis is the result of my own work. I have, however, received technical help from four colleagues as detailed below.

Sarah Stöcker and I performed the quantitative real-time PCR experiments. **Sarah Stöcker** also performed parts of the experiments for protein stability and RNA stability assays for death receptor 5 shown in **Figure 5-1**. **Marina L. Georgiou** and I performed all experiments carried out to assess the levels of extracellular acidification (ECAR) and oxygen consumption rate (OCR) using a Seahorse analyser (**Figure 6-8**). **Marina L. Georgiou** also performed the analysis of NAD+/NADH and NADP+/NADPH levels (**Figure 6-8**), whereas the glutathione (GSH) assay was kindly performed by **Emily Chater** (**Figure 6-9**). I am grateful to **Marina L. Georgiou** and for her contribution to the NF-κB western blots and luciferase assays shown in **Chapter 5.** (**Figure 5-6**). I am indebted to **Maria M. Misterek** for her technical assistance with some of the western blots in **Chapter 5** and **Chapter 6.** I am appreciative of the help from the aforementioned.

Parts of **Chapter 4** and **Chapter 5** have been published with myself as first author in a research article entitled "DAPK2 is a novel modulator of TRAIL-induced apoptosis." in *Cell Death & Differentiation*, (11th of July 2014) (Schlegel et al., 2014). This article can be found at the end of this document under **9**. **Publications. Chapter 6**. Is has been published with myself as first author in a research article entitled with "DAPK2 regulates oxidative stress in cancer cells by preserving mitochondrial function." *Cell Death & Disease* (12th of

December 2014) (Schlegel et al., 2014) This article can be found at the end of this document under **9**. **Publications.**

Copyright Declaration

Abstract

Targeting molecules involved in Tumour necrosis factor (TNF)-related apoptosis-inducing ligand (TRAIL) -mediated signalling has been hailed by many as a potential magic bullet to efficiently kill cancer cells, with little side effects on normal cells. Indeed, initial clinical trials showed that antibodies against TRAIL receptors, death receptor (DR) 4 and DR5 are well tolerated by cancer patients. Despite the initial efficacy issues in the clinical setting, novel approaches to trigger TRAIL-mediated apoptosis are being developed and its clinical potential is being reappraised. Unfortunately, many patients develop resistance to TRAIL-induced apoptosis and there is thus impetus for identifying additional resistance mechanisms that may be targetable and usable in combination therapies. Here, we show that the death associated protein kinase (DAPK) 2 is a modulator of TRAIL signalling. DAPK2 is a serine/threonine kinase that belongs to the DAPK family. Like DAPK1, it has been implicated in programmed cell death, the regulation of autophagy and developmental processes. Ablation of DAPK2 using RNAi causes phosphorylation of NF-κB and its transcriptional activity in several cancer cell lines. This then leads to the induction of a variety of NF-κB target genes, which includes DR4 and DR5. DR4 and DR5 protein expression is correspondingly increased on the cell surface and this leads to the sensitisation of resistant cells to TRAIL-induced killing. As DAPK2 is a kinase, it is eminently druggable and our data thus offer a novel avenue to overcome TRAIL-resistance in the clinic. We have additionally identified a new role for DAPK2 in the regulation of mitochondrial integrity. RNAi-mediated depletion of DAPK2 leads to a number of metabolic changes, including a significantly decreased rate of oxidative phosphorylation in combination with an overall destabilised

mitochondrial membrane potential. This phenotype is further corroborated by an increase in the production of mitochondrial superoxide anions and general oxidative stress. This role of DAPK2 is completely novel and could impact significantly on the understanding of DAPK2's function in physiology and disease.

Acknowledgements

Many people have accompanied me on the journey that I have taken since starting my Ph.D. four years ago. The influence of three people has been fundamental to the decision of starting this journey therefore I would like to thank Miriam Weiss, Steven A. Johnsen and Ana P. Costa-Pereira. I am indebted to Ana for not only giving me the opportunity to work in her lab but also constantly support and push me, whilst also being patient and cope with all the difficulties that, I am convinced, are part of every Ph.D.. I am sure that this unique relationship has led to this fruitful outcome and hope it will continue over the years. I am also incredibly grateful to my second supervisor Michael J. Seckl for his constant support and helpful criticism at the right moments. I would also like to thank Rajat Roy and Olivier Pardo for intensive and helpful discussions that have broadened my scientific horizon and were a major driver for me. I am grateful to Charlotte Bevan for the opportunity to take part in her lab meetings and her supportive, and always helpful input. Without the preliminary work done by Katrina M. Sutton and Ana-Violeta Fonseca my project would have not been possible and I would like to express my gratitude to them too. I would also like to thank my colleagues who made the lab sometimes more of a home then a workplace. Here, I am especially grateful to Catriona E. Munro, who I met on my first day of my Ph.D. and who has become a very good friend. I know my time here would have been way less enjoyable without her. I am also grateful to Nair Bonito who, despite all the disagreements, always supported me. I would also like to thank Sarah Stöcker for her support and constant positive attitude. I am grateful for William Stokes and Emily Chater for entertaining times in tissue culture and their support.

I am also grateful to Marina L. Georgiou who has proven that Master's students are not just a burden and who has become a close friend. I would also like to thank Anna Maria Tommasi for being constantly supportive and for coping with me, and all of my complaints. I am also grateful to Maria M. Misterek for her help and support during tough times of my Ph.D.. I would also like to thank Arnhild Grothey, Derek Lavery, Dieter Walsh, Ezra Bird, Greg Brook, Hua Zhang, Jana Hechler, Jennifer Podesta, Llucia Albertí Servera, Loredana Pellegrino and Sebastian Trousil. Furthermore, I would like to thank Anja Makert, Ewa Rupniewska, Julian Hendrik Gronau and Cristina Tomas dos Santos for introducing me to the life of a Ph.D. student and helping me settle in in this big city. I am also grateful to Laura Roca Alonso.

The last four years would have not been the same without the friends in London that have been a constant source of energy and support and who also helped me to forget the lab when necessary! I would like to especially thank my old friend Victor Diran for providing me shelter and introducing me to the London life. I am in debt to Miriam Weiss for her constant support and always helpful advice in every situation. I am grateful to Antonio Jorke and Jan Runo, we had a blast. I am grateful to my flatmate and friend Seiji Lim for putting up with me in any situation and all the trouble that I brought home. I would like to thank Filipa Pinho and Rui Tostões for exceptional moments and their perspective on the difficulties of life. I would further like to thank Christian Stihl for always making me smile, taking care of what I wear, and proving the fact that life can be amazing without alcohol. I would further like to thank Anne-Katrin Kallenbach for the great events and great nights we had. I am grateful to Andy Palfreeman for showing me you

can actually surf in the Britain and all weekends that we had and that are there to come. I would like to thank Adnan Bey and Alice Noyelle for exceptional moments. A big thank you to Rob Powell and William Stokes: you were the best gym buddies and always helped me to clear my head. I am also grateful to the wolf pack: Daniel Schmidt, Daniel Naujoks, Julian Hendrik Gronau and Rob Laux, for giving me a perspective from the 'real world' that have had a significant impact on choices that I have made and will make in the future. I would also like to thank Victor Diran, Felix Forster, Johannes Steltner, Karl Läufer and Irena Steinerova for bringing my hometown to me. I am indebted to Amanda Cross for her love, patience, constant support and positive attitude making the last year an enjoyable journey. I would also like to thank my friends from back home that never made me forget where I came from. I am indebted to Johannes Bohne for his support and critical point of view. I would further like to thank Alexander Schoel, Annemarie Strupp, Christian Kranz, Christian Nützmann, Eldar Nagiev, Hendrik Moeller, Henning Kempf, Johannes Fleischer, Jonas Pohlmann, Juliane Bill, Karoline Hammer, Lars Bill, Robert Frahm, Theresa Gorsler, Tom Schulze and Tristan Winkler for being my friends and being there for me during all this time.

Ich widme diese Arbeit auch meiner Familie und möchte mich für ungebrochene Unterstützung bedanken. Allen voran Danke ich meiner Mutter, Heike Schomann, die ausnahmslos immer für mich da war und mir einen Weg aus den schwierigsten Situationen gezeigt hat. Ich möchte mich auch bei meinem Vater, Christoph Schlegel, für seine Unterstützung bedanken. Außerdem bedanken möchte ich mich bei Wladimir Kim und Bärbel Hammer. Ich danke weiterhin

meiner Großmutter, Anngret Schomann, meiner Tante Anke Bathel und meinem Onkel Detlef Bathel, für die schöne Zeit und immer aufmunternden Worte. Ich möchte mich weiterhin bei meinem verstorbenen Großvater, Peter Schomann, bedanken weil er immer ein Vorbild war und mir gezeigt, dass sich harte Arbeit und Fleiß lohnen. Auch wenn nicht namentlich erwähnt bin dem Rest der Familie dankbar dafür, dass Sie immer für mich da waren und mir als Quelle für Kraft und Ausgeglichenheit meine Arbeit ermöglicht haben.

Table of Contents

List of Figures

List of Abbreviations

5-FU	5-fluoruracil
AKT	RAC serine/threonine-protein kinase
AP-1	Activator protein-1
APAF-1	Apoptotic peptidase activating factor-1
APC	Adenomatous polyposis coli
APL	Promyelocytic leukaemia
ATP	Adenosine triphosphate
ATRA	All-trans retinoic acid
B cells	Bursa/bone-derived cells
BAFF	B cell activating factor
BAK	BCL-2-antagonist/killer
BAX	BCL-2-associated X protein
BC	Before Christ
BCL-2	B-cell CLL/lymphoma 2
BCL3	B cell lymphoma 3
BCR-ABL	Breakpoint cluster region - Abelson murine leukaemia viral oncogene homolog 1
BID	BCL-2 homology domain 3 (BH3) interacting domain death agonist
c-FLIP	FADD-like interleukin 1β-converting enzyme (FLICE)-like inhibitory protein
c-myc	V-myc avian myelocytomatosis viral oncogene homolog
Ca.	Circa
CaM	Calmodulin
Caspase	Cysteinyl-aspartate specific protease
CD95	Cluster of differentiation 95

CHX	Cycloheximide
cIAP	Cellular inhibitor of apoptosis protein
CML	Chronic myelogenous leukaemia
CoQ_{10}	Ubiquinone
$CoQ_{10}H_2$	Ubiquinol
cRel	v-rel reticuloendotheliosis viral oncogene homolog
CYLD	Cylindromatosis (turban tumour syndrome)
Cyt *c*	Cytochrome complex
Cytochrome *c*	Cytochrome complex
DAPK	Death-associated protein kinase
DcR	Decoy receptor
DD	Death domain
DED	Death effector domain
DIABLO	Direct IAP binding protein with low pI
DISC	Death-inducing signalling complex
DNA	Deoxyribonucleic acid
DR	Death receptor
DRAK	DAPK-related apoptosis-inducing protein kinase
ERK	Extracellular signal-regulated kinase
ETC	Electron transport chain
FAD+/FADH	Flavin adenine dinucleotide
FADD	Fas-Associated protein with death domain
FasL	Fas ligand
FasR	Fas receptor
FCS	Foetal calf serum
GLUT	Glucose transporter

GPI	Glycosyl-phosphatidylinositol
GSH	Glutathione
h	Hour
H^+	Hydrogen proton
HER2	Human epidermal growth factor receptor 2
HIF	Hypoxia-inducible factor
HSP90	Heat shock protein 90
IKK	IκB kinase
IL	Interleukin
IL-8	Interleukin-8
IκB	Inhibitors of κ B
LDH	Lactate dehydrogenase family
LPS	Lipopolysaccharide
MAPK	Mitogen-activated protein kinase
MCA	Methylcholanthrene
mDcR1	Murine decoy receptor 1
mDcR2L	Membrane bound murine decoy receptor 2
mDcR2S	Soluble murine decoy receptor 2
mDR4	Murine death receptor 5
MLC	Myosin light chain
MMP	Matrix metalloproteinase
MnSOD	Mn-superoxide dismutase
MOMP	Mitochondrial outer membrane permeabilisation
mOPG	Murine osteoprotegerin
mRNA	Messenger RNA
mV	Millivolt

NAD^+/NADH	Nicotinamide adenine dinucleotide
$NADP^+$/NADPH	Nicotinamide adenine dinucleotide phosphate
NEMO	NF-κB essential modulator
NF-κB	Nuclear factor 'kappa-light-chain-enhancer' of activated B-cells
NIK	NF-κB-inducing kinase
NK cells	Natural killer cells
NKT cells	Natural killer T cells
NSCLC	Non-small cell lung cancer
o/n	Overnight
OPG	Osteoprotegerin
OXPHOS	Oxidative phosphorylation
PFA	Paraformaldehyde
p53	Tumour protein p53
PAF	Platelet-activating factor
PARP1	Poly (ADP-ribose)-polymerase 1
PBL	Peripheral blood leukocyte
PDC	Pyruvate dehydrogenase complex
PHGPx	Phospholipid-hydroperoxide glutathione peroxidase
PI	Propidium iodide
PI3K	Phosphatidylinositol-3-kinase
PKM2	Pyruvate kinase isoenzyme M2
PML-RARA	Promyelocytic leukaemia - retinoic acid receptor alpha (fusion protein)
RANK	Receptor activator of NF-kB
RANKL	Receptor activator of NF-kB ligand
RAS	Rat sarcoma gene

RAS	Rat sarcoma
RCF	Relative centrifugal force
REL	v-rel reticuloendotheliosis viral oncogene homolog
RHD	Rel homology domain
RIPK1/RIP1	Receptor-interacting serine/threonine-protein kinase 1
RNA	Ribonucleic acid
RNAi	RNA interference
ROS	Reactive oxygen species
Sec	Second
SEM	Standard error of the mean
Ser	Serine
siLuc	siLuciferase
siNS	Non-targeting siRNA
siRNA	Short-interfering RNAs
SMAC	Second mitochondria-derived activator of caspases
SOD2	Mn-superoxide dismutase
sTNF-α	Soluble tumour necrosis factor alpha
T	Temperature
T cells	Thymus cells
TACE	TNF alpha converting enzyme
TAD	C-terminal transactivation domain
TCA	Tricarboxylic acid
TCR	T cell receptor
Tet	Tetracycline
TetR	Tet repressor
TGFBR1	Transforming growth factor beta receptor 1

Thr	Threonine
TNF-β	Tumour necrosis factor beta
TNFR	Tumour necrosis factor receptor
TNF-α	Tumour necrosis factor alpha
TRADD	Tumour necrosis factor receptor type 1-associated DEATH domain protein
TRAF	TNF receptor associated family
TRAIL	Tumour necrosis factor (TNF)-related apoptosis-inducing ligand
TRAs	TRAIL-receptor agonists
Δψm	Mitochondrial membrane potential

1. Introduction

1.1 Cancer

Cancer defines a group of diseases that are caused by abnormal cellular proliferation and have the potential to invade and metastasise to other parts of the body. It is not a disease that is exclusive to humans, mammals or even vertebrates, but is in fact postulated to have arisen in parallel to the development of multi-cellular organisms (Strachan et al., 1999, Ratcliff et al., 2012, Merlo et al., 2006). Complexity of multi-cellular organisms seems to inversely correlate with their propensity to develop cancer (Domazet-Loso et al., 2014), however, cancer can already be found in the nematode *Caenorhabditis elegans*, an invertebrate with low organisational complexity (Kirienko et al., 2010) or the very well studied arthropod model *Drosophila melanogaster* (known as the common fruit fly) (Vidal and Cagan, 2006). Interestingly, with a significantly reduced incidence, chimpanzees (*Pan troglodytes*), one of our most closely related species have also been described to develop cancer (Puente et al., 2006). The earliest known description of cancer, a breast cancer, in humans (*Homo sapiens*) was found in the 'Edwin Smith Papyrus' that is believed to be written as early as 3000 BC (Stiefel et al., 2006, Breasted and New-York Historical Society. Library., 1930). Other evidence, dating back to approximately 1500 BC describes a fatty tumour for the first time, and gives further reference to potential cancers of the skin, uterus, stomach and rectum (Ebbell, 1937). The Greek physician and scientist Hippocrates (460 - 370 BC) used the term *Karkinos* (ulcerated malignant tumour) *and Karkinoma* (malignant tumour) (Greek word for crab) (Weiss, 2000) to describe cancer as its growth and vascularisation is said to have reminded him

of a moving crab. This word was later translated into the Latin word for cancer [thoroughly reviewed in (Hajdu, 2011)].

In the last 120 years medical and specifically cancer research has led to a thorough understanding of the aetiology and potential treatment options for this disease. Today, cancer is characterised by distinct properties and differentiated from benign lesions that are also caused by deregulated cellular growth. In 2000 Douglas Hanahan and Robert Weinberg published the review article 'The Hallmarks of Cancer', arguing that cancer cells share six hallmarks that pave the way for the transformation of normal cells to malignant (cancer) cells. These hallmarks are (1) self-sufficiency in growth signals, (2) insensitivity to anti-growth signals, (3) evading apoptosis, (4) limitless replicative potential, (5) sustained angiogenesis and (6) tissue invasion and metastasis (Hanahan and Weinberg, 2000).

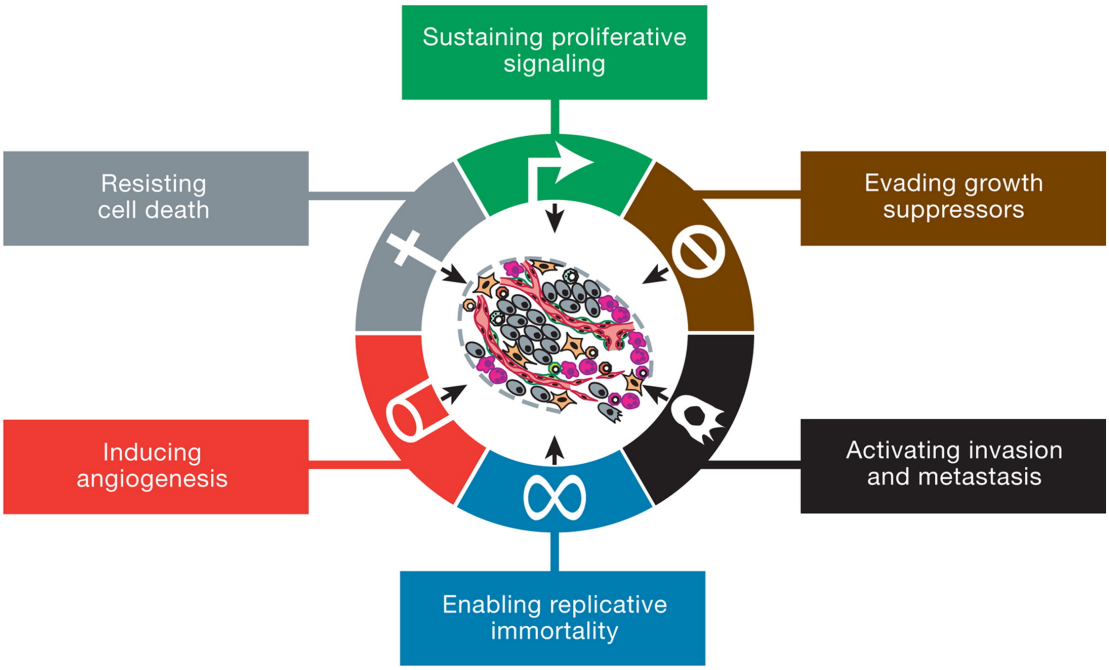

Figure 1-1. The hallmarks of cancer.

In 2000 Douglas Hanahan and Robert Weinberg published their first model of the six hallmarks of cancer that are acquired during tumour development. (Taken from (Hanahan and Weinberg, 2011))

In 2010 the authors extended their initial hallmarks and added the following: (7) deregulated cellular energetics and (8) avoiding immune destruction as well as two enabling characteristics, (1) genome instability and mutation and (2) tumour promoting inflammation.

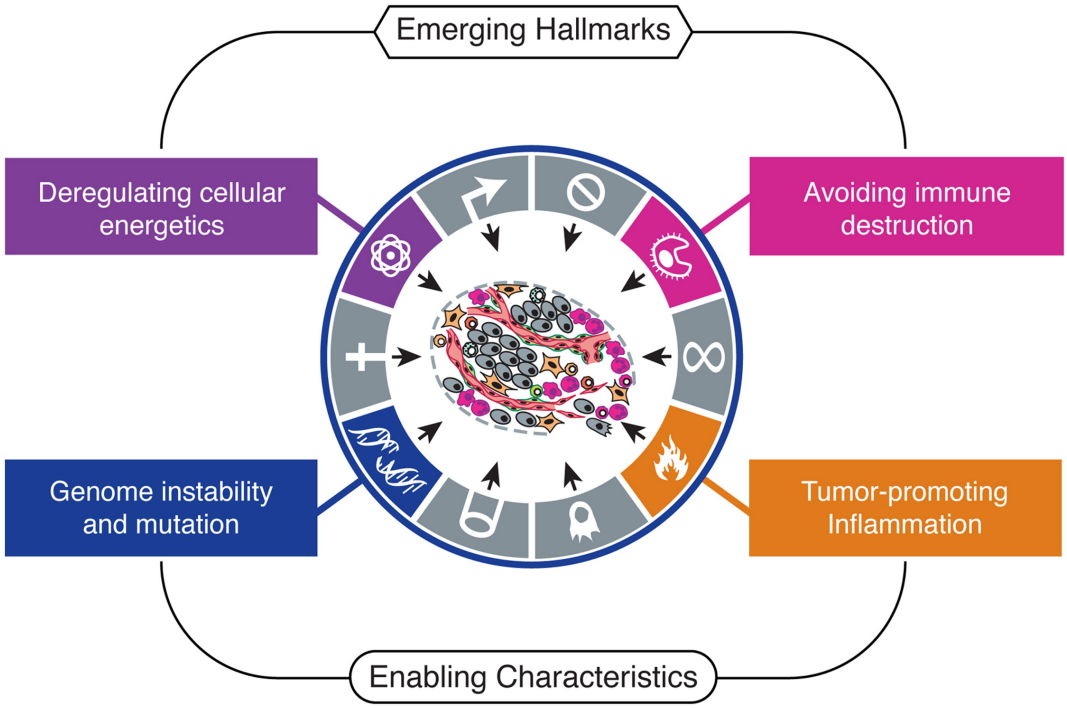

Figure 1-2. Emerging hallmarks and enabling characteristics of cancer.

In 2011 Douglas Hanahan and Robert Weinberg extended their initial model of six hallmarks of cancer with the two emerging hallmarks: (i) deregulated cellular energetics and (ii) avoiding immune destruction. Deregulated cellular energetics referred to the capability of tumour cells to re-program cellular metabolic processes in order to increase energy supply for the tumour. Avoiding immune destruction refers to the capability of tumour cells to change the expression of cytokines and surface molecules in order to actively evade destruction by the immune system. In addition, the authors postulated the two enabling characteristics (i) genome instability and mutation, which drives tumour formation and (ii) tumour promoting inflammation, which actively promotes tumour formation. (Taken from (Hanahan and Weinberg, 2011))

Cancer is believed to be caused by the accumulation of genetic mutations within a cell. Normal cells can either carry a genetic pre-disposition or acquire genetic alterations which then lead to the failure of growth regulation and ultimately cause any of the above mentioned hallmarks of cancer (Hanahan and Weinberg, 2011). Two main groups of genes have been described to be key regulators of 'oncogenesis', the development of cancer. In 1989 J. Michael Bishop and Harold E. Varmus received the Nobel Prize in Physiology and Medicine for the discovery of the first group, the so-called pro-oncogenes. In normal cells, these genes are responsible for the induction of cellular growth and differentiation. Upon

deregulation, these genes become so-called oncogenes and can then induce uncontrolled cellular proliferation (Varmus, 1985). Their counter players are so-called tumour suppressor genes, which protect cells from oncogenesis. In contrast to oncogenes these genes need to be affected on both alleles, which in 1971 has led to the development of the two-hit hypothesis by A.G. Knudson. He discovered that for the onset of retinoblastoma cancer, two genetic events were necessary (Knudson, 1971). In addition to genetic changes, epigenetic changes have been associated with the development of cancer. Germline mutations or inherited DNA changes and accumulated DNA damage and thereby, somatic mutations are fundamental to the aetiology of cancer. Somatic mutations can be caused by environmental factors and the inability of cells to maintain DNA integrity in the process of aging. Cancer has even been proposed to be the 'natural end-state of multicellular organisms' (Strachan et al., 1999). From an evolutionary point of view, mutations are the base of genetic variation and under selection pressure lead to survival of the most successful organism and its proliferation. Equivalent to the evolution of multicellular organism, the accumulation of somatic mutations allows 'normal cells' to escape its genetic control and faster proliferation. However, in the evolution of multicellular organisms there has been strong genetic selection favouring mechanisms that prevent 'normal cells' from escaping proliferation control. At least up to the point that multicellular organisms were able to reproduce themselves, no selection has favoured a long-term suppression of oncogenic lesion. Therefore, environmental factors, in combination with the decreased capability of the aging multicellular organism to prevent somatic mutations, inherited genetic alterations and epigenetic changes are believed to cause the development of cancer. This is

strongly supported by the fact that age is the most significant risk factor for the development of cancer (Simpson and Camargo, 1998, Stewart and Weinberg, 2006).

As mentioned previously, cancer cells are derived from 'normal cells' hence their physical appearance and properties are highly variable. Cancer is also described as malignant neoplasms, which are classified according to the cell type of which they originated. Five types have been described: (1) carcinomas, derived from epithelial cells (2) sarcomas, derived from connective tissue (3) lymphomas, derived from hematopoietic cells (4) germ line tumours, derived from pluripotent cells and (5) blastomas which are derived from immature precursor cells or embryonic tissue (Weinberg, 2007). The induction of oncogenesis is not only caused by genomic mutations but can also be induced by pathogens such as viruses. Upon integration into the host genome, these pathogens can introduce oncogenic genetic material, thereby favouring the development of cancer. A prominent example is the human papillomavirus (HPV), which upon integration expresses proteins that interfere with the tumour suppressors p53 and retinoblastoma protein (Rb), thus promoting oncogenesis (Munger and Howley, 2002). Interestingly, in humans, cancer exclusively develops out of endogenous cells, which cannot be easily passed onto others. However, dogs (*Canis lupus familiaris*) and Tasmanian devils (*Sarcophilus harrisii*) have developed parasitic cancers that are transmitted between individuals, so cancer cells themselves in this instance are infections agents (Rebbeck et al., 2009, Murchison et al., 2010).

1.2 Cancer therapies

As old as the description of cancer are approaches to cure this disease. Many routes were taken to treat cancer. In ancient Egypt cancer was treated with cautery, knives, salts and arsenic paste that was used until the 19th century as 'Egyptian ointment' (Hajdu, 2004). Other advanced civilisations in the same epoch applied herbal medicine or pastes containing metallic compounds such as iron or copper. In the middle ages until the beginning of the 20th century, surgery was the only treatment options that, under some circumstances, provided a cure [reviewed in (Hajdu, 2011)]. The evolutionary advantage of cancer cells compared to normal cells in multicellular organism, their evasion of proliferation control, also represents their Achilles heel and has been exploited by many modern therapeutic strategies. The discovery of radiation by Marie and Pierre Curie led to the development of radiation therapy, which specifically targets fast proliferating cells. This therapy was the first effective non-surgical cancer treatment and revolutionised cancer therapy (Slater, 2012). In the 1940s and 1950s the first chemical therapeutics were discovered and used to treat various types of cancer. Similar to radiation therapy chemotherapeutic agents target proliferating cells, thus the faster cells proliferate the more they are affected and in consequence cell death is induced. Some of the drugs that were discovered during that period are still in clinical use and provide a powerful weapon against some types of cancer such as methotrexate (Hashkes et al., 2014, DeVita and Chu, 2008). Many more classes of chemotherapeutic drugs have been discovered since. They all share a common mechanism of action as they target proliferating cells and thereby tumour cells. However, some 'normal cells' display

high proliferation rates, too e.g. immune cells. Thus chemotherapeutic and radiation therapy are characterised by more or less severe side effects on those fast proliferating cells. Even though surgery has been one of the first cancer treatments that provided a cure, it has not been replaced and, as surgical techniques advance, is still used successfully in combination with radiation and chemotherapy. As described earlier, not only organisms underlie evolutionary pressure, but also every single cell of a multicellular organism does. The development of cancer can be described as the failure of the whole organism to control growth of its individual components. The accumulation of genetic changes leads to the development of cancer cells, suggesting that these cells have acquired an evolutionary advantage compared to 'normal cells' (Simpson and Camargo, 1998, Tian et al., 2011). Upon chemotherapeutical or radiation treatment cancer cells lose their advantage to 'normal cells' and preferentially undergo cell death. However, evolution does not stop here and various strategies of cancer cells have been described leading to the evasion of therapeutic intervention (Holohan et al., 2013). Extensive research has been performed in this area and many mechanisms have been described, from temporarily stopped proliferation to enhanced tolerability towards treatment. All of them share the common cause of on-going evolution of cancer cells and the accumulation of favourable genetic changes in response to the evolutionary pressure generated by therapeutic intervention (Gottesman, 2002, Michor et al., 2006). To overcome this development, so-called 'targeted therapies' have been developed which, in contrast to classical treatment options, aim to specifically target cancer cells whilst sparing 'normal cells'.

1.3 Targeted cancer therapies

Opposed to classical non-specific chemotherapy or radiotherapy, targeted therapies aim to specifically interfere with molecular structures that are believed to play a crucial role in the development or progression of cancer. The central aim of targeted therapies is to discriminate 'normal' and cancerous cells and thereby increase efficiency and reduce adverse effects of cancer therapy. The fundamental background for the development of targeted therapies is the identification of potential targets. Very often the targeted structures are involved in oncogenesis and can be specifically targeted in cancer cells (Sawyers, 2004). One of the first targeted therapies, successfully used in the clinic, is Imatinib (trade name Gleevac). A small molecule inhibitor, which specifically targets the Bcr-Abl (breakpoint cluster region - Abelson murine leukaemia viral oncogene homolog 1) fusion kinase. This fusion kinase, which is the product of a chromosomal translocation, causes 90% of cases of chronic myelogenous leukaemia (CML) (O'Brien et al., 2003). Many more small molecules have been developed since and many of them target tyrosine kinases, due to their druggability, (Arora and Scholar, 2005). However, others have been developed, that for example modulate hormone receptors (Tamoxifen) (Jordan, 2006), target other types of kinases (Zhang et al., 2009) or inhibit heat shock protein 90 (HSP90) (Neckers and Workman, 2012). The other big class of targeted therapies are antibody-based treatments, which use monoclonal antibodies (mAb) to specifically target cancer cells or their secreted products. Upon binding of these mAb the cellular immune response may be activated and clears the body of tumour cells. One of the most successful antibody-based targeted

therapies is the mAb trastuzumab (trade name Herceptin), which interferes with the receptor-tyrosine-protein kinase epidermal growth factor receptor (ERBB)-2, also known as human epidermal growth factor receptor 2 (HER2). This receptor is specifically upregulated in approximately 20% of breast cancer cases and provides an ideal target for mAb-based therapies (Hudis, 2007, Wolff et al., 2007).

Even though the use of targeted therapies has the advantage over classic cancer therapies to affect 'normal' and cancer cells differentially, both approaches still face the same problem of resistance development. Evolutionary pressure and on-going mutation events can lead to tumour cells becoming resistant to treatment (Holohan et al., 2013, Lackner et al., 2012). To overcome this, many targeted therapies are used in combination with classic cancer therapies. In addition new, more advanced strategies are currently being developed, which for example combine the cell specificity of mAb with the powerful induction of cell death by chemotherapeutic drugs e.g. trastuzumab emtansine (trade name Kadcyla) (Niculescu-Duvaz, 2010). As the name implies, for the development of targeted therapies there is a need to identify targets that allow differentiation between 'normal' and cancer cells. Much excitement was generated in the mid-nineties when tumour necrosis factor (TNF)-related apoptosis-inducing ligand (TRAIL, also known as APO2L) was identified (Wiley et al., 1995, Pitti et al., 1996, Sanchez-Perez et al., 2002, Kirienko et al., 2010). This cytokine binds and thereby activates so-called death receptors (DRs) that then specifically induce the induction of cell death in cancer cells. By virtue of preferentially killing cancer cells, TRAIL is seen by many as a 'magic bullet' against cancer. Therefore, DRs

represent an ideal structure for targeted therapy. Extensive preclinical and clinical research has been performed on TRAIL as well as TRAIL receptor agonists (TRAs). Unfortunately, as many other targeted therapies, TRAIL-based clinical applications face the development of resistance, hindering their clinical success. Several resistance mechanisms have been described but they do not account for all cases of resistant cells [reviewed in (Mellier et al., 2010)]. In this work we describe a novel approach to overcome the resistance to TRAIL.

1.4 TRAIL Signalling

1.4.1 TRAIL ligand

The molecule TRAIL was identified in the mid-nineties of the last century. Two research groups independently reported a novel protein with significant homology to the already known extracellular domain of FasL and TNF-α [47, 66]. They further reported, that picomolar concentrations of this protein were capable of inducing apoptosis in a variety of cultured cell lines (Pitti et al., 1996, Wiley et al., 1995). The 20 kb TRAIL gene is located on chromosome 3 and is composed of five exons and four introns (Mellier et al., 2010). Transcriptome analysis revealed that TRAIL can be found in a variety of human tissues, most predominantly in spleen, lung and prostate [67]. Immunostaining, using TRAIL specific Abs confirms this observation, and, interestingly reveals relatively high TRAIL expression levels in the brain and thyroid (Daniels et al., 2005). Human TRAIL consist of 281 amino acids and the homologous protein in mice consists of 291 amino acids [66]. TRAIL has been characterised as a type II membrane protein, which can exhibit biological function as membrane bound, released in microvesicles (Martinez-

Lorenzo et al., 1999) , or cleaved by proteases into its soluble form sTRAIL (Liabakk et al., 2002). To achieve full biological activity, soluble TRAIL forms a homotrimeric structure, stabilised by a cystein residue at position 230. Mutation of this residue to alanine or glycine abolished TRAILs biological activity, suggesting that the trimeric structure is crucial for the activity of TRAIL [reviewed in (El-Deiry, 2005)].

1.4.2 TRAIL Receptors

It was observed that specific types of cancer cells express death receptors (DRs) on their cell surface such as DR4 (death receptor 4 or TRAIL-R1) and DR5 (death receptor 5 or TRAIL-R2) (**Figure 1-3a**). These receptors belong to the TNF superfamily, contain a conserved death domain, are triggered by TRAIL and lead to the induction of apoptosis (Pan et al., 1997b, Sheridan et al., 1997, MacFarlane et al., 1997). DR4 and DR5 are type I transmembrane polypeptides that, like other members of the TNF superfamily contain cysteine-rich pseudorepeats that are fundamentally involved in ligand binding (Smith et al., 1994). Both receptors share a high homology in their extracellular domain (58% identity and 70% similarity) also the intracellular domain and death domain are highly homologous. (Pan et al., 1997b, Chaudhary et al., 1997). The death domain of both receptors has been shown to be crucially involved in the induction of apoptosis (Chaudhary et al., 1997, McDonald et al., 2001, Dechant et al., 2004) and both receptors require the adaptor molecule Fas-associated protein with death domain (FADD) to recruit the executioner cysteinyl-aspartate specific proteases (caspases) caspases-8 and/or caspases-10 [3, 7, 44]. Besides the recruitment of FADD, DR4 and DR5 have further been shown to interact with the

adaptor molecule tumour necrosis factor receptor type 1-associated death domain protein (TRADD), an important adaptor molecule for TNF signalling (Hsu et al., 1995) and receptor-interacting serine/threonine-protein kinase 1 (RIPK1, also known as RIP1), a kinase that has been associated with NF-κB signalling and necroptosis (Jouan-Lanhouet et al., 2012, Bertrand and Vandenabeele, 2010). In addition to their pro-apoptotic function, it has been shown that DR4 and DR5 can activate NF-κB (nuclear factor kappa-light-chain-enhancer of activated B-cells) signalling. The use of caspase inhibitors in combination with the activation of DR4 and/or DR5 by TRAIL has further revealed that NF-κB activation occurs independent of TRAIL-induced apoptosis (Chaudhary et al., 1997). Activation of NF-κB by DR4 and DR5 has been shown to be associated with TNF receptor-associated factor (TRAF) 2, NF-κB-inducing kinase (NIK), IκB kinase (IKK) α and β. It has also been demonstrated that the execution of TRAIL-mediated apoptosis requires the inhibition of NF-κB (Kim et al., 2002).

In addition to their role in extrinsic apoptotic cell death induced by TRAIL, DR4 and DR5 have also been involved in the modulation of intrinsic apoptosis in response to DNA damage. RNAi mediated inactivation of DR5 was described to promote tumour growth and increase resistance to 5-fluoruracil (5-FU) (Wang and El-Deiry, 2004). Furthermore, it has been shown that DR4 is upregulated in a p53 dependent manner in response to treatment with 5-FU, and that depletion or down regulation of FADD or DR4 itself significantly reduced 5-FU induced cell death (Henry et al., 2012). Underlining the important role of TRAIL induced apoptosis in innate tumour surveillance, mutations of the human TRAIL receptors DR4 and DR5 have been reported in a variety of tumours e.g. osteosarcoma,

non-Hodgkin lymphoma, head/neck and lung cancer (Dechant et al., 2004, Lee et al., 2001, McDonald et al., 2001, Pai et al., 1998, Shin et al., 2001).

In addition to DR4 and DR5, TRAIL has also been shown to interact with the decoy receptors DcR1 (also known as TRAIL-R3) and DcR2 (also known as TRAIL-R4) and to bind to a soluble receptor called osteoprotegerin (OPG) (Marsters et al., 1997, Pan et al., 1997a). These receptors are, similar to DR4 and DR5, also type I transmembrane polypeptides and members of the TNF superfamily (Pan et al., 1997b, Sheridan et al., 1997, MacFarlane et al., 1997). Like other members of the TNF superfamily they also contain cysteine-rich pseudorepeats that are fundamentally involved in ligand binding (Smith et al., 1994). In strong contrast to DR4 and DR5, binding of TRAIL to DcR1 and DcR2 does not lead to the activation of apoptosis. DcR1 was described as glycosyl-phosphatidylinositol (GPI)-anchored membrane molecule that lacks an intracellular domain. Moreover, DcR1 has been described to inhibit TRAIL-induced apoptosis upon overexpression, suggesting a rather modulating effect on TRAIL signalling. The extracellular domain of DcR1 is highly homologous to DR4 (60%) and DR5 (50% DR5) (Sheridan et al., 1997). Under physiological conditions, expression of DcR1 is mostly restricted to peripheral blood leukocytes (PBLs) (Degli-Esposti et al., 1997b). In contrast to DcR1, DcR2 contains a cytosolic domain. This cytosolic domain of DcR2 contains only a portion of the consensus death motif, having lost 52 of 76 amino acids that encode the death domain of DR4 and DR5 (Walczak et al., 1997). As described for DR4 and DR5, DcR2 has been shown to be capable of activating NF-κB. Since NF-κB has been reported to mediate pro survival cues, DcR2 is likely to regulate TRAIL-induced

apoptosis *via* competition for TRAIL and *via* the induction of pro-survival signalling (Degli-Esposti et al., 1997a). Interestingly, DcR2 has also been reported to negatively regulate the cellular response to chemotherapeutic agents (Liu et al., 2005). In contrast to DcR1, DcR2 shows a widespread tissue distribution and was found to be highly expressed in several cancer cell lines (Degli-Esposti et al., 1997a). In addition to DcR1 and DcR2, TRAIL has also been shown to interact with osteoprotegerin (OPG) (Emery et al., 1998). In contrast to all the other TRAIL receptors, OPG is not membrane bound but a secreted receptor of the TNF receptor superfamily and also plays a fundamental role in the biology of bone remodelling. OPG also acts as a decoy receptor for the osteoclast activator receptor activator of NF-κB ligand (RANKL), inhibiting the binding of RANKL to the osteoclatogenesis receptor, RANK (receptor activator of NF-κB) and thereby preventing the formation of multinucleated osteoclasts. The ratio of RANKL/OPG determines bone mass and skeletal integrity (Boyce and Xing, 2007). Binding of TRAIL to OPG happens, however, with a weaker affinity then binding to all the other receptors (Truneh et al., 2000). Overexpression of OPG did suppress TRAIL-induced apoptosis and TRAIL has been shown to release the osteoclastogenesis block by OPG *in vitro* (Emery et al., 1998). Despite its regulation of OPG *in vitro,* TRAIL knockout mice did provide evidence for aberrant bone biology, suggesting that TRAIL is not essential for maintaining proper bone biology under physiological conditions (Sedger et al., 2002). Of note, DcR1 and DcR2 do not have a higher affinity for TRAIL and are expressed at substantially lower levels then DR4 and DR5 (Kimberley and Screaton, 2004). The exact mechanisms by which decoy receptors counteract TRAIL function remain to be unravelled.

Mice, however, compared to humans only express one functional TRAIL death receptor (mDR5) and three TRAIL decoy receptors (mDcR1, mDcR2 and mOPG), whereas mDcR2 can be expressed in two splicing variants, one membrane bound (mDcR2L) and one secreted form (mDcR2s) (**Figure 1-3**) (Schneider et al., 2003).

Four of the human TRAIL receptors, DR4, DR5, DcR1 and DcR2 are clustered on chromosome 8q22-q21 (Wu et al., 1997, Marsters et al., 1997, Truneh et al., 2000, Walczak et al., 1997). Their genomic close proximity and the complete lack of a second death inducing TRAIL receptor in mice, suggests that the development of the TRAIL system is a quite recent event in evolution and that all receptors have arisen from duplication (Wu et al., 1999). OPG has been mapped more distant but to the same chromosome, to 8q24 (Tan et al., 1997) (All receptors are depicted in **Figure 1-3**).

Given their potential common ancestry it is not surprising that TRAIL receptors share a number of transcription factors. In humans it has been shown that DR4, DR5, DcR1 and DcR2 can be transcriptionally activated by the tumour suppressor p53 (Shetty et al., 2005, Henry et al., 2012, Toscano et al., 2008, Liu et al., 2005). Conversely, the NF-κB transcription factor family has been shown to induce the transcription of DR4, DR5 and DcR1 (Mendoza et al., 2008, Shetty et al., 2005, Bernard et al., 2001). Remarkably, the NF-κB family member RELA, under certain circumstance, inhibits the expression of DR4 and DR5 thus, blocks TRAIL-induced apoptosis. This effect has been shown to be counter played by another member of the NF-κB family, cREL (Chen et al., 2003). Taken together,

this suggests that a balance of pro-survival and pro-apoptotic pathways is likely to regulate the expression of TRAIL receptors. However, the exact mechanisms defining whether a cell is prone to express a pro-apoptotic or pro-survival ratio of TRAIL-receptors has not been determined yet.

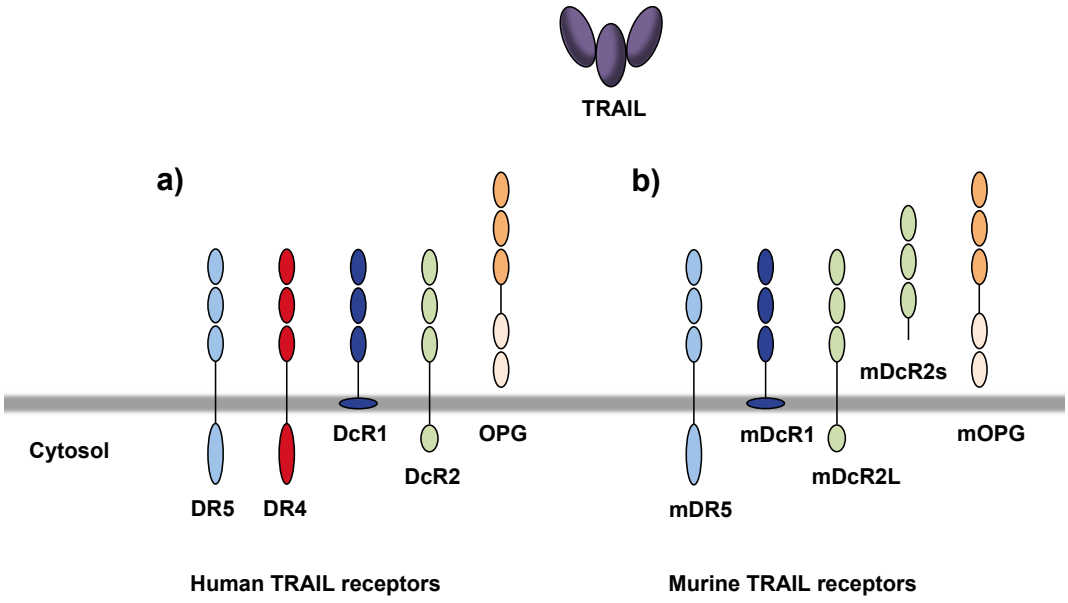

Figure 1-3. Human and murine TRAIL receptors.

Humans express five different receptors for TRAIL (**a**). DR4 and DR5 possess a fully functional intracellular domain and can induce apoptosis. DcR1 is a GPI-anchored membrane molecule without intracellular domain, DcR2 possess an intracellular domain with truncated death domain and has been shown to activate pro-survival cues *via* NF-κB. Both function as decoy molecules and inhibit the pro-apoptotic role of TRAIL. OPG has a lower affinity towards TRAIL and is involved in osteoclastogenesis. Mice express only four TRAIL receptors (**b**). Murine DR5 is the only fully functional receptor, capable of inducing apoptosis in mice. Murine DcR1 is equivalent to the human form a GPI-anchored membrane molecule without intracellular domain. Murine DcR2 is present as membrane bound form (mDcR2L) with truncated intracellular domain and capable of activating NF-κB. The soluble form of murine DcR2 (mDcR2S), which is cleaved of the membrane functions as soluble decoy receptor. Equivalent to humans, mice express OPG.

1.4.3 TRAIL-induced apoptosis

The induction of apoptosis in DR-expressing cells is mediated by the binding of TRAIL to DR4 and/or DR5. Only trimerised TRAIL is able to activate the receptor

complex by leading to a conformational change of their respective death domains (DD), receptor clustering and activation of the extrinsic apoptotic pathway. Activated receptors recruit Fas-associated protein with death domain (FADD) by interacting with their respective death domains. Subsequently, FADD, functioning as an adaptor protein, allows the recruitment of pro-caspase-8 and pro-caspase-10 *via* death effector domain (DED)-DED interactions triggering the formation of a multi-protein complex called death induced signalling complex (DISC) (Medema et al., 1997). This formation results in the auto activation of the initiator caspases (Kischkel et al., 2000). Moreover, cellular FADD-like interleukin 1β-converting enzyme (FLICE)-like inhibitory protein (c-FLIP), another DED-containing protein, is also able of binding FADD. c-FLIP possesses strong homology to caspase-8 with its two DEDs at the N-terminus and is a major inhibitor of the extrinsic cell death pathway. The activation of caspase-8, or caspase-10, as part of the DISC, leads to proteolytic cleavage of caspase-3, downstream cleavage of further caspases and other numerous regulatory and structural proteins (Danial and Korsmeyer, 2004). This results in hallmarks of apoptosis such as membrane blebbing, DNA fragmentation and cellular shrinkage (Galluzzi et al., 2007).

Moreover, initiator caspases are able to cleave BID (BCL-2 homology domain 3 (BH3) interacting domain death agonist), a pro-apoptotic member of the B-cell CLL/lymphoma 2 (BCL-2) family. It has been shown that the cell type determines how BID operates: (i) BID cleavage can provide an amplification loop for the apoptotic signal as in type I cells, where the main mechanism is mediated by extrinsic apoptotic signalling, or (ii) as in type II cells, it serves as the primary mechanism of TRAIL- induced apoptosis (Ozoren and El-Deiry, 2002). In the

latter, proteolytic processing of BID leads to the activation of the intrinsic apoptotic pathway including activation of BCL-2-associated X protein (BAX) and BCL-2 homologous antagonist-killer (BAK) resulting in decreased mitochondrial membrane potential (Δψm) and subsequent pore formation leading to mitochondrial outer membrane permeabilisation (MOMP) (Waterhouse et al., 2002). In addition, MOMP leads to the release of pro-apoptotic proteins such as cytochrome complex (cytochrome *c*) and SMAC (second mitochondria-derived activator of caspases/direct inhibitor of apoptosis-binding protein with low pI). Furthermore, cytochrome *c*, adenosine triphosphate (ATP) and apoptotic peptidase activating factor 1 (APAF-1) form the so-called apoptosome, which activates caspase-9. Active caspase-9 then activates caspase-3, caspase-6 and caspase-7 (Zou et al., 1997), finally resulting in DNA fragmentation and cell death.

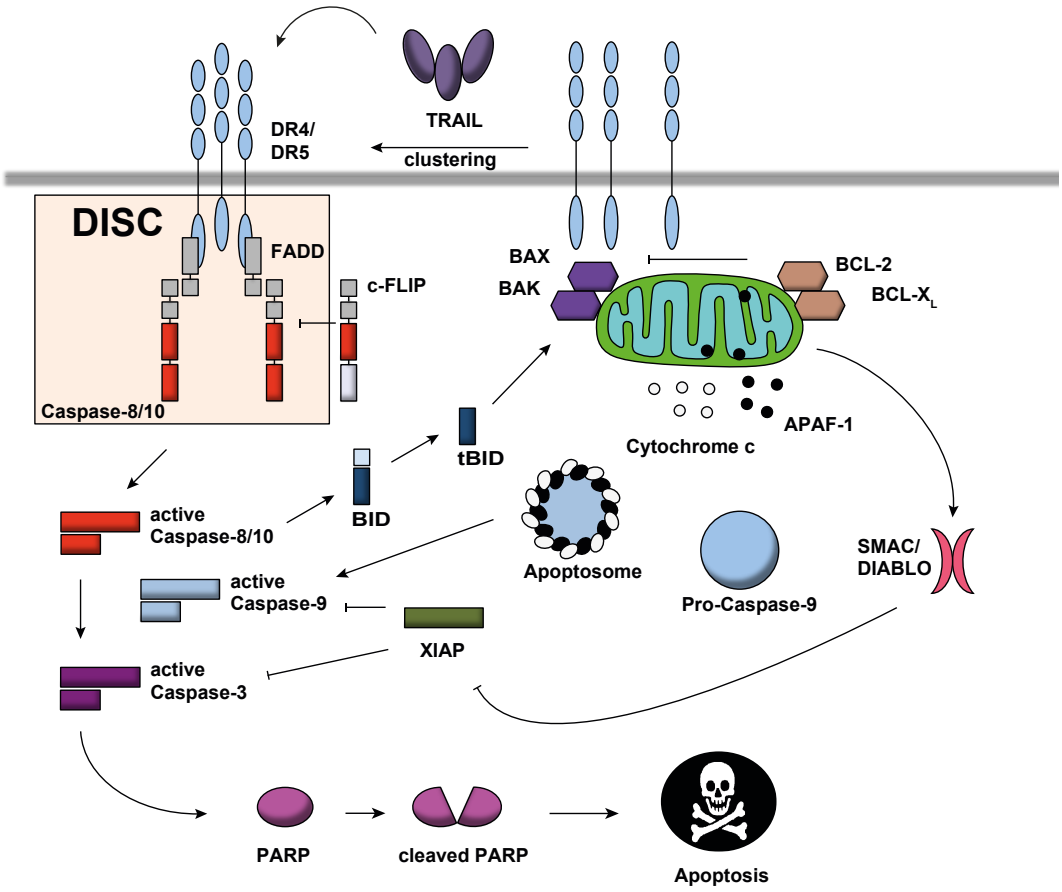

Figure 1-4. TRAIL-induced apoptosis signalling pathway.

Death receptor activation by TRAIL results in the formation of homotrimeric receptor complexes and primarily activates the extrinsic apoptotic pathway. TRAIL activation leads to an intracellular conformational change of the receptor and DISC formation. The DISC is composed of FADD, caspase-8, caspase-10 and potentially c-FLIP. Activation of initiator caspases-8 and caspases-10 lead to proteolytic cleavage and activation of downstream effector caspases, such as caspase-3 finally leading to the cleavage of downstream substrates e.g. PARP and ultimately to the induction of apoptosis. Furthermore, TRAIL can also activate the intrinsic apoptotic pathway *via* BID, which activates BAK and BAX, counteracted by BCL-2 and BCL-X_L and induces mitochondrial outer membrane permeabilisation (MOMP). Consequently, APAF-1 and cytochrome *c* form the apoptosome, activating caspases-9, which further activates downstream caspases. IAPs counteract the activation of caspases.

The use of TRAIL itself, or TRAs (TRAIL receptor agonists), in experimental tumour therapy is frequently confronted with resistance to TRAIL-based treatments that often arises during the course of therapy (Mellier et al., 2010). Many cancer cells develop resistance to treatment after an initial good response. Several resistance mechanisms have been described and it is believed that alterations at multiple levels from the receptor to initiator caspases are responsible. However, a general mechanism for the development of resistance has not yet been found. Several other signalling pathways have been associated with TRAIL-resistant phenotypes including activation of transcription factor NF-κB, mitogen-activated protein kinase (MAPK)/ extracellular signal-regulated kinase (ERK) signalling pathways and the phosphatidylinositol-3-kinase (PI3K)/ RAC serine/threonine-protein kinase (AKT) survival axis (Mellier et al., 2010). Commonly known mechanisms of resistance are described as follows.

The apoptotic function of TRAIL is mediated by signalling triggered by its receptor, which activates downstream death executor caspases. Thus, reduced cell surface expression, or receptor mutations leading to impaired function, can severely affect TRAIL-mediated signalling and thus constitute mechanisms of resistance. Indeed, reduced expression of DR4 caused by epigenetic silencing is associated with resistance to TRAIL-treatment in ovarian cancer cells (Hopkins-Donaldson et al., 2003, Horak et al., 2005). Furthermore, deficiencies in surface transport, loss of function mutations or endocytosis of DR4 and DR5 have been reported in various carcinomas (Fisher et al., 2001, Jin et al., 2004, Zhang and Zhang, 2008). There are also the so-called decoy receptors, DcR1 and DcR2, which compete with DR4 and DR5 for ligand binding. Hence, the ratio of TRAIL

decoy to DRs also determines the responsiveness of cells to TRAIL (Merino et al., 2006). After receptor activation, the formation of the DISC and auto-proteolytic cleavage of caspase-8 are key factors in TRAIL-induced apoptosis. High levels of c-FLIP, a DED-containing protein that can bind FADD, are associated with resistance to TRAIL. c-FLIP binds to the DISC and inhibits the activation of caspase-8. Thus, c-FLIP/caspase-8 ratio can also determine the responsiveness of cells to TRAIL-induced apoptosis and can lead to resistance in various types of cancer (Horak et al., 2005). Resistance can, therefore, be the result of c-FLIP overexpression and/or reduction of caspase-8 levels (Zhang and Fang, 2005). In addition, downregulation, increased turnover and mutations in several caspases have been linked to resistance to TRAIL-induced apoptosis (Crowder and El-Deiry, 2012, Lane et al., 2006, Van Geelen et al., 2010).

Despite the fact that TRAIL-induced cell death triggers the classical extrinsic apoptotic pathway, it also involves intrinsic, mitochondrial-associated, pathways. MOMP formation is a key event in the activation of the intrinsic apoptotic pathway and inhibitors of MOMP have been shown to inhibit signalling downstream of TRAIL ligation. Pro-apoptotic members of the BCL-2 family mediate the decrease in $\Delta\psi m$. It was shown that the ratio of pro- *versus* anti-apoptotic BCL-2 members is also responsible for the sensitivity to TRAIL (Zhang and Fang, 2005). The inhibitors of apoptosis proteins (IAP) interfere with the activation of executioner caspases. Members of this family possess an evolutionary conserved domain called baculovirus IAP repeat (BIR), as well as a caspase activation and recruitment domain (CARD) and are, therefore, as the name indicates, inhibitors of cell death. After the formation of MOMP, mitochondrial proteins such as

SMAC/DIABLO are released thus disrupting the interactions between caspases and IAPs. Hence, defects in SMAC/DIABLO release alter this balance and counteract apoptotic stimuli. The existence of a major resistance factor downstream of mitochondrial activation, which could be reverted by overexpressing SMAC/DIABLO, has been suggested (Ng and Bonavida, 2002).

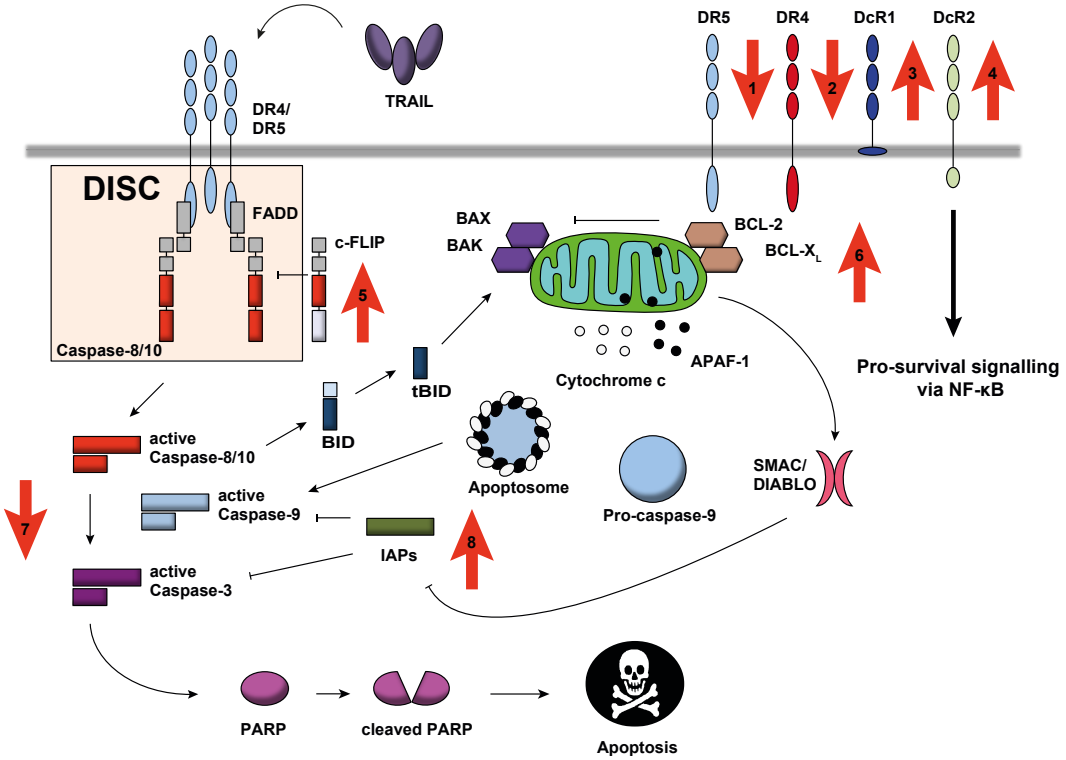

Figure 1-5. TRAIL-induced apoptosis signalling pathway and mechanisms of resistance.

Resistance mechanisms can occur at different stages of the cascade. The function or expression of the death-inducing receptors DR5 (**1**) and/or DR4 (**2**) can be altered. Overexpressed DcR1 (**3**) or DcR2 (**4**) can compete for TRAIL binding and DcR2 can activate pro survival cues *via* NF-κB. Upregulation of c-FLIP (**5**) can inhibit the activation of initiator caspases-8/10. Anti-apoptotic members of the BCL-2 family, such as BCL-XL and BCL-2 are known inhibitors of intrinsic apoptosis pathways by counteracting pro-apoptotic members of the family and are often upregulated (**6**). Mutations, downregulation or increased turnover of caspases has been linked to TRAIL-resistance (**7**). Increased expression of IAPs is capable of blocking the action of effector caspases (**8**).

1.4.4 Physiological roles

Since the discovery of TRAIL and its corresponding receptors, much effort was put in elucidating the potential therapeutic role of TRAIL. However, fewer research groups have focused on the physiological function of TRAIL. Today, more and more TRAIL-receptor agonists (TRAs) have finished phase 2 clinical trials and have all over led to disappointing clinical outcomes. Understanding the physiological role of TRAIL is more important than ever and might pave new avenues to make TRAs a successful strategy in the end.

As described earlier, TRAIL has been shown to induce tumour cell selective cell death in a variety of experimental setups *in vitro* and *in vivo*. As tightly regulated apoptosis has been demonstrated to be a crucial event during development (Fuchs and Steller, 2011) and, given the fact, that TRAIL has been shown to selectively induce apoptosis in tumour cells, several studies have focused on the role of TRAIL in development. The majority of these studies have been carried out in mouse models, but as mentioned earlier the TRAIL signalling system varies slightly between humans and mice (**Figure 1-3**). Interestingly, TRAIL and mDR5 knockout mouse models did not display any developmental of fertility defects (Sedger et al., 2002, Finnberg et al., 2005, Cretney et al., 2002). However, it has been described that TRAIL and/or mDR5 knockout mice show an enlarged thymus that contains more thymocytes than in wild type mice (Finnberg et al., 2005, Cretney et al., 2002). Furthermore, it has been postulated, that the expression of TRAIL is needed for negative selection of thymocytes and that TRAIL knockout mice are more susceptible to autoimmune diseases (Lamhamedi-Cherradi et al., 2003). Interestingly, TRAIL has further been shown

to play an important role in the adaptive immune system when controlling an infection with influenza (Ishikawa et al., 2005). In contrast, TRAIL deficient mice showed increased survival upon infection with the bacterium *Listeria monocytogenes*, most likely due to the abrogation of pro-apoptotic signalling in innate immune cells, normally induced by the bacteria (Zheng et al., 2004). Studies in mice and humans into the expression of TRAIL on the surface of isolated T cells, natural killer T cells (NKT) cells, B cells, dendritic cells (DC), monocytes or natural killer (NK) cells have shown that none of these cell types express detectable levels of TRAIL *in vivo*. Only a subset of mouse liver NK cells was found to express considerable amounts of TRAIL, in a, what appears to be, type II IFN-dependent manner. However, upon stimulation with interleukin (IL) -2, interferons (IFNs) or IL-15, most NK cells induce TRAIL expression [reviewed in (Smyth et al., 2003)]. TRAIL expression has been shown to increase in monocytes treated with lipopolysaccharide (LPS) or type I/II IFN, correlating with a potentiated toxicity towards tumour cells (Halaas et al., 2000, Ehrlich et al., 2003). T cells also induce TRAIL expression in response to type I IFN stimulation (Kayagaki et al., 1999), and, similarly DCs increase their surface expression upon type I IFN stimulation, which enhances their cytotoxicity towards tumour cells (Liu et al., 2001, Kemp et al., 2003) [thoroughly reviewed in (Mellier et al., 2010)].

Given the fact, that TRAIL has proven to induce cell death selectively in tumour cells, it has been postulated to be involved in anti-tumour immune surveillance. Surprisingly, TRAIL knockout or mDR5 knockout mice *per se*, did not show an increased susceptibility to tumour development in younger mice (Sedger et al.,

2002). However, an increase in lymphoid malignancies has been reported in mice older than 500 days (Zerafa et al., 2005). TRAIL or mDR5 deficiency has been shown to increase the susceptibility towards experimentally induced cancer and/or cancer allografts. Induction of primary fibrosarcomas by the chemical carcinogen methylcholanthrene (MCA) comparing TRAIL deficient and wild type mice revealed a greater sensitivity and increased tumour burden in TRAIL deficient mice. The authors further report, that TRAIL not only prevents formation of primary tumours, but also contributes to the NK cell-mediated protection from tumour metastasis (Cretney et al., 2002). Another primary tumour model using a multistage model for the development of primary squamous cell carcinoma revealed that mDR5 deficiency does not increase the number of observed tumours or tumour progression rate. However, mDR5 depleted cells showed a significantly increased number of lymph node metastasis, suggesting an involvement of TRAIL signalling in immune surveillance of metastasis (Grosse-Wilde et al., 2008). Furthermore, several studies revealed that TRAIL deficiency in mice leads to an increased tumour burden and more severe disease progression upon transplantation of e.g. lymphoma cells (Sedger et al., 2002), or renal carcinoma cells (Cretney et al., 2002). In contrast, is has also been shown that the development of thymic or intestinal tumours in mice with mutated p53 and adenomatous polyposis coli (APC) was independent of TRAIL expression status (Yue et al., 2005). Other studies however, have shown a clear involvement of monoallelic mDR5 loss in the development of *c-myc*-driven lymphomas (Finnberg et al., 2008). It has been hypothesised that exogenously introduced or chemically introduced tumours are highly immunogenic and activation of NK- and T cells might lead to bystander killing (Yue et al., 2005). Other publications

contradict this and have reported a protective effect of TRAIL expression on the induction of spontaneous tumours following the loss of one p53 allele, but report no protective effect of TRAIL on the development of HER2-driven breast cancer (Zerafa et al., 2005). It has been argued that this lack of TRAIL-induced protection against certain cancers could be caused by the ameliorated signalling of TRAIL decoy receptor, or receptor independent functions of TRAIL. Taken together, TRAIL-induced apoptosis has been demonstrated to be involved in several immunological processes. Besides a potential role in the negative selection of thymocytes, it can be associated with anti-tumorigenic role of NK cells and most likely other cells of the innate immune system. Furthermore, TRAIL-signalling is clearly involved in the anti-tumorigenic and anti-metastatic functions of the immune system, however it does not seem to be involved in the immune surveillance against all tumour types. It is highly likely, that TRAIL-signalling plays a role in the innate immune response against a subset of tumorous lesions. However, most functional insight into the physiological role of TRAIL has been gained using mouse models, which show fundamental differences in their TRAIL receptor expression and therefore cannot be transferred to humans without further validation.

1.4.5 Clinical success

As mentioned previously, binding of TRAIL to death inducing receptors DR4 and DR5 has been shown to selectively induce apoptosis in tumour cells. Several routes have been taken to utilise this tumouricidal function of TRAIL in cancer therapy. Two fundamental different categories of TRAIL-receptor agonists (TRAs)

are currently being tested in clinical trials. The first category are recombinant forms of TRAIL, the second category are monoclonal antibodies that target either DR4 or DR5. Several recombinant forms of TRAIL have been developed in preclinical studies; however, dulanermin is the only recombinant TRAIL that has been tested in clinical trials. This molecule is a shortened form of human TRAIL (amino acids 114–281) and devoid of foreign sequences (Ashkenazi et al., 1999). Several other TRAIL-based molecules have been developed for clinical applications, most recently a genetically engineered molecule (APG350) that represents two homotrimers fused to the Fc- part of a human IgG showing superior induction of TRAIL induced apoptosis compared to TRAIL and DR5 agonistic antibodies (Gieffers et al., 2013). In comparison to mAbs, use of TRAIL-based molecules has the disadvantage that they could also trigger signalling via TRAIL-decoy receptors and therefore induce side effects. When using TRAIL-receptor specific antibodies they will only target DR4 or DR5, which could also hinder clinical success. As mentioned before, some types of cancer express primarily DR4 and/or DR5. Therefore use of the therapeutic antibody would rely on the specific tumour type and require diagnostic testing beforehand. It has been shown that DR4 and/or DR5 specific Abs are capable of inducing clustering of TRAIL receptors and subsequent induction of extrinsic apoptosis (Belyanskaya et al., 2007). Opposed to recombinant TRAIL, which has a half-life of approximately 10 min (Lim et al., 2011) recombinant antibodies have a half-life in the range of days to weeks [reviewed in (Lemke et al., 2014b)].

As mentioned above, dulanermin is the only recombinant TRAIL molecule that has been tested in clinical trials. Initial studies confirmed its safety, however

phase II trials were disappointing. Treatment with dulanermin in combination with chemotherapy revealed no benefit over the use of chemotherapy alone (Soria et al., 2011). Besides dulanermin, several TRAIL receptor agonists have been tested in clinical trials. One of them targets DR4 (mapatumumab) whereas all others are directed against DR5 (conatumumab, lexatumumab, tigatuzumab, drozitumab and LBY-135). All of the antibodies demonstrated tumouricidal activity in preclinical testing and phase I studies proofed their safety in clinical use. However, clinical trials, comparing these TRAs with/without chemotherapy or the proteome inhibitor bortezomib to standard therapy, revealed no advantage over standard therapy [thoroughly reviewed in (Lemke et al., 2014b)]. Interestingly, some TRAs led to dramatic responses in some cases e.g. the DR4 agonist lexatumumab led to the resolution of symptoms of an unresectable chest wall/lung osteosarcoma after 2 years of treatment and the patient remained stable for at least 1 year after cessation of therapy (Merchant et al., 2012). Given the promising results in pre-clinical models the overall result of clinical trials with TRAs is surprisingly disappointing. Despite anticancer effect in certain cases, no TRA has yet been approved for clinical use. Many reasons for these disappointing results have been discussed. It is highly likely that the clinical failure of TRAs so far is caused by a combination of reasons. TRAs that are based on monoclonal therapeutic antibodies for example have the disadvantage that they are only capable of clustering two death receptors instead of the three receptors usually clustered by endogenous TRAIL (Wilson et al., 2011, Haynes et al., 2010). As mentioned above, cancer cells are known to develop resistance against TRAIL-induced apoptosis, which has been shown could be overcome by chemotherapeutic drugs or proteasome inhibitors *in vitro*. However, *in vivo*

results obtained from clinical trials do not resemble these initial findings for reasons that are yet not fully understood. To overcome these hurdles and to bring TRAIL-based therapies into the clinic, several routes are taken at present. More efficient TRAs are in development at the moment e.g. APG350 and, more sophisticated therapies are tested currently to overcome TRAIL-resistance *in vivo.* These methods include Smac and BH3 mimetics, helping to overcome TRAIL-resistance associated with intrinsic apoptotic signalling [reviewed in (Fulda, 2014)], inhibition of CDK9 (Lemke et al., 2014a) as well as the development and search of completely novel, selective strategies to counteract resistance to TRAIL-induced apoptosis.

1.5 Fas Signalling

The FAS signalling pathway is composed of FasL (also known as CD95L) and its corresponding receptor FasR (CD95). FasL is 40 kDa type II transmembrane protein and a member of the TNF family, which can be cleaved into a soluble form (Gregory et al., 2011). As all the other members of the TNF family, FasL forms a homotrimeric ligand that induces a specific cellular response upon binding to its corresponding receptor, FasR. FasR, a type I membrane protein, is a member of the TNF receptor family. Binding of FasL to FasR has been shown to induce receptor trimerisation and downstream activation of apoptosis (Krammer, 2000). FasL-induced apoptosis demonstrates a high degree of signalling overlap with TRAIL-induced apoptosis. Similar to TRAIL-induced cell death, binding of FasL and subsequent receptor trimerisation leads to the recruitment of FADD (Chinnaiyan et al., 1996) followed by the binding of initiator caspases procaspase-8 and/or procaspase-10 and the formation of a multi-protein complex called DISC. Downstream cleavage of caspases leads to the induction of cell death *via* the extrinsic apoptotic signalling pathway, with activated initiator caspases cleaving effector caspases such as caspases-3. In so-called type I cells this pathway is sufficient to induce apoptosis. Equivalent to TRAIL-induced apoptosis, so-called type II cells require a mitochondrial amplification loop as DISC assembly might be impaired or not sufficient enough to trigger apoptosis (Peter and Krammer, 2003). Partial activation of initiator caspases leads to proteolytic processing of BID, which subsequently activates the intrinsic apoptotic pathway that involves the mitochondria, as described by Werner et al. (Werner et al., 2002). Identical to TRAIL-induced apoptosis, FasL-

induced signalling can be very efficiently inhibited by upregulation of cFLIP or anti-apoptotic members of the BCL-2 family (Oyarzo et al., 2006, Srinivasan et al., 1998).

Physiologically, Fas signalling has been linked to the immune privileged status of certain organs. By using FasL deficient mice, it has been shown that FasL expression protects the anterior chamber of the eye, an immune privileged organ, from an inflammatory response (Griffith et al., 1995). In addition, FasL has been shown to be involved in maintaining the immune privileged status of the thyroid gland. Normal thyrocytes constitutively express FasL, protecting the organ from an immune reaction by negatively regulating lymphocytes through FasL. Interestingly, in the autoimmune disease Hashimoto thyroiditis, thyrocytes start to express FasR, which subsequently leads to the destruction of thyrocytes (Giordano et al., 1997). Mice with either FasR or FasL mutations exhibit severe autoimmune diseases that resemble systemic lupus erythematosus in humans (Furukawa et al., 1996, McNally et al., 1997). Mutations in the human FasR gene have been described to cause the autoimmune lymphoproliferative syndrome or Canale-Smith syndrome. These patients exhibit all signs of systemic autoimmunity including a massive non-malignant lymphadenopathy, hepatosplenomegaly and altered T cell populations (Drappa et al., 1996). Similar to TRAIL, FasL has been associated with negative selection of thymocytes (Castro et al., 1996). Moreover, the association of Fas signalling with autoimmune disorders is linked to the impaired regulation of autoreactive lymphocytes.

In contrast to TRAIL, Fas signalling has not been associated with innate tumour surveillance. The regulation of cytotoxic T lymphocytes by FasL is mandatory for a functional immune system and the prevention of autoimmune disorders. However, in some types of cancer, FasL expression has been shown to be disadvantageous. Of interest, many cancer cells themselves are resistant to FasL-induced apoptosis and/or show downregulation of the corresponding FasR. However, FasR is rarely lost completely and some tumours exhibit particularly high levels of FasR. Moreover, FasL expression by tumours has been postulated to protect tumour tissue from an immune response (Strand et al., 1996, O'Connell et al., 1996, Hahne et al., 1996). Recently, it has been shown that under certain conditions FasR activation by FasL could act tumorigenic and promote tumour growth and invasion in various cancer cell lines (Chen et al., 2010). In a glioblastoma mouse model, FasL signalling was shown to promote tumour invasion and migration through the PI3K, AKT, NF-κB and MMP (matrix metalloproteinase) pathways (Kleber et al., 2008). These findings have led to the development of a fusion protein that functions as a soluble FasR, inhibiting Fas signalling, which has recently been clinically approved as an orphan drug targeting glioblastoma multiforme (GBM) (Wick et al., 2011, Tuettenberg et al., 2012). Taken together, despite great similarities in the intracellular signalling of TRAIL and FasL, FasL does not play a role in the innate immune response to tumours but under certain conditions can exhibit pro-invasive and pro-metastatic functions.

1.6 TNF-α Signalling

Over 40 years ago, it was reported for the first time, that cytokines might be involved in the anti-tumour response of the immune system (Ruddle and Waksman, 1968, Kolb and Granger, 1968). Around 20 years later, in 1984, two cytokines, involved in a cytotoxic response were cloned and identified. It was then discovered that they bind to the same receptor (Aggarwal et al., 1985a) and share 50% sequence homology. They were subsequently called tumour necrosis factor (TNF) -α and TNF-β (also known as lymphotoxin-α) (Aggarwal et al., 1984, Aggarwal et al., 1985b). Identification of these cytokines led to the discovery of the whole TNF superfamily and their receptors. Equivalent to the other members of the TNF superfamily, TNF-α is a trimeric type II transmembrane protein (sometimes referred to as mTNF-α) (Kriegler et al., 1988). It can be shed of the membrane by the metalloproteinase TNF alpha converting enzyme (TACE) and forms soluble homotrimers as most other members of the TNF superfamily (sometimes referred to as sTNF-α) (Tang et al., 1996, Black et al., 1997). Both, membrane bound and soluble TNF-α, have been shown to exhibit biological activity (Decoster et al., 1995). Equivalent to the other members of the TNF superfamily, TNF-α exerts biological function by binding to its corresponding receptors. There are two receptors described for TFN-α, tumour necrosis factor receptor (TNFR) 1 and 2. Both of them are members of the TNF receptor superfamily and are capable of binding membrane bound TNF-α whereas soluble TNF-α only activates TNFR1 [reviewed in (Cabal-Hierro and Lazo, 2012)]. TNFR1 is a ubiquitously expresses 55 kDa transmembrane protein, which can be activated by both, membrane bound and soluble TNF-α. Ligand binding induces

a conformational change in its intracellular domain and receptor trimerisation. TNFR1 contains a death domain (DD) and can recruit other DD containing proteins and induce apoptosis. Moreover, TNFR1 has been shown to recruit members of the TNF receptor associated family (TRAF) and subsequently activate the NF-κB family of transcription factors (Schulze-Osthoff et al., 1998). The second TNF receptor, TNFR2 is a 75 kDa transmembrane protein, that has been shown to be mostly expressed in specific cell types such as oligodendrocytes (Dopp et al., 2002), astrocytes (Li et al., 2002), T cells (Ware et al., 1991), myocytes (Irwin et al., 1999), thymocytes (Grell et al., 1998), endothelial cells (Choi et al., 2005) and human mesenchymal stem cells(Faustman and Davis, 2010) [reviewed in (Cabal-Hierro and Lazo, 2012)]. TNFR2 does not contain a DD and in contrast to TNFR1 it can only be efficiently activated by membrane bound TNF-α. Downstream signalling in response to TNF-α binding differs significantly between TNFR1 and TNFR2 (for differences in NF-κB activation see **Figure 1-8**). As mentioned above, TNFR1 contains a DD and can subsequently activate apoptotic processes. However, dependent on the cellular context TNFR1 activation can also activate pro-survival and proliferative pathways. Upon ligation of TNF-α, two different intracellular signalling complexes have been described for TNFR1. The first complex (referred to as complex-I, **Figure 1-6a**) is formed by the recruitment of TRADD to TNFR1 via its DD. In the next step, further adaptor molecules such as TRAF2, cellular inhibitors of apoptosis (cIAP) -1, -2 and RIPK1 (also known as RIP1) are recruited to the receptor (Hsu et al., 1996a, Chen et al., 2008). This complex is referred to as complex I, which is capable to activating survival cues via NF-κB and activator protein (AP) 1 (Micheau and Tschopp, 2003, Mahoney et al., 2008, Hsu et al.,

1996a, Chen et al., 2008). The activation of NF-κB family of transcription factors by TNFR1 involves the polyubiquitination of RIPK1 (Lee et al., 2004), this process is further described in **1.7.1**..

Under certain conditions, RIPK1 can be deubiquitinated by the ubiquitin carboxyl-terminal hydrolase (CYLD), which subsequently leads to the formation of complex-II (**Figure 1-6b**). This complex does further contain TRADD, FADD and pro-caspase-8 and is called DISC (Micheau and Tschopp, 2003, Hitomi et al., 2008). Equivalent to the DISC formed upon ligation of TRAIL to DR4/DR5 this complex leads to the activation of the initiator caspases-8/10 and the activation of extrinsic apoptotic signalling.

As mentioned earlier, TNFR2 does not contain a DD and can only be activated by membrane bound TNF-α. Binding of membrane bound TNF-α to TNFR2 induces receptor trimerisation and subsequently recruitment of the key adaptor protein TRAF2. Then, TRAF2 further recruits TRAF1, TRAF3, cIAP1 and cIAP2. The final result is activation of the non-canonical signalling branch of NF-κB *via* the NIK (Hauer et al., 2005) and is described in more detail in **1.7.2**. In addition, crosstalk between TNFR1 and TNFR2 has been observed under certain conditions. TNFR2 can increase pro-apoptotic signalling of TNFR1. As TRAF2 is the main adaptor molecule for TNFR2, activation of TNFR2 and subsequent degradation of TRAF2 leads to a cellular environment favouring the formation of TNFR1 complex II (Rodriguez et al., 2011), and thus, induction of apoptosis. This suggests that the cellular outcome of cellular TNF-α depends on a fine balance of intracellular events mediated by ligand binding to different receptors.

When first identified, TNF-α showed striking anti-tumour activity in mice (Carswell et al., 1975). Since its discovery extensive research has been done on the physiological role of TNF-α and its potential clinical application. It is commonly believed that the expression of TNF-α is regulated by most pattern-recognition receptors, including Toll-like receptors, various cytokine receptors and the T cell receptor (TCR). Given the ubiquitous expression of TNFR1, the consequences of TNF-α signalling can be local as well as systemic [reviewed in (Kruglov et al., 2008)]. Utilising knockout mice, it was shown that TNF-α signalling is crucially involved in the immune response towards a variety of pathogens (Grivennikov et al., 2005, Deepe, 2007). However, in some cases, production of TNF-α can contribute to life threatening conditions such as sepsis in response to the exposure to bacterial endotoxins (Beutler et al., 1985). Remarkably, TNF-α signalling was also shown to be over-activated in a number of auto-inflammatory disorders such as arthritis (Keffer et al., 1991), which led to the development of the anti-TNF therapy, a breakthrough in the treatment of rheumatoid arthritis (Elliott et al., 1994). Despite its potential to induce apoptosis in certain types of tumours, TNF-α signalling was also found to promote tumourigenesis via activation of NF-κB and activator protein 1 (AP-1) survival cues and inflammation of the tumour (Balkwill, 2006).

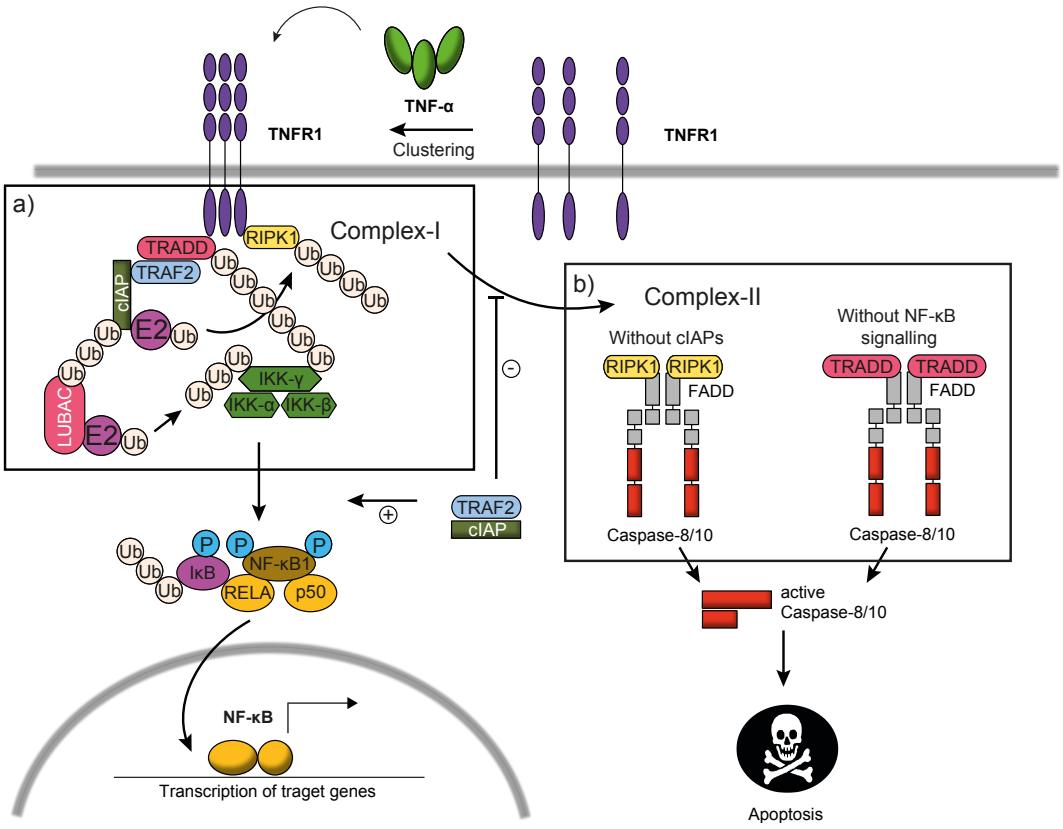

Figure 1-6. TNF-α signalling through TNFR1.

Ligation of TNF-α to TNFR1, induces receptor trimerisation and recruitment of TRADD, TRAF2 and cIAPs. cIAPs function as E3 ubiquitin ligases for RIPK1 and LUBAC. These non-degradative ubiquitination processes lead to the recruitment of the IKK complex (composed of IKK-α, IKK-β and IKK-γ (NEMO)). The E3 ubiquitin ligase complex LUBAC mediates polyubuquitination of IKK-γ, which stabilises complex-I (**a**). Spatial accumulation of the IKK complex mediates the phosphorylation of IκB proteins and subsequent polyubiquitination and proteasomal degradation. The IKK complex further phosphorylates NF-κB1 (p105) leading to proteolytic processing and increased levels of p50. RELA (p65) – p50 dimers translocate to the nucleus and regulate the expression of target genes, representing the canonical activation of NF-κB. NF-κB family members, TRAF2 and cIAPs suppress the formation of the death-inducing complex-II (**b**). This complex is formed in the absence of TRAF2, cIAP or NF-κB signalling and depending on the cellular context contains of RIPK1, FADD and initiator caspases-8/10 or TRADD, FADD and initiator caspases-8/0 and leads to the induction of the extrinsic apoptotic pathway.

1.7 NF-κB Signalling

All multicellular organisms face the necessity to react towards external changes in order to maintain integrity and survival. Such changes may require immediate or sustained responses. Many molecular switches can be modulated in response to external changes. Amongst the most powerful are transcription factors, which induce mRNA expression, and subsequently regulate protein levels. This generates an immediate, but transient molecular response towards extracellular changes. The NF-κB family of transcription factors is a textbook example for the complexity and plasticity of these molecular switches. Discovered in 1986, NF-κB family members were identified as proteins that bind to enhancers of the κ light chain in B cells (Sen and Baltimore, 1986, Singh et al., 1986, Staudt et al., 1986, Weinberger et al., 1986). Since then, extensive research has been done on the biology of the NF-κB family of transcription factors and much progress has been made on deciphering the extremely complex regulation of NF-κB. The transcriptional activation of NF-κB depends on the activation/formation of NF-κB dimers, their translocation to the nucleus, binding to NF-κB consensus sequences and activation of the transcription machinery (Wang et al., 2012a). DNA binding and nuclear translocation of NF-κB dimers is tightly regulated by a number of positive and negative regulators. Without stimulation, in a so-called “resting state” NF-κB dimers are prevented from entering the nucleus by members of the inhibitors of κ B (IκB) family (Beg and Baldwin, 1993, Hayden and Ghosh, 2012). NF-κB dimers are released and become transcriptional active upon phosphorylation of IκB, which is followed by ubiquitination and proteasomal degradation. Phosphorylation of IκB in response to external changes is facilitated

by proteins of the IκB kinase (IKK) complex, composed of IKK-α, IKK-β and the structural/regulatory component NF-κB essential modulator (NEMO, also known as IKK-γ) (**Figure 1-7**). The activation of the IKK complex is a very complex process and depending on the stimuli involves different receptors, adaptors and scaffolding proteins (Israel, 2010) and is described in more detail in **1.7.1**. There are five members of the NF-κB transcription factor family in humans (**Figure 1-7**). NF-κB1 (also known as p105) and NF-κB2 (also known as p100) require proteolytic processing to become active. NF-κB1 (p100) is cleaved and gives rise to NF-κB1 (p50) and NF-κB2 (p105) forms NF-κB2 (p52) after cleavage. The other three members RELA (also known as p65), RELB and cREL (often referred to as v-rel reticuloendotheliosis viral oncogene homolog (REL) proteins) do not require processing (Hayden and Ghosh, 2012). It has been revealed that so-called REL homology domains (RHDs) at the N-terminus of NF-κB members are required for binding to the DNA. To become functionally active, NF-κB proteins form homo- heterotrimers and bind to the DNA where they can either inhibit or promote transcription of target genes (Muller et al., 1995, Wolberger, 1998). Interestingly, only RELA, RELB and cREL contain so-called C-terminal transactivation domains (TADs), which are required for activating the transcription machinery. NF-κB1 (p50) and NF-κB2 (p52) do not contain TADs but are capable of positively regulating transcription upon formation of heterodimers with TAD containing NF-κB proteins or other transcription factors that have the ability for transactivation (Hayden and Ghosh, 2012). In addition, NF-κB1 (p50) and NF-κB2 (p52) homodimers have also been shown to bind NF-κB consensus sites, inhibiting NF-κB mediated transcription by competing

with TAD containing dimers (Zhong et al., 2002, Muller et al., 1995, Hayden and Ghosh, 2012).

Prior to external activation, NF-κB proteins are inhibited by members of the IκB family (**Figure 1-7**). In humans, this protein family has eight different members: IκBα, IκBβ, IκBε, IκBζ, BCL3 (B-cell lymphoma 3), IκBNS (also known as NF-κBδ) plus the precursor proteins NF-κB1 (p105) and NF-κB2 (p100) (Basith et al., 2013). NF-κB1 (p105) and NF-κB2 (p100) lose their ability to inhibit NF-κB dimers after proteolytic processing to NF-κB1 (p50) and NF-κB2 (p52) (Basith et al., 2013, Hayden and Ghosh, 2012). Proteins of the IκB family share the so-called destruction box serine residue (DSGXXS) domain. Phosphorylation of serine residues in this domain leads to polyubiquitination and subsequent proteasomal degradation and/or processing of IκB proteins (Xu et al., 2011, Kanarek et al., 2010).

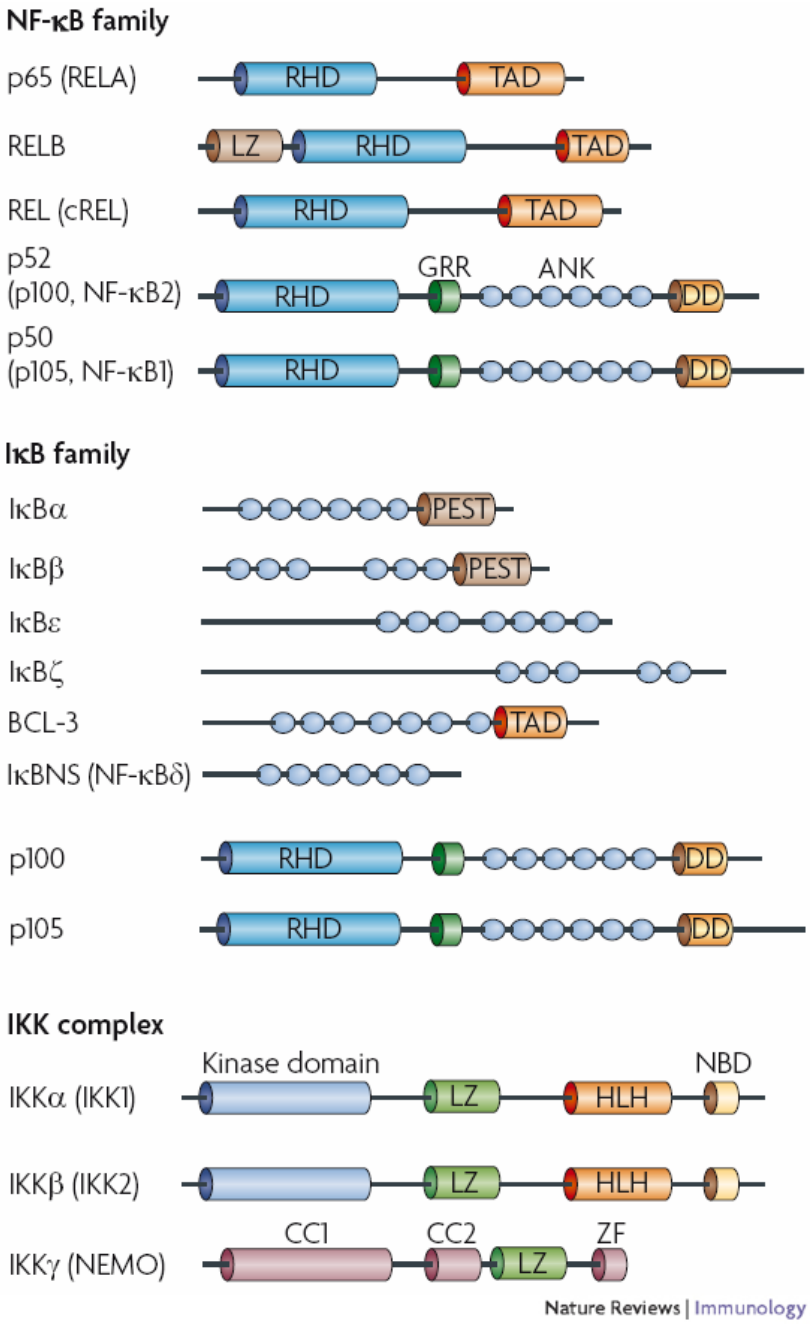

Figure 1-7. Proteins of the NF-κB, IκB and IKK families.

Protein names are depicted on the left and alternative names can be found in brackets. The NF-κB family members NF-κB1 (p105) and NF-κB2 (p100) function in the unprocessed form as IκB. When processed to NF-κB1 (p50) and NF-κB2 (p52) they function as NF-κB family members. The following protein domains are indicated: ANK, ankyrin repeats; CC, coiled-coil; DD, death domain; GRR, glycin rich region; HLH, helix-loop-helix; LZ; leucin-zipper; NBD, NF-κB-essential-modulator-binding domain; PEST, proline-glutamic, serine- and threonine-rich; RHD, REL homology domain; TAD, transactivation domain; ZF, zinc-finger. (Taken from (Ghosh and Hayden, 2008))

1.7.1 Canonical activation

As mentioned earlier, NF-κB becomes activated in response to phosphorylation, subsequent ubiquitination and proteasomal degradation of IκB proteins. This targeted phosphorylation is facilitated by proteins of the IKK family. A large number of extracellular stimuli like oxidative stress (Kratsovnik et al., 2005, Rupec and Baeuerle, 1995, Schreck et al., 1991), DNA damage (Janssens and Tschopp, 2006, McCool and Miyamoto, 2012) or cellular ligands such as TNF-α are capable of activating IKKs (Cabal-Hierro and Lazo, 2012). IKKs are activated by the formation of IKK complexes. Depending on the actual stimuli these complexes vary slightly in composition and can lead to different downstream signalling events. Activation of NF-κB has been categorised as so-called canonical, also known as classical activation and the non-canonical or alternative pathway depending on the extracellular stimuli (Hayden and Ghosh, 2008, Wajant and Scheurich, 2011, Hayden and Ghosh, 2012). As depicted in **Figure 1-6** and **Figure 1-8**, NF-κB can be canonically activated upon binding of TNF-α to TNFR1 and subsequent receptor trimerisation. This conformational change of the receptor complex induces the recruitment of the E3 ubiquitin ligase TRADD to TNFR1 via its DD. In addition the E3 ubiquitin ligases TRAF2, cIAP1, cIAP2 and the protein kinase RIPK1 are recruited to the complex, referred to as complex-I (Aggarwal et al., 1996, Chen et al., 2008, Hsu et al., 1996a). This interaction leads to the cIAP-mediated polyubiquitination of RIPK1 with non-degradative ubiquitin, which in the next step leads to the recruitment of the dimeric linear ubiquitin chain assembly complex (LUBAC). Furthermore, ubiquitination of complex-I members also recruits the IKK complex composed of IKK-α, IKK-β and

IKK-γ. Consequently, LUBAC mediates the polyubiquitination of IKK-γ, thereby stabilising complex-I (Haas et al., 2009, Tokunaga et al., 2009). The activated IKK complex subsequently phosphorylates IκB proteins and induces their proteasomal degradation (Ea et al., 2006, Kovalenko and Wallach, 2006) leading to the translocation of NF-κB (p50)/ RELA (p65) dimers into the nucleus (Basak et al., 2007, Wajant and Scheurich, 2011). IKK complex proteins have also been shown to phosphorylate NF-κB family members directly and thereby alter their transcriptional response, e.g. RELA pS536 (Yoboua et al., 2010, Syrovets et al., 2005).

1.7.2 Non-canonical activation

A certain subset of cellular stimuli activates the NF-κB family of transcription factors *via* the so-called non-canonical or alternative NF-κB pathway. This pathway has been shown to be activated after binding of TNF-β, B cell activating factor (BAFF), RANKL or TNF-α to their corresponding receptors (Gardam and Brink, 2014, Madge et al., 2008, Cabal-Hierro and Lazo, 2012). TNF-α activates the canonical pathway after binding to the TNFR1, whereas ligation of TNF-α to TNFR2 activates the non-canonical pathway (Cabal-Hierro and Lazo, 2012). Here, ligation induced receptor trimerisation induces the recruitment of TRAF2 to the receptor complex, which functions as an adaptor protein to recruit TRAF1, TRAF3, cIAP and cIAP2 (Rothe et al., 1995a, Rothe et al., 1995b, Rothe et al., 1994). The fundamental difference between the canonical and non-canonical activation of NF-κB is the involvement of NIK, which becomes recruited by the TRAF proteins and phosphorylates and thereby activates IKK-α (Sun, 2011). In

contrast to the canonical activation *via* TNF-α, IKK-β does not play a fundamental role. IKK-α mediated phosphorylation and downstream degradation of IκB proteins, triggers the proteolytic processing of NF-κB2 (p100) to NF-κB2 (p50). This event relieves the inhibition of NF-κB dimers by NF-κB2 (p100) and increases the number of NF-κB2 (p50) containing dimers, inducing a transcriptional response (Hayden and Ghosh, 2012, Sun, 2011).

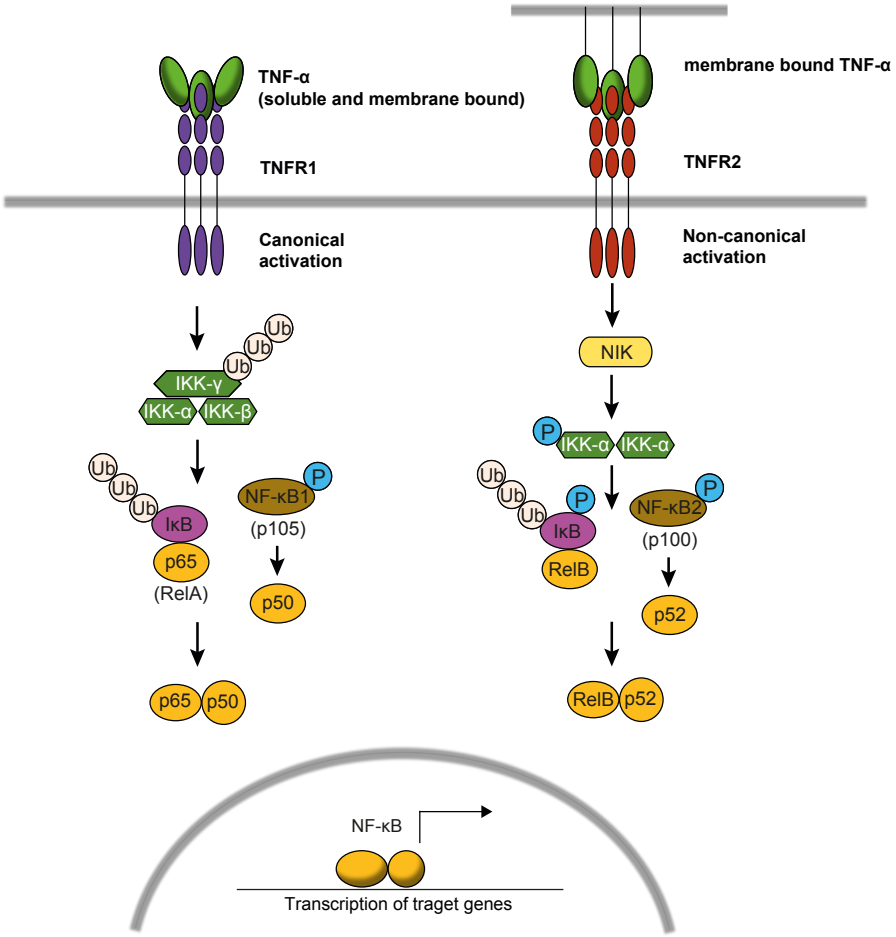

Figure 1-8. Canonical and non-canonical activation of NF-κB *via* TNF-α.

The canonical NF-κB pathway can be activated *via* TNFR1. Activation of the IKK complex (IKK-α, IKK-β and IKK-γ (NEMO)) leads to the phosphorylation of IκB proteins and subsequent polyubiquitination and proteasomal degradation. The IKK complex further phosphorylates NF-κB1 (p105) leading to proteolytic processing and increased levels of p50. RELA (p65) – p50 dimers translocate to the nucleus and regulate the expression of target genes. When TNFR2 is activated this leads to the activation of NIK which phosphorylates and thereby activates IKK-α. Downstream of IKK-α, phosphorylation of NF-κB2 (p100) leads to an increased proteolytic processing towards p52 and phosphorylation of IκB proteins release the block of RELB. RELB - p52 dimers translocate to the nucleus and regulate the expression of target genes.

1.8 The Death-Associated Protein Kinase (DAPK) family

The Death-Associated Protein Kinase (DAPK) family comprises serine/threonine kinases that are associated with several cell death-related signalling pathways. The family is formed by DAPK1 (also referred to as DAPk) and two closely related homologues, DAPK2 (also known as DRP-1) and DAPK3 (also known as ZIPK/DLK). This family also includes DAPK-related apoptosis-inducing protein kinase (DRAK) 1 and 2, which display a lower level of homology. DAPK2 and DAPK3 share 83% and 80% identity respectively with DAPK1´s catalytic domain at the amino acid level. Outside this domain they vary greatly in size and structure (**Figure 1-9**). DAPK1 was originally identified as a factor regulating apoptosis in response to the cytokine Interferon (IFN) -γ (Deiss et al., 1995). All family members have been shown to mediate apoptosis upon overexpression (Cohen et al., 1997, Kawai et al., 1998, Kawai et al., 1999). Furthermore, the DAPK1 gene is often methylated in tumour cells, thereby transcriptionally silent, supporting the hypothesis that members of the DAPK family act as tumour suppressors (Bialik and Kimchi, 2006). However, it has also been reported that a DAPK1 isoform protects cells from TNF-induced apoptosis. This cytoprotective effect has been shown to be mediated through intrinsic and extrinsic apoptotic signalling pathways (Jin et al., 2001). In addition, DAPK1 has been described as a sensor for Δψm (Shang et al., 2005) and a player in oxidative stress response pathways (Eisenberg-Lerner and Kimchi, 2007).

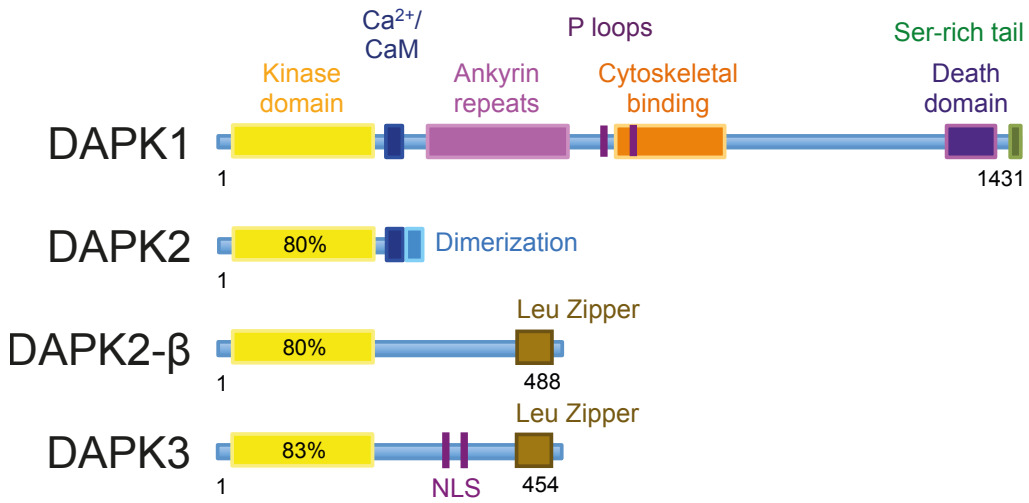

Figure 1-9. The DAPK family.

Protein domains of the DAPK family members are shown in different colours. The percentage in the kinase domain depicts homology to the family founder DAPK1. Whereas the proteins show a strong homology at the kinase domain, the C-termini of these proteins differ significantly.

1.8.1 DAPK2

DAPK2 is a member of the DAPK family and shares a high level of homology in its kinase domain with the other two family members, DAPK1 and DAPK3. The Kimchi group also identified DAPK2, which they characterised in 1999(Kawai et al., 1999). Like DAPK1, it is a Ca^{2+}/calmodulin (CaM) regulated serine/threonine (Ser/Thr) kinase. The kinase domain is located at its N-terminus and the CaM regulated domain is located after the kinase domain and inhibits catalytic activity by functioning as a so-called pseudosubstrate (**Figure 1-9** and **Figure 1-10**) (Shani et al., 2001, Bialik and Kimchi, 2006). Similar to DAPK1, the kinase activity of DAPK2 can be inhibited by autophosphorylation at the Serine residue 308 (S308), which reduces its affinity to CaM (Shani et al., 2001, Shohat et al., 2001). Therefore, the activation of DAPK2 requires two distinct events: First, Ca^{2+}-activated CaM binds to the CaM regulated domain and releases this domain

from the catalytic cleft. Second, unique to members of the DAPK family, S308 dephosphorylation increases DAPK2's affinity towards CaM and allows low levels of activation even in the absence of CaM (Shani et al., 2001, Shohat et al., 2001) [reviewed in (Bialik and Kimchi, 2006)]. Furthermore, it has been shown that DAPK2 dephosphorylated at S308 tends to form dimers and higher oligomeric forms. Homodimerisation is facilitated by its C-terminal 40-amino acid tail. Remarkably, it has been shown, that homodimerisation adds another level of complexity to the regulation of DAPK2, as mutants that lack this tail were not only unable to dimerise but required higher CaM concentrations to function properly (Shani et al., 2001). More recent work carried out by Patel et al. shed more light into this complex activation process. Upon evaluating crystallised DAPK2 it was shown that dimerised DAPK2 itself does not resemble the activated form. However, dimerised CaM bound to DAPK2 is suggested to play a crucial role in the generation of S308 dephosphorylated, monomeric and active DAPK2 (Patel et al., 2011) (**Figure 1-10**). DAPK2 is ubiquitously expressed in several different cells and tissue types (Kawai et al., 1999). As mentioned above, activation of DAPK2 requires binding of Ca^{2+}-activated CaM followed by the dephosphorylation of S308 leading to activated DAPK2 monomers. Interestingly, the potentially apoptotic TNF family members FasL and TNF-α were found to induce dephosphorylation of DAPK2 S308 and formation of DAPK2 dimers, required for the activation of active monomers, suggesting that DAPK2 becomes activated downstream of TNF receptor activation (Shani et al., 2001). It has been suggested, that under physiological conditions two different processes are capable to activate DAPK2. An increase in cellular Ca^{2+} levels, often associated with the induction of apoptosis, can induce the CaM modulated activation of

DAPK2. Alternatively, mostly independent of increased Ca^{2+} levels, phosphatases can dephosphorylate S308 in response to extracellular stimuli leading to the activation of DAPK2 (Bialik and Kimchi, 2006). In addition to the reported activation of DAPK2 in response to the activation of TNF-α, it has also been described to directly interact with the transforming growth factor, beta receptor 1 (TGFBR1) (Barrios-Rodiles et al., 2005). However, no functional work characterising this interaction has been carried out so far.

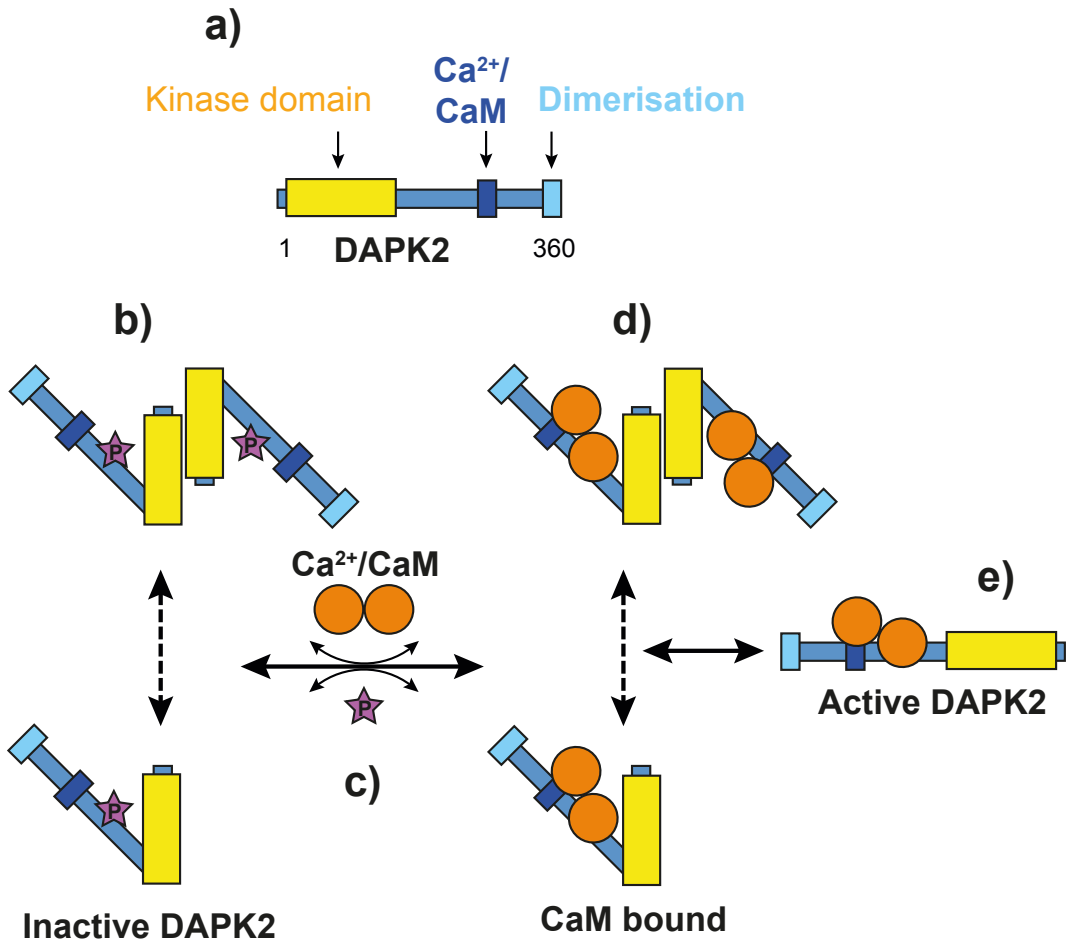

Figure 1-10. Model of DAPK2 activation.

Structure of DAPK2 with its kinase domain in yellow, Ca^{2+}/calmodulin (CaM) binding domain in dark blue and dimerization domain in light blue (**a**). Possible activation mechanism of DAPK2 according to Patel et al. (**b - e**). CaM binding domain functions as pseudo substrate for DAPK2s kinase domain and pS308 reduces the affinity of DAPK2 towards CaM, leading to autophosphorylated, monomeric or dimeric inactive DAPK2. Homodimerisation is dependent on the C-terminal dimerisation domain (**b**). Dephosphorylation of pS308 increases the affinity of DAPK2 towards CaM and/or increase of cellular Ca^{2+} levels leads to an activation of CaM. In consequence, CaM binds to dephosphorylated DAPK2, leading to the formation of CaM bound dimeric form (**d**) which is required to form the CaM bound monomeric active form of DAPK2 (**e**) (Reproduced and adapted from (Patel et al., 2011)).

The activation of DAPK2, as it is the case with DAPK1, has been associated with autophagy and caspase-independent cell death. During autophagic processes, DAPK2 can be found in the lumen of autophagic vesicles (Inbal et al., 2002). The majority of investigations into its functional role are solely based on induction of death related changes in overexpression studies. Interestingly, involvement in

death-inducing processes have often been shown to also involve DAPK1 and DAPK3, and the formation a so-called 'death-associated multi-protein complex' has been postulated (Gozuacik and Kimchi, 2006). Interestingly, kinase dead DAPK2, that contains alanine instead of lysine at the residue 42, which destroys the ATP binding pocket, has been shown to block TNF-α induced membrane blebbing (Inbal et al., 2002, Kawai et al., 1999). Together with other reports, linking DAPK2 expression to the induction of membrane remodelling and loss of matrix adherence, this suggests that DAPK2 could be partly involved in the induction of apoptotic features in response to extracellular stimuli (Inbal et al., 2002). This effect on membrane remodelling by DAPK2 is likely to be modulated *via* phosphorylation of myosin light chain (MLC), which is a known target of DAPK2 (Inbal et al., 2000, Kawai et al., 1999). Furthermore, DAPK2 is capable of phosphorylating DAPK1 and DAPK3 (Shani et al., 2004), which have also been associated with cytoskeletal remodelling [reviewed in (Bialik and Kimchi, 2006)].

In contrast to DAPK1 and DAPK3, DAPK2 has not been identified as a tumour suppressor in solid tumours. Interestingly, DAPK2 is emerging as a tumour suppressor in several types of leukaemia, especially in acute promyelocytic leukaemia (APL), a subtype of acute myelogenous leukaemia (AML), which responds to treatment with all-trans retinoic acid (ATRA) (Rizzi et al., 2007).

Further insight into the physiological role of DAPK2 has been found upon identification of DAPK2 as a key player during granulopoiesis. It has been shown to be specifically expressed in normal granulocytes *versus* monocytes/ macrophages and CD34+ progenitor cells. Remarkably, the induction of

neutrophil differentiation by means of all-trans retinoic acid (ATRA) resulted in increased DAPK2 mRNA and protein expression. On the other hand, RNAi mediated DAPK2 depletion in an acute promyelocytic leukaemia cell line (NB4) resulted in reduced ATRA mediated granulocytic differentiation (Rizzi et al., 2007). The expression of DAPK2 during neutrophil differentiation was demonstrated to be mediated by the myeloid master regulator PU.1. It can be blocked by the main driver of acute promyelocytic leukaemia (APL), the fusion protein, PML-RARA, linking DAPK2 function not only to neutrophil differentiation but the origin of leukemic disorders (Humbert et al., 2013). Recently, it has been shown that the role of DAPK2 in granulocytes does not seem to be restricted to their differentiation but is also involved in motility and response to chemoattractants. Pharmacological inhibition of DAPK2 in granulocytes resulted in decreased motility and block of an intermediary chemoattractant (e.g. IL-8, Leukotriene B4, platelet-activating factor) response with no effect on the response to end target molecules (e.g. formyl-methionyl-leucyl phenylalanine (fMLF) or complement component C5 (C5a)) that are secreted at the actual site of inflammation. This suggest a direct involvement of DAPK2 in an pro-inflammatory response mediated by granulocytes which might be linked to previously described mechanism of MLC phosphorylation by DAPK2 (e.g. fMLF or C5a) (Geering et al., 2013).

Remarkably, DAPK2 has also been associated with differentiation processes in the erythropoietic lineage. DAPK2 was proposed to be a new candidate attenuator of erythropoiesis. Interestingly, DAPK2 expression levels are significantly increased in early stages of erythrocyte development (bone marrow

stage and late stage erythroblasts). DAPK2 knock in mice failed to reverse induced anaemia and showed a decreased response to EPO treatment. Moreover, RNAi mediated depletion of UT7/Epo (erythroleukemic cells) led to substantial survival advantages in response to EPO treatment. These findings suggested that DAPK2 might exert fundamental regulatory effects on proerythroblast development (Fang et al., 2008). The described function of DAPK2 in myeloid differentiation sheds light into the so far enigmatic role of DAPK2's physiological function.

Most recently, DAPK2 has also been linked to the induction of tubulointerstitial fibrosis in mice kidneys upon chronic cisplatin exposure. Interestingly, no malformation or increased tumour rate was reported in these mice (Guay et al., 2014).

Adding another level of complexity into the biology of DAPK proteins, an alternative splicing variant of DAPK2 has been identified recently. This isoform lacks the above-mentioned CaM regulated domain and contains a leucin zipper domain equivalent to DAPK3 (**Figure 1-9**). This isoform was named DAPK2-β and reported to be exclusively expressed in embryonic and early developmental tissues (Shoval et al., 2011).

1.9 Cancer and glucose metabolism

In 2011, when Hanahan and Weinberg extended their initial hallmarks of cancer theory, they included the ‘emerging hallmark: reprogramming energy metabolism’

(Hanahan and Weinberg, 2011) (**Figure 1-2**). This hallmark of cancer characterises the metabolic changes in cancer cells that fundamentally contribute to carcinogenesis.

Under physiological conditions, ATP is generated *via* two distinct metabolic pathways, depending on the cell type and environmental changes. Glycolysis is the first step in both pathways, degrading one molecule of glucose into two molecules of pyruvate, thereby producing two molecules of ATP. As depicted in **Figure 1-11**, most eukaryotic cells produce their majority of energy using the aerobic respiratory pathway. Here, pyruvate, as the main energy source, is transported into the mitochondria, where it becomes decarboxylated by enzymes of the pyruvate dehydrogenase complex (PDC) and enters the tricarboxylic acid (TCA)/Krebs cycle. The TCA/Krebs cycle is composed of a number of sequential reactions, that, in the end, lead to the oxidisation of two pyruvate molecules and production of 6 NADH, 2 FADH, as well as 2 ATP and the by-products H_2O and CO_2 [reviewed in (Zheng, 2012)]. In the next step, NADH is metabolised in the oxidative phosphorylation (OXPHOS), which utilises NADH to generate an electron gradient between the inner and outer mitochondrial membrane, in the so-called intermembrane space. The enzyme ATP synthase uses this electron gradient to produce ATP. One molecule of glucose ultimately yields 36 ATP molecules (Rich, 2003).

The other main pathway to generate ATP is the so-called anaerobic respiration (**Figure 1-11**). When oxygen supply is limited, this pathway bypasses the pyruvate transport to the mitochondria. Instead an enzyme of the lactate

dehydrogenase family (LDH) converts pyruvate to lactate, under the expense of one NADH molecule, freeing NAD^+ for glycolysis and leading to the accumulation of lactate. Under physiological conditions anaerobic respiration happens in all cells automatically, as pyruvate always accumulates to a certain extend. Accumulated lactate is transported out of the cells and can be converted back into pyruvate, producing NADH. (Miao et al., 2013). In addition, cells can increase anaerobic respiration in response to hypoxia due to intensive muscular work, injuries or necrosis (Miao et al., 2013, Dashty, 2013).

In 2011, Hanahan and Weinberg (Hanahan and Weinberg, 2011) stated, that tumour cells in hypoxic environments, or even in the presence of oxygen switch from aerobic to anaerobic respiration. This metabolic change in cancer cells has been described as early as in 1930 [35]. However, switching towards anaerobic respiration forces cancer cells to cope with an approximately 18 fold reduced production of ATP (36 molecules after oxidative phosphorylation *versus* 2 molecules after anaerobic respiration) (Hanahan and Weinberg, 2011). Increasing evidence suggests that this switch in metabolism is not only caused by hypoxia but also driven by well characterized oncogenes such as myelocytomatosis viral oncogene homolog (*c-Myc*) and rat sarcoma (*RAS*) or mutated tumour suppressors such as (*p53*). As mentioned above, pyruvate is converted into lactate by enzymes of the LDH family. Five different LDH isozymes play a major role in human metabolism. These isozymes are tetramers composed of the subunits LDH-A and/or LDH-B, encoded by two different genes (von Eyben, 2001). Composition of the LDH complex determines whether the enzyme complex favours the conversion of pyruvate to lactate or the other way

round. The more LDH-A subunits are present in the isozyme tetramer, the more the enzyme complex favours the reaction of pyruvate to lactate, whereas the number of LDH-B subunits correlates with the conversion of lactate to pyruvate. Cancer cells primarily express LDH-A, which therefore has been discussed as a potential biomarker for cancer (Miao et al., 2013, Girgis et al., 2014).

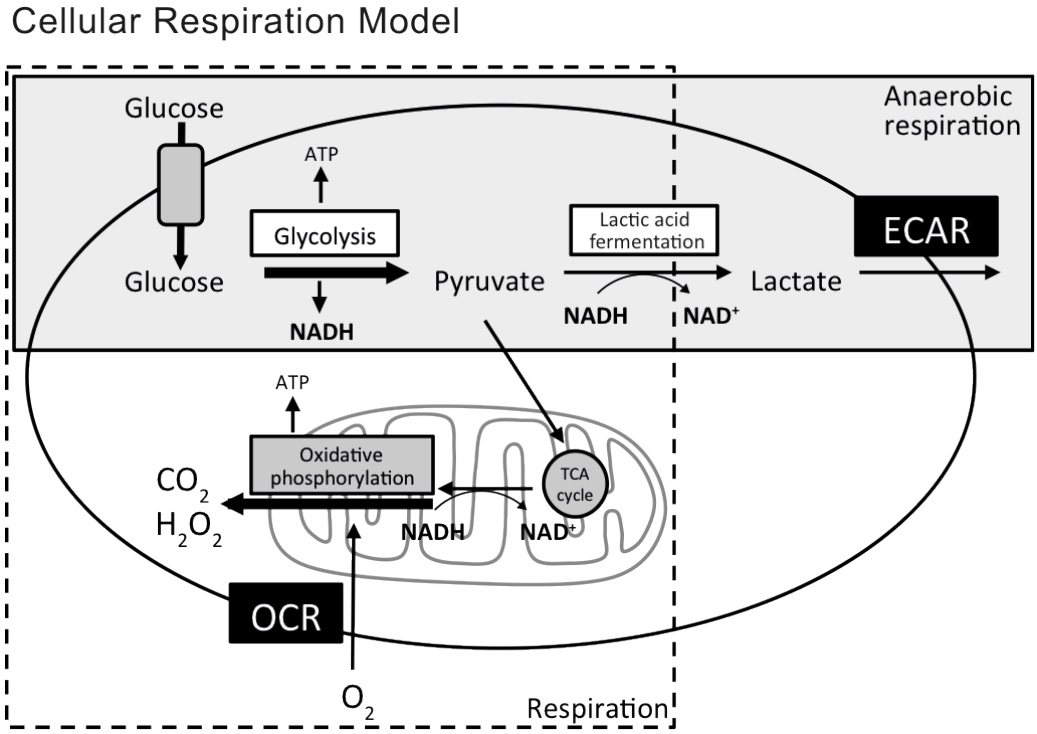

Figure 1-11. Simplified cartoon of cellular metabolism pathways.

Simplified cartoon depicting cellular metabolism pathways with glycolysis as the first step of glucose breakdown, and oxidative phosphorylation and anaerobic respiration as subsequent steps.

Reprogramming of cancer cells towards anaerobic glycolysis has been shown to be associated with the regulation of hypoxia-inducible factors (HIFs). HIFs are a family of transcription factors that are activated under hypoxic conditions and upregulate the expression of LDH-A mRNA amongst other transcriptional targets. Several oncogenic lesions, such as c-myc deregulation or overactivation of

Her2/neu promote the expression of LDH-A *via* activation of HIFs [reviewed in (Miao et al., 2013)]. Activation of HIFs also induces the expression of glucose transporters (GLUT), further increasing the amount of cytosolic glucose available for anaerobic respiration (Fantin et al., 2006). In addition, other factors have been linked to HIF proteins: e.g. HIF-1α has been linked to pyruvate kinase isoenzyme M2 (PKM2). PKM2 is an isoenzyme of the pyruvate kinase family, which dephosphorylates phosphoenolpyruvate to pyruvate whilst producing ATP as the final step of glycolysis. Under physiological conditions, PKM2 is mostly expressed during embryogenesis and development. Cancer cells however have been shown to induce expression of this protein so that it can contribute to the metabolic reprogramming towards anaerobic respiration (Luo et al., 2011). Recently, PKM2 has also been shown to be directly regulated by DAPK1, a member of the DAPK family, which phosphorylates PKM2 and thereby increases cellular lactate production (Mor et al., 2012).

Despite the obvious reason for favouring anaerobic respiration in cancer cells under hypoxic conditions, the described metabolic reprograming is not necessarily associated with a hypoxic environment. It has been postulated, that an increased glycolysis *per se* represents an advantage for rapidly dividing cells. Synthesis of cellular components such as nucleotides and proteins require a constant supply with glycolytic intermediates. Interestingly, not only cancer cells, but also embryonic tissues exhibit an increase in anaerobic glycolysis. This suggests, that an increased glycolytic rate, despite its poor metabolic efficiency, contributes to cellular growth (Vander Heiden et al., 2009, Potter, 1958). Interestingly, induction of LDH-A has not only been shown to promote the

conversion of pyruvate to lactate, but LDH-A inhibition or lack seems to increase the rate of oxidative phosphorylation (Le et al., 2010). Remarkably, LDH-A is upregulated in a variety of human tumours and has further been associated with resistance to chemotherapy (Zhou et al., 2010, Miao et al., 2013).

1.10 Mitochondria and ROS

As mentioned above, there are two main pathways of glucose metabolism. During glycolysis, glucose is broken down into two pyruvate molecules generating two molecules of ATP. The anaerobic respiratory pathway further converts pyruvate to lactate, generating NADH. Oxidative phosphorylation is the far more efficient metabolic pathway, which in the end produces 36 ATP molecules from one molecule of glucose. Here, pyruvate is transported into the mitochondria and decarboxylated by enzymes of the PDC and enters the TCA/Krebs cycle. At the end of this cycle, composed of a series of enzymatic reactions, two pyruvate molecules become oxidised to 6 NADH, 2 FADH, as well as 2 ATP and the by-products H_2O and CO_2. As mentioned in **1.9**, Mitochondria are the key compartments that, subsequently utilise NADH and FADH to generate ATP in processes referred to as oxidative phosphorylation or chemiosmosis (Mitchell and Moyle, 1967). As depicted in **Figure 1-12**, this process is driven by the generation of a proton gradient between the mitochondrial matrix and the intermembrane space alongside the inner mitochondrial membrane. NADH and FADH serve as electron donors to electron acceptors such as O_2. Part of this process is the oxidation of NADH and FADH and the transport of hydrogen protons (H^+) into the inner mitochondrial membrane space by a protein complex referred to as electron transport chain (ETC), which is located in the inner mitochondrial membrane. The ETC consists of four different protein complexes, (Complex I, II, III and IV). Each of these is involved in the electron transfer process and functions as electron donor and acceptor leading to the accumulation of H^+ in the mitochondrial intermembrane

space. This leads to the generation of an electron potential between the mitochondrial intermembrane space and the mitochondrial matrix, which is also referred to as mitochondrial membrane potential (Δψm). Here, Complex I (NADH dehydrogenase), transfers two electrons from NADH to the coenzyme ubiquinone (CoQ_{10} or Q_{10}) resulting in the production of its reduced form ubiquinol ($CoQ_{10}H_2$) and the transfer of four H^+ protons into the intermembrane space. Complex II (succinate dehydrogenase) functions similar to Complex I, facilitating the reduction of CoQ_{10} to $CoQ_{10}H_2$ using FADH, which is produced during the oxidisation of succinate to fumarate as the last step of the TCA cycle. Note, this complex does not transport H^+ to the intermembrane space. In the next step, Complex III (CoQ_{10} - cytochrome *c* reductase) removes two electrons from CoQ_{10} and transfers them to the haemoprotein cytochrome *c*; Complex III also transfers four H^+ into the mitochondrial intermembrane space. This reaction is followed by Complex IV (cytochrome *c* oxidase), which removes electrons from cytochrome *c* and leads to the oxidisation of O_2, resulting in the formation of H_2O and also transferring two molecules of H^+ into the mitochondrial intermembrane space. The last step of OXPHOS is the oxidative phosphorylation of ADP, resulting in the production of ATP, the central energy storage unit of the cells. This is facilitated by Complex V, also referred to as ATP synthase, a multi-protein complex that functions as an ion channel allowing an influx of H^+ protons, along the proton gradient, back into the mitochondrial matrix. The energy freed during this proton flux is used to phosphorylate ADP, leading to the production of ATP.

During the process of oxidative phosphorylation, single protons can escape and reduce oxygen to the superoxide anion ($\bullet O_2^-$), which further results in the

generation of a variety of reactive oxygen species (ROS) such as H_2O_2, and highly reactive hydroperoxyl radical (HO2•). Accumulation of ROS can lead to oxidative damage and as end consequence induction of apoptosis [reviewed in (Fariss et al., 2005)]. It has been postulated that approximately 1% of consumed O_2 contributes to the generation of ROS, the majority of which is being produced in the mitochondria (Petrosillo et al., 2004) [reviewed in (Fariss et al., 2005)]. Electron leakage has been reported for Complex I, which is usually released into the matrix, making Complex I an important site for the production of $\bullet O_2^-$ (Hirst et al., 2008, Muller et al., 2004). Interestingly, Complex II has only been associated with the generation of ROS when mutated or Complex I and Complex III are inhibited, leaving it as a minor source for mitochondrial ROS (Drose, 2013, Quinlan et al., 2012). Complex III has been described by many groups to be a major source of mitochondrial ROS and is, together with Complex I, regarded as the main mitochondrial site involved in the production of ROS. During the electron transfer by Complex III the highly reactive ubisemiquinone radical anion ($\bullet CoQ_{10}^-$) is formed, which can induce electron leakage leading to the generation of $\bullet O_2^-$. This oxygen radical is released into the matrix as well as the intermembrane space (Muller et al., 2004). The generation of ROS by complexes of the ETC can be increased by a large proton gradient during OXPHOS. Such increase can be caused by an increased production of NADH or a defect in proteins of the ETC by e.g. aging or mutations (Fariss et al., 2005). Mitochondrial ROS are controlled by two proteins, phospholipid-hydroperoxide glutathione peroxidase (PHGPx) and Mn-superoxide dismutase (MnSOD or SOD2). PHGPx functions as electron donor for peroxidised lipids under oxidation of glutathione, protecting mitochondria from toxic lipid radicals (Nakagawa, 2004). SOD2 is a

mitochondrial protein that can be found in the mitochondrial matrix, transforming $\bullet O_2^-$ into less toxic H_2O_2 (Muscoli et al., 2003).

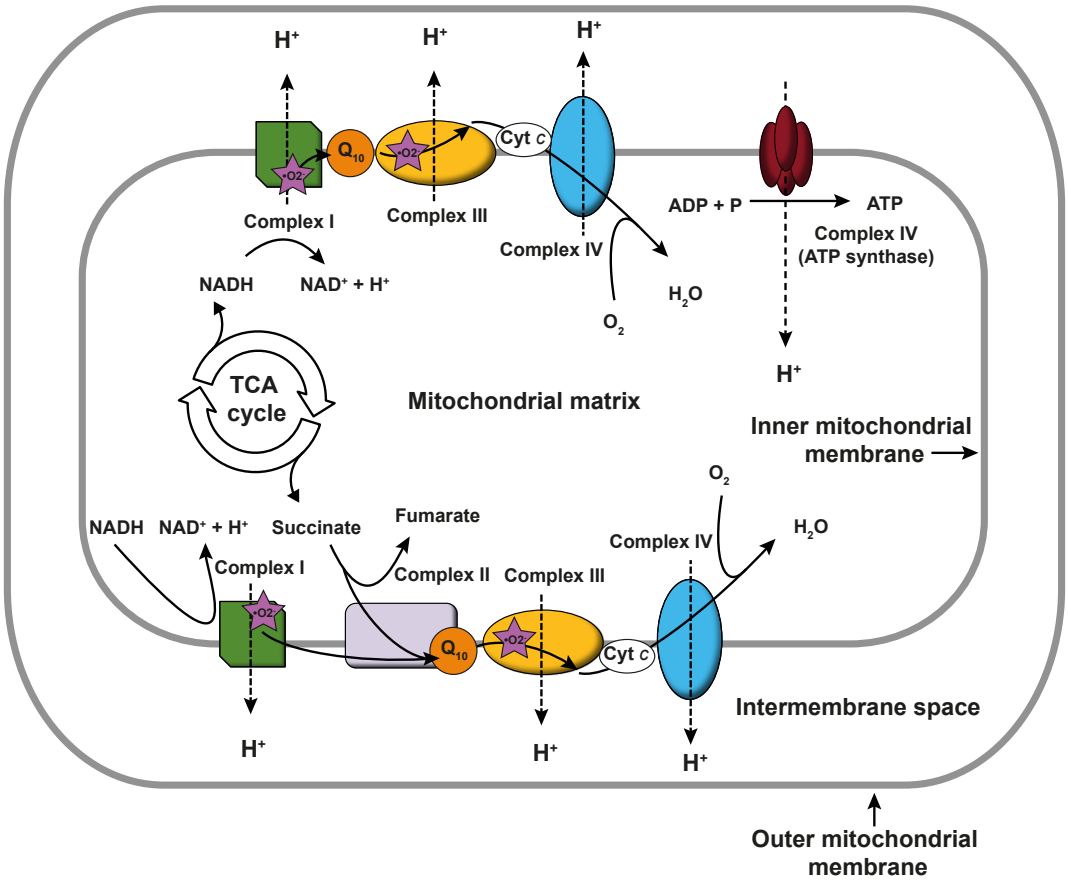

Figure 1-12. Simplified cartoon of the electron transport chain.

NADH is generated by the TCA cycle. **Complex I** (depicted as green square) transfers electrons to the coenzyme ubiquinone (Q_{10}) and utilises the freed energy to transfer H^+ protons into the intermembrane space. During this process superoxide ($\bullet O_2^-$, depicted as purple stars) can be generated. As part of the TCA cycle succinate is oxidised to fumarate. This reaction is carried out by **Complex II** (depicted as light purple square). During this process energy is stored in FADH as an intermediate and electrons are transferred to Q_{10}. **Complex III** (depicted as yellow oval) removes electrons from Q_{10} and transfers them to cytochrome *c* (Cyt *c*) whereby H^+ protons are pumped into the intermembrane space. This process bears the risk of $\bullet O_2^-$ generation. **Complex IV** (depicted as blue oval) removes electrons from Cyt *c* and oxidises O_2 under generation of H_2O and also utilises the generated energy to pump H^+ protons into the intermembrane space. **Complex V**, also known as ATP synthase (depicted in brown), uses the mitochondrial membrane potential to generate ATP. H^+ proton flux along the proton gradient frees energy, which is utilised to phosphorylate ADP to ATP.

2. Aims

Previous work in Dr. Ana P. Costa-Pereira's' laboratory, carried out by Dr. Katrina M. Sutton and Dr. Ana-Violeta Fonseca, revealed that the depletion of DAPK2 resulted in sensitisation of U2OS osteosarcoma cells to TRAIL-induced apoptosis, whilst having no impact on other apoptosis stimuli such as taxol and H_2O_2 (**Figure 2-1a** + **b**), and the death-inducing cytokine TNF-α (**Figure 2-1d**).

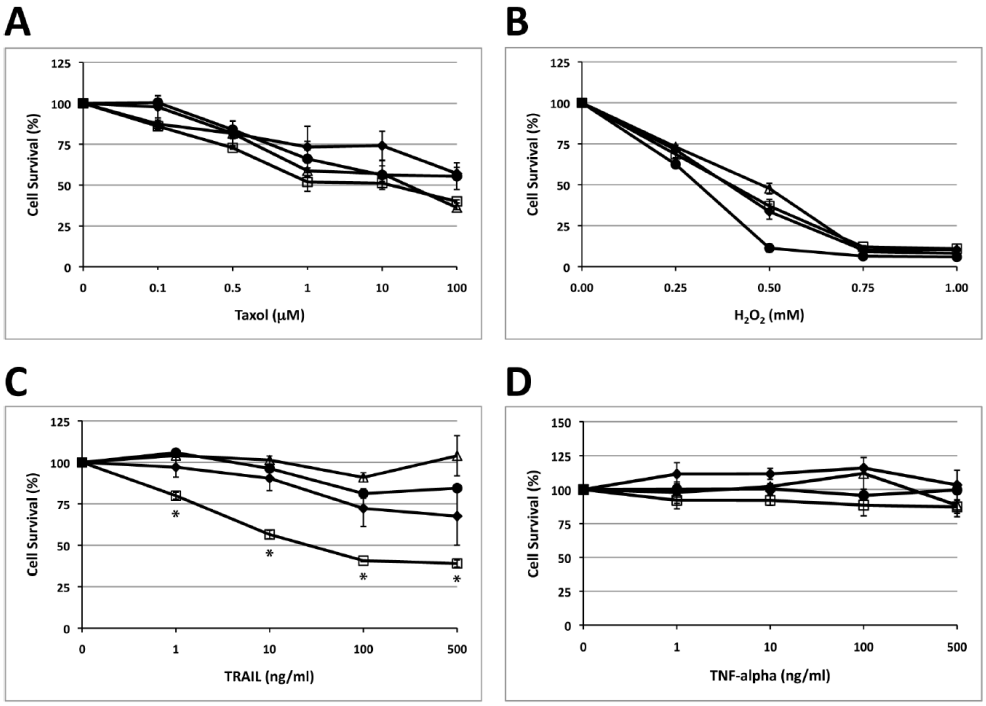

Figure 2-1. DAPK2 is a modulator and inhibitor of TRAIL-induced apoptosis in cancer cells.

U2OS osteosarcoma cells were left untransfected, mock-transfected or transfected with siRNA oligonucleotides targeting four different regions of DAPK2 (previously validated by deconvolution analysis), or with a nontargeting (NT) siRNA. After 48 h, cells were counted and re-plated at equivalent numbers. Cells were then challenged with Taxol, H_2O_2, TRAIL or TNF-**α** for 24 h and cell death measured using crystal violet. All samples were set in triplicate and the data shown here represent the average of 3 independent experiments. * $p < 0.05$ two-tailed students *t*-test; ♦ Untransfected; • Mock; ∆ NT siRNA; DAPK2 siRNA. Dr. Ana-Violeta Fonseca generated this figure.

We hypothesised that DAPK2 is a novel modulator of TRAIL-induced apoptosis. Therefore, the aim of this work was thus to decipher and better understand the underlying mechanism(s) leading to the sensitisation of TRAIL-resistant cancer cells to TRAIL-induced apoptosis.

3. Materials and Methods

3.1 Materials

3.1.1 Equipment

Applied Biosystems 7900HT Fast Real-Time PCR System was from Applied Biosystems, (Foster City, CA, USA). FACS Canto flow cytometer was from Becton Dickinson (Franklin Lakes, NJ, USA). Orbital shaker Stuart SSL1 was from Bibby Scientific (Stone, UK). Mini-PROTEAN® electrophoresis system and PowerPac™ Universal Power Supply were from BioRad (Hercules, CA, USA). PHERAstar *Plus* luminescence microplate reader was from BMG Labtech (Ortenberg, Germany). The BioMAT 2 Microbiological Safety Cabinet was from CAS (Manchester, UK). Centrifuge 5810, centrifuge 5411 D, –80 °C Premium U570 Upright Freezer and the Thermomixer Compact were from Eppendorf (Hamburg, Germany). PIPETMAN Classic™ pipets were from Gilson (Middleton, WI, USA). The water bath was from Grant Instruments (Shepreth, UK). The Konica SRX-101A film processor was from Konica Minolta (Marunouchi, Japan). The iBlot® Dry Blotting system was from Invitrogen, a brand of Life Technologies (Carlsberg, CA, USA) and the Veriti® 96-Well Thermal Cycler was from Life Technologies. Milli-Q® Integral Water Purification Systems was from Merck Millipore (Billerica, MA, USA). The MP225 General Purpose GLP pH /mV / T Meter was from Mettler-Toledo (Greifensee, Switzerland). The AutoFlow Direct Heat CO_2 Incubator was from NuAire (Plymouth, MN, USA). The inverted research microscope IMT-2 was from Olympus (Tokio, Japan). The FUSION Solo™ quantitative luminescence system was from PEQLAB (Erlangen, Germany). The bacterial incubator was from Sanyo (Moriguchi, Japan). CERTOMAT® BS-1 Incubation-Shaking Cabinet was from B. Braun Biotech International, now part of Sartorius (Göttingen, Germany). Seahorse XF96

analyser was from Seahorse Bioscience (North Billerica, MA, USA). Films were scanned using an EPSON PERFECTION V500 photo scanner from Seiko Epson (Nagano, Japan). Freezing container, Nalgene® Mr. Frosty was from Sigma-Aldrich (St. Louis, MO, USA). The VORTEX GENIE 2 was from Scientific Industries (Bohemia, NY, USA). Sunrise™ microplate absorbance reader was from Tecan Group (Männedorf, Switzerland). Heraeus™ Fresco™ 17 Microcentrifuge, rotamixer Denley Spiramix, magnetic stirrer IKAMAG RO 15 POWER, Sorvall™ Legend™ T Plus/RT Plus Centrifuge, Matrix™ Equalizer Electronic Multichannel Pipetters and NanoDrop 1000 Spectrophotometer were from Thermo Fisher Scientific (Waltham, MA, USA). The gel documentation system was from UVITEC (Cambridge, UK).

3.1.2 Software

Data was analysed using Microsoft® Excel® for Mac 2011 from Microsoft (Redmond, WA, USA). Statistical analysis was performed and the majority of graphs were generated using GraphPad Prism from GraphPad software (La Jolla, CA, USA). Flow cytometry data was analysed and graphs were generated using FlowJo Version 8.8.7 (Tree Star, Ashland, OR, USA). Quantitative polymerase chain reaction data was analysed using the Applied Biosystems 7900HT Fast Real-Time PCR System Software SDS v2.3 from Applied Biosystems. Further gene expression analysis was performed using the qbase+ software from Biogazelle (Ghent, Belgium). Western blot images were obtained using the FUSION-CAPT software from PEQLAB (Erlangen, Germany). Images were further analysed using the Image Studio Lite software from LI-COR

Biosciences (Lincoln, NE, USA). Manuscript figures were assembled using Microsoft® PowerPoint® for Mac 2011 (Microsoft) and Adobe Illustrator CS6 from Adobe Systems Incorporated (San Jose, CA, USA).

3.1.3 Consumable materials

All pipette tips were from Starlab (Milton Keynes, UK) and VWR (Radnor, PA, USA). Cell scrapers, centrifuge tubes, tissue culture dishes, tissue culture flasks and sterile serological pipettes were from VWR. Aspiration pipettes were from Sarstedt (Nümbrecht, Germany). Cloning cylinders were from Sigma-Aldrich. Microcentrifuge tubes and all remaining plastic ware were from Starlab and XF96 microplates were from Seahorse Bioscience.

3.1.4 General reagents

The $NADP^+$/ NADPH assay kit was from Abcam (Cambridge, UK). The Glutathione Assay Kit was from BioAssay Systems (Hayward, CA, USA). The NAD^+/ NADH assay kit was from BioVision (San Francisco, CA, USA). Foetal calf serum (FCS) was purchased from FirstLink (Wolverhampton, UK). L-glutamine, Lipofectamine® RNAiMax transfection reagent, Lipofectamine® 2000 transfection reagent, OneShot® TOP10 Chemical competent cells, Proteinase K, Dynabeads® Protein G-magnetic beads, iBlot® nitrocellulose Transfer Stacks, High-Capacity cDNA Reverse Transcription Kit, Fast SYBR® Green Master Mix, PureLink® HiPure Plasmid Midiprep Kit, Opti-MEM® Reduced Serum Media and Zeocin™ were obtained from Life Technologies. 5-(and-6)-chloromethyl-2',7'-

dichlorodihydrofluorescein diacetate, acetyl ester (CM-H2DCFDA), dihydroethidium (DHE), the MitoProbe™ JC-1 Assay Kit and MitoSOX™ Red mitochondrial superoxide indicator were purchased from Molecular Probes®, a brand of Life Technologies. Glycine, nonidet-P40 (NP-40) and paraformaldehyde (p-FA) were from VWR (Radnor, PA, USA). Dithiothreitol (DTT) and powdered milk were obtained from AppliChem (Darmstadt, Germany). BioRad protein assay and bromophenol blue were obtained from BioRad. Ethanol, glycerol, isopropyl alcohol, methanol, ethylenediamine tetraacetic acid (EDTA), Tris(hydroxymethyl)-aminomethan (Tris), hydrochloric acid (HCl, 37% v/v), glacial acetic acid, phosphate buffered saline, sodium chloride (NaCl), sodium dodecyl sulphate (SDS), Ultrapure Protogel 30% (w/v) acrylamide, 0.8% bis-acrylamide (37.5:1), Fermentas PageRuler^{TM} prestained protein markers, Pierce ECL Western Blotting Substrate were obtained from Thermo Fisher Scientific. All siGENOME siRNA sequences were obtained from Dharmacon, now a brand of GE Healthcare (Little Chalfont, UK). Enhanced chemiluminescence (ECL) detection reagents were purchased from Amersham a brand of GE Healthcare and aprotinin and leupeptin were purchased from Calbiochem, now a brand of Merck Millipore. Attractene transfection reagent, MinElute® PCR Purification Kit, QIAprep® Spin Miniprep Kit, RNeasy® kit and Ribonuclease A (RNase A) and FlexiTube siRNA were obtained from Qiagen (Hilden, Germany). FUJI medical x-ray film was from FUJIFILM (Tokyo, Japan). Dual-Glo® Luciferase assay system was obtained from Promega (Madison, WI, USA). All restriction enzymes and T4 DNA Ligase were from New England Biolabs (Ipswich, MA, USA). Tet System Approved FBS was from Clontech a brand of Becton Dickinson. The cOmplete and Mini EDTA-free protease inhibitor cocktail was from Hoffmann-La

Roche (Basel, Switzerland). All remaining reagents were purchased from Sigma-Aldrich.

3.1.5 Antibodies and cytokines

Anti-DAPK2 was purchased from Epitomics (Burlingame, CA, USA). Anti-DAPK1 and pDAPK1 (Ser308) were from Abcam. DAPK3 antibody was from Calbiochem. Antibodies against Caspase-3, Caspase-8 and Caspase-9, CHOP, BID, BCL-X_L, DR5, pERK1/2 (Thr202/Tyr204), NF-κB1 (p50, p105), NF-κB2 (p52, p100), PARP, RELA (p65), and phosphorylated pRELA (pp65-Ser536), were bought from Cell Signaling Technology (Danvers, MA, USA). The antibodies against β-Actin, Flag, HA and α-Tubulin were obtained from Sigma-Aldrich and the one against HSP90 from NeoMarkers (Fremont, CA, USA). The antibodies against ERK1/2, KEAP1, Lamin-B and NRF2 were from Santa Cruz Biotechnology (Santa Cruz, CA, USA). Anti-FAS IgM was from Merck Millipore. Secondary antibodies were from DAKO (Glostrup, Denmark). For flow cytometry, the antibody against DR5 and FAS were from eBioscience (Hatfield, UK) and the one against DR4 from Abcam. TRAIL and TNF-α were purchased from PeproTech (London, UK).

3.1.6 Cell lines

The majority of work in this study was carried out using U2OS and A549 cells. U2OS is an adherent epithelial cell line derived from a moderately differentiated osteosarcoma from the tibia of a 15-year-old Caucasian female (Ponten and Saksela, 1967). A549 is an adenocarcinomic, non-small cell lung cancer (NSCLC) cell line derived from a 58-year-old Caucasian male (Giard et al., 1973). Additionally used were T24 cells, a transitional cell carcinoma, bladder cancer cell line derived from an 81-year-old female Caucasian (O'Toole et al., 1972) and PC3 cells, a prostate adenocarcinoma cell line, derived from a 62-year-old male Caucasian (Kaighn et al., 1979). Characteristics and p53 status of these cell lines are depicted in **Table 3-1**. All cell lines were obtained from the American Type Culture Collection (ATCC).

Table 3-1. Cell lines used in this study and corresponding p53 status.

Cell line	Tumour type	Origin	p53 status
U2OS	Osteosarcoma	Bone	wt / wt (Diller et al., 1990)
A549	NSCLC, adenocarcinoma	Lung	wt / wt (Lehman et al., 1991)
T24	Transitional cell bladder carcinoma	Bladder	wt / mt (Y126 → Stop) (Cooper et al., 1994)
PC3	Prostate	Prostate	- / mt (codon 138, C nucleotide deletion → frame shift) (Isaacs et al., 1991)

For further functional studies and the generation of tetracycline (Tet) inducible cell lines, U2OS cells stably transfected with the Tet repressor (TetR) gene were used (henceforth referred to as U2OS-TetR). These cells were characterised in 2003 (Monroe et al., 2003) and are identical to parental U2OS cells but contain a

stably transfected pcDNA™6/TR plasmid as part of the inducible T-REx™ System (Life Technologies).

3.2 Methods

3.2.1 Cell culture

U2OS, A549, T24 and PC3 cells were cultured in Dulbecco's Modified Eagle's Medium (DMEM) supplemented with 10% (v/v) foetal calf serum (FCS), 2 mM L-glutamine, 50 units/ml penicillin and 50 µg/ml streptomycin (henceforth referred to as Full-DMEM) in a humidified atmosphere of 10% CO_2 at 37 ˚C. U2OS-TetR cells were cultured in Full-DMEM (with Tet System Approved FBS) media supplemented with 5 µg/ml blasticidine. U2OS-TetR cells stably transfected with pcDNA™4/TO based constructs were cultured in Full-DMEM (with Tet System Approved FBS) media supplemented with 5 µg/ml blasticidine and 500 µg/ml Zeocin™. All cell culture work was performed under a laminar flow hood and materials were disinfected using 70% (v/v) ethanol. Medium and buffers were warmed up in a 37 °C water bath. Cells were sub-cultured at circa 80% confluency. For passaging, cells were rinsed generously with PBS and any leftover media and cellular debris were aspirated. Next, cells were incubated with the protease Trypsin-EDTA [2.5 mg/ml trypsin in 0.02% (w/v) EDTA, 0.09% (w/v) NaCl], which detaches adherent cells. Soft beating and incubation at 37 °C eased cell detaching. Cells were re-suspended in Full-DMEM and spun down at 200 RCF for two min to remove any leftover PBS and trypsin. In the next step, cells were seeded into new culture flasks according to the experimental requirements, for passaging usually at a 1:10 ratio. Cells were frozen as follows: upon media removal and washing with PBS, cells were covered with

Trypsin-EDTA. The majority of liquid was aspirated instantly so that the culture flask was covered with a thin layer of Trypsin-EDTA. Upon incubation and cell detachment, cells were re-suspended into freezing media [DMEM, 30% FCS (v/v), DMSO 10% (v/v)], transferred into freezing vials (>1x10^6 cells/vial) and frozen at -80 ˚C using a Mr. Frosty Nalgene® freezing container. Twenty-four h later, freezing vials were transferred into vapour phase nitrogen in liquid nitrogen storage tanks.

Cells were thawed in a water bath at 37 ˚C and upon thawing re-suspended drop-wise in Full-DMEM (37 ˚C). To remove leftover DMSO from the freezing media, cells were spun down at 200 RCF for two min and re-suspended in Full DMEM. Cells were then grown in a humidified atmosphere of 10% CO_2 at 37 ˚C.

3.2.2 Generation of stable inducible cell lines.

For functional studies of DAPK2 mutants, tetracycline inducible cell lines were generated. Therefore U2OS-TetR cells were stably transfected with pcDNA™4/TO plasmids containing N-terminal human influenza haemagglutinin (HA) tagged DAPK2 constructs. The different DAPK2 constructs and their sub-cloning into pcDNA™4/TO plasmids are further described in section **3.2.14**. To achieve higher integration efficiency, HA-DAPK2 constructs cloned into the pcDNA™4/TO vector, were linearised using the restriction enzyme PvuI and complete digest was verified using agarose gel electrophoresis. Linearised plasmids were transfected into U2OS-TetR cells using Lipofectamine® 2000. Forty-eight h later, cells were split into selection antibiotic containing media [Full-

DMEM (with Tet System Approved FBS) supplemented with 5 µg/ml Blasticidine and 500 µg/ml Zeocin™] in a 1:20 and 1:40 ratio. After around four days in selection media, visible colonies began to form. When colonies reached an appropriate size they were picked using cloning cylinders and autoclavable silicon grease as follows. Colonies were assessed for their physical appearance and only those equivalent to the parental cell line were chosen and marked with a pen at the bottom of the cell culture plate. Next, cells were washed twice with PBS and the majority of liquid was aspirated. The bottom of cloning cylinders was covered in grease and then pressed on the surface of the cell culture plate enclosing a selected colony. Subsequently trypsin was added drop wise into the cylinder and cells were incubated at 37 °C for ca. two min. Cell were then transferred into a multiwell culture plate containing selection media. Cells were grown and expanded for further analysis. Induction of DAPK2 constructs with doxycycline (10 ng/ml) and background expression were assessed by SDS-PAGE/western blotting. For each construct, at least five inducible clones were generated and tested. To avoid the possible loss of transgenes, cells were constantly cultured in selection media.

3.2.3 RNA interference (RNAi)

Transfection of small interfering (si) RNA oligonucleotides was performed using Lipofectamine^{TM} RNAiMax according to the manufacturer's instructions. The concentrations of Lipofectamine^{TM} RNAiMax and siRNAs were optimised for all cell lines prior to each experimental procedure. Single knockdowns were performed at a conc. of 20 nM and for double knockdowns (knocking down two

different targets at once) a total siRNA conc. of 40 nM was used, by combining 20 nM of each target siRNA. Silencing of target mRNAs was performed using either siGENOME pooled siRNA (Dharmacon) (containing four different siRNAs targeting the same mRNA), custom designed siRNA (Dharmacon) or Qiagen FlexiTube siRNA. The individual siGENOME siRNAs were characterised by Dharmacon using genome wide microarrays analyses identifying minimal off-target signatures (Parsons et al., 2009) and further characterised throughout the study by deconvolution. Knockdown efficiency was assessed by qPCR and/ or western blotting. RNAi experiments were controlled by using two non-specific siRNA controls, AllStars Negative Control siRNA (Qiagen) and Luciferase GL3 Duplex (Dharmacon), as well as untransfected cells. siRNA oligonucleotides used in this study are depicted in **Table 3-2**.

Table 3-2. siRNA oligonucleotide sequences used throughout the study.

Target gene	Target sequence	Manufacturer's ID
Non targeting (AllStars)	Not disclosed by Qiagen	Qiagen-SI03650318
Luciferase GL3 Duplex	CUUACGCUGAGUACUUCGA	Dharmacon-001400-01-20
BID_3	GCACCUACGUGAGGAGCUU	Dharmacon-004387-03
BID_18	GAGUAAGGGCACUGACGGA	Dharmacon-004387-18
BID_19	GCCAGAAGCUACUGCGAUG	Dharmacon-004387-19
BID_20	UGCAAUACAUACCACGCUA	Dharmacon-004387-20
~~DAPK2_1~~[#]	~~GAGGAGAGCUCUUCGAUUU~~	~~Dharmacon-004418-01~~
DAPK2_3	GGAAACGGCUCACAAUCCA	Dharmacon-004418-03
DAPK2_4	GGAAUUUGUUGCUCCAGAA	Dharmacon-004418-04
~~DAPK2_5~~[#]	~~GAGAUGGGCCCAAGGAAUU~~	~~Dharmacon-004418-05~~
DAPK23'UTR	GAGUGUGGACUUAGGAAAA	Dharmacon-custom
DAPK2 Qiagen 11	CAGCAUUCCCAAAGCTCUU	Qiagen-SI04988298
DAPK3_1	GAACAUUCCUGGAUUAAGG	Dharmacon-004947-01
DAPK3_2	CCACGCGUCUGAAGGAGUA	Dharmacon-004947-02
DAPK3_3	GAGCCAGGCCCGUAAGUUC	Dharmacon-004947-03
DAPK3_4	GAGGAGUACUUCAGCAACA	Dharmacon-004947-04
DR4_6	UGACAAUUCUGCUGAGAUG	Dharmacon-008090-06

DR4_15	CAACAAAACUGGACGGAAC	Dharmacon-008090-15
DR4_16	GAACAUAGCCCUUUGGGAG	Dharmacon-008090-16
DR4_17	CGGCAGAUUUGACAGGUGU	Dharmacon-008090-17
DR5_1	GGACAGAAGCUCACAACGA	Dharmacon-004448-01
DR5_2	UCAUGUAUCUAGAAGGUAA	Dharmacon-004448-02
DR5_3	ACACGAUGCUGAUAAAGUG	Dharmacon-004448-03
DR5_4	CAAGGUCGGUGAUUGUACA	Dharmacon-004448-04
NFKB1_1	GCAGGUAUUUGACAUAUUA	Dharmacon-003520-01
NFKB1_2	GCAAUAGCCUGCCAUGUUU	Dharmacon-003520-02
NFKB1_3	GAACCACGCCUCUAGAUAU	Dharmacon-003520-03
NFKB1_5	GGGCUACACCGAAGCAAUU	Dharmacon-003520-05
NFKB2_1	CCAAACAGUUCACCUAUUA	Dharmacon-003918-01
NFKB2_2	GGACGUGUCUGAUUCCAAA	Dharmacon-003918-02
NFKB2_3	GGUGAUGGAUCUGAGUAUA	Dharmacon-003918-03
NFKB2_18	GUAGACACGUACCGACAGA	Dharmacon-003918-18
RELA_3	GGAUUGAGGAGAAACGUAA	Dharmacon-003533-03
RELA_4	CUCAAGAUCUGCCGAGUGA	Dharmacon-003533-04
RELA_5	GGCUAUAACUCGCCUAGUG	Dharmacon-003533-05
RELA_18	GAUUGAGGAGAAACGUAAA	Dharmacon-003533-18
RELB_1	CAUCAGAGCUGCGGAUUUG	Dharmacon-004767-01
RELB_4	GCCCGUCUAUGACAAGAAA	Dharmacon-004767-04
RELB_5	GCACAGAUGAAUUGGAGAU	Dharmacon-004767-05
RELB_18	GUACCUGCCUCGCGACCAU	Dharmacon-004767-18

Excluded from the siRNA pool following deconvolution analysis due to off-target effects.

3.2.4 Protein extraction

Upon treatment according to the experimental procedures, cell culture plates were placed on ice. When assessing apoptotic processes, the supernatant containing dead cell bodies was transferred into separate tubes. Both the latter and cells that remained attached to the plate (live cells) were washed with ice-cold PBS and lysed using radioimmunoprecipitation assay (RIPA) buffer [50 mM Tris-HCL pH 7.4, 0.5% (v/v) NP-40, 150 mM NaCl, 1 mM EDTA, 1 mM Na_3VO_4 and ‘cOmplete and Mini, EDTA-free protease inhibitor cocktail’ (Hoffmann-La Roche), the latter used as instructed by the manufacturer]. Proteins isolated from

live and dead cells were combined, incubated on ice for 30 min and DNA was removed by centrifugation at 16.2 RCF for 20 min at 4 ˚C and transfer of protein lysate to new tubes. Protein concentrations were determined using a Bradford assay according to the manufacturer's instructions. In brief, this is a dye-binding assay based on a differential colour change of a dye in response to different concentrations of protein (Bradford, 1976). For long-term storage samples were frozen at -80 ˚C. To prepare samples for subsequent SDS-polyacrylamide gel electrophoresis (PAGE) protein concentrations were equalized and samples were re-suspended in Laemmli buffer [0.25 M Tris HCl, pH 6.8, 8% (w/v) SDS, 40% glycerol, 0.042% (w/v) bromophenol blue, 10% β-mercaptoethanol] and boiled at 95 ˚C for 5 min.

3.2.5 SDS-PAGE and western blotting

Sodium dodecyl sulphate polyacrylamide gel electrophoresis (SDS-PAGE) and western blotting were used to separate proteins according to their molecular weights. For that purpose 5% acrylamide stacking gels [5% (v/v) acrylamide, 0.125 M Tris, pH 6.8, 0.1% (w/v) SDS, 0.075% (w/v) ammonium persulphate (APS) and 0.083% (v/v) tetramethylethylenediamine (TEMED)] together with 6%, 10% or 12.5% acrylamide resolving gels [6%, 10%, 12.5% (v/v) acrylamide, 0.0375 M Tris pH 8.8, 0.1% (w/v) SDS, 0.06% (w/v) APS, 0.07% (v/v) TEMED] were set up. The latter depended on the molecular mass of proteins being analysed. Gels were run at 90 V in a Tris-glycine buffer [2.5 mM Tris, 0.2 M glycine and 0.1% (w/v) SDS]. Separated proteins were transferred onto nitrocellulose membranes using the Invitrogen iBlot®-system according to

manufacturer's instructions. To prevent non-specific antibody binding, membranes were blocked in 5% (w/v) bovine serum albumin (BSA)/ Tris-buffered saline/ Tween (TBST) [0.01 M Tris pH 7.4, 75 mM NaCl, 1.25 mM EDTA pH 8.0, 0.1% (v/v) Tween 20] containing 0.02% (v/v) sodium azide at room temperature for 1 to 2 h. Alternatively, depending on the antibodies, blocking was performed in 5% (w/v) milk powder/TBST. Primary antibodies were diluted in 5% (w/v) BSA/ TBST, containing 0.02% (v/v) sodium azide, according to manufacturer's instructions and incubated for either one h at room temperature, or o/n at 4 °C overnight. Before applying the secondary antibody, membranes were washed three times for 10 min in TBST. Secondary antibodies, conjugated to horseradish peroxidase (HRP), were diluted in 5% (w/v) milk powder/ TBST and incubated for one to two h at room temperature. Before detecting antibody binding by exposing to ECL reagent, membranes were washed at least six times for 5 min in TBST. If re-probing was necessary, antibodies were removed overnight using stripping buffer [2 M glycine pH 2.5, 0.1% (w/v) of SDS, 0.02% (w/v) sodium azide]. When phosphorylated proteins were assessed, phosphorylated forms were always probed first, followed by the total proteins. Western blots were analysed using the quantitative luminescence system FUSION Solo™. Images were analysed using Image Studio Lite software.

3.2.6 RNA extraction

Total RNA was isolated using the RNeasy® Mini kit according to the manufacturer's instructions. Briefly, cells were collected in 350 µl RLT lysis buffer and homogenized using the QIAshredder spin column. After adding ethanol, the

flow-through was run through an RNeasy spin column. RNA bound to the column was washed with 750 µl of RW1 buffer and twice with 500 µl RPE buffer. In the final step, RNA was eluted using RNase free water and RNA concentration was determined using the NanoDrop 1000 Spectrophotometer. If RNA was not isolated the day of lysis, cells were stored at -80 °C in RLT lysis buffer until RNA was extracted.

3.2.7 Quantitative polymerase chain reaction (qPCR)

Gene expression analysis was done by quantitative two-step reverse transcription PCR. Reverse transcription was performed using total RNA and the High-Capacity cDNA Reverse Transcription kit, using random hexamers. qPCR was done using the Fast SYBR® Green Master Mix with specific primer pairs (**Table 3-3**). For each target mRNA analysed, 2.5 µl of Fast SYBR® Green Master Mix, 0.5 µM of each primer pair and 2 µl of cDNA in deionised water (5 ng/µl) were mixed in 384-well plates in duplicates using Matrix™ Equalizer Electronic Multichannel Pipetters. qPCR was carried out on an ABI PRISM 7900HT using the following settings: initial activation of 20 sec at 95 ˚C, 40 cycles; denaturation for 1 min at 95 ˚C; annealling/ extension for 20 sec at 60 ˚C; final melting curve was carried out for 15 sec at 95 ˚C and then 15 sec at 60 ˚C. Quantification of target messages was performed using qbase+ software. HPRT and GAPDH were the reference genes used for normalisation.

Table 3-3. Oligonucleotide qPCR primer pair sequences used throughout this study.

Oligonucleotide Name	Oligonucleotide sequence (5' → 3')	Published source
BID fwd	TCCACACATGAATCTGCACATC	
BID rev	GGGAACCTGCACAGTGGAA	
c-FLIP fwd	TCTCACAGCTCACCATCCCTG	(Zhang et al., 2004)
c-FLIP rev	CAGGAGTGGGCGTTTTCTTTC	
c-JUN fwd	TCCAAGTGCCGAAAAAGGAAG	
c-JUN rev	CGAGTTCTGAGCTTTCAAGGT	
COX2 fwd	CGGTGAAACTCTGGCTAGACAG	(Mologni et al., 2012)
COX2 rev	GCAAACCGTAGATGCTCAGGGA	
cREL fwd	AGTTGCGGAGACCTTCTGACCA	
cREL rev	CGTGATCCTGGCACAGTTTCTG	
DAPK2 fwd	TCCTGGATGGGGTGAACTAC	
DAPK2 rev	CAGCTTGATGTGTGGAATGG	
DcR1 fwd	TCCCCAAGACCCTAAAGTTCG	
DcR1 rev	CAGTGGTGGCAGAGTAAGC	
DcR2 fwd	TACCACGACCAGAGACACC	(Cui et al., 2011)
DcR2 rev	CACCCTGTTCTACACGTCCG	
DcR3 fwd	TGCAGAAGATGTAGATTGTGTGATGA	
DcR3 rev	GGGTCCGGGTGCAGTTTATT	
DR4 fwd	CATCGGCTCAGGTTGTGGA	(Galligan et al., 2005)
DR4 rev	TGCCGGTCCCAGCAGACA	
DR5 fwd	GCACTCACTGGAATGACCTC	(Pellerito et al., 2010)
DR5 rev	GCCTTCTTCGCACTGACAC	
FasR fwd	GTACGCGGAGTGGCAGAAA	
FasR rev	CAGAGGACGTTGCAGTAGC	
GAPDH fwd	AGCCACATCGCTCAGACAC	
GAPDH rev	GCCCAATACGACCAAATCC	
HPRT fwd	TGACCTTGATTTATTTTGCATACC	
HPRT rev	CGAGCAAGACGTTCAGTCCT	
KEAP1 fwd	CAGATTGGCTGTGTGGAGTT	
KEAP1 rev	GCTGTTCGCAGTCGTACTTG	
NF-κB1 fwd	GCAGCACTACTTCTTGACCACC	
NF-κB1 rev	TCTGCTCCTGAGCATTGACGTC	
NF-κB2 fwd	GGCAGACCAGTGTCATTGAGCA	
NF-κB2 rev	CAGCAGAAAGCTCACCACACTC	
NRF2 fwd	GAGAGCCCAGTCTTCATTGC	(Lister et al., 2011)
NRF2 rev	TTGGCTTCTGGACTTGGAAC	
OPG fwd	TCCTGGGTGGTCCACTTAAT	
OPG rev	CTCCAAGCCCCTGAGGTT	
p21 fwd	TGAGCCGCGACTGTGATG	(Chen et al., 2013)
p21 rev	GTCTCGGTGACAAAGTCGAAGTT	
p53 fwd	TAACAGTTCCTGCATGGGCGGC	(Chew et al., 2012)

p53 rev	AGGACAGGCACAAACACGCACC	
RELA fwd	CCAGGTTCTGGAAACTGTGGAT	(Higai et al., 2006)
RELA rev	CCCCACGAGCTTGTAGGAAAG	
RELB fwd	TGTGGTGAGGATCTGCTTCCAG	
RELB rev	TCGGCAAATCCGCAGCTCTGAT	
RIPK1 fwd	TATCCCAGTGCCTGAGACCAAC	
RIPK1 rev	GTAGGCTCCAATCTGAATGCCAG	
RIPK2 fwd	AGACCACTCCATGCTCTTCAGC	
RIPK2 rev	GATCCACTGCTGGGCTATACCA	
SOD1 fwd	AGGGCATCATCAATTTCGAG	
SOD1 rev	TGCCTCTCTTCATCCTTTGG	
SOD2 fwd	CGACCTGCCCTACGACTACG	
SOD2 rev	TGACCACCACCATTGAACTT	
TNFR1 fwd	TCACCGCTTCAGAAAACCACC	
TNFR1 rev	GGTCCACTGTGCAAGAAGAGA	
TNFR2 fwd	CGGGCCAACATGCAAAAGTC	
TNFR2 rev	CAGATGCGGTTCTGTTCCC	
TNF-α fwd	TCTTCTCGAACCCCGAGTGA	(Giulietti et al., 2001)
TNF-α rev	CCTCTGATGGCACCACCAG	
TRAIL fwd	AAGACTGTCAGCTTCCAAACATTAA	(Giulietti et al., 2001)
TRAIL rev	GTGATACACTACTTGAGAGATGGAT	

3.2.8 mRNA and protein stability assays

Cells were transfected with siRNA oligonucleotides as described before. Forty-eight h after transfection cells were treated with 5 µg/ ml actinomycin D for 1 - 4 h. Subsequently, RNA was isolated using an RNeasy® kit following the manufacturer's instructions. Gene expression analysis was performed by qPCR as described before, using HPRT and GAPDH as housekeeping genes. For protein stability, cells were incubated with cycloheximide (CHX) (1 µg/mL) for 2, 4 or 6 h and protein measured by SDS-PAGE/western blotting using the FUSION Solo™ quantitative luminescence system and normalised to the housekeeping gene HSP90.

3.2.9 Flow cytometry

3.2.9.1 Detection of surface molecules

Cells were cultured and transfected with siRNA as described earlier. Forty-eight h later, cells were washed thoroughly with PBS and any leftover media and cellular debris were aspirated. Next, cells were incubated with trypsin to detach the adherent cells. Soft beating and incubation at 37 °C eased cell detaching. Upon blocking the trypsin with FCS-containing Full-DMEM and a washing step with PBS, cells were incubated with anti-DR4-FITC, anti-DR5-PE or anti-FAS-PE for 1 h at 4 ˚C, washed five times with cold PBS and fixed with PBS containing 1% (w/v) p-FA. Cells were analysed using a FACS Canto and data was analysed with FlowJo Version 8.8.7. Geometric means were used for the analyses essentially as described earlier (Hajdu, 2011).

3.2.9.2 Detection of oxidative stress and mitochondrial superoxides

Cells were cultured and transfected with siRNA as described before, or treated with 0.5 mM H_2O_2 for 24 h, which was used as a positive control for ROS production. For the detection of general ROS using 5-(and-6)-chloromethyl-2',7'-dichlorodihydrofluorescein diacetate, acetyl ester (CM-H2DCFDA) (Molecular Probes®) (referred throughout the text as DCFDA) cells were incubated with 10 µM CM-H2DCFDA dissolved in pre-warmed PBS for 30 min at 37 ˚C. Next, cells were trypsinised, re-suspended in Full-DMEM, washed twice with PBS and analysed by flow cytometry. Cellular superoxides were detected using dihydroethidium (DHE) (Molecular Probes®). Therefore, 48 h after transfection, cells were trypsinised, re-suspended in Full-DMEM, washed twice with PBS and

incubated in 10 µM DHE dissolved in pre-warmed PBS for 15 min, washed twice with pre-warmed PBS and analysed by flow cytometry.

For the detection of mitochondrial superoxides, MitoSOX™ Red mitochondrial superoxide indicator (Molecular Probes®) was used. Briefly, cells were transfected as described earlier, or they were treated for 24 h with 1 mM 1-Methyl-4-phenylpyridinium iodide (MPP^+), or with 0.5 mM H_2O_2, which were used as positive controls. Forty-eight h later, cells were washed with PBS and incubated for 10 min at 37 ˚C in the dark with 5 µM MitoSOX™ Red reagent diluted in pre-warmed PBS. Samples were subsequently washed twice with PBS before being analysed. Depolarised mitochondria were studied using the MitoProbe™ JC-1 Assay Kit (Molecular Probes®) according to the manufacturer's instructions. Briefly, 48 h after transfection, cells were trypsinised, re-suspended in Full-DMEM, washed twice with PBS and incubated in two µM 5',6,6'-tetrachloro-1,1',3,3'-tetraethylbenzimidazolylcarbocyanine iodide (JC-1) dissolved in pre-warmed PBS at 37 °C, 10% CO2, for 15 min and analysed by flow cytometry. To induce complete mitochondrial depolarisation the protonophore, carbonyl cyanide m-chlorophenyl hydrazone (CCCP) (50 mM) was used for 5 min previous to JC-1 incubation. Cells were analysed by flow cytometry.

All flow cytometry analyses were performed using a FACS Canto and data mining was done using FlowJo version 8.8.7. Fluorescence geometric means were used for the analyses and samples were normalised to siNS-transfected control cells, essentially as described earlier (Hajdu, 2011).

3.2.9.3 Cell cycle analysis using propidium iodide (PI)

Cells were cultured and transfected with siRNA as described before. To assess the effect of TRAIL treatment on DNA hypoploidy, cells were treated with TRAIL (100 ng/ml) for six h. PI staining was carried out as follows; Cell corpses and cellular debris were removed and washed with pre-warmed PBS. Remaining cells were washed thoroughly with pre-warmed PBS and trypsinised. Detached cells were re-suspended in Full-DMEM, washed with pre-warmed PBS and after combination with cell corpses/debris, they were fixed with ice cold 70% (v/v) ethanol for 30 min. After two additional washing steps, cells were incubated with Ribonuclease A (20 µg/ml) and stained with PI (50 µg/ml) for 15 min in the dark. Cells were analysed using a FACS Canto and data was analysed with FlowJo Version 8.8.7.

3.2.10 Metabolic assays

3.2.10.1 Analysis of OCR and EACR using a Seahorse XF96 analyser

Seahorse XF96 analyser was used to measure the oxygen consumption rate (OCR) and the extracellular acidification rate (ECAR) under basal conditions, as recommended by the manufacturer. A cell titration assay was used in order to determine a suitable cell seeding density for both A549 and U2OS cells. For the experiment, $0.5x10^6$ cells were plated per 10 cm dish and reverse transfected with targeted siRNAs and controls on day one as detailed earlier. Forty-eight h post-transfection, cells were re-plated into the XF96 microplates at a density of $4x10^4$ cells/well (100 µl/well) in Full-DMEM and cultured overnight. In addition, the XF calibrant solution was added into the XF sensor cartridge and incubated

at 37 °C with no CO_2 overnight. The next day, growth media was replaced with XF Assay Medium Modified DMEM (1000 µg/ml glucose, pH~ 7.4) and incubated at 37 °C without CO_2 for one h prior to the assay. Analyses were performed according to the manufacturer's instructions, using the eight measurements the instrument recorded for OCR (nmoles/min) and ECAR (mpH/min) pertaining to each well. Results were obtained using the XF^e Wave software.

3.2.10.2 Glutathione (GSH) colorimetric assay

Cells were cultured and transfected as described earlier. As controls, cells were treated for 48 h with either 50 µM ethacrynic acid (EA) or 40 µM buthionine sulphoximine (BSO). Cell lysates were collected and sonicated in 50 mM PBS and 1 mM EDTA. The concentrations were determined using a Bradford assay according to the manufacturer's instructions and subsequently normalised to 1 µg/µl of protein. GSH levels in each sample were quantified using the Glutathione Assay Kit essentially as recommended in the manufacturer's protocol.

3.2.10.3 NADH/NADPH colorimetric assay

Cells were plated and transfected as previously described. As positive control, cells were treated for 24 h with 1 mM MPP^+. Forty-eight h after transfection $NADP^+$/NADPH levels for each sample were quantified using the $NADP^+$/NADPH assay kit and NAD^+/NADH levels using the NAD^+/NADH assay kit according to the manufacturer's protocols.

3.2.11 Molecular cloning and plasmid propagation

Molecular cloning was performed as follows. Vector and insert were cut using restriction enzymes under conditions according to the manufacturer's protocol. Digested DNA was run on an agarose gel, cut out of the gel, purified using the MinElute® PCR Purification Kit and DNA concentration was quantified using the NanoDrop 1000 Spectrophotometer. The ligation reaction was set up as follows by mixing, the linearised vector (50 - 400 ng), insert DNA (1:1 to 3:1 molar ratio of insert DNA to vector DNA), ligation buffer, T4 DNA Ligase and nuclease free water according to the manufacturer's instructions. Ligation mixtures were incubated at room temperature for one h. After ligation the samples were mixed with One Shot® TOP10 Chemically Competent *Escherichia coli (E. coli)* and incubated on ice for 10 min. Next, a heat shock was performed at 42 °C for exactly 30 sec followed by another incubation step of 10 min on ice. In the next step, the ligation mix was incubated in 250 µl of pre-warmed Super Optimal broth with Catabolite (SOC) (Hanahan, 1983) repression medium for one h at 37 ˚C on a thermal shaker. Then, cell suspension was spread on lysogeny broth (LB) (Bertani, 1951) agar plates supplemented with 100 µg/ml ampicillin or 50 µg/ml kanamycin (depending on the bacterial resistance marker) and allowed to grow o/n at 37 ˚C. Positive clones were picked and cultured in LB media, containing the appropriate antibiotics, for at least six h at 37 ˚C. DNA was isolated using the QIAprep® Spin Miniprep Kit and subjected to control digests and sequencing. Positive clones were further cultured in a larger volume of LB media containing the appropriate antibiotics. DNA was isolated using the PureLink® HiPure Plasmid Midiprep Kit and used for the experimental procedures described in this study. Glycerol stocks were prepared by mixing LB media containing the

respective plasmid carrying *E. coli* with an equal amount of glycerol and freezing the mix at -80 °C. Plasmids were propagated equal to the above mentioned protocol starting with the heat shock.

3.2.12 Transient transfection of plasmids

Plasmids were transfected using Attractene Transfection Reagent according to the manufacturer's instructions. Briefly, cells were plated at density of $4x10^5$ in 6-well plates transfected with 1.2 µg of plasmid DNA or empty vector control. Protein expression was analysed by quantitative western blotting.

3.2.13 Cotransfection of siRNA and plasmid DNA

Cotransfection was performed using Attractene Reagent. Briefly, cells were plated at a density of $4x10^5$ in 6-well plates and co-transfected with either 40 nM AllStars negative control siRNA, or 40 nM siDAPK2 and 1.2 µg DNA of empty vector control or pcDNA3 FLAG-BCL-X_L plasmid. Protein expression was analysed by quantitative western blotting and cell death in response to TRAIL by using crystal violet assays.

3.2.14 Plasmids used in this study

DAPK2 pcDNA3 plasmids containing N-terminal human influenza hemaglutinin (HA) tagged DAPK2 were kindly provided by Professor Adi Kimchi (Weizmann Institute of Science, Rehovot, Israel). Five constructs were received and used in

this study including the HA-DAPK2 wild-type (wt) and HA-DAPK2 K42A, (K42 → A42) (kinase dead). Further information about these constructs can be found in **Table 3-4**. For the generation of tetracycline inducible cell lines each of these constructs was sub-cloned into a pcDNA™4/TO vector using BamHI and XhOI restriction sites. The DR5 full-length promoter pGL3 construct and DR5 promoter-intron wild-type (wt) and NF-κB mutated (mt) pGL3 constructs were kindly provided by Professor Spencer Gibson (University of Manitoba, Canada). pNF-κB-Luc reporter vector was from Clontech (Mountain View, CA, USA). The pRL Renilla Luciferase Control Reporter Vector was from Promega. The N-terminal FLAG tagged BCL-X_L pcDNA3 expression plasmid was a gift from Dr Ingram Iaccarino (Institute of Human Genetics, University Hospital Schleswig-Holstein, Kiel, Germany) an overview of all plasmids can be found in **Table 3-4**.

Table 3-4. Plasmids used throughout this study.

Backbone	Insert	Origin	Citation
pcDNA3	HA-DAPK2 wild-type	Prof Adi Kimchi	(Inbal et al., 2000)
pcDNA3	HA-DAPK2 K42A	See above	See above
pcDNA™4/TO	HA-DAPK2 wt	Sub-cloned from pcDNA3 using BamHI and XhOI restriction sites.	
pcDNA™4/TO	HA-DAPK2 K42A	See above	
pGL3	DR5 full-length promoter	Prof Spencer Gibson	(Shetty et al., 2002)
pGL3	DR5 promoter-intron wild-type	See above	See above
pGL3	DR5 promoter-intron NF-κB mutated	See above	See above
pRL	Renilla Luciferase Control Reporter Vector	Promega	
pNF-κB-Luc	pNF-κB-Luc	Clontech	
pcDNA3	FLAG-BCL-X_L	Dr Ingram Iaccarino	
pcDNA3	empty	Invitrogen (now Life Technologies)	
pcDNA™4/TO	empty	See above	

3.2.15 Luciferase Assays

Cells were transfected with siRNA oligonucleotides as described earlier. Twenty-four h later, cells were co-transfected with 100 ng of pNF-κB-Luc, DR5 full length promoter *Firefly*-luciferase pGL3, DR5 promoter-intron wild-type (wt) Firefly-luciferase pGL3, or DR5 promoter-intron NF-κB mutated (mt) *Firefly*-luciferase pGL3 constructs and 10 ng of *CMV* promoter *Renilla*-luciferase

pRL construct using Attractene Transfection Reagent. The day after, both *Firefly*- and *Renilla*-luciferase activities were quantified using the Dual-Glo® Luciferase Assay System according to the manufacturer's instructions. Luminescence was detected using a PHERAstar *Plus* plate reader. The measured luminescence for *Firefly* luciferase activity was normalised to that of *Renilla* luciferase.

3.2.16 Crystal violet cell survival assay

Crystal violet is a dye that stains cellular proteins and DNA (Bonnekoh et al., 1989, Yang et al., 2001, Lu et al., 2009). Here, it was used to quantify cell survival, thus to discriminate between detached (dead) and attached cells (presumably alive) quantifying the number of life cells on the cell culture plate. For cell survival assays, cells were transfected as described earlier and 24 h later re-plated into 96-well plates at a density of $2x10^4$ cells per well. The following day cells were treated with TRAIL, TNF-α, FAS-IgM, cisplatin or H_2O_2 for 24 h. Cells were then fixed using methanol and stained as follows: Cells were washed in PBS, and fixed and stained with 100 µl per well 0.5% (w/v) crystal violet in 25% (v/v) methanol for 30 min. The plates were then thoroughly washed with water, dried o/n and the dried dye dissolved in 10% (v/v) acetic acid for 30 min by incubating on a horizontal shaker. In the next step crystal violet stain was quantified by measuring the absorbance at 595 nm using a Sunrise^{TM} microplate absorbance reader. Values were normalised to the untreated samples and each experiment was performed in triplicates.

4. Depletion of DAPK2 sensitises tumour cells to TRAIL-induced apoptosis

4.1 Introduction

Despite the effort and resources invested in cancer research, cancer remains a serious public health problem. Most patients are treated surgically and/or with combinations of a systemic treatment with chemotherapeutic drugs, antibodies and small molecule inhibitors. The big disadvantage of systemic tumour therapy is that most treatments affect the body as a whole and do not target the tumorigenic cells and tissues specifically. Further, although patients generally respond well to the various types of tumour therapy, they frequently develop resistance to it. This poses a challenge to their treatment and calls for more tumour specific and alternative approaches to be developed. Indeed, much excitement was generated in the mid nineties when TRAIL was identified (Wiley et al., 1995, Pitti et al., 1996, Sanchez-Perez et al., 2002, Kirienko et al., 2010). In contrast to chemotherapeutic and small molecule-based strategies, TRAIL-based therapies directly and specifically targeted cancer cells with relatively weak side effects. However, the use of TRAIL itself, or TRAIL agonistic antibodies, in experimental tumour therapy has been frequently confronted with the development of resistance to TRAIL-based treatments that often arises during the course of therapy (Mellier et al., 2010). Here, we report a novel approach to overcome resistance to TRAIL-mediated cell death, based on the depletion of death associated protein kinase (DAPK) 2 by siRNAs. Silencing DAPK2 resulted in re-sensitisation of resistant cancer cells to TRAIL.

TRAIL is a death receptor (DR) ligand that signals through DR4 and DR5, two members of the TNF receptor family [(Sawyers, 2004, Strachan et al., 1999),

reviewed in (Gonzalvez and Ashkenazi, 2010)]. DR5 has two isoforms that differ by 29 amino acids and which are functionally indistinguishable (Sawyers, 2004, Screaton et al., 1997). TRAIL binding activates primarily the extrinsic apoptotic pathway (**Figure 1-4**). The formation of ligand/receptor complexes leads to the assembly of a multi-protein DISC, which in the case of TRAIL is typically composed of FADD, the initiator caspases, caspase-8 and caspase-10 and/or c-FLIP. The initiator caspases subsequently proteolytically cleave effector caspases, such as caspase-3, caspase-6 and/or caspase-7 thereby activating them. This leads to the destruction of key cellular components such as the cytoskeleton, nucleus and DNA, and the appearance of typical features of apoptosis such as membrane blebbing and nuclear shrinkage. TRAIL can also activate intrinsic apoptotic pathways *via* BID and thus involve mitochondria (**Figure 1-4**). By virtue of preferentially killing tumour cells, TRAIL is seen by many as a 'magic bullet' against cancer cells. Some cancer cells, however, are resistant, or develop resistance, to TRAIL-induced apoptosis. Several resistance mechanisms have been described but do not account for all cases of resistance [reviewed in (Mellier et al., 2010) and (van Dijk et al., 2013)], suggesting that additional but yet unidentified mechanisms exist. Deregulation at the receptor, DISC and mitochondria level have all been described, and the involvement of MAPKs and PARP1 have also been suggested (Azijli et al., 2013, Yuan et al., 2013). Here we show that DAPK2 can be used as a target to overcome resistance to TRAIL-induced apoptosis.

DAPK2 (also known as DRP-1) belongs to the DAPK family, which comprises a number of proteins regulated by calcium (Ca^{2+})/calmodulin (CaM) that are

involved in death-inducing pathways. The three main members (DAPK1, DAPK2 and DAPK3) share a high degree of homology in the kinase domain but vary greatly outside this key region (**Figure 1-9**, described in detail in **1.8**). The most studied protein is the founder molecule DAPK1, which has been implicated in Interferon-γ, FAS ligand, TNF-α and ceramide-induced cell death, amongst others [reviewed in (Bialik and Kimchi, 2006)]. The gene is often methylated in tumour cells and is thought to be a tumour suppressor (Raval et al., 2007). DAPK3 (also known as ZIPK) lacks the Ca^{2+}/CaM regulatory domain, is characterised by a nuclear localisation signal (NLS) and has been described as a tumour suppressor and to be involved in cardiovascular pathologies [reviewed in (Usui et al., 2014)]. DAPK2 is a much smaller protein than DAPK1 (42 *versus* 120 kDa); it lacks ankyrin repeats, and, critically, the death domain (**Figure 1-9**). Evidence for a pro-apoptotic role is largely based on its ability to induce apoptosis-like cell morphology upon overexpression (Puente et al., 2006, Inbal et al., 2000, Breasted and New-York Historical Society. Library., 1930). Moreover, siRNA mediated depletion of DAPK1 has recently been shown to re-sensitise TRAIL-resistant endometrial carcinoma cells to TRAIL-induced apoptosis suggesting in some circumstances an anti-apoptotic role of DAPK1 (Bai et al., 2010). We thus hypothesized that endogenous DAPK2 may under some circumstances have anti-apoptotic properties and provide cancer cells with pro-survival cues.

4.2 Results

4.2.1 DAPK2 depletion sensitises resistant cells to TRAIL-induced apoptosis

The DAPK2 molecule lacks a recognisable death motif. We, therefore, asked what the contribution of endogenous DAPK2 to cell death induced by different apoptotic triggers was. For these studies, we used U2OS osteosarcoma cells and A549 NSCLC cells, two cell lines with different mutational backgrounds that have been extensively characterised in our laboratory (Shiloh et al., 2013, Watling et al., 2008). Both osteosarcoma and NSCLC are solid tumours that have been described to frequently develop resistance to TRAIL-based treatments (Locklin et al., 2007, Voortman et al., 2007) and indeed, the two model cell lines used here, U2OS and A549, have been previously reported to be resistant to TRAIL-mediated apoptosis (Mirandola et al., 2006, Zhuang et al., 2010).

RNAi was used to modulate the levels of DAPK2 in U2OS and A549 cells. Although most experiments described in this Thesis used a pool of siRNAs, the specificity of each individual siRNA oligonucleotide was analysed meticulously. Molecules targeting different regions of DAPK2, efficiently reduced DAPK2 protein levels without affecting protein levels of DAPK1 and DAPK3 (**Figure 4-1a, b, c,** note: knockdown of DAPK3 in U2OS better visible in **a,** but siDAPK2 Dharmacon_5 was not loaded). Of note, U2OS lysates did not contain detectable levels of DAPK1 protein when compared to A549 cell lysates loaded on the same gel (**Figure 4-1a** + **b)**. Using qPCR we further established that DAPK1 cDNA was only amplified after more then 30 PCR cycles, indicating very low, to non-detectable mRNA expression levels of DAPK1 in U2OS cells. Evaluating the

effect of DAPK2 depletion on DAPK3 was not trivial as the polyclonal DAPK3/ZIPK (279-298) antibody (Calbiochem) detects multiple bands and siRNA-mediated knockdown of DAPK3 was not as efficient as siRNA-mediated depletion of DAPK1 and DAPK2. However, a DAPK3 specific band was identified by knocking down DAPK3 itself and it could be seen in all blots on **Figure 4-1** (can be easiest detected in **Figure 4-1a**, disappears in the 10th lane, siDAPK3).

Off-target effects associated with oligonucleotides 1 and 5 were, however, observed. These were thus excluded from our analyses and a pool containing only oligonucleotides 3 and 4 were used throughout the study (henceforth referred to as siDAPK2). To further validate the effect of DAPK2 depletion we purchased a custom made Dharmacon DAPK2 siRNA oligonucleotide that specifically targeted the DAPK2 3'UTR as well as a DAPK2 siRNA from an alternative supplier (QIAGEN) (Hs_DAPK2_11 FlexiTube siRNA) also targeting the DAPK2 3'UTR. This supplier uses an algorithm completely different from the one used by Dharmacon to select its sequences. Reassuringly, this siRNA yielded results identical to those shown by the other siRNAs. Both of the 3'UTR targeting siRNAs were specific to DAPK2 and did not target DAPK1 or DAPK3 (**Figure 4-1a, b, c**). Cells transfected with a non-targeting siRNA pool (siNS) were used as controls in all experiments presented in this Thesis and that involved RNAi.

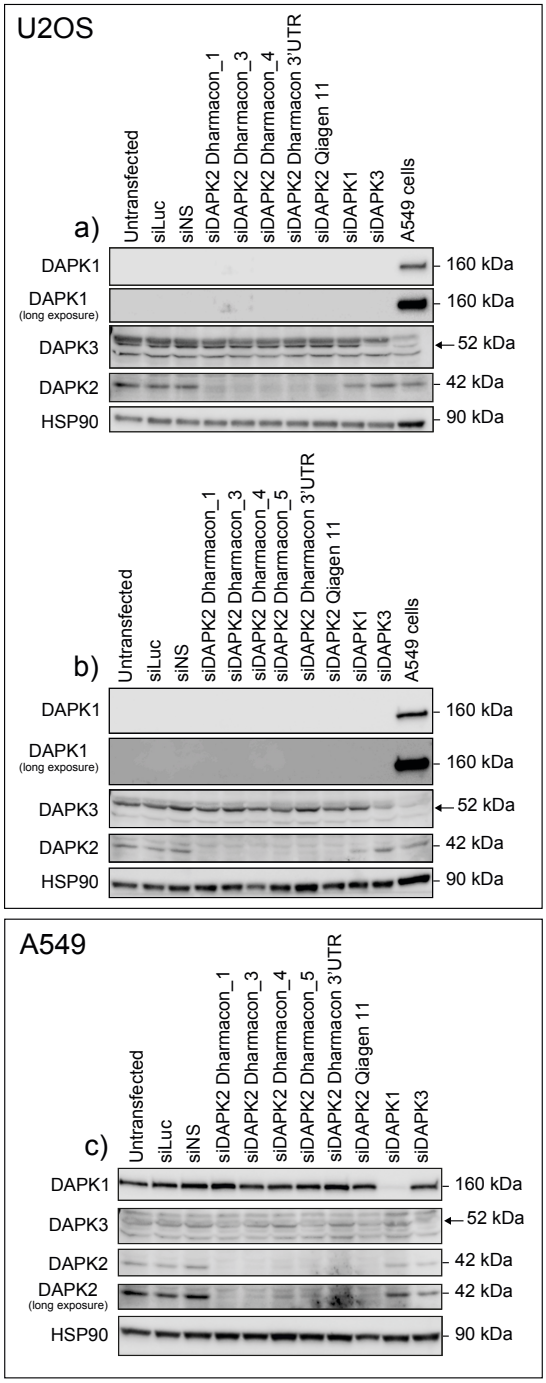

Figure 4-1. Deconvolution of DAPK2 siRNAs used in this study and their effect on other members of the DAPK family.

U2OS (**a** + **b**) or A549 (**c**) cells were left untransfected or were transfected with non-targeting siLuc, siNS, different DAPK2 siRNA oligonucleotides, siDAPK1 or siDAPK3 as indicated in the figure. Forty-eight h after transfection effects of each individual oligonucleotide, effects on DAPK1, DAPK2 and DAPK3 protein levels were assessed by SDS-PAGE/western blotting. U2OS cells (**a** + **b**) did not express detectable amounts of DAPK1 protein, lysates of untransfected A549 cells with equal amount of protein were loaded as control. HSP90 served as loading control. Data is representative of two independent repeats.

To assess the contribution of endogenous DAPK2 to cell death induced by different apoptotic triggers, the siDAPK2 pool (consisting of oligonucleotide 3* and 4*, henceforth referred to as siDAPK2) was used to deplete endogenous levels of DAPK2. As shown in **Figure 4-2**, in contrast to the non-targeting siRNA pool (siNS), siDAPK2 efficiently downregulated DAPK2 mRNA and protein levels in U2OS (**Figure 4-2a**) and A549 (**Figure 4-2f**) cells. To study cell death, cells were transfected with either siNS or siDAPK2, 24 h later re-plated into 96 well plates and the next day challenged with TRAIL (**Figure 4-2b** and **g**), cisplatin (**Figure 4-2c** and **h**), hydrogen peroxide (H_2O_2) (**Figure 4-2d** and **i**) and TNF-α (**Figure 4-2e** and **j**) for 24 h. Cell death levels were assessed using crystal violet viability assays. Crystal violet is a dye that stains cellular proteins and DNA (Bonnekoh et al., 1989, Yang et al., 2001, Lu et al., 2009) and it can be used to measure cell survival by discriminating between detached (dead) and attached cells (presumably alive) in cell culture plates. The susceptibility of cells with near to none DAPK2 expression was compared to that of control cells (siNS). Data from three independent experiments (each with technical triplicates) is shown as the mean percentage of live cells ± standard error of the mean (SEM) (**Figure 4-2**). U2OS were readily killed by cisplatin (**Figure 4-2c**) and oxidative stress (**Figure 4-2d**), which was not dependent on DAPK2. A549 were less susceptible than U2OS to the killing effects of cisplatin (**Figure 4-2h**), or H_2O_2 (**Figure 4-2i**) but, as for U2OS cells, the induction of apoptosis was also independent of DAPK2 expression levels. As reported previously, U2OS and A549 were resistant to DR-mediated cell death induced by TRAIL (**Figure 4-2b** and **g**, black bars) or TNF-α (**Figure 4-2e** and **j**, black bars). Both cell types could not be sensitized to TNF-α-induced death by silencing DAPK2 (**Figure 4-2e** and **j**, green

bars). In contrast, reducing the levels of DAPK2 significantly sensitised U2OS and A549 cells to TRAIL-induced cell death (**Figure 4-2**b and g, green bars), suggesting that DAPK2 potentially functioned as an inhibitory molecule that modulated TRAIL signalling.

The effect of DAPK2 depletion on sensitisation to TRAIL-induced apoptosis was further validated using a different cell death assay, which involved quantifying DNA hypoploidy (**Figure 4-3**). U2OS and A549 were transfected with either siDAPK2 or siNS and 48 h post-transfection challenged with TRAIL for 6 h. As for the crystal violet viability assays, DNA hypoploidy measurement with propidium iodide (PI) showed significant killing in DAPK2-depleted cells (**Figure 4-3c** + **d** and **h** + **i**) compared to cells transfected with the non-targeting control siRNA (**Figure 4-3a** + **b** and **f** + **g**). Cell cycle profiles are graphically summarised in bar charts (**Figure 4-3e** and **j**).

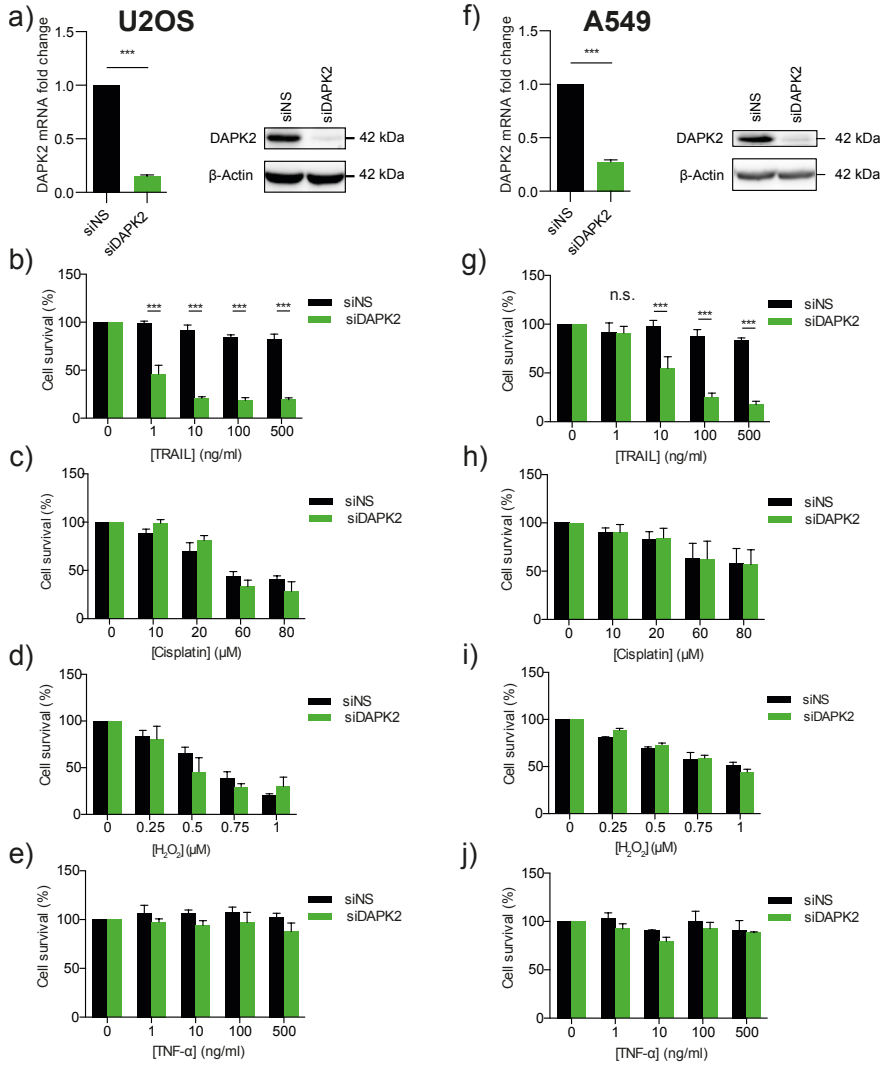

Figure 4-2. Knockdown of DAPK2 sensitises U2OS and A549 cells to TRAIL-induced cell death.

U2OS (**a - e**) and A549 (**f - j**) cells were transfected with either siNS, or DAPK2 siRNA. Forty-eight h after transfection knockdown efficiency was determined by SDS-PAGE/western blotting and qPCR (**a** + **f**). Data represent mean ± SEM of three independent experiments. Statistical analyses were done using Student's t-test (paired, one tailed) (*** p< 0.005). For cell survival assays (U2OS, **b - e** and A549, **g - j**), cells were re-plated into 96 well plates at a density of $2x10^4$ cells per well 24 h after siRNA transfection. The following day cells were treated with the indicated concentrations of TRAIL (**b** + **g**), cisplatin (**c** + **h**), H_2O_2 (**d** + **i**) and TNF-α (**e** + **j**) for 24 h. Cells were then fixed using methanol and stained with crystal violet. Crystals were dissolved in 10% (v/v) acetic acid and quantified by measuring the absorbance at 595 nm. Values were normalised to the untreated samples. Data represent mean ± SEM of three independent experiments performed in triplicates. Statistical analyses were done using two-way ANOVA test (*** p< 0.005).

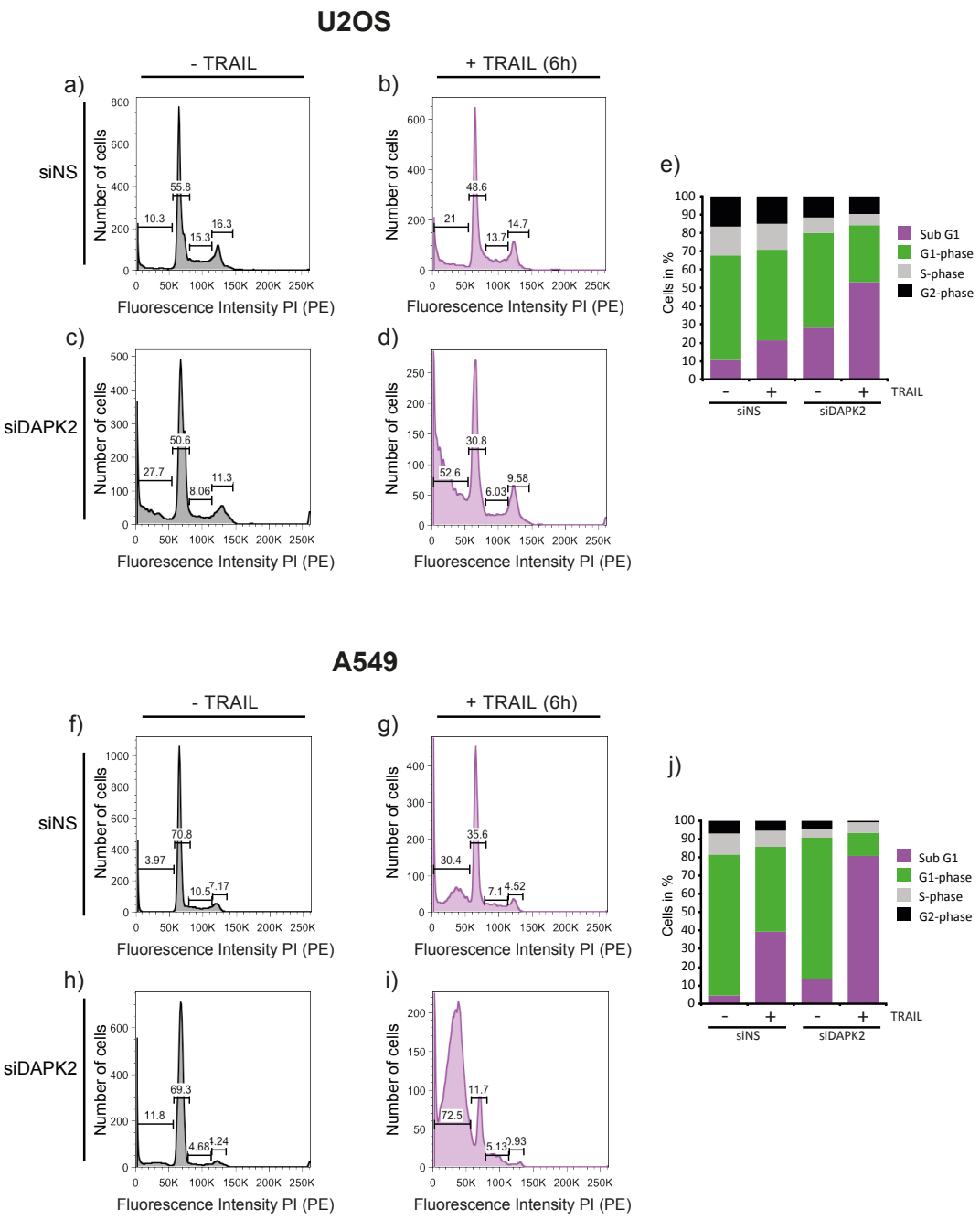

Figure 4-3. Silencing DAPK2 sensitises TRAIL resistant cancer cell lines to TRAIL-induced cell death.

U2OS and A549 cells were transfected with either siNS, or siDAPK2. Forty-eight h after transfection U2OS (**a - e**) and A549 (**f - j**) cells were treated with TRAIL (100 ng/ml) for 6 h. Cells were then fixed with ethanol, incubated with RNase A and PI. Cell sub-populations were analysed using FlowJo software. Representative cell cycle profiles of three independent experiments are shown in histograms (**1 - d** and **f - i**) and summarised graphically in bar charts (**e** + **j**). Data is representative of two independent repeats.

4.2.2 The effect of sensitisation to TRAIL upon DAPK2 depletion was validated by deconvoluting the siRNA pools and by using additional siRNAs

The experiments demonstrating a sensitisation of U2OS and A549 cells to TRAIL-induced apoptosis upon DAPK2 depletion were carried out using a pool of siGENOME DAPK2 oligonucleotides 3 and 4 (siDAPK2), as validation experiments demonstrated that siDAPK2 oligonucleotides 1 and 5 had off-target effects. To further validate these findings and exclude any additional potential off-target effects still unidentified, sensitisation experiments described in **Figure 4-2** were repeated using the individual siDAPK2 oligonucleotides 3 and 4, a custom made 3'UTR-specific DAPK2 siRNA from Dharmacon and another one from QIAGEN (Hs_DAPK2_11 FlexiTube). Cells were transfected with either siNS or single siDAPK2 oligonucleotides, 24 h later re-plated into 96 well plates and the next day, challenged with TRAIL. Cell death levels were assessed using crystal violet cell viability assays. The susceptibility of DAPK2-depleted cells was compared to that of siNS-transfected cells. Data from three independent experiments (each with three technical replicates) are shown as the mean percentage of live cells ± SEM (**Figure 4-4**). As demonstrated earlier, U2OS and A549 were resistant to DR-mediated cell death induced by TRAIL when transfected with siNS. (**Figure 4-4a - j**, black bars). Consistent with the results obtained using the siDAPK2 pool, U2OS and A549 cells were readily killed when DAPK2 was depleted from cells following transfection with individual siGENOME DAPK2 oligonucleotides 3 or 4 (**Figure 4-4a** + **b, f** + **g**). Reassuringly, transfection of U2OS and A549 cells with the 3'UTR specific DAPK2 siRNAs also sensitised to TRAIL-induced apoptosis (**Figure 4-4c** + **d, h** + **i**), providing further evidence in favour of the notion that the sensitisation to TRAIL-induced apoptosis

is a specific effect resulting from DAPK2 knockdown. Interestingly, when comparing the effect of sensitisation to TRAIL upon DAPK2 knockdown between U2OS and A549 cells, U2OS exhibited a stronger sensitivity to TRAIL treatment with significant cell death at a TRAIL concentration as low as 1 ng/ml (**Figure 4-4a** - **d**). A549 cells however required a concentration of at least 10 ng/ml of TRAIL to induce significant killing (**Figure 4-4f** - **i**). This suggested that A549 cells possessed an inhibitory mechanism, which protected them from TRAIL that was not fully overcome by solely depleting DAPK2.

To additionally exclude the possibility that the transfection of cells with siRNA oligonucleotides *per se* induced sensitisation to TRAIL-induced apoptosis, further control experiments were performed. Cells were transfected with siRNA against Luciferase (siLuc). This targeted the luciferase gene, which can be found in the common eastern firefly (*Photinus pyralis*) and is not expressed in mammalian cells. Cells were left untransfected (Untr), or they were transfected with either siNS or siLuc, and cell death was assessed using crystal violet assay as described before. As shown in **Figure 4-4e** and **j**, transfection of U2OS and A549 cells with siLuc (purple bars) yielded in results identical to transfection with siNS (black bars) but there was no evidence for significantly increased sensitisation to TRAIL-induced apoptosis. These results were almost identical to cells that were left untransfected (Untr, grey bars), which also exhibited resistance to TRAIL induced apoptosis.

Taken together these data strongly supported the initial observation and suggested that depletion of DAPK2 specifically sensitised TRAIL resistant U2OS and A549 cells to TRAIL-induced apoptosis.

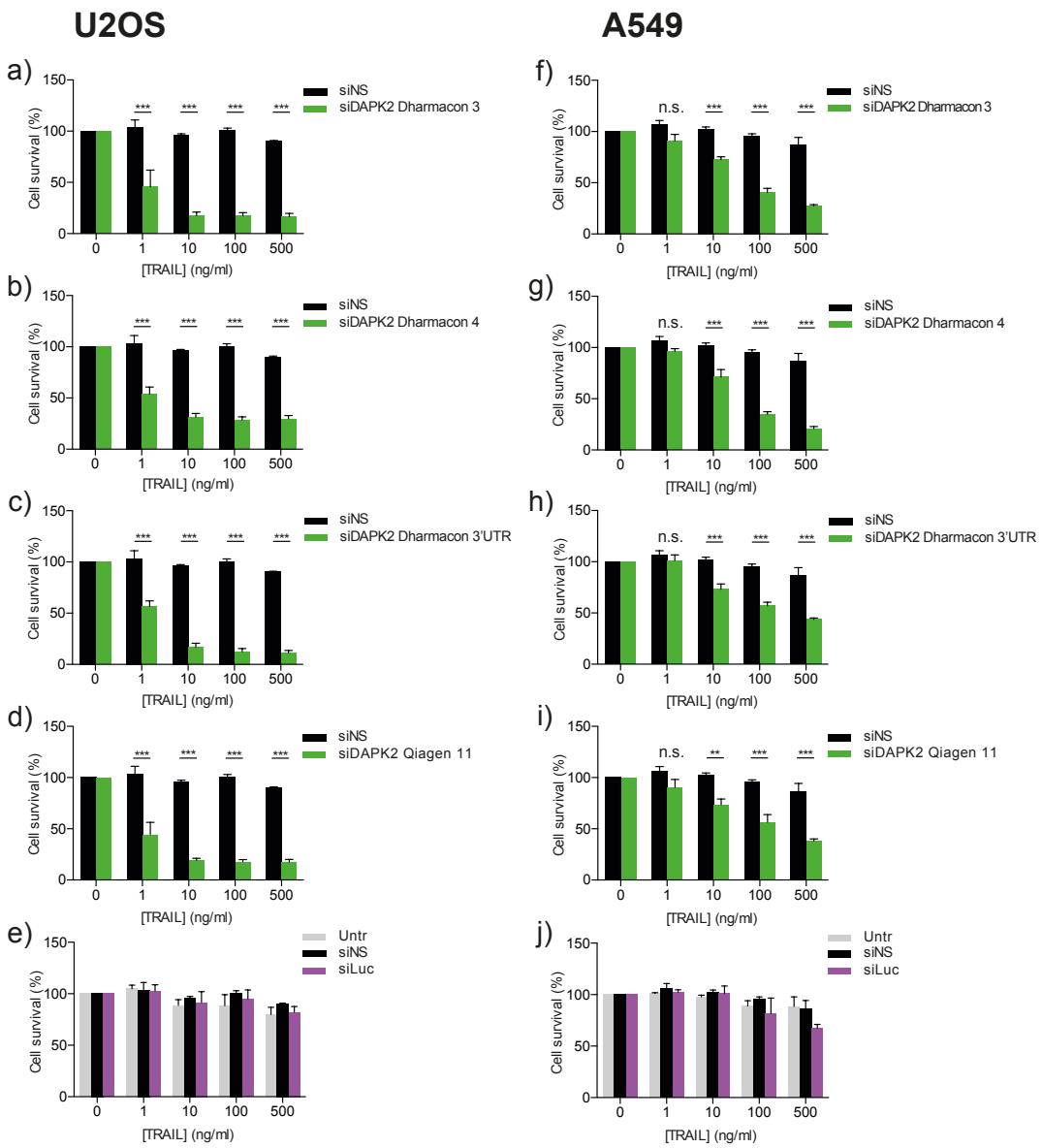

Figure 4-4. Validation of siRNA oligonucleotide molecules that target different sequences of DAPK2 mRNA, designed using different algorithms.

U2OS (**a - e**) or A549 (**f - j**) cells were transfected with non-targeting siNS or siLuc, different DAPK2 siRNA oligonucleotides or left untransfected (Untr), as indicated in the figure. Forty-eight h after transfection cell survival in response to TRAIL ligation was measured using crystal violet viability assays. For that purpose, 24 h after transfection cells were re-plated into 96-well plates at a density of $2x10^4$ cells per well. The following day, cells were treated with the indicated concentrations of TRAIL for 24 h. Cells were then fixed using methanol and stained with crystal violet. Crystals were dissolved in 10% (v/v) acetic acid and quantified by measuring the absorbance at 595 nm. Values were normalised to the untreated samples. Data represent mean ± SEM of at least three independent experiments, performed in triplicate. Statistical analyses were done using two-way ANOVA test (** $p<0.01$, *** $p< 0.005$).

4.2.3 Downregulation of DAPK2 sensitises cells to TRAIL-induced apoptosis *via* increased apoptotic signalling

Having observed that U2OS and A549 cells were more susceptible to TRAIL-induced cell death after DAPK2 knockdown, we next asked what the molecular consequences of DAPK2 silencing were. Accordingly, cells were transfected with siDAPK2, as before, treated with TRAIL for varying periods of time as indicated, and proteins extracted and separated on a polyacrylamide gel (**Figure 4-5**). Western blot membranes were subsequently probed with antibodies specific to key molecules known to be activated downstream of TRAIL. TRAIL-induced apoptosis was studied over a period of 1-24 h. Focus was given to earlier time points (up to 4 h) as caspase activation is generally a rapid event in cells sensitive to TRAIL. Caspase-8 and caspase-10 are two initiator caspases downstream of DRs and were thus analysed first. Activation of caspase-8 was faster and stronger in siDAPK2-transfected cells than in control cells (siNS) (**Figure 4-5a** + **d**), as seen by both the emergence of smaller caspase fragments (43, 41 and 18 kDa) and the reduction of the full-length 55 kDa protein. Indeed, in cells transfected with siNS, caspase-8 cleavage 1 h after TRAIL treatment (100 ng/ml) was much weaker in siNS-transfected cells than in cells transfected with siDAPK2. Activation of caspase-8 leads to cleavage of the effector caspase-3 and subsequent degradation of molecules such as PARP, which ultimately results in cellular demise. Accordingly, DAPK2 silencing also resulted in increased caspase-3 (**Figure 4-5b** and **e**) and PARP cleavage (**Figure 4-5c** and **f**). In addition, the reduction of BID expression and increased caspase-9 cleavage after DAPK2 silencing indicated the recruitment of the intrinsic apoptotic pathway (**Figure 4-5a** + **d** and **b** + **e**). Collectively, these data suggested that

DAPK2 inhibited caspase activation downstream of TRAIL by interfering with both the extrinsic and intrinsic apoptosis pathways.

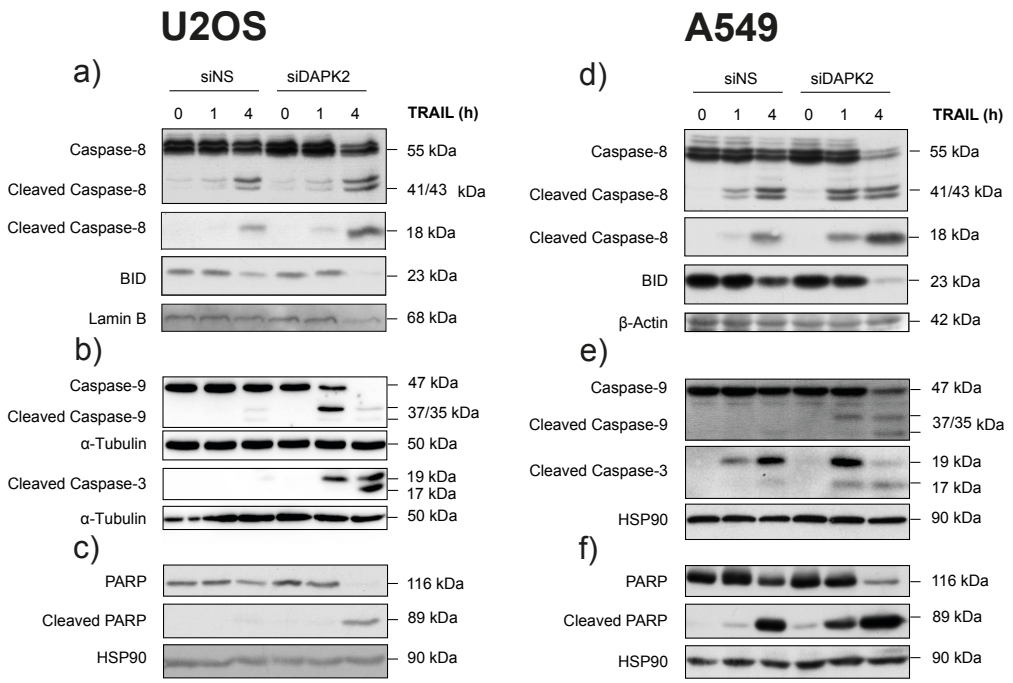

Figure 4-5. Knockdown of DAPK2 increases apoptotic extrinsic and intrinsic apoptotic signalling in response to TRAIL treatment.

Molecular events of TRAIL-induced apoptosis **(a - f)** were assessed by SDS-PAGE/western blotting. Forty-eight h after A549 and U2OS cells were transfected with siNS and siDAPK2, cells were treated with TRAIL (100 ng/ml) for the indicated time points. Activation of the extrinsic and intrinsic pathways was assessed by SDS-PAGE/qualitative western using cleavage of BID and caspase-8 (**a** + **d**), caspase-9 and caspase-3 (**b** + **e**) and PARP (**c** + **f**) as read-outs. Lamin B, α-Tubulin, β-Actin and HSP90 served as loading controls. Data is representative of at least three independent repeats.

4.2.4 siDAPK2 mediated sensitisation to TRAIL-induced apoptosis is independent of c-FLIP

Having observed that DAPK2-depleted U2OS and A549 cells were more susceptible to TRAIL-induced apoptosis and that there was a concomitant more pronounced activation of the effector caspase in these cells, we next asked what could cause this increased activation of caspase-8. As described earlier, c-FLIP possesses strong homology to caspase-8 with its two DEDs in the N-terminus and it is, in fact, a major inhibitor of the extrinsic cell death pathway. Accordingly, cells were transfected with siNS or siDAPK2 oligonucleotides and mRNA, as well as protein, was extracted to assess the cellular levels of c-FLIP in response to DAPK2 knockdown. As depicted in **Figure 4-6a** + **b**, RNAi-mediated DAPK2 depletion did not alter mRNA induction of c-FLIP in U2OS or A549 cells. Consistently, protein levels of the c-FLIP isoforms c-FLIP$_L$, c-FLIPγ and c-FLIP$_s$ were also unaffected by DAPK2 knockdown (**Figure 4-6c** + **d).** Suggesting that DAPK2 depletion mediated sensitisation to TRAIL-induced apoptosis is independent of the modulation of c-FLIP.

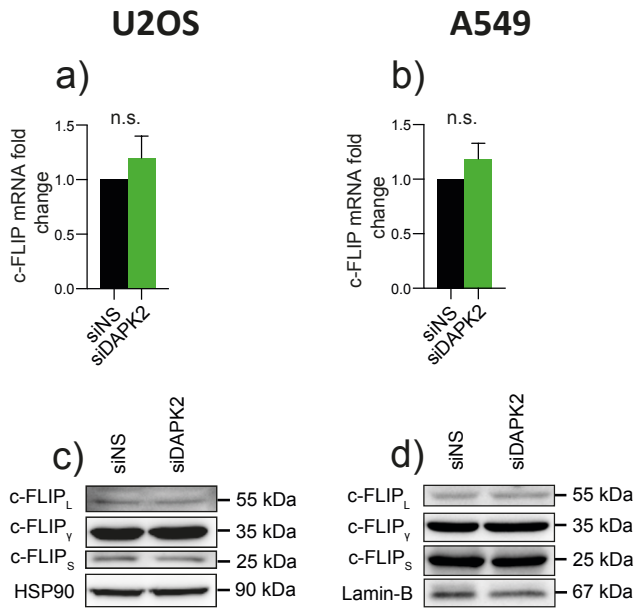

Figure 4-6. Silencing DAPK2 does not affect the levels of c-FLIP.

U2OS **(a** + **c)** and A549 **(b** + **d)** cells were transfected with either siNS or DAPK2 siRNA. Forty-eight h after transfection the levels of c-FLIP mRNA were analysed by qPCR **(a** + **b)**. qPCR data represent mean ± SEM of three independent experiments with duplicate samples. Statistical analysis was done using Student's *t*-test (paired, one tailed). Protein expression levels of c-FLIP were evaluated by quantitative western blotting **(c** + **d)** blots shown are representative of three independent experiments yielding identical results.

4.2.5 DAPK2 silencing leads to the upregulation of DR5 and DR4 mRNA, key receptors for TRAIL-induced apoptosis

The involvement of both the extrinsic and intrinsic cell death pathways, evidenced by increased activation of caspase-8 and increased cleavage of the downstream molecules, such as caspase-9 and BID, suggested that knocking down DAPK2 affected an upstream event common to both arms of the TRAIL apoptotic pathway (**Figure 1-4**). As both pathways are activated *via* the engagement of TRAIL receptors, the effect of DAPK2 depletion on the levels of TRAIL-receptor expression was assessed. It is known that TRAIL can induce cell death *via* either of its two receptors, namely DR4 and DR5. In addition, there are

also the so-called decoy receptors, DcR1 and DcR2, which can compete with DR4 and DR5 for ligand binding. Hence, the ratio of TRAIL decoy to DRs also determines the responsiveness of cells to TRAIL (Merino et al., 2006). A fifth receptor named OPG has been identified but its activity so far has not been linked to TRAIL-induced apoptosis. All receptor types have been described in **1.4.2** and depicted in **Figure 1-3**). To assess receptor levels in U2OS and A549 cells, cells were transfected with siDAPK2 or siNS, and mRNA levels of TRAIL receptors were assessed by qPCR. Transfection of U2OS and A549 cells with siDAPK2 led to the induction of DR5 mRNA (**Figure 4-7a** + **d**), one of the receptors through which TRAIL can signal to kill. DR4, the second death-inducing receptor was not expressed in U2OS cells but was expressed in A549 and its mRNA levels were also increased after silencing DAPK2 (**Figure 4-7d**). Messenger RNA levels of the decoy receptors DcR1 and DcR2 were neither elevated in U2OS, nor in A549 cells (**Figure 4-7b** + **e**). Interestingly, the mRNA levels of the soluble receptor OPG showed the trend of an increase in U2OS cells, (**Figure 4-7c**) but remained unaffected after DAPK2 depletion in A549 cells (**Figure 4-7f**). These data suggested that the sensitisation of TRAIL-resistant U2OS and A549 cells to TRAIL-induced apoptosis was possibly modulated by the increased expression of DRs.

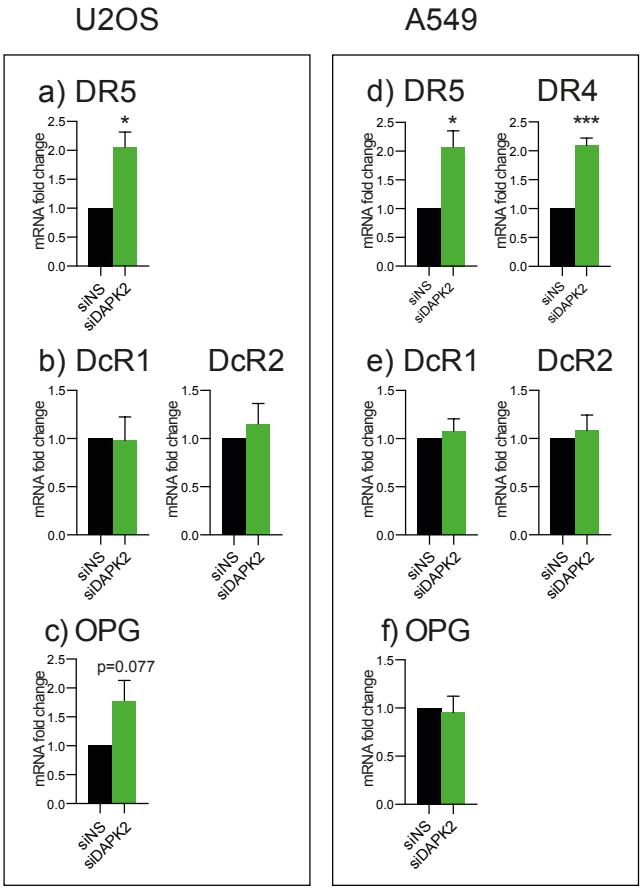

Figure 4-7. Knockdown of DAPK2 induces expression of DR4 and DR5 mRNA.

U2OS **(a - c)** and A549 **(d - f)** cells were transfected with either siNS or siDAPK2 oligonucleotides. Forty-eight h after transfection RNA was harvested and DR5 (U2OS, A549) (**a** + **d**), DR4 (A549) (**d**), DcR1 (U2OS, A549), DcR2 (U2OS, A549) (**b** + **e**) and OPG (U2OS, A549) (**c** + **f**) mRNA levels were analysed by qPCR. qPCR data represent mean ± SEM of at least three independent experiments with technical duplicate samples. Statistical analysis was done using Student's *t*-test (paired, one tailed) (* $p<0.05$, *** $p< 0.005$).

4.2.6 DAPK2 silencing induces protein expression of DR4 and DR5.

Having observed a clear upregulation of DR mRNA levels upon DAPK2 depletion, DR5 in U2OS and both DR4 and DR5 in A549 cells, we sought to establish if this mRNA induction translated into protein expression. The induction of DR5 was analysed using SDS-PAGE/quantitative western blotting in both cell lines. DR5 has two isoforms that differ by 29 amino acids and which are functionally indistinguishable, as described earlier. The antibody used here recognises both isoforms and the identity of DR5 was further confirmed using DR5-specific RNAi. Silencing of DAPK2 did not only significantly increase DR5 mRNA levels as shown in **Figure 4-7**; it significantly induced DR5 protein expression in U2OS and A549 cells (**Figure 4-8**). Densitometric analyses of western blots, normalising DR5 expression levels to the housekeeping gene HSP90 and siNS transfected cells, revealed an protein level increase of approximately three fold in U2OS for both DR5 isoforms and an increase of around five fold of $DR5_S$ and approximately four fold of $DR5_L$ in A549 cells. (**Figure 4-8a** + **c).** To analyse the cell surface expression of DR4 and DR5 upon DAPK2 knockdown, unpermeabilised U2OS and A549 cells were stained with DR specific, fluorophore-coupled, antibodies. As opposed to the quantification of total DR protein levels using SDS-PAGE/quantitative western blotting, this technique specifically captures the levels of extracellular and thus potentially functional DRs. As shown in **Figure 4-8** (**b** + **d**) RNAi-mediated DAPK2 silencing led to a two - three fold induction of DR5 surface expression in U2OS and A549 cells, RNAi targeting DR5 served as a control. Furthermore, the surface expression of DR4 was increased in A549 cells upon RNAi-mediated DAPK2 knockdown and, here too, siDR4 served as a control for antibody specificity.

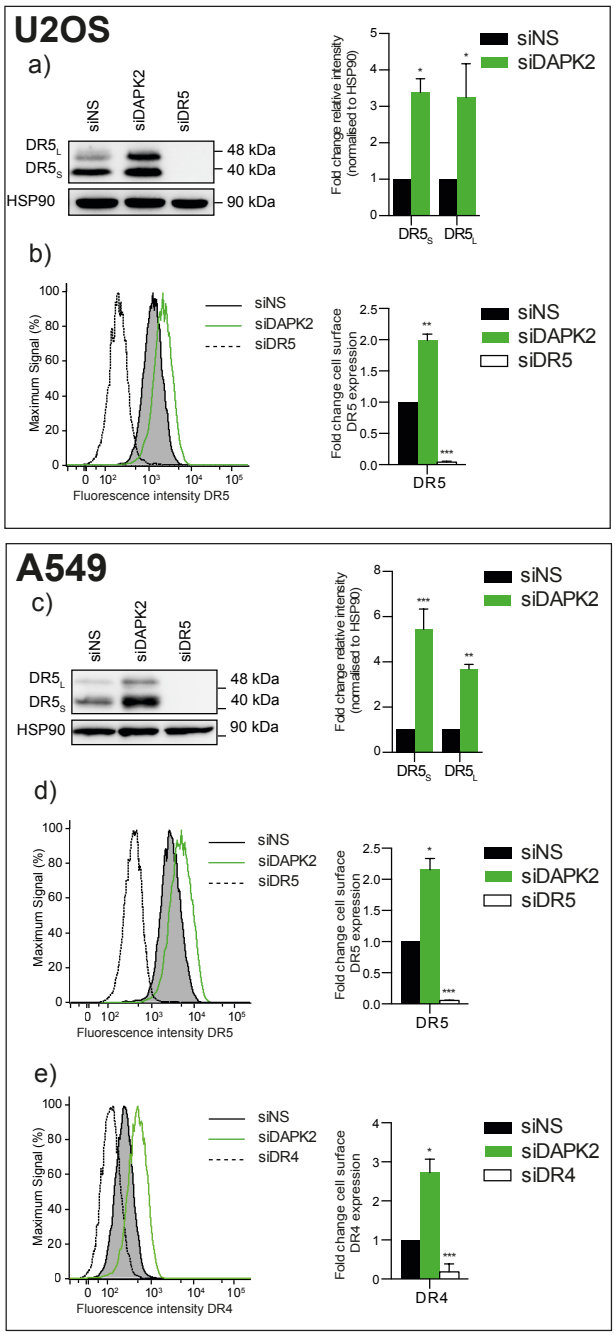

Figure 4-8. DAPK2 silencing leads to the upregulation of DR5 and DR4, key receptors for TRAIL.

U2OS **(a** + **b)** and A549 **(c** - **e)** cells were transfected with either siNS, or siDAPK2 for 48 h. Proteins were isolated and the level of DR expression was assessed by western blotting **(a** + **c),** or flow cytometry **(b, d, e)**. Densitometric analyses of western blots were plotted as fold change of DR5 expression relative to the siNS control. Data represent mean ± SEM of three independent experiments. Statistical analyses were done using one-way ANOVA test (* $p< 0.05$, ** $p<0.01$, *** $p< 0.005$). Cell surface expression was quantified using geometric means of three independent experiments and plotted as fold change of surface expression. Statistical analysis was done using Student's *t*-test (paired, one tailed) (* $p< 0.05$, ** $p<0.01$).

4.2.7 The effect of DR4 and DR5 upregulation upon DAPK2 knockdown was validated by deconvolution and additional siRNAs

To further validate the finding that DR expression was induced specifically in response to DAPK2 depletion and not due to an off-target effect, the siDAPK2 pool was deconvoluted as before and additional siDAPK2 oligonucleotides used. The latter included the custom made Dharmacon 3'UTR-specific DAPK2 siRNA mentioned previously and the Hs_DAPK2_11 FlexiTube siRNA from QIAGEN. U2OS and A549 cells were transfected with individual siDAPK2 oligonucleotides or siNS as control, and cell surface DR expression was assessed by flow cytometry. As depicted in **Figure 4-9** depletion of DAPK2 by each of the siRNA oligonucleotides significantly increased the surface expression of DR5 in U2OS cells. The same result was obtained in A549 cells (**Figure 4-10a - d**) where cell surface expression of DR5 was induced upon transfection with each of the individual siDAPK2 oligonucleotides. In addition, in A549 cells, the knockdown of DAPK2 using each of the single siRNAs also led to upregulation of DR4 surface expression (**Figure 4-10e - h**).

As shown in **Figure 4-11** the upregulation of DR5 surface expression upon DAPK2 knockdown was further compared to the effect of the additional non-targeting siRNA oligonucleotides, such as siRNA siLuc and cells that were left untransfected (Untr). Depletion of DAPK2 using the siDAPK2 pool specifically induced expression of DR5 in U2OS (**Figure 4-11a**) and A549 cells (**Figure 4-11b**), as shown before. Leaving cells untransfected or transfecting them with siLuc did not cause any detectable/significant change in DR5 surface expression compared to the siNS control. Taken together, these data thus suggest that

siDAPK2-induced sensitisation to TRAIL was accompanied by, and likely to be modulated *via*, upregulation of DR receptors.

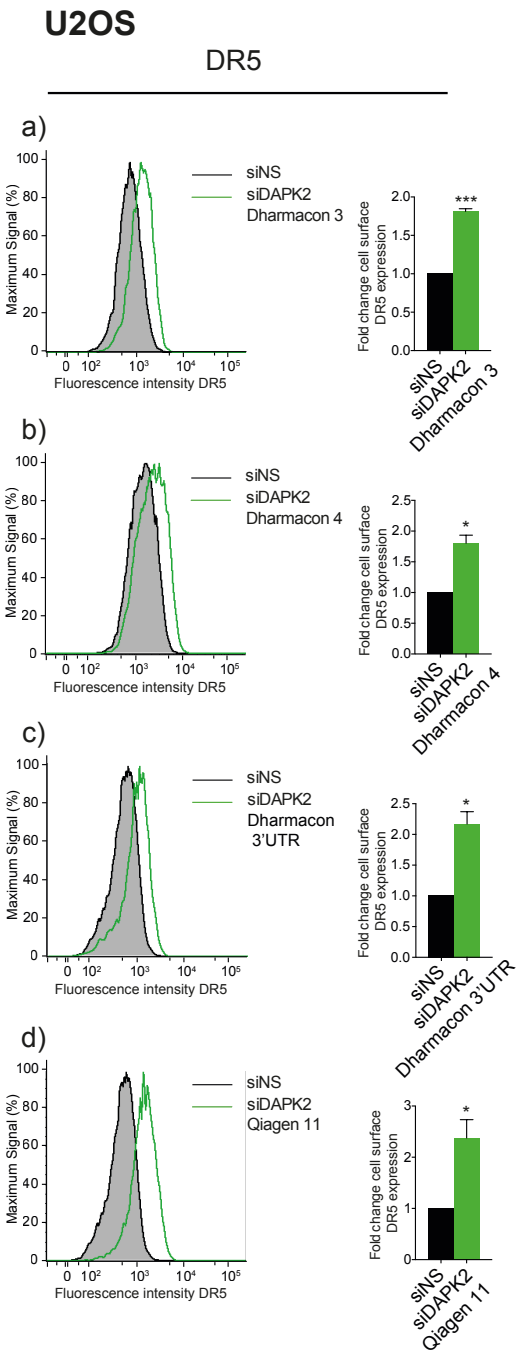

Figure 4-9. Validation of different siRNA oligonucleotide molecules for their ability to induce DR5 expression in U2OS cells.

U2OS cells were transfected with non-targeting siNS, or different DAPK2 siRNA oligonucleotides, as indicated in the figure. Flow cytometry was used to assess the levels of DR5 (**a - d**). Data represent mean ± SEM of at least three independent experiments. Cell surface expression was quantified using geometric means of those independent experiments and plotted as fold change of surface expression in relation to siNS. Statistical analysis was done using Student's t-test (paired, one tailed) (* $p < 0.05$, ** $p<0.01$, *** $p < 0.005$).

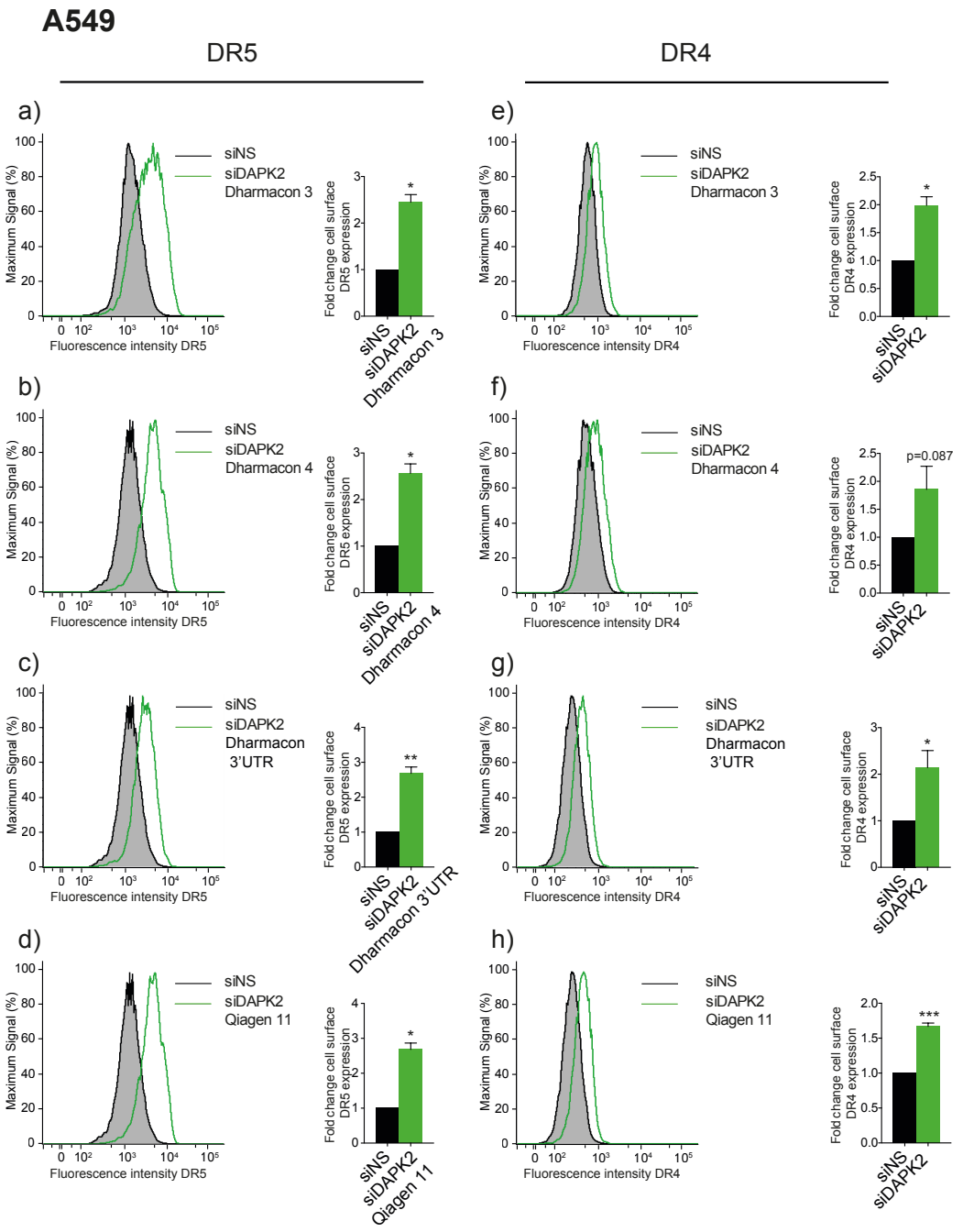

Figure 4-10. Validation of different siRNA oligonucleotide molecules for their ability to induce DR5 and DR4 expression in A549 cells.

A549 cells were transfected with non-targeting siNS, or different DAPK2 siRNA oligonucleotides, as indicated in the figure. Flow cytometry was used to assess the levels of DR5 (**a - d**) and DR4 (**e - h**). Data represent mean ± SEM of at least three independent experiments. Cell surface expression was quantified using geometric means of those independent experiments and plotted as fold change of surface expression in relation to siNS. Statistical analysis was done using Student's t-test (paired, one tailed) (* $p < 0.05$, ** $p < 0.01$, *** $p < 0.005$).

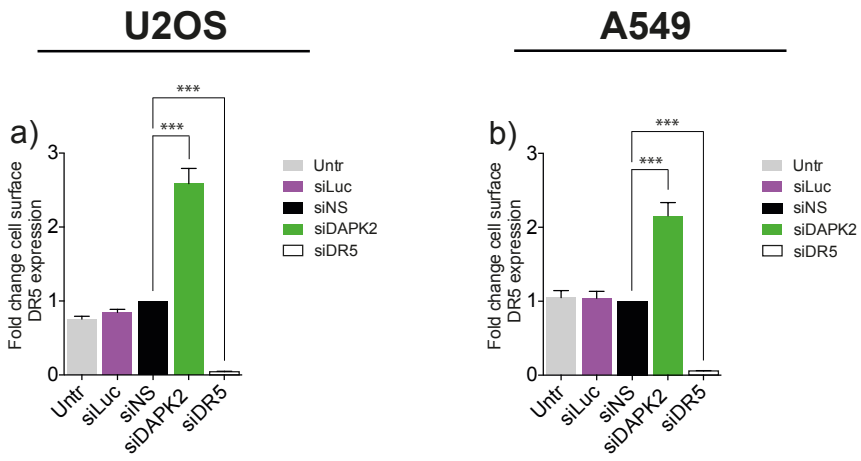

Figure 4-11. Upregulation of DR5 expression is specific to DAPK2 depletion.

U2OS and A549 cells were transfected with non-targeting siNS and siLuc, siDAPK2 and siDR5 oligonucleotides or left untransfected (Untr), as indicated. Flow cytometry was used to assess the levels of DR5 (**a** + **b**). Data represent mean ± SEM of at least three independent experiments. Cell surface expression was quantified using geometric means of those independent experiments and plotted as fold change of surface expression in relation to siNS. Statistical analysis was done using Student's t-test (paired, one tailed) (* $p < 0.05$, ** $p<0.01$, *** $p < 0.005$).

4.2.8 In the absence of DR5, siDAPK2 can neither sensitise U2OS, nor A549 cancer cells to TRAIL-induced apoptosis

The upregulation of DR5 may have been necessary but not sufficient for the sensitisation to TRAIL-induced apoptosis observed after silencing DAPK2. In order to determine its relevance, double knockdowns targeting concomitantly DAPK2 and DR5 in U2OS cells and additionally DR4 in A549 cells were performed. As controls, cells were transfected with siNS, siDR5, or siDR4. Cells were transfected with all permutations of siRNA to a final concentration of 40 nM: siNS/siNS, siDAPK2/siNS, siDR5/siNS, siDAPK2/siDR5 in U2OS and in A549 cells additionally siDR4/siNS and siDAPK2/siDR4. The efficiency of the double knockdown experiments was validated using qPCR (**Figure 4-12b** + **e**). As

predicted, downregulation of DR5 slightly increased resistance of U2OS or A549 to TRAIL-induced death (**Figure 4-12a** + **c**). In contrast, the downregulation of DAPK2 sensitised cells, as shown previously, provided that the expression of DR5 was not downregulated (compare cells transfected with siDAPK2/siNS *versus* siDAPK2/siDR5). This suggested that the upregulation of DR5 following silencing of DAPK2 was indeed critical to sensitise the resistant cells to apoptosis. A549 cells also express DR4 and double knockouts of DR4 and DAPK2 suggested that in these cells DR4 was partially required to sensitise A549 cells to TRAIL-induced apoptosis. The effect does not seem to be as pronounced as that seen when DR5 was silenced and, despite the trend shown, it was not statistically significant (**Figure 4-12d**). At higher concentrations of TRAIL, DR5 knockdown did not fully reverse the phenotype, suggesting that in these cells DR4 might be engaged to overcome impaired DR5 expression (**Figure 4-12c** + **d**).

Indeed, silencing of DR5 would almost certainly reverse the phenotype observed when DAPK2 was silenced, as this is a key receptor for TRAIL. To study whether DR5 upregulation was the crucial step in siDAPK2-induced sensitisation to TRAIL, we titrated siDR5 (**Figure 4-13a**), measured its impact on DR5 protein expression (**Figure 4-13a** + **b**) and established the concentration at which only the DAPK2 RNAi effect was reverted, which was deemed to be 1.25 nM (**Figure 4-13a**). By co-transfecting siDAPK2 (20 nM) and siDR5 (1.25 nM) in U2OS cells, which only express DR5, we were able to revert the induction of DR5 levels. Furthermore, reverting DR5 levels successfully impaired siDAPK2-mediated TRAIL sensitisation (**Figure 4-13c**) and thus confirms the data shown in (**Figure**

4-12a + **c**). Overall, these findings strongly support the role of DR induction in siDAPK2-induced TRAIL sensitisation. In particular DR5 seemed to be the key molecule which was upregulated in response to DAPK2 knockdown and which, when reverted to its initial level can no longer facilitate TRAIL-induced apoptosis.

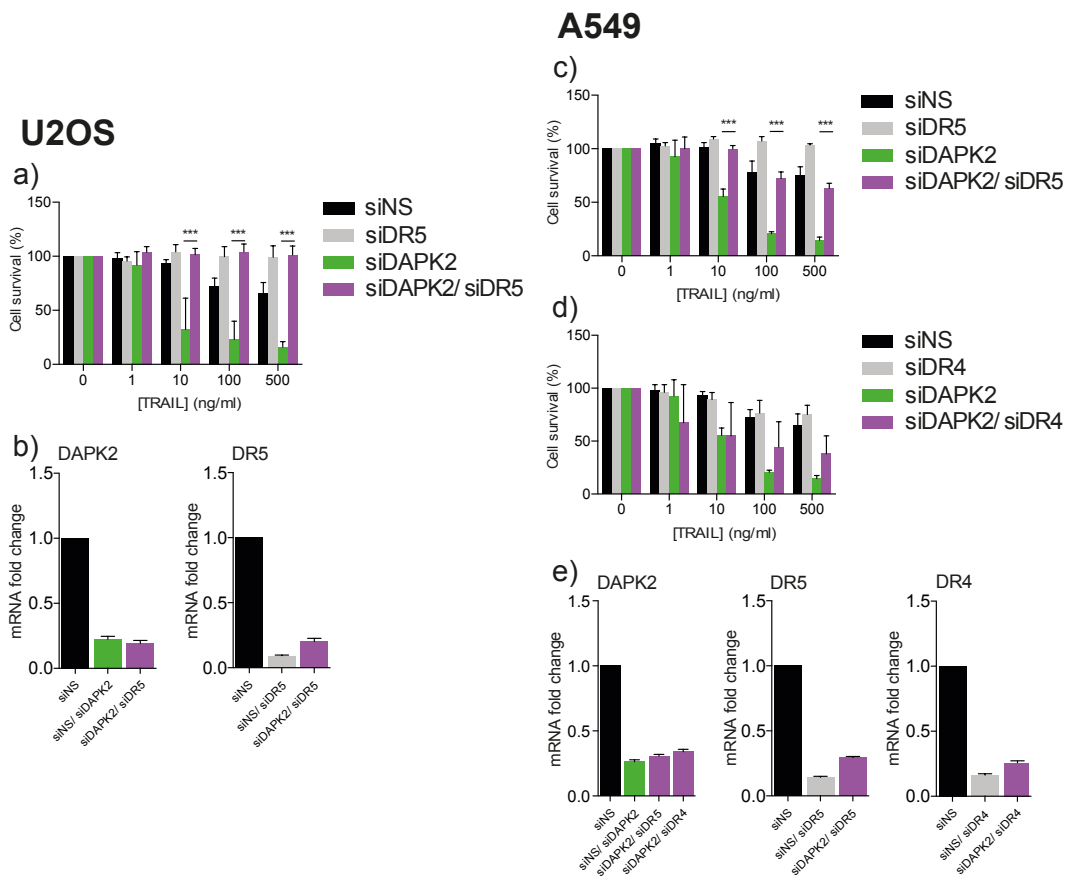

Figure 4-12. In the absence of DR5, siDAPK2 can neither sensitise U2OS, nor A549 to TRAIL-induced apoptosis.

Double knockdowns were carried out in U2OS (**a** + **b**) and A549 (**c - e**) cells. For this purpose, U2OS and A549 cells were transfected with 40 nM of: siNS+siNS, siDR5+siNS, siDAPK2+siNS, siDR5+siDAPK2 (**a** + **c**) and siNS+siBID and siBID+siDAPK2 (**e**). A549 cells were also transfected with siNS+siDR4 and siDR4+siDAPK2 (**d**). Twenty-four h after transfection cells were re-plated into 96 well plates at a density of $2x10^4$ cells per well. The following day cells were treated with TRAIL for 24 h at the indicated final concentrations. Cells were methanol-fixed and stained with crystal violet. Staining was dissolved in acetic acid and quantified by measuring the absorbance at 595 nm. Values were normalised to the untreated samples. Data represent mean ± SEM of three independent experiments performed in triplicates. Statistical analysis was done using two-way ANOVA test (* $p< 0.05$, ** $p<0.01$, *** $p< 0.005$). Forty-eight h after transfection and re-plating, RNA was harvested and double knockdown efficiency was confirmed (**b** + **e**). DAPK2 DR4 and DR5 mRNA levels were analysed by qPCR, data represent mean ± SD of one representative experiment with technical duplicate samples.

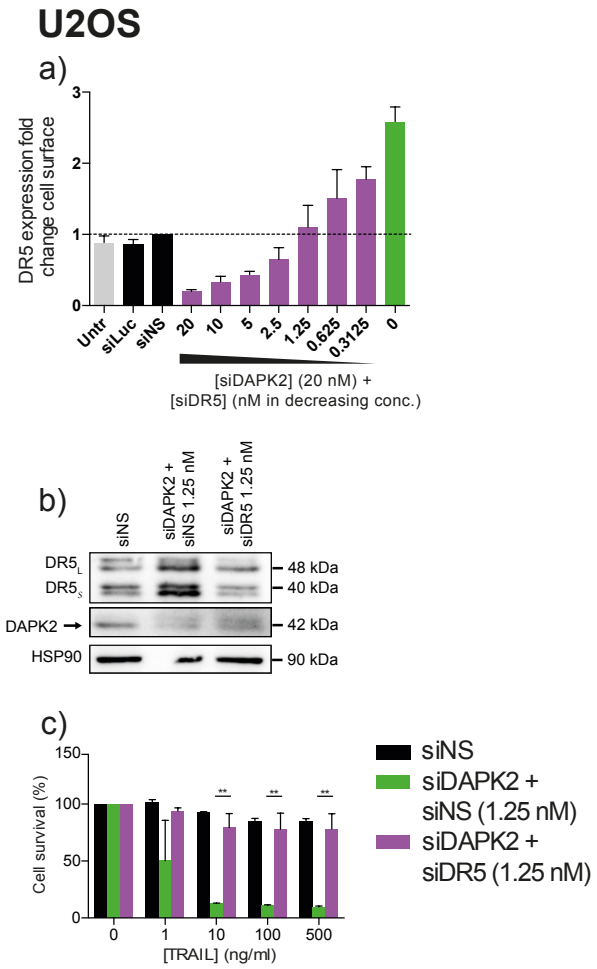

Figure 4-13. Titration of DR5 siRNA sufficient to block TRAIL-induced apoptosis in U2OS cells.

(**a**) U2OS cells were transfected with either siNS, siLuc (both controls for RNAi off-target effects), siDAPK2 or with siDAPK2 (20 nM) concomitantly with siDR5 (0.31-20 nM) for 48 h. DR5 expression was measured by flow cytometry and cell surface expression quantification performed as before. Co-transfection of U2OS cells with 1.25 nM siDR5 and 20 nM siDAPK2 abolished siDAPK2-mediated DR5 induction. (**b**) The effect of co-transfection was also assessed using quantitative western blotting, which confirmed the results obtained by flow cytometry. [The shadow bands seen in the DAPK2 panel correspond to DR5, since the membrane was probed for with this antibody after being stripped from the anti-DR5 antibody.] (**c**) To assess the impact of reverting the siDAPK2-mediated effects on DR5 protein levels on cell survival after TRAIL U2OS cells were transfected with either siDAPK2 (20 nM) and siNS (1.25 nM), or siDAPK2 (20 nM) and siDR5 (1.25 nM). Cells were re-plated into 96-well plates at a density of $2x10^4$ cells per well 24 h after siRNA transfection and treated the following day with the indicated concentrations of TRAIL for another 24 h. Cells were methanol-fixed and stained with crystal violet. Staining was dissolved in acetic acid and quantified by measuring the absorbance at 595 nm. Values were normalised to the untreated samples. Data represent mean ± SEM of three independent experiments performed in triplicates. Statistical analysis was done using two-way ANOVA test (* p< 0.05, ** p<0.01, *** p< 0.005).

4.2.9 TRAIL downstream signalling differs significantly between U2OS and A549 cells.

Having established that siDAPK2-mediated sensitisation to TRAIL-induced apoptosis was caused by upregulation of DR5 and, to some extent DR4; further experiments were carried out to more fully understand downstream processes. BID is a pro-apoptotic member of the BCL-2 family and part of a well-known amplification loop downstream of TRAIL, which in some cells is required to induce death. It has been shown that the cell type determines how BID operates: BID cleavage can provide an amplification loop for the apoptotic signal as in type I cells, where the main mechanism is mediated by extrinsic apoptotic signalling, or as in type II cells, it serves as the primary mechanism of TRAIL-induced apoptosis, as described in **1.4.3.**

U2OS and A549 cells were transfected with all permutations of siRNA to a final concentration of 40 nM: siNS/siNS, siDAPK2/siNS, siBID/siNS and siDAPK2/siBID. Downregulation of BID *per se* did not impact significantly on the susceptibility of U2OS or A549 to TRAIL-induced death (**Figure 4-14a** and **c**). In U2OS cells, the downregulation of DAPK2 sensitised cells, as shown previously, and siBID did not have an impact on the sensitisation process (**Figure 4-14a** compare cells transfected with siDAPK2/siNS *versus* siDAPK2/siBID). Interestingly, in A549 cells siBID rescued siDAPK2 mediated sensitisation to TRAIL (**Figure 4-14c,** compare cells transfected with siDAPK2/siNS *versus* siDAPK2/siBID), suggesting that A549 require a mitochondrial amplification loop. These results indicated that the induction of TRAIL-induced apoptosis in U2OS cells downstream of DR signalling was fundamentally different to A549 cells.

While U2OS cells showed characteristics of type I cells with a dispensable mitochondrial amplification loop, A549 behaved like type II cells by depending on the mitochondrial amplification of TRAIL-induced apoptosis. To validate the finding that the mitochondrial amplification loop was indeed dispensable in U2OS cells, mitochondrial amplification of extrinsic apoptotic signalling was blocked by overexpressing the anti-apoptotic BCL-2 family member, BCL-X_L. The impact of BCL-X_L overexpression on DAPK2 and BCL-X_L protein endogenous levels in U2OS cells was addressed using a plasmid with a BCL-XL expression cassette and an empty vector as a control, in combination with transfection of siDAPK2 or siNS oligonucleotides (**Figure 4-15a**). Interestingly, overexpression of BCL-X_L did not rescue siDAPK2-induced TRAIL sensitisation in U2OS cells (**Figure 4-15b** + **c**). Hence, the mitochondrial amplification loop seems to be dispensable when inducing apoptosis *via* TRAIL in DAPK2 depleted U2OS cells. Overall, these findings reveal different signalling process in U2OS and A549 cells downstream of DR activation. The fact that amplification *via* BID is of fundamentally different importance in the two cell lines studied lends further support to the hypothesis that siDAPK2-induced sensitization to TRAIL is mediated at the receptor level.

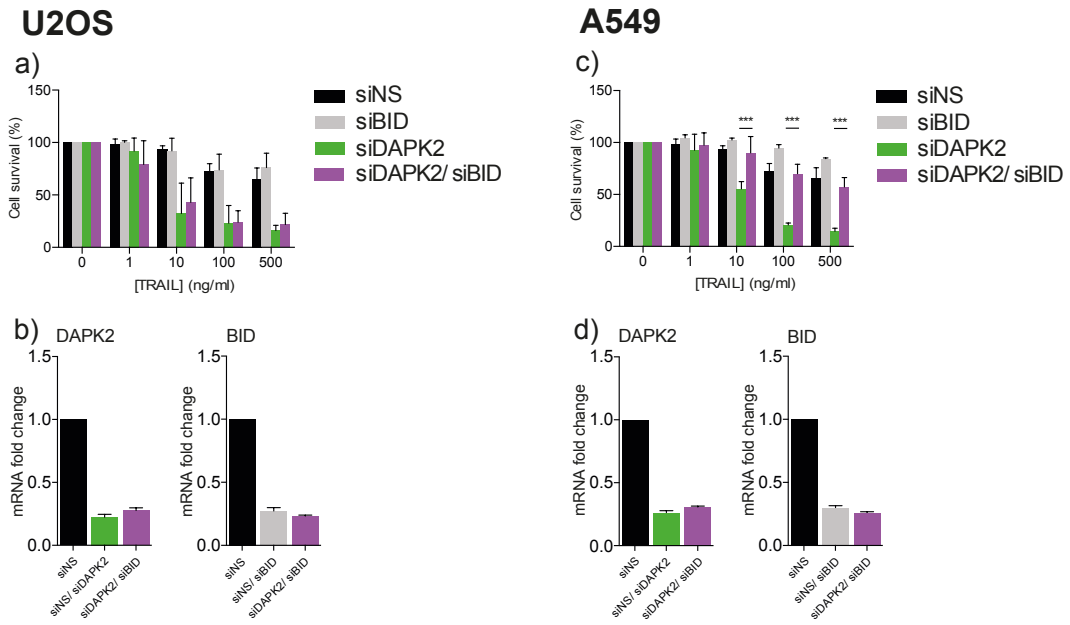

Figure 4-14. In the absence of BID, siDAPK2 can sensitise U2OS but not A549 to TRAIL-induced apoptosis.

Double knockdowns were carried out in U2OS (**a**) and A549 (**c**) cells. For this purpose, cells were transfected with 40 nM of the following siRNA mixtures: siNS+siNS, siDAPK2+siNS, siNS+siBID and siBID+siDAPK2. Twenty-four h after transfection cells were re-plated into 96 well plates at a density of $2x10^4$ cells per well. The following day cells were treated with TRAIL for 24 h at the indicated final concentrations. Cells were methanol-fixed and stained with crystal violet. Staining was dissolved in acetic acid and quantified by measuring the absorbance at 595 nm. Values were normalised to the untreated samples. Data represent mean ± SEM of three independent experiments performed in triplicates. Statistical analysis was done using two-way ANOVA test (* $p< 0.05$, ** $p<0.01$, *** $p< 0.005$). Forty-eight h after transfection and re-plating, RNA was harvested and double knockdown efficiency was confirmed (**b** + **d**). DAPK2 and BID mRNA levels were analysed by qPCR, data represent mean ± SD of one representative experiment with duplicate samples.

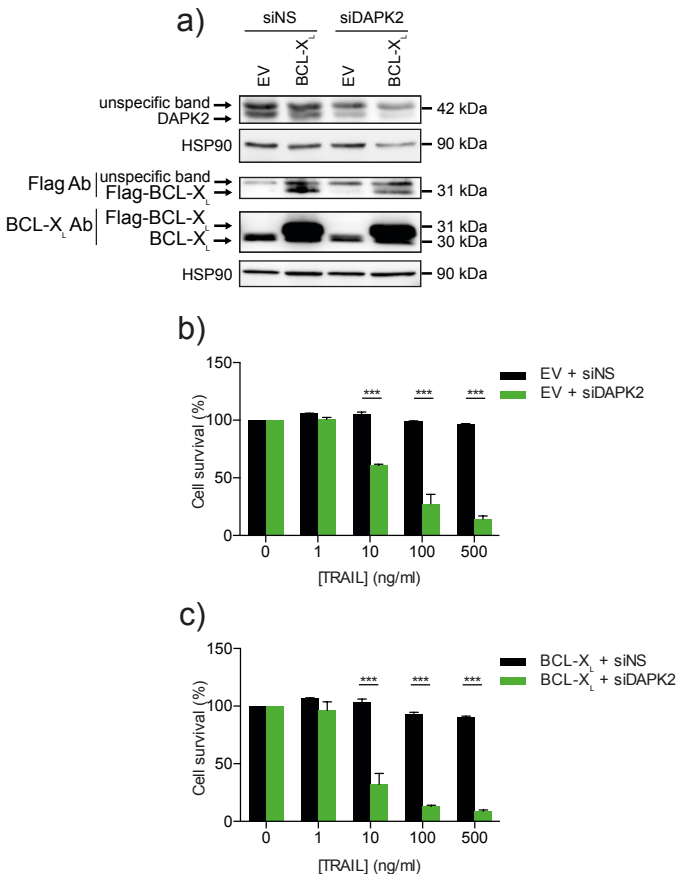

Figure 4-15. Overexpression of BCL-X_L does not rescue siDAPK2-mediated sensitisation of U2OS cells to TRAIL.

(**a**) U2OS cells were transfected with either siNS, or siDAPK2 in combination with an 'empty' pcDNA3 control vector (EV), or with a pcDNA3 BCL-X_L expression plasmid, and the knockdown and over-expression efficiencies determined by quantitative western blotting. Cells transfected with the empty vector (**b**), or with the BCL-X_L-expressing vector (**c**) were re-plated into 96-well plates at a density of $2x10^4$ cells per well 24 h after siRNA transfection. The following day cells were treated with the indicated concentrations of TRAIL for 24 h and cell death assessed using crystal violet assays, as described before. Values were normalised to the untreated samples. Data represent mean ± SEM of two independent experiments performed in triplicate. Statistical analyses were done using two-way ANOVA test (* $p< 0.05$, ** $p<0.01$, *** $p< 0.005$).

4.2.10 Depletion of DAPK2 also sensitises U2OS and A549 cells to FAS ligand-induced apoptosis

The process by which TRAIL binds to DR4 and DR5 and leads to caspase cleavage and apoptosis are very similar to another receptor of the TNFR family, known as FasR (also known as CD95). This receptor, however, can only be ligated by the death-inducing ligand FasL (also known as CD95L). In contrast to TRAIL, which specifically targets tumour cells, FasL induces apoptosis in a variety of tissues as described earlier in the Introduction. Interestingly, the upregulation of c-FLIP has been described as a common mechanism of FasL-resistance, as is the case for TRAIL. Given the high degree of signalling overlap between TRAIL- and FasL, we asked whether the lack of DAPK2 also affected the cells susceptibility to FasL-mediated apoptosis. To induce FasL-mediated apoptosis, we used an anti-Fas IgM antibody that is capable of clustering FasR, thus mimicking FasL-induced apoptosis (henceforth referred to as FasL) (Yonehara et al., 1989). U2OS and A549 cells were transfected with siNS, siDAPK2 and siFLIP, which served as a positive control for sensitisation to FasL-induced apoptosis. As shown in **Figure 4-16a**, DAPK2 knockdown sensitised U2OS cells to FasL-induced apoptosis, just like what was observed for c-FLIP, a known inhibitor of Fas-induced death. Interestingly, in A549 cells (**Figure 4-16e**) neither siDAPK2, nor siFLIP-sensitised cells to FasL-induced apoptosis. As what was seen for mRNA upregulation of DR4 and DR5 in response to DAPK2 knockdown (**Figure 4-7a** + **d**), we found significantly elevated levels of FasR mRNA upon DAPK2 depletion in both cell lines studied (**Figure 4-16b** + **f**). Upregulation of FasR messenger RNA levels also translated into increased surface FasR protein expression (**Figure 4-16c** + **g**), which was further confirmed

using additional DAPK2 siRNAs (**Figure 4-16d** + **h**). Given the differential response to FasL in DAPK2-depleted U2OS and A549 cells, the levels of the FasL decoy receptor (DcR3); a putatively soluble protein which expression levels have been described to negatively correlate with FasL-induced cell death was assessed (Li et al., 2007). Interestingly, DcR3 mRNA expression levels were decreased upon DAPK2 knockdown in U2OS cells (**Figure 4-16b**), whereas DcR3 mRNA levels remained unaffected in A549 cells (**Figure 4-16f**), suggesting that DcR3 levels might correlate with cellular sensitivity to FasL-induced cell death. These results indicated that, besides sensitising U2OS and A549 cells to TRAIL-induced apoptosis, DAPK2 knockdown could also sensitise cells to FasL-induced cell death. However, sensitization to FasL seems to be associated not only with the upregulation of its corresponding receptor, FasR, but also with significant downregulation of its decoy receptor, DcR3. On the face of it, it seems that the way depletion of DAPK2 leads to Fas-sensitisation is a process fundamentally different from that that led to the sensitization to TRAIL, where decoy receptors appeared unimportant.

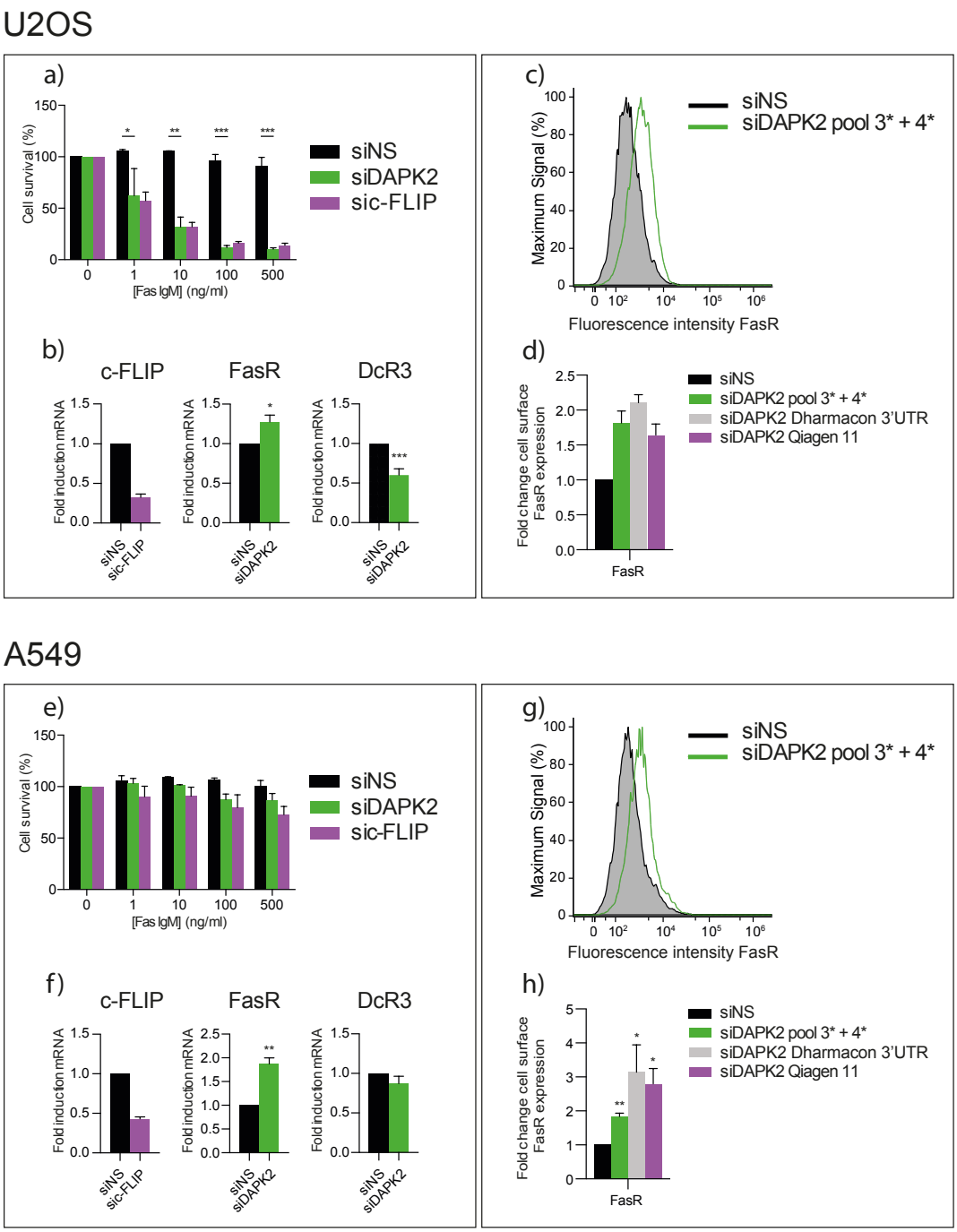

Figure 4-16. Depletion of DAPK2 sensitises U2OS but not A549 cells to FAS-induced apoptosis.

U2OS (**a** + **b**) or A549 (**e** + **f**) cells were transfected with non-targeting siNS, siDAPK2 and siFLIP, as indicated in the figure. Forty-eight h after transfection cell survival rates in response to FAS-IgM were measured using crystal violet viability assays. For cell survival assays (**a** + **e**), 24 h after transfection, cells were re-plated into 96-well plates at a density of $2x10^4$ cells per well. The following day, cells were treated with the indicated concentrations of TRAIL for 24 h. Cells were then fixed using methanol and stained with crystal violet. Crystals were dissolved in 10% (v/v) acetic acid and quantified by measuring the absorbance at 595 nm. Values were normalised to the untreated samples. Data represent mean ± SEM of at least three independent experiments, performed in triplicate. (Legend continued on the next page)

(Continued from last page) Statistical analyses were done using two-way ANOVA test (* p<0.05, ** p<0.01, *** p< 0.005). Forty-eight h after transfection and re-plating, RNA was harvested and c-FLIP, FasR and DcR3 mRNA levels were analysed by qPCR. c-FLIP qPCR data represent mean ± SD of one representative experiments with duplicate samples, FASR and DcR3 qPCR data represent mean ± SEM of at least three independent experiments with duplicate samples. Statistical analysis was done using Student's *t*-test (paired, one tailed) (* p<0.05, ** p<0.01, *** p< 0.005). U2OS (**c** + **d**) or A549 (**g** + **h**) cells were transfected with non-targeting siNS, or different DAPK2 siRNA oligonucleotides, as indicated in the figure. Flow cytometry was used to assess the levels of FasR (**c, d, g** and **h)**. For U2OS cells, data represent mean ± SEM of two independent experiments (**d**), whereas for A549 cells, data represent mean ± SEM of three independent experiments (**h**). Cell surface expression quantification was done using geometric means of those independent experiments and plotted as fold change of surface expression in relation to siNS. Statistical analysis was done using Student's t-test (paired, one tailed) (* p< 0.05, ** p<0.01, *** p< 0.005).

4.3 Discussion

DAPK1 was the first member of the DAPK family to be identified by Adi Kimchi in the mid-nineties (Deiss et al., 1995). DAPK1 is a serine/threonine kinase with a well-defined death domain, implicated in apoptotic pathways triggered by diverse stimuli(Shiloh et al., 2013). DAPK2 is a much smaller kinase, with approximately 80% of homology to DAPK1 in the kinase domain, a dimerization domain but with no discernible death domain(Inbal et al., 2000) (**Figure 1-9**). Most reports on DAPK2 involve exogenously expressed, and thus overexpressed, DAPK2. We hypothesised that depending on the cellular content and expression levels of DAPK2 this kinase would work either as a pro- or anti-apoptotic protein.

Death-inducing ligands of the TNF superfamily have been a focus of translational cancer research for the last 20 years. Due to their potentially tumour-eliminating characteristics, work has been specifically focused on TNF-α, FasL (CD95) and TRAIL. Whereas TNF-α and FasL have proven to cause significant and potentially life-threatening side effects when administered systemically (MacEwan, 2002, Nagata, 1997), TRAIL had a promising debut as a therapeutic

agent. In contrast to TNF-α and FasL, TRAIL specifically induced cell death in transformed cells whereas exhibiting little to none systemic toxicity (Kirienko et al., 2010). It soon became clear that numerous cancer cells that readily died after the initial treatment quickly acquired resistance to TRAIL (Sanchez-Perez et al., 2002), hindering the development of successful clinical applications. Several resistance mechanisms have been described since, such as downregulation of TRAIL receptors and upregulation of the inhibitory molecule c-FLIP, to mention but the most prominent ones. Much effort has thus focused on overcoming this resistance. To date, the most successful ways to overcome TRAIL resistance involve synergistic pro-apoptotic treatments and/or the induction of ROS (Mellier and Pervaiz, 2012, Ganten et al., 2004). Additional strategies that focus on specific re-sensitisation of tumour cells to TRAIL, potentially with few side effects, are thus highly desirable. Recently, siRNA mediated depletion of DAPK1 has been shown to re-sensitise TRAIL-resistant endometrial carcinoma cells to TRAIL-induced apoptosis suggesting in some circumstances an anti-apoptotic role for DAPK1 (Bai et al., 2010).

Here, we have shown using crystal violet-based cell survival assays that RNAi-mediated depletion of another DAPK family member, DAPK2, compared to a non-targeting control siNS (**Figure 4-2a** + **f**), specifically sensitises U2OS and A549 cells to TRAIL-induced apoptosis (**Figure 4-2b** + **g**). The findings seemed *bona fide* since multiple DAPK2 siRNAs with different targeting sequences did not cross-targeted other DAPK family members (**Figure 4-1**). Interestingly, in cells depleted of DAPK2 there is no sensitisation to a wide range of other apoptotic stimuli (**Figure 4-2c - e** and **h - j**). These results were further confirmed

by measuring DNA hypoploidy (**Figure 4-3**), which can be used as a readout for apoptosis. Deconvolution of the siDAPK2 pool and two additional unrelated DAPK2 siRNAs validated these initial observations and ascribed the effects to specific silencing of DAPK2 (**Figure 4-4a - d** and **f - i**). In addition, a second non-specific siRNA (siLuc) confirmed that the observed sensitisation is not an unspecific response to the transfection with siRNA oligonucleotides (**Figure 4-4e** and **j**).

Downregulation of DAPK2 leads to TRAIL-mediated activation of both extrinsic and intrinsic death pathways, which is quicker in A549 cells than in U2OS cells (**Figure 4-5**). Interestingly, activation of the intrinsic signalling, which includes a mitochondrial amplification loop, appears dispensable in U2OS cells (**Figure 4-14a** and **Figure 4-15**) but represents a crucial part of TRAIL-induced apoptosis upon DAPK2 depletion in A549 cells (**Figure 4-14c**). Many mechanisms of TRAIL-resistance and strategies to overcome these involve the DISC complex, including down-regulation of c-FLIP, which mimics caspase-8 and thus inhibits its binding to the DISC (Ganten et al., 2004). Inhibition of anti-apoptotic members of the BCL-2 family, such as BCL-2 and BCL-X_L, has also been shown to re-sensitise TRAIL-resistant cancer cells to TRAIL-induced apoptosis (Sinicrope et al., 2004, Huang and Sinicrope, 2008). There was no change on FLIP levels upon siDAPK2 (**Figure 4-6**) and overexpressing BCL-X_L had no impact on DAPK2-mediated sensitisation of U2OS to TRAIL (**Figure 4-15**), suggesting that these molecules are unlikely factors of TRAIL resistance that can be overcome by silencing DAPK2. However, perhaps the most prominent mechanism to overcome TRAIL-resistance is the up-regulation of its receptors, DR4 and/or

DR5. DAPK2 depletion leads to a significant increase of DR5 mRNA levels in U2OS and A549 cells (**Figure 4-7a** + **d**). In A549 cells, silencing DAPK2 also increases the expression of DR4 mRNA levels (**Figure 4-7d**). Such mRNA upregulation translated into significantly increased levels of total DR5 protein in U2OS and A549 cells (**Figure 4-8a** + **c**), as well as increased cell surface expression of DR5 in U2OS and A549 cells (**Figure 4-8b** + **d** and **Figure 4-11a** + **b**) and DR4 in A549 cells (**Figure 4-8e**). Deconvolution and use of two additional siDAPK2 oligonucleotides revealed that depletion of DAPK2 specifically induces protein expression of DR5 in U2OS and A549 cells and DR4 in the A549 cell line (**Figure 4-9** and **Figure 4-10**). The upregulation of DRs is one of the most common mechanisms leading to the re-sensitisation of resistant cells to TRAIL-induced apoptosis. Several combination treatments and methods combining TRAIL-agonists and compounds have been described leading to the induction of DRs and thus re-sensitisation to TRAIL-induced apoptosis. These strategies range from co-treatment with DNA damaging agents (Naka et al., 2002), (Mendoza et al., 2008) to the use of proteasome inhibitors (Liu et al., 2008b, Liu et al., 2007). However, other possible receptor-associated mechanisms of sensitisation such as a shift in the ratio between DcRs and DRs (Prasad et al., 2011) or a change of DR formation in lipid rafts (Delmas et al., 2004, Psahoulia et al., 2007) have been described. Simultaneous knockdowns of DAPK2/DR5 in U2OS and A549 as well as DAPK2/DR4 in A549 cells reveals that, in both cell lines, DR5 is the main receptor for inducing TRAIL-mediated apoptosis (**Figure 4-12**). To test whether the observed induction of DR5 is sufficient for re-sensitisation and to exclude other potential sensitising processes, siDR5 was titrated and a concentration of siDR5 was established, capable of reverting the

DAPK2 RNAi mediated induction of DR5 (1.25 nM). These experiments were carried out in U2OS cells, as they do not express DR4 (**Figure 4-13a** + **b**), thus simplifying the results' interpretation. Co-transfection of siDAPK2 (20 nM) and siDR5 (1.25 nM) successfully rescues cells from siDAPK2 mediated TRAIL-sensitisation, suggesting that the TRAIL-resensitised phenotype of DAPK2-depleted cells is dependent on the upregulation of its key receptor DR5.

Having already established that depletion of DAPK2 did not impact on the sensitisation to TNF-α (**Figure 4-2e** + **j**) further investigations into the effect of DAPK2 knockdown on sensitisation to FasL were carried out. For that purpose, an anti-FAS IgM antibody that was first described in 1989 (Yonehara et al., 1989) and that is capable of clustering FasR, thus mimicking FasL-induced apoptosis (**Figure 4-16**) (henceforth referred to as FasL) was used. Our analysis revealed that under certain conditions DAPK2 depleted cells can also be sensitised to FasL-induced cell death. Interestingly, DAPK2 depleted U2OS cells are significantly sensitised to FasL-induced apoptosis to the same extent as U2OS cells with silenced c-FLIP (**Figure 4-16a**), whereas no sensitising effect is observed in A549 cells, which is also not sensitised to FasR by simply using RNAi against siFLIP (**Figure 4-16e**). As for the upregulation of DR5 and/or DR4 upon DAPK2 knockdown, FasR mRNA and surface-protein levels are also elevated in U2OS and A549 cells after transfection with siDAPK2 (**Figure 4-16**). Interestingly, mRNA of the soluble FasL decoy receptor, DcR3, is significantly downregulated in U2OS cells, whereas no such effect is observed in A549 cells (**Figure 4-16b** + **f**).

It thus seems likely that the mechanisms of sensitisation to FasL-induced cell death and TRAIL-induced cell death in DAPK2-depleted cells are essentially different. Under the experimental conditions used here, siDAPK2 leads to a significant downregulation of the FasR decoy receptor DcR3 transcript in U2OS cells (**Figure 4-16b**). Previously, it has been shown that the expression of DcR3 inversely correlates with the sensitivity to FasL-induced apoptosis (Li et al., 2007). This could explain the selective sensitivity of DAPK2 depleted U2OS cells to FasL. This is in contrast to DAPK2-depleted A549 cells, which remain resistant to FasL-induced cell death even after depletion of the well-described intracellular Fas signalling inhibitor c-FLIP (**Figure 4-16e** and **f**) (Scaffidi et al., 1999).

Overall, our work suggests that inhibition of DAPK2 in combination with TRAIL or TRAIL mimics may provide an alternative, novel approach to overcome TRAIL-resistance and may ultimately open new avenues for treatments of certain types of malignancies. Interestingly, DAPK2 depletion seems to induce expression of a variety of death receptors e.g. DR4, DR5 and FasR. This increased expression is facilitated most likely *via* a common transcription factor. Interestingly, DR4, DR5 and FasR share, amongst others, the transcription factor p53 (Liu et al., 2004), (Shetty et al., 2005, Muller et al., 1998) and can all be induced by members of the NF-κB-family of transcription factors (Mendoza et al., 2008, Shetty et al., 2005, Chan et al., 1999). The potential role and/or activation of these factors upon DAPK2 depletion will be described in **Chapter 5**.

5. DAPK2 depletion leads to the upregulation of DRs *via* NF-κB-family activation

5.1 Introduction

In **Chapter 4.** it has been shown that the depletion of DAPK2 sensitises TRAIL-resistant U2OS and A549 cells to TRAIL-induced apoptosis (**Figure 4-2**). It was further demonstrated that the siRNA-mediated knockdown of DAPK2 induced the upregulation of DR4, DR5 and FasR at the mRNA and protein level (**Figure 4-7** and **Figure 4-8**). Sensitisation to TRAIL-induced apoptosis was mainly facilitated by upregulation of DR5, as reverting DR5 levels to the levels of siNS-transfected cells rescued the sensitisation to TRAIL in U2OS cells (**Figure 4-12** and **Figure 4-13**). Besides transcriptional induction, it has been shown that DR5 can be upregulated *via* mRNA stabilisation or by an increase in protein stability. Treatment with the proteasome inhibitor PS-341 (Bortezomib or Velcade®) has been shown to induce DR5 *via* mRNA stabilisation at the 3′-untranslated region (Kandasamy and Kraft, 2008). Treatment with the plant flavonoid Quercetin has been described to increase protein stability but not mRNA stability of DR5 (Jung et al., 2010). In this chapter we sought to elucidate the mechanism(s) behind siDAPK2-mediated upregulation of DR5. Classical experiments were performed to assess the mRNA and protein stability of DR5 in DAPK2 depleted cells. Having established that the induction of DR5 in cells after DAPK2 depletion occurred at the transcriptional level, based on published work, we focused on the role of the transcription factors p53 and the NF-κB on the induction of DR5. The transcription factor p53, which has been described as the so-called ‘guardian of the genome’ (Lane, 1992), is a central regulator of the DNA damage response and is frequently mutated in cancer cells (Muller and Vousden, 2013). Tightly regulated by its ubiquitin ligase MDM2, p53 is activated by various types of

cellular stress (e.g. DNA damage, metabolic stress and ROS [reviewed in (Lakin and Jackson, 1999, Liu et al., 2008a, Puzio-Kuter, 2011)]) and it has been described to regulate the transcription of DRs and FasR. These receptors can be upregulated by p53 in response to DNA damaging agents such as 5-fluoruracil (5-FU) and cisplatin, or the inhibitor of p53's E3 ubiquitin ligase, Nutlin-3 (Henry et al., 2012, Meijer et al., 2013, Vassilev et al., 2004). When incorrectly regulated, the NF-κB family of transcription factors has been linked to many pathological conditions, especially cancer and inflammation [reviewed in (Karin et al., 2002, Lawrence, 2009)]. Similar to p53, activation of NF-κB upon treatment with etoposide, phorbol myristate acetate (PMA) and ionomycin (PMA/I) (Chan et al., 1999), or 2,3,7,8-tetrachlorodibenzo-p-dioxin (TCDD) (Singh et al., 2007) (Mendoza et al., 2008) has been shown to activate DR5, DR4 or FasR. To understand further the events downstream of siRNA-mediated depletion of DAPK2 and upstream of DR mRNA upregulation, we studied the role of p53 and NF-κB in siDAPK2-mediated TRAIL sensitisation and established that NF-κB is absolutely required for siDAPK2-mediated sensitisation to TRAIL-induced cell death whilst p53 is dispensable. We thus investigated the regulation of NF-κB by DAPK2 and, in the process, identified DAPK2 as a potential novel regulator of NF-κB signalling.

5.2 Results

5.2.1 Increased DR5 expression following DAPK2 knockdown is transcriptionally regulated and not due to altered mRNA or protein stability

To gain insight into the mechanism underlying the upregulation of DR5 mRNA and protein levels in response to DAPK2 knockdown, mRNA transcription and protein translation were inhibited and mRNA and protein stability assessed (**Figure 5-1**). Transcription was blocked by treating cells with actinomycin D (Act-D), a polypeptide antibiotic (Waksman et al., 1946), which prevents transcription by intercalating with DNA at the transcription initiation complex and thereby preventing mRNA elongation (Sobell, 1985). The experimental procedure for analysing DR5 mRNA stability is represented schematically (**Figure 5-1a**). Cells were treated with Act-D as indicated 48 h after transfection with either siNS or siDAPK2 oligonucleotides. Gene expression analysis was performed by qPCR, using HPRT and GAPDH as housekeeping genes. Fold change was calculated by normalising mRNA expression to samples that were not treated with Act-D for each transfection individually. As shown in **Figure 5-1 (b** + **c),** no significant difference in the mRNA stability of siNS or siDAPK2-transfected cells was observed. Interestingly, the DR5 mRNA half-life (50% of mRNA transcript) in U2OS cells was approximately 240 min, whereas it was longer than the time range assessed in A549 cells. To analyse protein stability, translation was blocked by cycloheximide (CHX) an inhibitor of the elongation phase of eukaryotic translation (Obrig et al., 1971, Schneider-Poetsch et al., 2010), which blocks translation and thus *de novo* protein synthesis, was used. The experimental procedure for analysing DR5 protein stability is represented schematically (**Figure 5-1d)**. Cells were treated with CHX as indicated 48 h after

transfection with either siNS or siDAPK2 oligonucleotides. DR5 protein levels were measured over time using SDS-PAGE/quantitative western blotting followed by densitometric analysis, where each value was normalised to the corresponding HSP90 loading control. Fold change was calculated by normalising protein expression of each set of transfections to samples that were not treated with CHX. For these analyses the $DR5_L$ isoform was used. As depicted in **Figure 5-1 (e** + **f)**, protein stability remained the same in U2OS and A549 cells regardless of DAPK2 expression levels. Protein half-life was approximately 1 h in both cell lines. There was a trend towards a shorter half-life in DAPK2-depleted cells in relation to siNS-transfected cells, which was not statistically significant. In short, the depletion of DAPK2 led to an up-regulation of DR5 mRNA and protein levels, which was not mediated by an increase in mRNA or protein stability, and which is consistent with a transcriptional effect.

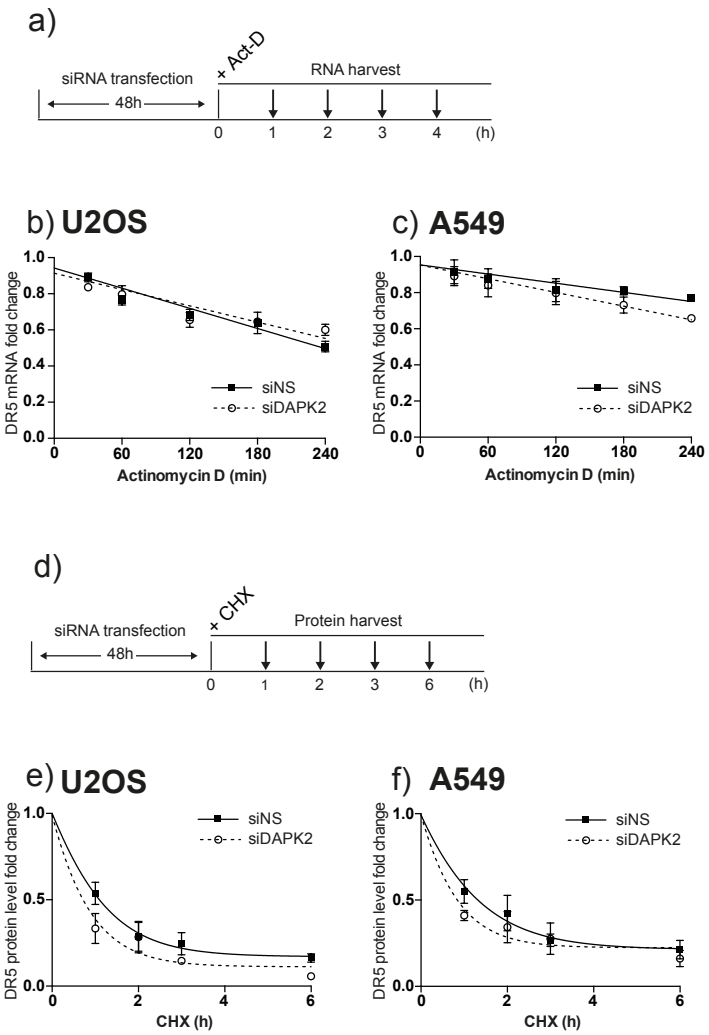

Figure 5-1. DR5 increased expression following the knockdown of DAPK2 is transcriptionally regulated and not due to alterations on mRNA or protein stability.

The experimental procedure for analysing DR5 mRNA stability is represented schematically in **(a)**. RNA stability was determined after RNAi against DAPK2 by inhibiting RNA synthesis with actinomycin D (Act-D) over the time periods indicated in the figure **(b, c)**. Experimental procedures used to analyse DR5 protein stability are represented in **(d)**. Protein synthesis was inhibited using cycloheximide (CHX) after 48 h transfection with siNS and siDAPK2 **(e, f).** DR5 protein levels were measured over time using SDS-PAGE/western blotting followed by densitometric analysis, where each value was normalised to the corresponding HSP90 loading control. For these analyses the $DR5_L$ isoform was used. The data represent the mean of three independent experiments ± SEM and no significant changes were detected using a two-way ANOVA test. I am grateful to Ms Sarah Stöcker for her contribution to these experiments.

5.2.2 DAPK2 depletion mediated sensitisation to TRAIL is independent of p53

Investigations into the role of p53 in siDAPK2-mediated upregulation of DR mRNA and sensitisation to TRAIL were also carried out. For that purpose, p53 mRNA levels in U2OS and A549 cells were measured, as p53 itself is one of the first transcriptional targets of p53 as part of a positive feedback loop (Deffie et al., 1993). As shown in **Figure 5-2**, RNAi-mediated depletion of DAPK2 in either U2OS or A549 cells did not lead to transcriptional induction of p53 mRNA. The cell cycle regulator p21 (CIP1/WAF1), one of the most studied and most immediate transcriptional targets of p53, can also provide a readout for p53 activation since it is mostly, but not exclusively, activated by p53 (Macleod et al., 1995). Interestingly, although p53 mRNA was not upregulated, there was a statistically significant ~2-fold upregulation of p21 mRNA in response to DAPK2 knockdown in U2OS and A549 cell (**Figure 5-2a** and **b**).

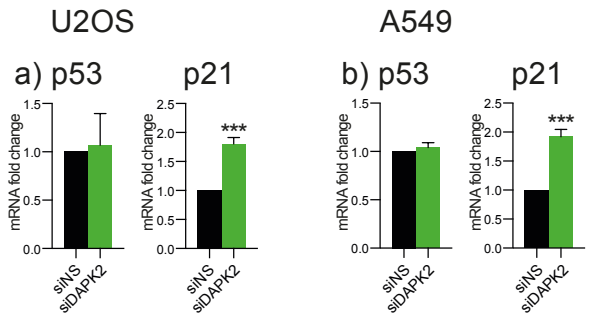

Figure 5-2. Depletion of DAPK2 does not affect p53 mRNA expression levels but induces its target p21.

U2OS **(a)** and A549 **(b)** cells were transfected with either siNS or siDAPK2 RNA oligonucleotides. Forty-eight h after transfection RNA was harvested, and p53 and p21 mRNA levels were analysed by qPCR. Data represent mean ± SEM of four independent experiments with duplicate samples. Statistical analysis was done using Student's *t*-test (paired, one tailed) (*** p< 0.005).

To further test whether p53 was involved in DAPK2 depletion-induced sensitisation to TRAIL-mediated apoptosis, p53-null prostate cancer PC3 cells and p53-mutated bladder carcinoma T24 cells were used. Whereas PC3 is a prostate adenocarcinoma cell line that lacks both p53 alleles, T24 cells carry a p53 mutant allele with an in-frame deletion of the TAC triplet encoding tyrosine 126 (**Table 3-1**) that leads to impaired activation of p53 upon induction of DNA damage (Konstantakou et al., 2009). As shown in **Figure 5-3 (a** + **c),** transfection of PC3 or T24 cells with siDAPK2 successfully downregulated DAPK2 protein levels. Interestingly, PC3 as well as T24 were readily sensitive to TRAIL-induced apoptosis at a concentration of more than 100 ng/ml (**Figure 5-3b** + **d,** black bars). Depletion of DAPK2 in p53-null PC3 cells, or in p53-mutated T24 cells led to a significant further increase in sensitivity towards TRAIL-induced apoptosis (**Figure 5-3b** + **d,** black bars *versus* green bars).

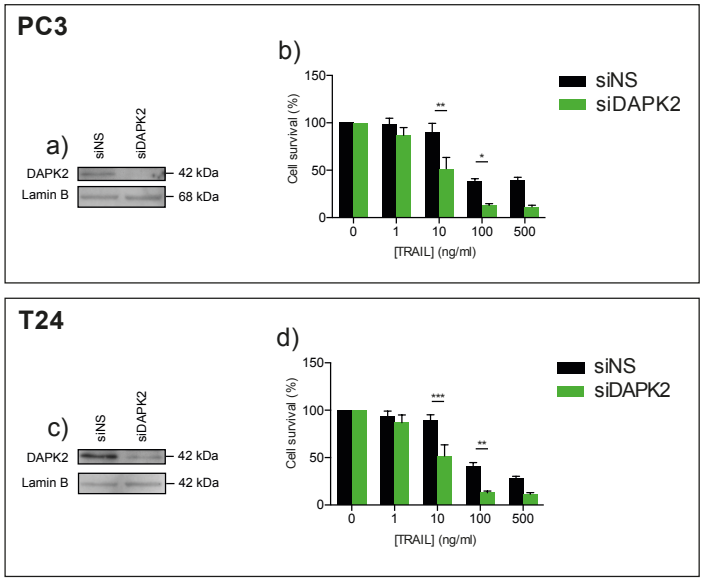

Figure 5-3. Knockdown of DAPK2 sensitises PC3 and T24 cells to TRAIL-induced cell death, in a p53-independent manner.

PC3 (**a**, **b**) and T24 (**c**, **d**) cancer cells were transfected with either siNS, or DAPK2 siRNA. Forty-eight h after transfection knockdown efficiency was determined by SDS-PAGE/western blotting (**a**, **c**). Data represent mean ± SEM of three independent experiments. For cell survival assays (PC3, **b** and T24, **d**), cells were re-plated into 96 well plates at a density of $2x10^4$ cells per well 24 h after siRNA transfection. The following day cells were treated with the indicated concentrations of TRAIL for 24 h. Cells were then fixed using methanol and stained with crystal violet. Crystals were dissolved in 10% (v/v) acetic acid and quantified by measuring the absorbance at 595 nm. Values were normalised to untreated control samples. Data represent mean ± SEM of three independent experiments performed in triplicates. Statistical analyses were done using two-way ANOVA test (* $p< 0.05$, ** $p<0.01$, *** $p< 0.005$).

Despite the fact that p53 itself was not found to be transcriptionally activated (**Figure 5-2a** + **b,** left graph), the data suggest that p53 was likely activated upon siRNA-mediated depletion of DAPK2, as, mRNA levels of p21 were upregulated by two-fold (**Figure 5-2a** + **b,** right graph). However, further experiments with p53-null PC3 and p53-mutated T24 cells revealed that wild-type, fully functional, p53 was dispensable for the molecular mechanism involved in the sensitization of these cells to TRAIL-induced apoptosis (**Figure 5-3b** + **d**). This suggested that while p53 might be transcriptionally activated in response to DAPK2 knockdown, it was not crucial for the observed sensitisation.

5.2.3 Depletion of DAPK2 activates the NF-κB-family of transcription factors

Given the fact that cellular p53 was dispensable to sensitise cells to TRAIL-induced apoptosis, the induction/activation of other transcription factors known to be involved in the regulation of the TNF receptor superfamily was analysed. As described earlier, the induction of DR4, DR5 and FasR has been linked not only to p53 but also the NF-κB-family of transcription factors. Experiments using NF-κB luciferase reporter assays to detect potential NF-κB activation in response to DAPK2 depletion were, therefore, performed. U2OS and A549 cells were transfected with either siNS or siDAPK2 and 24 h later with pNF-κB-Luc reporter *Firefly*-luciferase and CMV promoter/*Renilla*-luciferase plasmids. Forty-eight h later, luminescence was detected and normalised to the internal transfection control and to siNS. Interestingly, a significant increase in pNF-κB-Luc reporter activity in U2OS and A549 cells depleted of DAPK2 compared to siNS was observed (**Figure 5-4**).

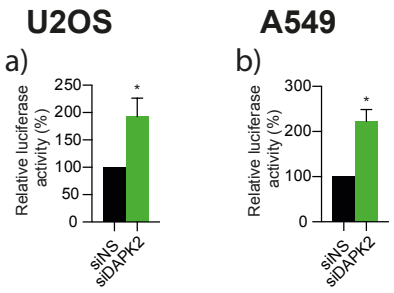

Figure 5-4. NF-κB is transcriptionally active in response to DAPK2 depletion.

Luciferase assays were performed to assess the transcriptional activity of NF-κB in response to DAPK2 knockdown in U2OS **(a)** and A549 **(b)**. RNAi-mediated DAPK2 depletion was induced 24 h prior to co-transfection with a pNF-κB-Luc reporter *Firefly*-luciferase and a CMV promoter/ *Renilla*-luciferase constructs. Twenty-four h later, both *Firefly- and Renilla*-luciferase activities were measured. Data were analysed by normalising the *Firefly*-luciferase to the luminescence obtained for the *Renilla*-luciferase construct. Data represent mean ± SEM of three independent experiments performed in triplicates. Statistical analysis was done using Student's *t*-test (paired, two tailed) (* $p < 0.05$). I am grateful to Ms Marina L. Georgiou for her contribution to the luciferase assays.

NF-κB signalling is highly complex and different members assemble into different dimers that then participate in canonical and non-canonical signalling pathways. The canonical pathway tends to involve NF-κB1 (p105/p50) and RELA (p65) or cREL, whereas the non-canonical pathway is thought to involve primarily NF-κB2 (p100/p52) and RELB. This distinction is not absolute and a great deal of signalling specificity is determined by the cell type and cellular environment (Ghosh and Karin, 2002, Tergaonkar, 2006). To further understand the effect of DAPK2 knockdown on NF-κB signalling, qPCR analyses of all five human NF-κB family members, namely NF-κB1, NF-κB2, RELA, RELB, and cREL were performed. U2OS and A549 cells were transfected with either siNS control or siDAPK2, and 48 h later RNA was harvested, reverse transcribed, and qPCR performed. These analyses revealed that the mRNA expression of NF-κB family members such as NF-κB1, NF-κB2 and RELB was strongly induced (2-3 fold) in both cell lines in response to DAPK2 knockdown (**Figure 5-5**). In addition, RELA

and cREL were found to be slightly but significantly upregulated in U2OS cells but not in A549 cells. Taken together, these results suggested that RNAi-mediated genetic ablation of DAPK2 led to the activation of NF-κB responses and to the transcriptional upregulation of NF-κB-family transcription factors.

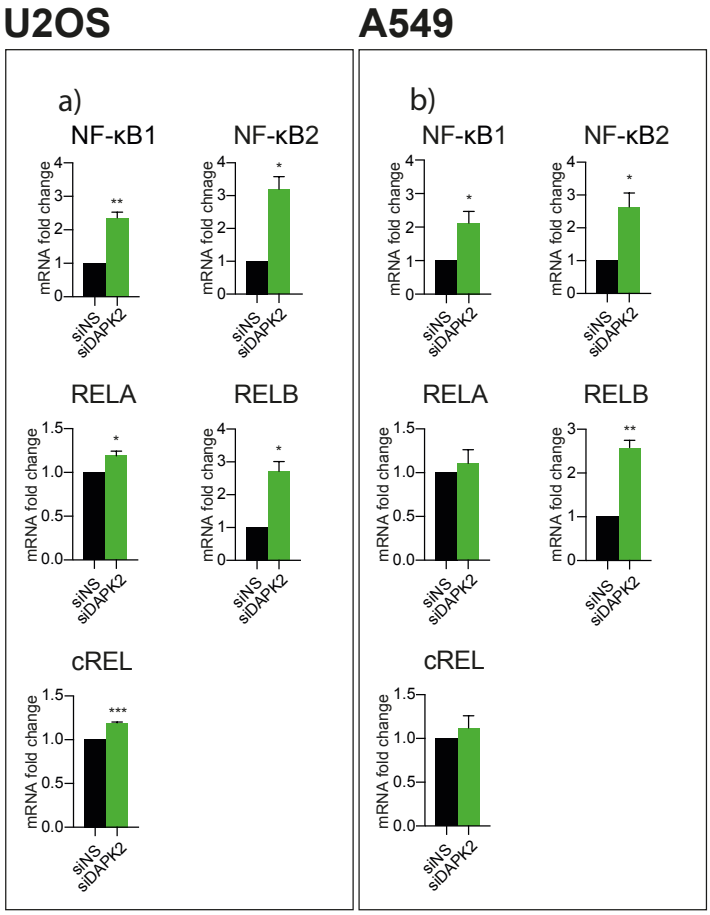

Figure 5-5. mRNA levels of NF-κB family members are upregulated in response to siDAPK2.

U2OS **(a)** and A549 **(b)** cells were transfected with either siNS or siDAPK2 RNA oligonucleotides. Forty-eight h after transfection RNA was harvested and NF-κB mRNA levels were analysed by qPCR. Data represent mean ± SEM of at least three independent experiments with duplicate samples. Statistical analysis was done using Student's *t*-test (paired, one tailed) (* p< 0.05, ** p<0.01, *** p< 0.005).

5.2.4 Elevated transcription of NF-κB in response to siDAPK2 translates into increased protein expression.

Using luciferase reporter assays it was established that the RNAi-mediated ablation of DAPK2 induced the NF-κB response. Indeed, in response to DAPK2 knockdown, the transcription of NF-κB1, NF-κB2 and RELB was strongly induced in both U2OS and A549 cells. In addition, RELA and cREL were also significantly upregulated in U2OS cells. To elucidate whether the elevated mRNA levels also translated into increased NF-κB activation, cells were transfected as before and proteins were extracted and separated on a polyacrylamide gel. Western blot membranes were then probed with antibodies specific to NF-κB1, NF-κB2, RELA and the activating phosphorylation of RELA (pS536). Protein expression analysis revealed that p100 and p52 (NF-κB2) were induced (**Figure 5-6c** + **d**) in response to DAPK2 knockdown, whilst p105 (NF-κB1) levels remained unchanged, with a slight increase in its proteolytic cleavage as demonstrated by a 1.5 and 2-fold increase in p50 expression in U2OS and A549 cells, respectively (**Figure 5-6a** + **b**). Importantly, RELA was robustly phosphorylated on S536 in both cell lines (**Figure 5-6e** + **f**). This suggested that the transcriptional upregulation at the mRNA level of NF-κB1 and NF-κB2 led to increased protein expression in DAPK2-depleted cells. Consistent with the mRNA results (**Figure 5-5a** and **b**), NF-κB2 was more strongly induced than NF-κB1 and no changes in the levels of total RELA protein were detectable. However, RELA was strongly phosphorylated on S536. These results suggest that in response to DAPK2 knockdown both branches of NF-κB signalling (canonical and non-canonical)

were engaged with phosphorylated RELA S536 as part of the canonical NF-κB activation and upregulated NF-κB2 as part of the non-canonical activation.

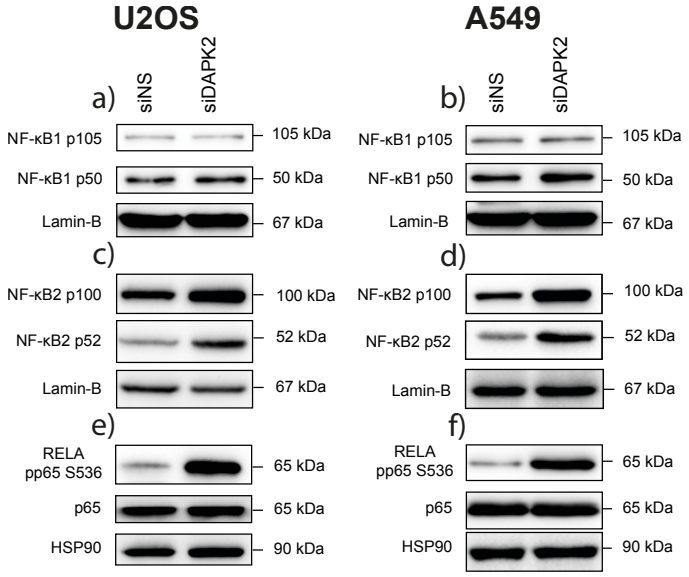

Figure 5-6. NF-κB family members are upregulated at the protein level in response to DAPK2 depletion.

U2OS **(a, c, e)** and A549 **(b, d, f)** cells were transfected with either siNS or DAPK2 siRNA. Forty-eight h after transfection the expression levels of NF-κB1 **(a, b)**, NF-κB2 **(c, d)**, RELA pp65-S536 and RELA **(e, f)** were evaluated by SDS-PAGE/western blotting. Lamin-B and HSP90 served as loading controls. Blots shown are representative of three independent experiments. I am grateful to Ms Marina L. Georgiou for her contribution to the western blots.

5.2.5 NF-κB activation induces the transcription of a variety of NF-κB target genes

In **Chapter 4.,** it was shown that the TNFR family members DR5 and FASR were transcriptionally induced in both U2OS and A549 cells upon DAPK2 depletion, as was DR4 in DAPK2-depleted A549 cells. Subsequent experiments revealed that NF-κB mRNA was induced (**Figure 5-5**), protein translated (**Figure 5-6**) and this was transcriptionally active in DAPK2-depleted cells (**Figure 5-4**). Additional probing into the transcriptional activation of NF-κB target genes and NF-κB

signalling-associated genes was thus carried out. U2OS and A549 cells were transfected with siNS and siDAPK2, mRNA was harvested, reverse transcribed and gene expression was analysed by qPCR, as before. Results for NF-κB target genes that are commonly used as readouts for NF-κB-activation as well as genes that are associated with NF-κB signalling but have not been shown to be induced by NF-κB directly are depicted in **Figure 5-7**. The death inducing ligand TNF-α, as well as its corresponding receptor, tumour necrosis factor receptor (TNFR) 2, have both been described as NF-κB target genes and are often activated as part of a positive feedback loop in response to cytokine stimulation (Perrot-Applanat et al., 2011, Hamilton et al., 2011). Interestingly, TNF-α mRNA levels were also significantly upregulated (2-fold) in U2OS and A549 cells (**Figure 5-7a** + **b**), whilst the levels of TNFR2 remained unaffected in U2OS cell (**Figure 5-7a**) but were strongly upregulated (> 6-fold) in A549 cells (**Figure 5-7b**). The transcription of the death-inducing ligand TRAIL itself, whose signalling and downstream killing mechanism are the main focus of this study, has also been described as an NF-κB-target gene (Baetu et al., 2001, Matsuda et al., 2005). Interestingly mRNA levels of TRAIL were not affected in U2OS, or A549 cells (**Figure 5-7a** + **b**). The effect of siDAPK2-mediated NF-κB activation on the transcription of cyclooxygenase-2 (COX2) and SOD2, both described as NF-κB targets, was also assessed (Xu et al., 1999, Yamamoto et al., 1995). COX2, also known as prostaglandin-endoperoxide synthase 2, is involved in the production of prostaglandins and it has been shown to trigger pro-inflammatory responses upon NF-κB-mediated induction (Ulivi et al., 2008). SOD2 is the mitochondrial member of the SOD family and has been to exhibit have anti-oxidative and anti-

inflammatory effects (Zelko et al., 2002, Hernandez-Saavedra et al., 2005, Velarde et al., 2012). SOD2 expression was significantly increased in both cell lines, with a stronger activation in A549 cells than in U2OS cells (**Figure 5-7a** + **b**). COX2, however, was only induced in response to DAPK2 depletion in A549 cells (**Figure 5-7a** + **b**). The opposite was true for the receptor-interacting serine/ threonine-protein kinase (RIPK) 2, another NF-κB target gene (Matsuda et al., 2003) which has also been associated with activation of NF-κB in response to T-cell receptor signalling (Ruefli-Brasse et al., 2004), as it was elevated in U2OS but not in A549 cells (**Figure 5-7a** + **b**).

To probe further into the specificity of the transcriptional response in DAPK2-depleted cells, the mRNA levels of TNFR1 and RIPK1 were also measured. Both genes have been associated with NF-κB signalling (Wajant and Scheurich, 2011, O'Donnell et al., 2007) but, critically, have not been described as NF-κB response genes. Neither of these genes was significantly affected by DAPK2 depletion-mediated induction of NF-κB (**Figure 5-7c** + **d**). We further assessed the mRNA levels of the proto-oncogene c-JUN, which has been described previously to be activated in parallel with NF-κB (Kharkwal et al., 2012, Sanchez-Perez et al., 2002), shown to directly interact with NF-κB and to increase the DNA-binding capacity of NF-κB (Wolter et al., 2008, Stein et al., 1993). As shown in **Figure 5-7 (c** + **d**) it was modestly upregulated in DAPK2 depleted U2OS and A549 cells and this was statistically significant. Together the data show that the depletion of DAPK2 led to the transcriptional upregulation of previously described NF-κB target genes and that the response was not totally identical in U2OS and

A549 cells, since some genes appear to be activated in one but not the other cell line. Moreover, genes that have been associated with NF-κB signalling, but have not been so far described as NF-κB targets, remained unaffected by DAPK2 knockdown-induced NF-κB activation in either of the studied cell lines.

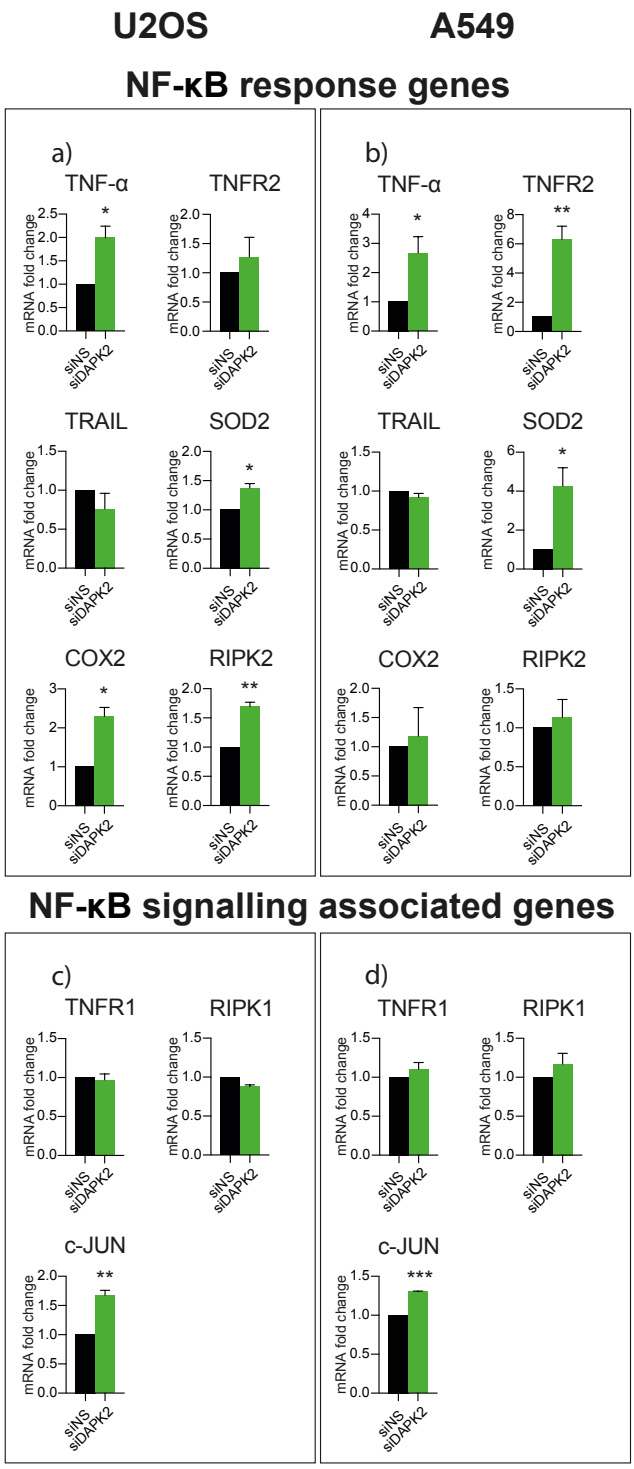

Figure 5-7. Effect of DAPK2 depletion on the induction of NF-κB-response and NF-κB-associated genes.

U2OS **(a** + **c)** and A549 **(b** + **d)** cells were transfected with either siNS or siDAPK2 RNA oligonucleotides. Forty-eight h after transfection RNA was harvested and mRNA levels of NF-κB target genes and NF-κB signalling associated genes were analysed by qPCR. Data represent mean ± SEM of at least three independent experiments with duplicate samples. Statistical analysis was done using Student's *t*-test (paired, one tailed) (* p< 0.05, ** p<0.01, *** p< 0.005).

5.2.6 Activation of NF-κB is causal for the sensitisation of U2OS and A549 cells to TRAIL in response to DAPK2 depletion

The absence of DAPK2 in U2OS and A549 cells sensitised these otherwise resistant cells to TRAIL-induced cell death *via* upregulation of DR5 and/or DR4 in what appeared to be a NF-κB-dependent manner. We hypothesised that if NF-κB activation was critical for the sensitisation, then knocking down its components should lead to a reversal of this phenotype. Cell survival assays were performed and RNAi against NF-κB1, NF-κB2, RELA and RELB with or without targeting DAPK2 concomitantly used to falsify the hypothesis. The efficiency of the double knockdown experiments was validated using qPCR (**Figure 5-8c** + **f** and **Figure 5-9c** + **f**). As depicted in **Figure 5-8a,** U2OS cells with silenced DAPK2 became resistant to TRAIL again only when NF-κB1 was absent. In contrast, A549 cells became resistant when either NF-κB1 or NF-κB2 was silenced (**Figure 5-8d** + **e**). Despite its strong phosphorylation (**Figure 5-6e** + **f**), RELA was redundant and its absence *per se* did not prevent DAPK2 silencing from sensitising U2OS or A549 cells to TRAIL-induced apoptosis (**Figure 5-9a** + **d**). Interestingly, silencing RELB did not effect the sensitisation of U2OS cells to TRAIL-mediated death (**Figure 5-9b**), but it partially blocked sensitisation of A549 cells (**Figure 5-9e**). Together the data suggested that NF-κB1 was necessary for the re-sensitization to TRAIL in DAPK2 depleted U2OS cell, whereas NF-κB1, NF-κB2 and RELB were involved in the re-sensitisation process of A549 cells. The canonical NF-κB pathway involves NF-κB1 (p105/p50) and RELA (p65), whereas the non-canonical pathway primarily involves NF-κB2 (p100/p52) and RELB. Thus, the absence of DAPK2 seems to activate both the canonical and the non-canonical

NF-κB pathway, and the activation seems to be different in U2OS and A549 cells.

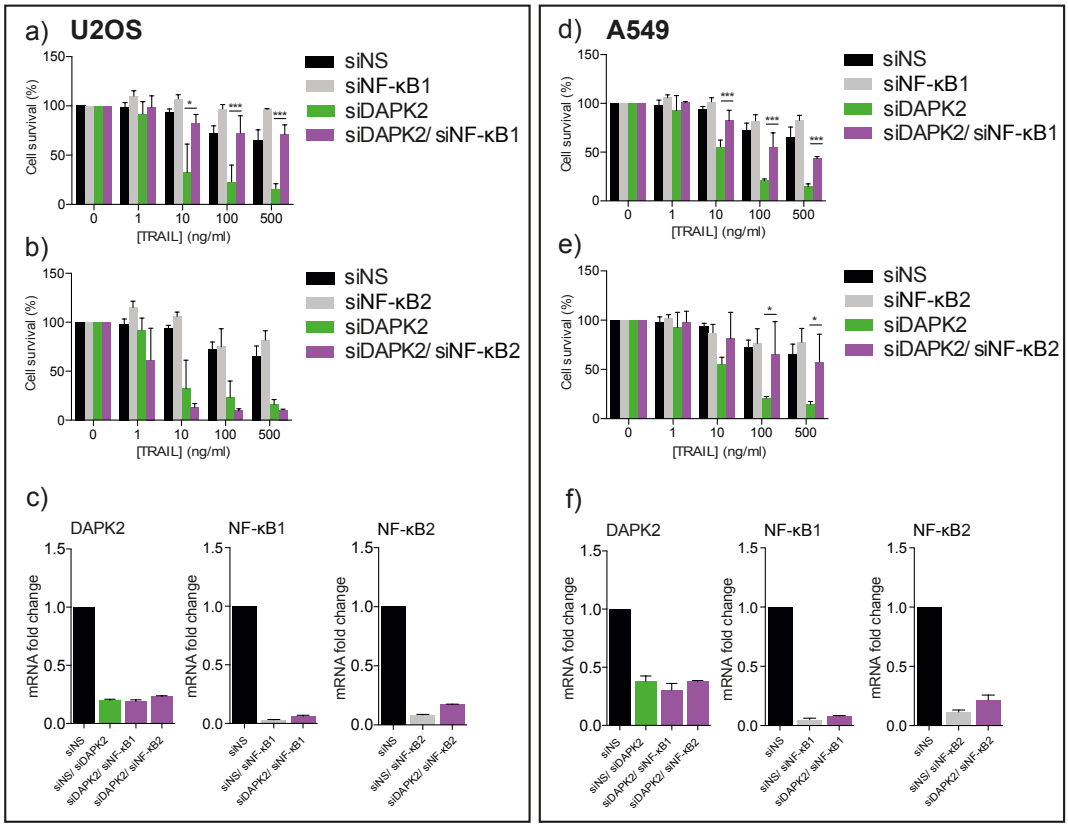

Figure 5-8. NF-κB1 and/or NF-κB2 are necessary for the sensitisation to TRAIL-induced cell death seen after DAPK2 silencing.

Double knockdowns were carried out in U2OS (**a, b, c**) and A549 (**d, e, f**) cells. For this purpose, cells were transfected with 40 nM of the following siRNA mixes: siNS+siNS, siDAPK2+siNS, siNS+NF-κB1 and siBID+NF-κB2. Twenty-four h after transfection cells were re-plated into 96 well plates at a density of $2x10^4$ cells per well. The following day cells were treated with TRAIL for 24 h at the indicated final concentrations (**U2OS: a, b; A549: d, e**). Cells were methanol-fixed and stained with crystal violet. Staining was dissolved in acetic acid and quantified by measuring the absorbance at 595 nm. Values were normalised to the untreated samples. Data represent mean ± SEM of three independent experiments performed in triplicates. Statistical analysis was done using two-way ANOVA test (* $p< 0.05$, ** $p<0.01$, *** $p< 0.005$). Forty-eight h after transfection and re-plating, RNA was harvested and double knockdown efficiency was confirmed (**U2OS: c; A549: f**). DAPK2, NF-κB1 and NF-κB2 mRNA levels were analysed by qPCR, data represent mean ± SEM of three independent experiments with duplicate samples.

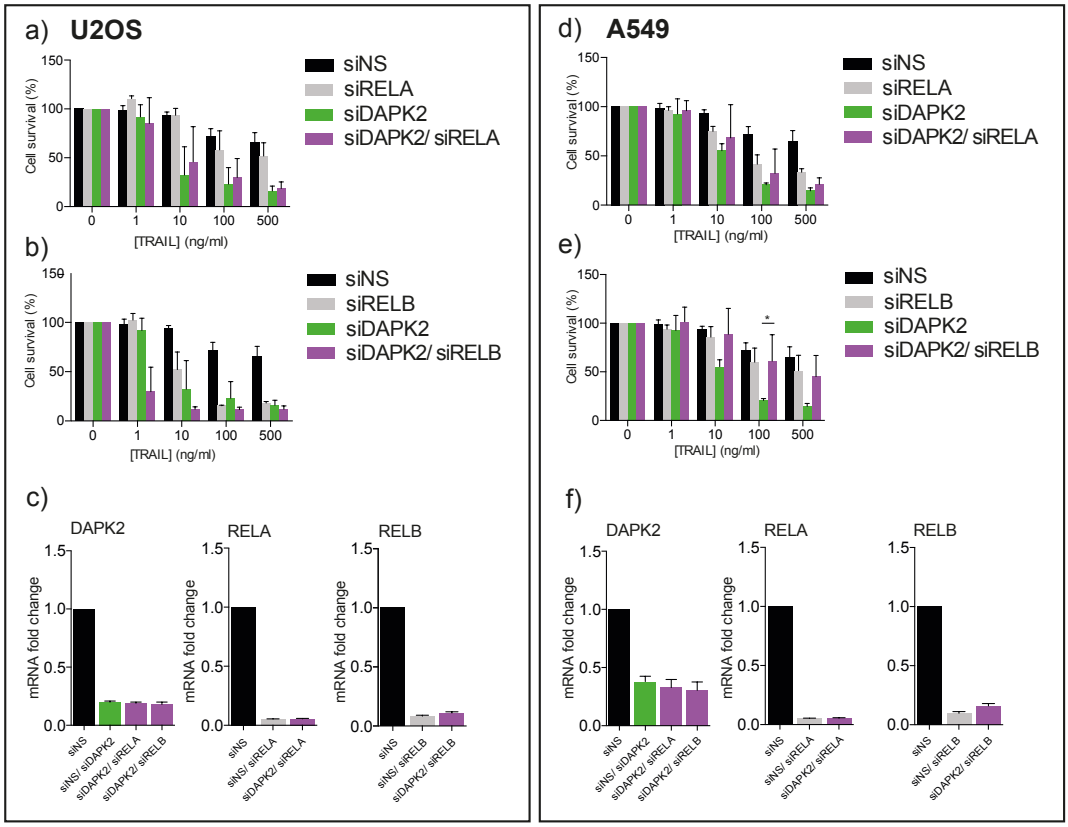

Figure 5-9. RELA and RELB are dispensable for the sensitisation to TRAIL-induced cell death seen after DAPK2 silencing.

Double knockdowns were carried out in U2OS (**a, b, c**) and A549 (**d, e, f**) cells. For this purpose, cells were transfected with 40 nM of the following siRNA mixes: siNS+siNS, siDAPK2+siNS, siNS+RELA and siBID+RELB. Twenty-four h after transfection cells were re-plated into 96 well plates at a density of $2x10^4$ cells per well. The following day cells were treated with TRAIL for 24 h at the indicated final concentrations (**U2OS: a, b; A549: d, e**). Cells were methanol-fixed and stained with crystal violet. Staining was dissolved in acetic acid and quantified by measuring the absorbance at 595 nm. Values were normalised to the untreated samples. Data represent mean ± SEM of three independent experiments performed in triplicates. Statistical analysis was done using two-way ANOVA test (* $p< 0.05$, ** $p<0.01$, *** $p< 0.005$). Forty-eight h after transfection and re-plating, RNA was harvested and double knockdown efficiency was confirmed (**U2OS: c; A549: f**). DAPK2, RELA and RELB mRNA levels were analysed by qPCR, data represent mean ± SEM of three independent experiments with duplicate samples.

5.2.7 Absence of DAPK2 leads to the NF-κB-mediated upregulation of DR5

Human DR5 is an NF-κB target gene, which possesses a NF-κB binding site in the first intronic region (Shetty et al., 2005) (depicted in **Figure 5-10a**). The effect of RNAi-mediated DAPK2 depletion on the activation of the DR5 promoter was investigated using luciferase reporter constructs. Accordingly, U2OS and A549 cells were transfected with either siNS or siDAPK2 and 24 h later with DR5 promoter pGL3 *Firefly*-luciferase constructs and CMV promoter/*Renilla*-luciferase plasmids. Forty-eight h later, luminescence was detected and normalised to the internal transfection control and to siNS. The DR5 promoter plasmids used in this study are schematically represented in **Figure 5-10a**. The full-length DR5 promoter plasmid spans over the whole promoter region of the DR5 gene from 1200 base pairs (bp) upstream of the transcription start site (TSS) to 2400 bp downstream into the gene and has been cloned into pGL3 vector. The other two constructs cover a smaller area of the DR5 promoter, mainly the intronic region of the DR5 promoter but include the well-characterised p53 and NF-κB binding sites of the human DR5 gene (Shetty et al., 2005) (**Figure 5-10a**). One of these promoter-intron plasmids contains a mutation of the NF-κB binding site (referred to as promoter-intron mt), which has been shown to abrogate NF-κB-mediated DR5 transcription (Shetty et al., 2005). The other second promoter-intron plasmid carries the wild-type sequence of the NF-κB binding site (referred to as promoter-intron wt). The DR5 promoter was clearly engaged upon transfection of both cell types with siDAPK2 (**Figure 5-10b** + **c** and **f** + **g**), and this engagement was abrogated if the NF-κB binding site on this promoter was mutated (**Figure 5-10c** + **g,** compare wt and mt), indicating the absolute requirement for NF-κB in

siDAPK2-mediated DR5 upregulation. All of the applied DR5 promoter luciferase constructs also contain the p53-binding site, which in case of the mutated NF-κB binding site (**Figure 5-10c** + **g**) was unable to compensate for the lack of NF-κB and promote full DR5 transcription. This was another piece of evidence lending further support to the hypothesis that DAPK2 depletion mediated re-sensitisation to TRAIL-induced cell death independently of p53 through mechanism(s) that relied on the activation of NF-κB.

NF-κB activation was clearly required for the transcriptional induction of DR5 in DAPK2 depleted cells. Further experiments, however, were carried out to verify these results by using RNAi against NF-κB1 with or without targeting DAPK2 concomitantly and assessing its effect on DR5 mRNA and protein levels. NF-κB1 was chosen, as previous double knockdown experiments revealed that RNAi-mediated depletion of NF-κB1 abrogated the re-sensitising effect of DAPK2 knockdown in both U2OS and A549 cells (**Figure 5-8a** + **d**). As shown in **Figure 5-10** (**d** + **h**) depletion of DAPK2 significantly induced DR5 mRNA in both cell lines, as described earlier. In contrast, knockdown of NF-κB1 on its own only had a small effect on DR5 mRNA levels in U2OS cells and none on the levels in A549. However, the combinatory knockdown of DAPK2 and NF-κB1 (compare green and purple bars) reverted the induction of DR5 in the absence of DAPK2. Importantly, these results were reproducible at the protein level (**Figure 5-10e** + **i**) where the induction of DR5 protein expression in response to DAPK2 depletion was reverted by simultaneous downregulation of NF-κB1 and DAPK2.

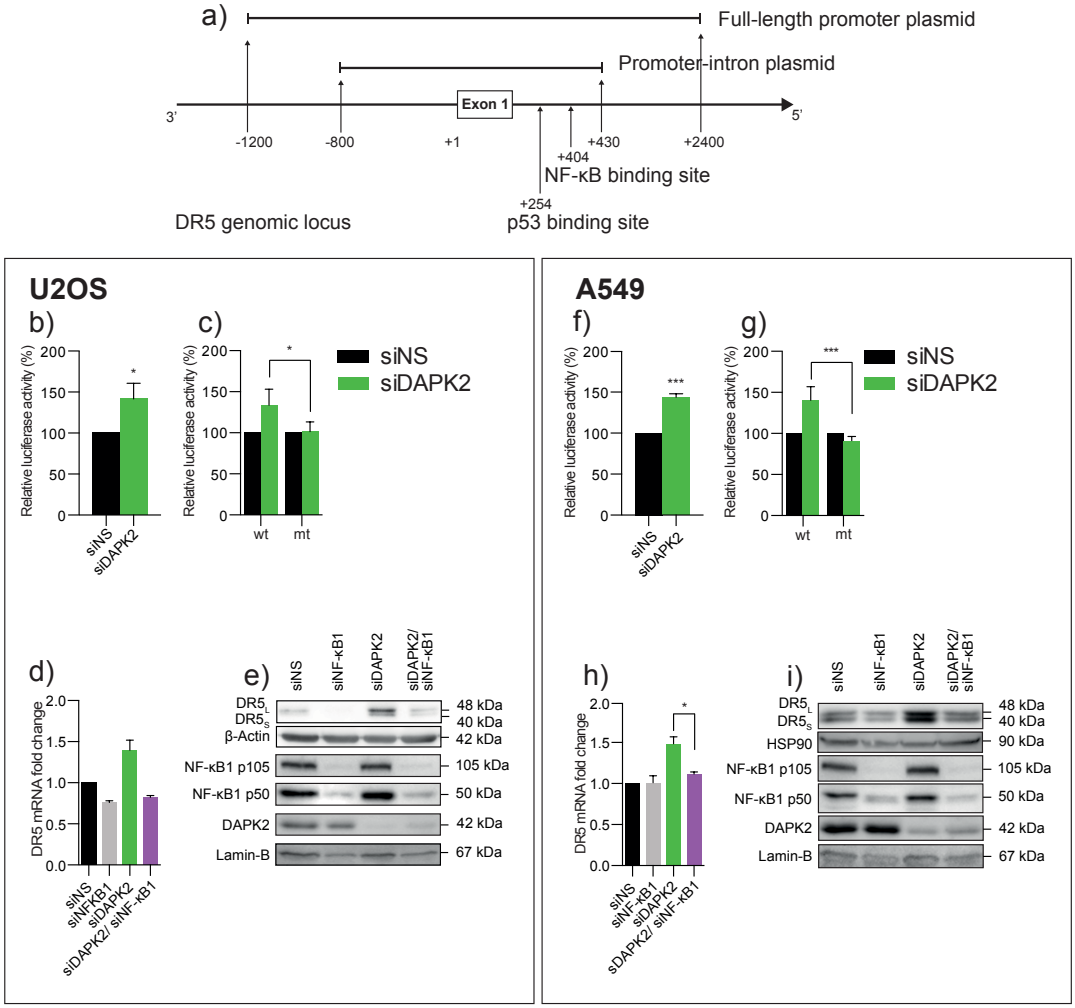

Figure 5-10. The transcription factor NF-κB is a critical component of DR5 expression and is necessary for the induction of DR5 after DAPK2 silencing.

The DR5 locus and plasmids used for DR5 promoter analyses are represented in **(a)**. As before, DAPK2 depletion was initiated in U2OS (**b** + **c**) and A549 cells (**f** + **g**) 24 h prior to co-transfection with the DR5 full-length promoter (**b, f**), DR5 promoter-intron wild-type (wt) or NF-κB mutated (mt) (**c, g**) plasmid *Firefly*-luciferase pGL3 construct and a CMV promoter/*Renilla*-luciferase construct. Twenty-four h later, both *Firefly- and Renilla*-luciferase activities were measured. Data were analysed by normalising the *Firefly*-luciferase to the luminescence obtained for the *Renilla*-luciferase activity. Data represent mean ± SEM of three independent experiments. Statistical analysis was done using Student's *t*-test (paired, two tailed) (* $p < 0.05$, *** $p < 0.005$). U2OS (**d** + **e**) and A549 (**h** + **j**) cells were transfected with either siNS or the following siRNA 1:1 mixes: siNF-κB1+siNS, siDAPK2+siNS, siDAPK2+ NF-κB1 (40 nM in total). Forty-eight h after transfection RNA and proteins were isolated and levels of DR5 mRNA (**d** + **h**) and protein were measured (**e** + **i**). I am grateful to Ms Marina L. Georgiou for her contribution to the luciferase assays.

5.2.8 Dissecting the upstream mechanisms leading to the activation of NF-κB in absence of DAPK2

DAPK2 depletion induced the activation of a NF-κB transcriptional response leading to the induction of a variety of NF-κB target genes, including DR5, which subsequently re-sensitised otherwise resistant cells to TRAIL-induced apoptosis. To gain a more dynamic insight into the NF-κB activation kinetics in DAPK2-depleted cells and gain further insight into the mechanisms upstream of such activation, a series of experiments were carried out using the death inducing ligand TNF. Besides activating the MAPK pathway and inducing extrinsic apoptosis, the third main pathway initiated by TNF-α is the activation of NF-κB (Wajant et al., 2003). As neither U2OS nor A549 were sensitive (or could be sensitised) to TNF-α-induced cell death by silencing DAPK2 (**Figure 4-2**), TNF-α was used to induce NF-κB signalling and study the effect of DAPK2 knockdown on the latter. Briefly, activation of NF-κB through TNF-α occurs as follows: IκBα inhibits NF-κB signalling by masking the nuclear localisation sequence of NF-κB transcription factors and thereby inhibiting nuclear translocation and DNA binding (Perkins, 2000). Downstream processes upon binding of TNF-α to TNFR1 remove this blockage (Pahl, 1999). Ligation of TNF-α to TNFR1 induces a conformational change in the intracellular domain of the receptor; leading to the recruitment of TRADD to its death domain. TRADD functions as an adaptor molecule for the binding of TRAF2 and RIPK1 (Hsu et al., 1996a, Hsu et al., 1996b). TRAF2 is needed for the recruitment of the IκB kinase (IKK) complex, whereas RIPK1 activates the IKKs by phosphorylation (Devin et al., 2000). The

activated IKK complex subsequently phosphorylates IκBα, induces its proteasomal degradation and activates NF-κB (Karin, 1999).

U2OS and A549 cells were transfected with either siNS or siDAPK2 as described before, treated with TNF-α for varying periods of time as indicated, and proteins were extracted and separated on a polyacrylamide gel. Western blot membranes were subsequently probed with antibodies specific to NF-κB key molecules known to be activated downstream of TNF-α. The results for U2OS cells and A549 cells are shown in **Figure 5-11 (a** + **b),** respectively**,** and are very similar in both cell lines. Transfection of U2OS or A549 with siDAPK2 caused a decrease of IκBα protein levels, and to the activation of NF-κB. The reduction of IκBα was already detectable independently of any stimulation with TNF-α, in untreated samples transfected with siDAPK2 when compared to cells transfected with a non-targeting siRNA control. However, *de novo* synthesis of IκBα was also reduced in response to TNF-α, (compare the TNF-α 30 min and 120 min time point with and without siDAPK2). It must be pointed out that DAPK2 and IκBα have very similar sizes. As the DAPK2 blot was done after the WB membranes were probed for IκBα, the signal from the IκBα antibody was still picked up when the membranes were re-probed for DAPK2. As described earlier (**Figure 5-6e** + **f**) absence of DAPK2 lead to increased baseline phosphorylation of RELA on S536. This was clearly independent of TNF-α, which in A549 cells was only visible after a long exposure of the WB (**Figure 5-11b**). Comparing the 120 min time point of TNF-α stimulation in siNS and siDAPK2 cells, the phosphorylation of RELA S536 in DAPK2-depleted cells was slightly increased, hinting towards a

prolonged activation of RELA S536 phosphorylation in DAPK2-depleted cells. Changes in total RELA levels in response to TNF-α, especially visible in A549 cells (**Figure 5-11b**), were unlikely to be caused by protein degradation as the timeframe here would be too short. More likely, the signal for phosphorylated RELA in A549 cells was so strong that it was difficult to fully strip the membrane and masked the RELA signal when the membrane was re-probed for total RELA. Furthermore, no changes in the total levels of IKK-α, part of the IKK complex were observed in either U2OS, or A549 cells. Taken together, it seemed that DAPK depletion led to chronic phosphorylation of RELA S536, independent of extrinsic NF-κB activation, which was accompanied by a chronic degradation of IκBα.

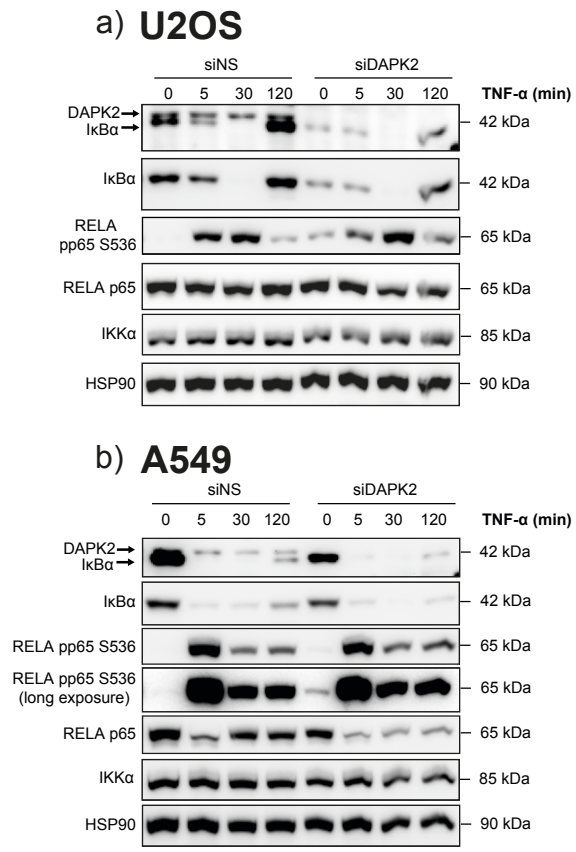

Figure 5-11. Effect of DAPK2 depletion on molecular NF-κB signalling events downstream of TNF-α stimulation.

U2OS (**a**) and A549 (**b**) cells were transfected with siNS and siDAPK2. Forty-eight h later, cells were treated with TNF-α (10 ng/ml) for the indicated time points. NF-κB signalling events were assessed by SDS-PAGE/western blotting. IκBα degradation, levels of RELA pS536 and total RELA used as readouts. Knockdown of DAPK2 was confirmed by SDS-PAGE/western blotting. HSP90 served as loading control. Blots shown are representative of two independent experiments. I am grateful to Ms Maria M. Misterek for her contribution to these western blots.

5.2.9 Effect of DAPK2 overexpression on the activation of NF-κB by TNF-α

The absence of DAPK2 led to a chronic decrease of IκBα and subsequently chronic increase of RELA S536 phosphorylation independent of extrinsic NF-κB stimulants. To shed further light into the role of DAPK2 in the regulation of NF-κB tetracycline-inducible U2OS cells, which contained either wild-type (HA-DAPK2.wt) or kinase-dead DAPK2 (HA-DAPK2.K42A) constructs were

generated. We wanted to assess whether overexpression of DAPK2 led to the opposite phenotype observed after DAPK2 knockdown. As DAPK2 is a protein kinase we also wanted to assess whether over-expression of a kinase mutant DAPK2, a so-called dominant-negative protein, would mimic the effect of DAPK2 siRNA on NF-κB. Single cell clones for DAPK2 wt and kinase-dead were produced as described in detail in **3.2.2**. The expression of DAPK2 constructs was induced with DOX 24 h prior to the exposure to TNF-α. Treatment with TNF-α for varying periods of time was performed as indicated. Western blot membranes were subsequently probed with antibodies specific to NF-κB key molecules known to be activated downstream of TNF-α. Wild-type DAPK2 was successfully overexpressed upon treatment with DOX with no leaky expression of HA-DAPK2 present in untreated cells (**Figure 5-12a**). Overexpression of DAPK2 without TNF-α stimulation seemed to slightly decrease basal levels of IκBα protein expression (compare 0 min time point of TNF-α stimulation - and + DOX treatment). More pronounced was the effect of DAPK2 overexpression on the phosphorylation of RELA S536. When DAPK2 was present in excess, TNF-α induced phosphorylation of RELA S536 was dampened (compare 5 min and 30 min time point of TNF-α stimulation - and + DOX treatment). Total levels of RELA remained unaffected and visible differences were most likely caused by antibodies for phosphorylated RELA masking the total RELA signalling.

As for the U2OS TetR cells overexpressing wild-type DAPK2, kinase-dead DAPK2 was successfully overexpressed upon DOX stimulation and no background expression was detectable (**Figure 5-12b**). Similarly to U2OS cells

transfected with siDAPK2 (**Figure 5-11a**), an increased baseline phosphorylation of RELA S536, independent of TNF-α stimulation, was observed. Overexpression of kinase-dead DAPK2 did not exert a significant impact on the kinetics of RELA S536 phosphorylation. Interestingly, basal IκBα protein levels remained unaffected upon overexpression of kinase dead DAPK2, whereas after 120 min of TNF-α stimulation the IκBα *de novo* synthesis appeared delayed, with is consistent with data obtained in the absence of DAPK2 (**Figure 5-11a** + **b**). Taken together, overexpression of wild-type DAPK2 dampened TNF-α mediated activation of NF-κB, as assessed by using phosphorylation of RELA S536 as a readout. When overexpressed, kinase-dead DAPK2 induced basal phosphorylation of RELA S536, as seen after siRNA-mediated depletion of DAPK2. However, the effect on IκBα was less pronounced in these cells than in cells depleted of DAPK2 after RNAi. Thus, the overexpression of wild-type DAPK2 inhibited the activation of NF-κB, whereas overexpression of kinase-dead DAPK2 partially mimicked the results obtained by knocking down DAPK2, leading to the phosphorylation of RELA S536.

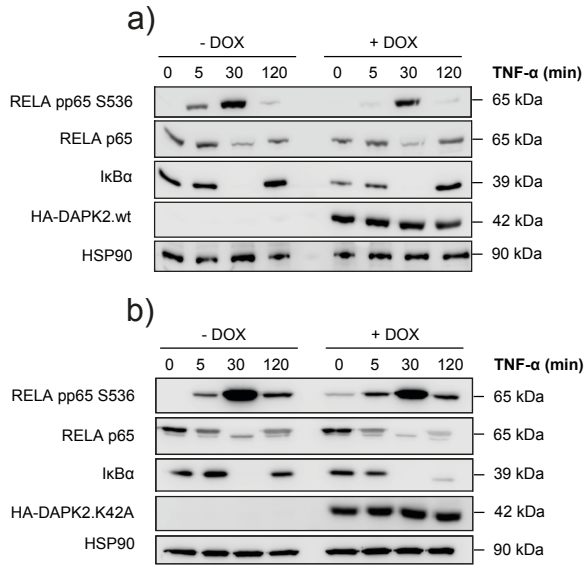

Figure 5-12. Overexpression of wild-type and kinase dead DAPK2 affects NF-κB signalling events downstream of TNF-α stimulation.

U2OS TetR HA-DAPK2.wt (wild type) (**a**) and U2OS TetR HA-DAPK2.K42 (kinase dead) (**b**) cells were stimulated with transfected with doxycycline (DOX) (10 ng/ml). Twenty-four h later, cells were treated with TNF-α (10 ng/ml) for the indicated time points. NF-κB signalling events were assessed by SDS-PAGE/western blotting. IκBα degradation, levels of RELA pS536 and total RELA were used as readouts. Overexpression of HA-DAPK2 was confirmed by SDS-PAGE/western blotting. HSP90 served as loading control. Blots shown are representative of three independent experiments. I am grateful to Ms Maria M. Misterek for her contribution to these western blots.

So far, all data provided evidence for cross-talk between NF-κB and DAPK2, with the lack of DAPK2 leading to basal activation of NF-κB (**Figure 5-11**) and DAPK2 overexpression suppressing NF-κB signalling (**Figure 5-12a**). To analyse the effect that NF-κB activation had on the expression levels of DAPK2, U2OS and A549 cells were incubated with TNF-α to induce the activation of NF-κB, as before. The effect of NF-κB activation on DAPK2 protein levels was studied over a time period of up to 72h. The levels of DAPK2 in U2OS cells were greatly decreased after 72 h of stimulation with TNF-α (**Figure 5-13a**), whereas in A549 cells a strong reduction of DAPK2 levels was already detectable after a period of 48 h (**Figure 5-13b**). These results should be considered preliminary as the

experiment was only carried out once. Taken at face value though, the results suggested, that DAPK2 was directly affected in response to the activation of NF-κB by TNF-α and lent further support to the concept that DAPK2 is a novel inhibitory protein for activation of NF-κB.

The founding member of the DAPK-family has been associated with various types of induced cell death and it has been found to be directly associated with the TNF-α receptor TNFR1, the adaptor molecule TRADD and, more interestingly, with the adaptor molecule FADD, which plays an important role in TRAIL-induced apoptosis (Henshall et al., 2003). DAPK2 has only been described to directly interact with transforming growth factor β receptor 1 (TGFBR1). To assess the possibility of a direct interaction between DAPK2 and the TRAIL receptor DR5, co-immunoprecipitation was performed. Due to the lack of suitable DAPK2 antibodies, expression of HA-tagged DAPK2 was induced in U2OS TetR HA-DAPK2.wt cells and HA-DAPK2 was precipitated using beads covalently coupled to an anti-HA antibody. Membranes were probed with a DR5 antibody (rabbit), revealing an interaction between DAPK2 and DR5 (**Figure 5-14**, compare lane five - DOX with lane six + DOX). As a control, membranes were additionally probed with a HA-specific mouse antibody, showing the specific induction and precipitation of HA-DAPK2 in DOX-treated cells.

Taken together these data suggest that DAPK2 was likely to play an important role in the regulation of NF-κB signalling, as its downregulation induced the activation of NF-κB upstream of IκBα and its overexpression clearly inhibited the activation of RELA in response to TNF-α-induced NF-κB. Moreover, the

overexpression of a kinase-dead DAPK2 partially mimicked knocking down DAPK2, as it also led to the basal phosphorylation of RELA. DAPK2 itself was clearly downregulated upon chronic activation of NF-κB, supporting the hypothesis of DAPK2 functioned as an upstream inhibitor of NF-κB signalling. The direct interaction with DR5 suggested that DAPK2 might interact with upstream modulators of TRAIL-induced apoptosis and/or activators of NF-κB.

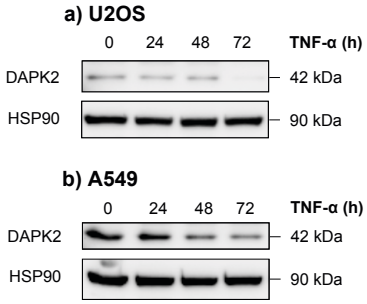

Figure 5-13. Effect of prolonged TNF-α stimulation on DAPK2 stability.

U2OS (**a**) and A549 (**b**) cells were treated with TNF-α (10 ng/ml) for the indicated time points. Levels of DAPK2 in response to TNF-α stimulation were assessed by SDS-PAGE/western blotting. HSP90 served as loading control. The experiment was performed once.

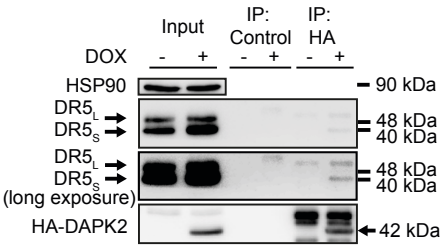

Figure 5-14. DAPK2 directly interacts with DR5.

U2OS TetR HA-DAPK2.wt cells were treated with doxycycline (DOX) at a concentration of 10 ng/ml to induce the expression of HA-DAPK2. Twenty-four h later, cells were lysed and incubated overnight with either beads that were covalently bound to anti HA antibodies or uncoupled beads. The next day input samples (1/10 of the pull down) and pull down samples were assessed by SDS-PAGE/western blotting. The membrane was subsequently probed with DR5 and anti-HA antibodies. HSP90 served as loading control for the input samples. Blots shown are representative of two independent experiments.

5.3 Discussion

In **Chapter 4.** it was shown that the depletion of DAPK2 by RNAi sensitised resistant cancer cell lines to TRAIL-induced apoptosis, but not to a wide variety of other death stimuli. It was additionally shown that the sensitising effect was due to the upregulation of DR5 and, in some cell lines, also DR4. Moreover, DAPK2 knockdown induced the expression of FasR and it sensitised U2OS cells to FasL-induced cell death.

Induction of all these receptors both at the mRNA and protein level led to the hypothesis that a common transcription factor was likely activated in response to DAPK2 knockdown and that this was responsible for inducing the transcription of DR4, DR5 and FasR. The transcription factor p53, as well as the NF-κB-family of transcription factors have both been described to be involved in the transcription of DR4, DR5 and FasR. To gain further insight into the mechanisms of siDAPK2-mediated sensitisation to TRAIL-induced apoptosis, we focused on the role of p53 and the NF-κB transcription factors. It has been previously described that DRs cannot only be induced through increased transcription but also *via* mRNA stabilization (Kandasamy and Kraft, 2008) or increased protein stability (Jung et al., 2010). DR induction leads to an increase of the number of receptor molecules on the cell surface thus overcoming the threshold required to sensitise cells to TRAIL cytotoxicity. As U2OS cells do not express DR4 and silencing DAPK2 led to the upregulation of DR5 in both U2OS and A549 cells (**Figure 4-8**), we focused on the regulation of DR5 induction/expression upon DAPK2 depletion. Using classical biochemical assays we were able to show that depletion of

DAPK2 did not increase the mRNA (**Figure 5-1b** + **c**) or protein (**Figure 5-1e** + **f**) stability of DR5. However, DR5 and DR4 mRNAs were elevated after silencing DAPK2 (**Figure 4-7**), suggesting that inhibition of DAPK2 led to the transcriptional regulation of DRs. As mentioned earlier, the well-studied DR5 receptor gene is regulated by a variety of transcription factors, such as p53 and NF-κB. We discovered that DAPK2 knockdown did not lead to a transcriptional induction of p53 mRNA. However, the cell cycle regulator p21 (CIP1/WAF1), one of the most studied and immediate transcription targets of p53 often used as a readout for p53 activation (Macleod et al., 1995), was upregulated when DAPK2 was silenced (**Figure 5-2a** + **b**). The fact that DAPK2 silencing could also sensitise p53-mutated T24 colon cancer cells and p53-null prostate cancer PC3 cells argues against the absolute requirement for p53 (**Figure 5-3**). However, it has been shown that the functions of p53-transcription factor family members p63 and p73 have certain redundancies with p53. Isoforms of p73 and p63 have also been shown to induce apoptosis in response to DNA damage (Ramadan et al., 2005, Petitjean et al., 2008) and both are capable of inducing p21 (CIP1/WAF1) (Levrero et al., 2000). Furthermore it has been shown that p21 can also be activated by NF-κB (Basile et al., 2003). We therefore focused on the activation of NF-κB upon DAPK2 depletion. Using NF-κB luciferase reporter assays it was shown that NF-κB is transcriptionally active in response to DAPK2 knockdown (**Figure 5-4**). This is interesting, as NF-κB plays an ambiguous role in TRAIL signalling. For example, there are reports suggesting an anti-apoptotic role for NF-κB, involving the up-regulation of the DcR1 (Bernard et al., 2001), or of anti-apoptotic BCL-X_L (Zender et al., 2005), whereas other reports suggest a pro-apoptotic role due to the induction of DR4 or DR5 (Mendoza et al., 2008,

Shetty et al., 2005). Interestingly, binding of TRAIL to DcR2, that contains a truncated DD, has been shown to activate NF-κB, which then initiates a negative feedback loop protecting cells from TRAIL-induced apoptosis (Degli-Esposti et al., 1997a). NF-κB signalling is highly complex and different members assemble in different dimers that then participate in canonical and non-canonical signalling pathways. Canonical pathways have been described to involve NF-κB1 (p105/p50) and RELA (p65) and the non-canonical pathway is thought to involve primarily NF-κB2 (p100/p52) and RELB. Distinction between these pathways is not absolute and much depends on the cellular environment and specific cell type (Tergaonkar, 2006). Further analyses using qPCR and SDS-PAGE/western blotting revealed that components of the canonical (RELA and NF-κB1) as well as components of the non-canonical (NF-κB2) pathways were transcriptionally upregulated upon DAPK2 depletion in both cell lines studied (**Figure 5-5**). RELA, an important factor of the canonical NF-κB activation was found to be consistently phosphorylated in response to RNAi-mediated DAPK2 depletion. Proteolytic processing of NF-κB1 p105 to NF-κB1 p50 seemed to be unaffected in U2OS cells (**Figure 5-6a**) but was slightly increased in A549 cells (**Figure 5-6b**). NF-κB1 p100 was found to be significantly processed in both cell lines studied (**Figure 5-6c** + **d**). Overall, DAPK2 depletion induced the activation of NF-κB-family transcription factors without specifically activating the canonical or non-canonical signalling branch. Further analysis of NF-κB target genes, that have previously been used as readouts for NF-κB activation, revealed a differential expression upon DAPK2 knockdown in U2OS compared to A549 cells. TNF-α and SOD2, however, were induced in both cell lines. Interestingly, c-

JUN, which has often been found to be co-activated with NF-κB was also induced after DAPK2 silencing (**Figure 5-7**) [22, 45]. To unravel the complex role of NF-κB in TRAIL signalling, we then performed double knockdown experiments (**Figure 5-8** and **Figure 5-9**). By analysing the effect of TRAIL on U2OS and A549 cells transfected with siRNA targeting DAPK2 concomitantly with siRNAs directed against NF-κB family members, we identified NF-κB1 as key molecules responsible for a sensitisation to TRAIL-induced apoptosis in response to DAPK2 depletion (**Figure 5-8a** + **b**). Interestingly, in A549 cells, knockdown of NF-κB2 and RELB in combination with DAPK2 also resulted in a partial rescue. Remarkably, RELA (p65), which was consistently phosphorylated on S536, did not seem to be involved in the siDAPK2 mediated sensitisation to TRAIL (**Figure 5-8e, Figure 5-9e**). It thus appears that U2OS cells require mainly the activation of the NF-κB canonical pathway, whereas A549 cells require the activation of both the canonical and non-canonical pathways. It is still unclear why this is, but it is fair to assume that, due to distinct cellular environments in these two cell lines, silencing DAPK2 leads to the formation of different NF-κB dimers which are nevertheless capable of resulting in an identical biological response, namely upregulation of DR5. As described in **Chapter 4**, the fact that A549 seems to also require BID to be fully sensitised to TRAIL after DAPK2 silencing may be related to the partial requirement for NF-κB2/RELB. It is also possible that NF-κB2 and/or RELB are required to induce DR4, which is not expressed in U2OS cells. In 2005, Shetty and colleagues characterised the specific NF-κB binding site in the first intron of the DR5 gene. Indeed, using DR5 promoter luciferase constructs with either wild type or mutated NF-κB consensus sites (**Figure 5-10a**)

we established the necessity of NF-κB as a transcription factor required for the induction of DR5 in response to DAPK2 depletion (**Figure 5-10c** + **g**). Recently, Yoo and colleagues have suggested that DAPK1 can function as a repressor for NF-κB activation (Yoo et al., 2012). Additionally, NF-κB activation downstream of T cell receptor signalling is increased in DAPK1 knockout T cells (Chuang et al., 2008). Moreover, DAPK1 has been found to interact with the TNF-α receptor TNFR1 (Henshall et al., 2003), NEMO [also known as inhibitor of nuclear factor kappa-B kinase subunit gamma (IKK-γ)] (Fenner et al., 2010) and the adaptor molecule FADD, which plays a crucial role in TRAIL-induced apoptosis (Henshall et al., 2003). As all DAPK family members are thought to form multi-protein complexes (Gozuacik and Kimchi, 2006), the activation of NF-κB proteins upon DAPK2 knockdown is likely to be caused by at least some of the same molecular events described for DAPK1. DAPK2 has only been described to directly interact with TGFBR1. Here, we showed that DAPK2 directly interacts with the TRAIL-receptor DR5 (**Figure 5-14**), which immediately suggests the possibility that DAPK2 may be part of a multi-protein complex influencing signalling downstream of DRs.

Interestingly, Yukawa and co-workers (Li et al., 2004) showed, using a high concentration of siDAPK1, that downregulation of DAPK1 in endometrial cancer cells led to cell death. They hypothesised that this was due to the induction of TRAIL, DR4 and DR5 mRNAs. In contrast to their findings for DAPK1, we did not observe an induction of TRAIL (**Figure 5-7**) or DcR expression (**Figure 4-7**), nor did we observe apoptosis 48 h post-siDAPK2 transfection. What we did observe after knocking down DAPK2, as they did for DAPK1, was the upregulation of DR4

and DR5, depended on the activation of NF-κB and on the integrity of NF-κB1 proteins (p50 and p105). Overall these observations suggests that DAPK2 is a potential novel modulator of NF-κB signalling, possibly associated with the multi-protein complex downstream of TNFR family members. The proposed model is depicted in Figure 5-15.

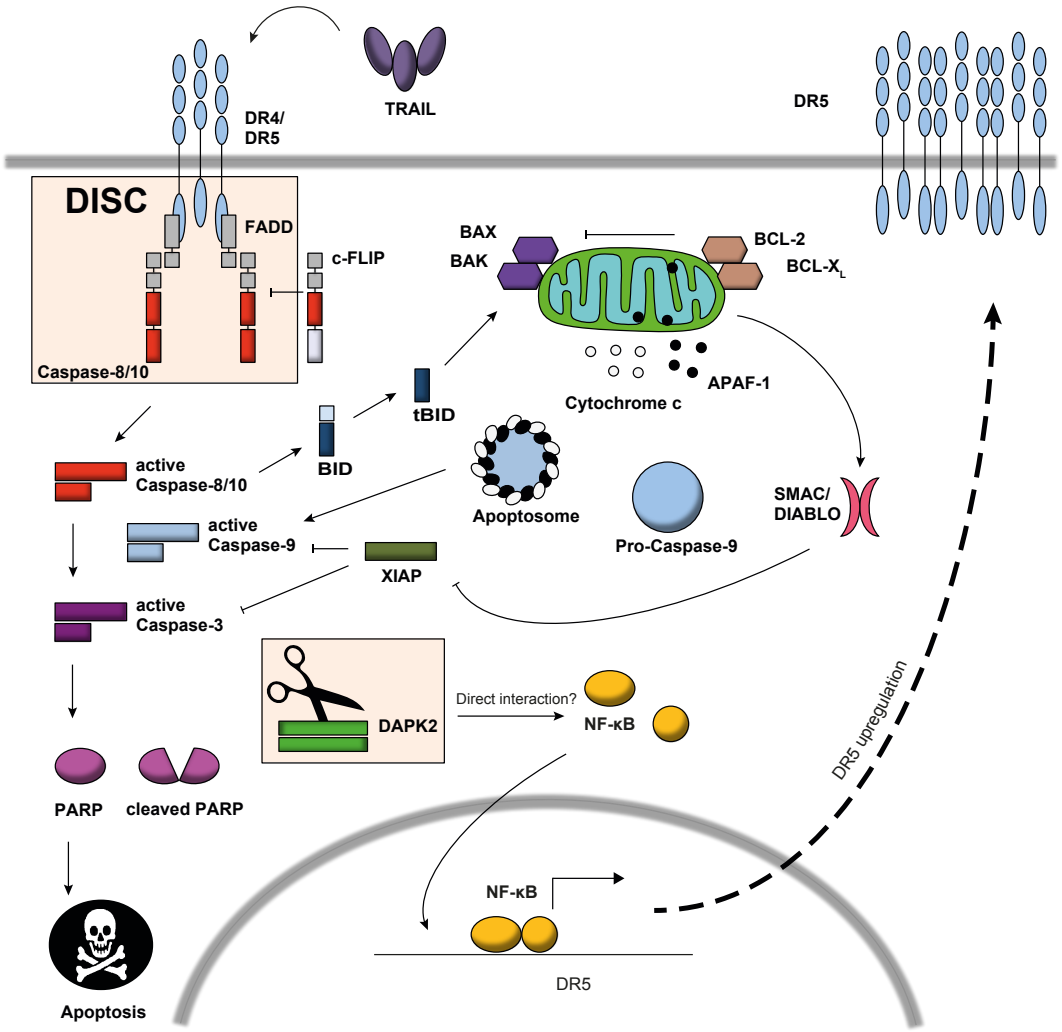

Figure 5-15. DAPK2 is a novel modulator of TRAIL-induced apoptosis.

Death receptor ligation by TRAIL primarily activates the extrinsic apoptotic pathway. TRAIL binding induces DISC formation. Activation of the initiator Caspases-8/10 leads to proteolytic cleavage and activation of downstream effector caspases, such as Caspase-3, which eventually culminates in apoptosis. TRAIL can also activate the intrinsic apoptotic pathway *via* BID. This involves depolarisation of the mitochondrial membrane potential *via* BAK and BAX, followed by cytochrome *c* release and downstream activation of Caspase-9. Resistance mechanisms can occur at many different stages of the cascade. c-FLIP can inhibit the activation of initiator caspases within the extrinsic pathway, XIAP can block the action of effector caspases and anti-apoptotic members of the BCL-2 family, such as BCL-X_L and BCL-2, which are known inhibitors of the intrinsic apoptosis pathway. Depletion of DAPK2 triggers the activation of NF-κB and leads to NF-κB-mediated induction of DR5 mRNA and to an increase in DR5 protein levels. The increase in the number of DR5 molecules presumably overcomes the inhibition threshold and lead to the re-sensitisation of cancer cells to TRAIL-induced apoptosis.

6. DAPK2 Regulates Oxidative Stress in Cancer Cells by Preserving Mitochondrial Function

6.1 Introduction

DAPK2 shares a high level of homology within its kinase domain with the other two DAPK family members, DAPK1 and DAPK3 (**Figure 1-9**). DAPK1 has been linked to key events in autophagy and it has been, more recently, implicated in mitochondrial maintenance (Shang et al., 2005) and metabolism (Mor et al., 2012). As described earlier, DAPK2 is significantly smaller than DAPK1 and it lacks the ankyrin repeats region, the cytoskeletal binding domain and the death domain, all of which are part of DAPK1's unique protein structure (Deiss et al., 1995). Several biological roles and functions have been ascribed to DAPK2 and, perhaps surprisingly, they often coincide with those of DAPK1. Indeed, it would appear that, like DAPK1, DAPK2 is also involved in the formation of autophagic vesicles (Cohen et al., 1997, Inbal et al., 2002), modulation of receptor induced cell death (Inbal et al., 2000, Lin et al., 2007) and several modes of intrinsic apoptotic cell death(Inbal et al., 2002). Whereas epigenetic silencing of DAPK1 has been reported in many different human cancers (Esteller et al., 2001, Katzenellenbogen et al., 1999), DAPK2 appears to be silenced mainly in haematological disorders (Rizzi et al., 2007). Most approaches used for studying the role of DAPK2 have, so far, relied on using tagged versions of this molecule and it is, therefore, still unclear whether these functions are also carried out by the native protein, when DAPK2 is expressed at much lower, endogenous, levels (Further discussed in **1.8.1**.)

DAPK1 has been shown to regulate mitochondrial integrity and to modulate the mitochondrial membrane potential (Shang et al., 2005) but, to the best of our

knowledge, no work has been carried out in this respect with regards to DAPK2. Since DAPK1 and DAPK2 appear to share many functions and both are thought to reside, at least partially, in the mitochondria, we hypothesised that DAPK2 depletion was also likely to regulate mitochondrial metabolism, which may also explain how silencing DAPK2 leads to NF-κB activation (**Chapter 5.**). Mitochondrial dysfunction is characterised by the induction of ROS in the cell (Turrens, 2003). Ultimately, dysfunctional mitochondria can no longer be powerhouses of use to the cell and are, therefore, targeted for degradation. Alternatively, their membrane can depolarise leading to the release of cytochrome *c*, which is part of a well-studied apoptotic process (Liu et al., 1996). As in previous chapters, depletion of DAPK2 through RNAi was carried out in both U2OS osteosarcoma and A549 NSCLC cells. In DAPK2-depleted cells there was an increase in the levels of intracellular ROS, such as peroxide (H_2O_2) and superoxide anion ($O_2^{\bullet-}$), mitochondrial depolarisation and severely impaired mitochondrial metabolism. The data thus suggested that DAPK2 exerted metabolic and mitochondria-regulating functions, which have not been described to date and that, can explain why this kinase is downregulated in several haematological malignancies (Humbert et al., 2014, Rizzi et al., 2007, Tur et al., 2009).

6.2 Results

6.2.1 RNAi-mediated ablation of DAPK2 induces oxidative stress and activates mitogen-activated protein kinases (MAPKs)

Although DAPK2 is structural significantly different from DAPK1, their kinase domains are highly homologous (80%) (Bialik and Kimchi, 2006) (**Figure 1-9**). In

order to determine whether DAPK2 modulated the level of cellular oxidative stress in U2OS and A549 cells were transfected as in previous chapters. Oxidative stress was studied by flow cytometry in cells transfected with siNS, siDAPK2 or challenged with H_2O_2, which was used as a positive control for the production of ROS. General oxidative stress was analysed using the chloromethyl 2',7'-dichlorodihydrofluorescein diacetate (CM-H_2DCFDA, henceforth referred to as DCFDA) probe (**Figure 6-1a** + **b** and **e** + **f)** and superoxide production was assessed using the dihydroethidium (DHE) probe (**Figure 6-1c** + **d** and **g** + **h**). The fluorescence of cells transfected with siDAPK2 or treated with H_2O_2 was compared to that of control cells (siNS). The histograms depict typical cell profiles obtained in each experiment and the bar charts on the right conglomerate mean percentage of fluorescence normalised to control cells ± SEM from three independent experiments. Both DAPK2 depletion and H_2O_2 treatment resulted in an increase in general oxidative stress in U2OS (**Figure 6-1a** + **b**) and A549 (**Figure 6-1e** + **f**) cells. The same was observed with regards to the generation of superoxide, which was elevated upon siDAPK2 depletion and upon treatment with H_2O_2 in both U2OS (**Figure 6-1c** + **d**) and A549 cells (**Figure 6-1g** + **h**).

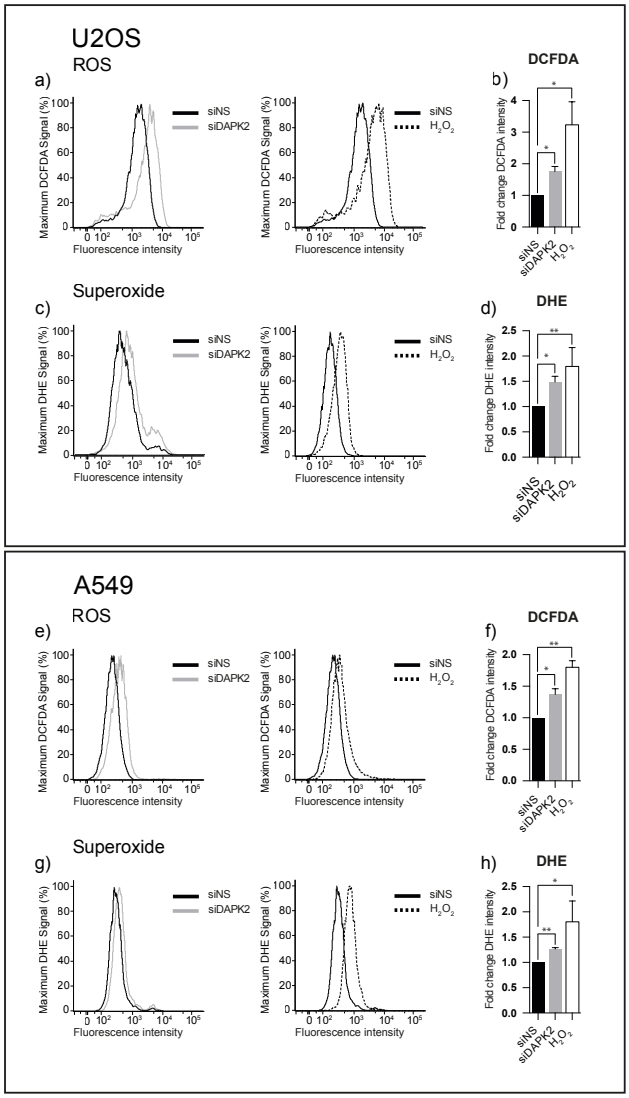

Figure 6-1. Depletion of DAPK2 induces oxidative stress.

U2OS (**a - d**) and A549 (**e - h**) cells were transfected with either siNS, or DAPK2 siRNA for 48 h and oxidative stress was detected by flow cytometry. Cells were also treated with H_2O_2 (0.5 mM, 24 h), which was used as a positive control for ROS production. The DCFDA probe was used to detect general ROS in U2OS (**a** + **b**) and A549 cells (**e** + **f**), whereas $O_2^{\bullet-}$ anions were detected in U2OS (**c** + **d**) and A549 cells (**g** + **h**) using the DHE probe. Staining intensity was quantified using geometric means of three independent experiments and plotted as fold change in relation to the siNS-transfected cells. Statistical analysis was done using Student's *t*-test (paired, one tailed) (* $p< 0.05$, ** $p<0.01$).

Having observed a clear induction of ROS (H_2O_2 and $O_2^{\bullet-}$) upon silencing DAPK2, we asked whether this led to the activation of mitogen-activated protein kinases (MAPKs), which are known to be activated by oxidative stress as part of a pro-survival response (Son et al., 2013). Therefore, U2OS and A549 cells were transfected with either siNS or with siDAPK2, proteins were extracted and then analysed by SDS-PAGE. Quantitative western blots in **Figure 6-2** confirmed the efficiency of the knockdown of DAPK2 in U2OS (**Figure 6-2a**) and A549 (**Figure 6-2c**) cells, when compared to the control siNS-transfected cells. Western blot membranes were also probed with antibodies raised against the phosphorylated forms of ERK1/2, p38 and JNK. Depletion of DAPK2, when compared to the siNS control, led to clear phosphorylation/activation of ERK1/2 (Thr202/Tyr204) and JNK (Thr183/Tyr185) in U2OS and A549 cells, whereas phosphorylation of p38 (Thr180/Tyr182) was only observed in U2OS cells but not in A549 lung cancer cells (**Figure 6-2a** *versus* **c**). Superoxide anion ($O_2^{\bullet-}$) is a potentially damaging free radical, which is converted into less reactive hydrogen peroxide (H_2O_2) by enzymes of the superoxide dismutase (SOD) family. To analyse the effect of DAPK2 depletion on the expression of SOD1, which is the predominant cytoplasmic SOD, and mitochondrial SOD2, cells were transfected as before and RNA was subsequently extracted. There was significant, albeit small (<1.5-fold), up-regulation of both SOD1 and SOD2 mRNA in U2OS cells (**Figure 6-2b**). In contrast, in A549 cells, SOD1 mRNA was not induced but SOD2 mRNA was greatly increased (>4-fold) (**Figure 6-2d**).

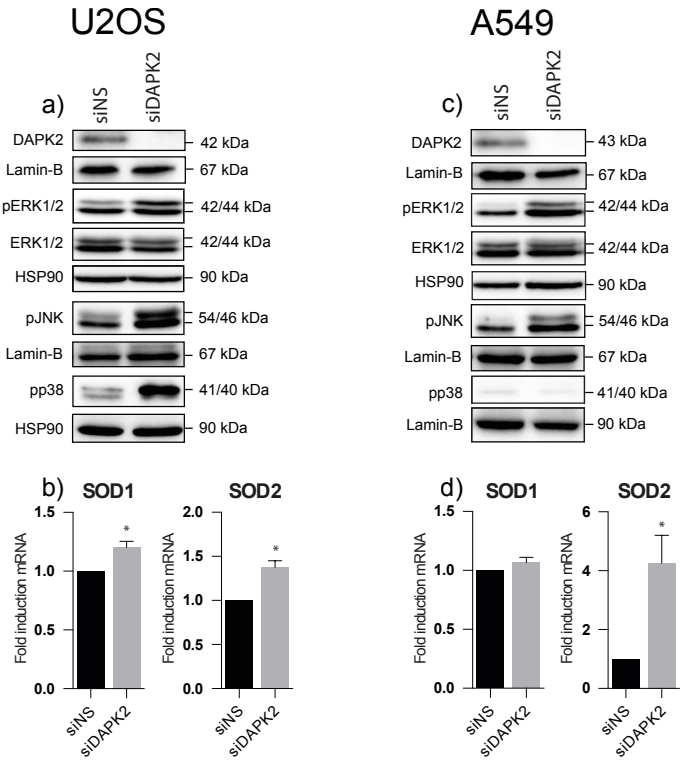

Figure 6-2. DAPK2 depletion induces phosphorylation of MAPKs and transcription of SODs.

U2OS (**a** - **b**) and A549 (**c** - **d**) cells were transfected with either siNS, or DAPK2 siRNA. Forty-eight h after transfection, the efficacy of DAPK2 silencing and phosphorylation of ERK1/2, JNK and p38 were assessed by SDS-PAGE/western blotting using Lamin B and HSP90 as loading controls (**a, c**), and the induction of SOD1 and SOD2 mRNA was measured by qPCR (**b, d**). Data represent mean ± SEM of three independent experiments. Statistical analyses were done using Student's *t*-test (paired, one tailed) (* $p < 0.05$). I am grateful to Ms Marina L. Georgiou for her contribution to the western blots and Ms Sarah Stöcker for performing the qPCR experiments.

6.2.2 DAPK2 knockdown increases the levels of mitochondrial $O_2^{\bullet-}$ and leads to spontaneous mitochondrial membrane depolarisation

Silencing DAPK2 in two different cell lines led to up-regulation of cellular ROS, activation of MAPKs and upregulation of mitochondrial SOD2, whereas SOD1 was only slightly upregulated in one of the cell lines (U2OS). We, therefore, asked whether the source of oxidative stress were mitochondria. Indeed, the production of ATP by oxidative phosphorylation is a major source for mitochondrial ROS, and mitochondrial proton and electron leaks can impact on

mitochondrial coupling efficiency and lead to increased production of mitochondrial ROS (Balaban et al., 2005). MitoSOX™ Red was used to assess mitochondrial $O_2^{\bullet-}$ levels since it selectively targets mitochondria and is exclusively oxidised by $O_2^{\bullet-}$ (**Figure 6-3**). Cells were transfected as before and treatments with H_2O_2 or the mitochondrial complex I inhibitor 1-methyl-4-phenylpyridinium (MPP^+) iodide served as positive controls for the experiment. Unsurprisingly, treatment of U2OS (**Figure 6-3a**) and A549 cells (**Figure 6-3d**) with either H_2O_2 or MPP^+ increased the levels of mitochondrial $O_2^{\bullet-}$. As hypothesised, RNAi-mediated depletion of DAPK2 resulted in a small but statistically significant increase of mitochondrial $O_2^{\bullet-}$ in U2OS (**Figure 6-3b** + **c**) and A549 cells (**Figure 6-3e** + **f**) compared to siNS-transfected control cells.

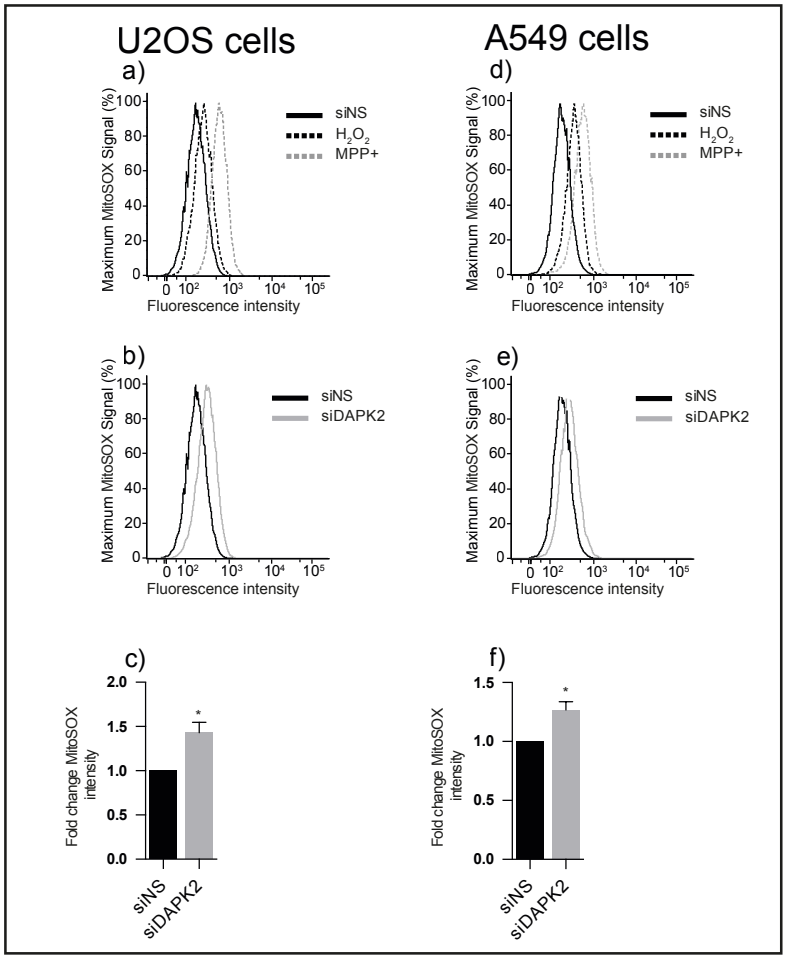

Figure 6-3. DAPK2 knockdown triggers mitochondrial $O2^{\bullet-}$ production.

U2OS (**a** - **c**) and A549 (**d** - **f**) cells were transfected with either siNS, or DAPK2 siRNA. Forty-eight h later, mitochondrial $O2^{\bullet-}$ levels were assessed using the MitoSOX™ Red probe. U2OS (**a**) and A549 (**d**) cells were also treated with H_2O_2 (0.5 mM) or MPP+ (1 mM) for 24 h, which were used as positive controls. The average of geometric means of four independent experiments was plotted as fold change (siNS *versus* siDAPK2) (**c, f**). Statistical analysis was done using Student's *t*-test (paired, two tailed) (* $p < 0.05$).

Another potential source for cellular ROS is the endoplasmic reticulum (ER) where the transcription factor CCAAT-enhancer-binding protein homologous protein (CHOP) is specifically activated upon ER stress (Nishitoh, 2012). Tunicamycin was used to induce ER stress (Kaufman, 1999), which triggered the expression of CHOP in both U2OS (**Figure 6-4a**) and A549 cells (**Figure 6-4b**). In contrast, DAPK2 knockdown did not lead to an increase in CHOP expression in either of the cell lines (**Figure 6-4a** + **b)**.

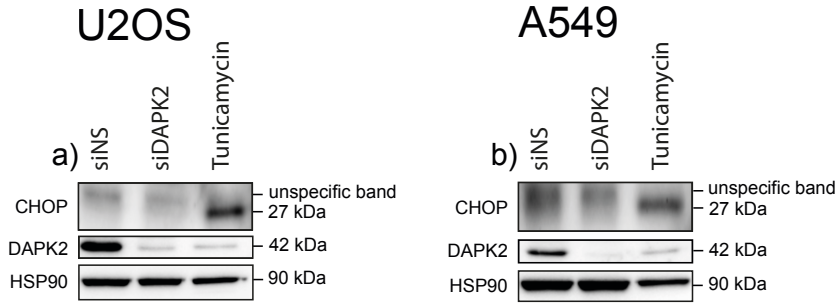

Figure 6-4. Depletion of DAPK2 does not induce the expression of CHOP.

U2OS (**a**) and A549 (**b**) cells were transfected with either siNS, or DAPK2 siRNA. Forty-eight h later, ER stress was assessed by SDS-PAGE/western blotting using CHOP expression as a readout. The induction of CHOP protein following treatment with tunicamycin for 24 h (0.5 µg/ml) served as positive control for CHOP induction and HSP90 expression was used as a loading control. Blots shown are representative of three independent experiments.

It is thought that elevated levels of mitochondrial $O_2^{\bullet -}$ can be both a cause and a consequence of mitochondrial depolarisation (Wang et al., 2012b), which is involved in apoptosis and inflammation(Lum and Nagley, 2003, Heiskanen et al., 1999). To study the effect of DAPK2 depletion on mitochondrial membrane potential (Δψm), the JC-1 probe, which forms red fluorescing aggregates at hyperpolarized mitochondrial membranes and green-fluorescing monomers at depolarised membranes, was used. U2OS and A549 cells were transfected with either siNS, or siDAPK2 and, as a control for Δψm depolarisation, cells were treated with carbonyl cyanide 3-chlorophenylhydrazone (CCCP), and then analysed by flow cytometry (**Figure 6-5c** + **e** and **i** + **k**). By gating the depolarised population that resulted from CCCP treatment, two distinct populations were identified: one with intact mitochondria and another that exhibited increased green fluorescence and thus harboured cells with depolarised mitochondria. Depletion of DAPK2 led to approximately 50% more depolarised mitochondria in both U2OS (**Figure 6-5a** + **b**) and A549 cells (**Figure 6-5g** + **h**), when compared

to siNS-transfected control cells. This pattern can also be seen in histograms measuring fluorescence in the green channels (FITC, ~525 nm) (**Figure 6-5d** + **e** and **j** + **k**). After normalising the absolute fluorescence of cells upon DAPK2 knockdown to that of siNS-transfected cells and applying appropriate statistical analyses (detailed in figure's legend), a significant overall increase in green fluorescence, a read-out for decreased Δψm, was measured in both cell lines (**Figure 6-5f** + **l**), suggesting that DAPK2 ablation led to an increase in mitochondria spontaneously depolarising.

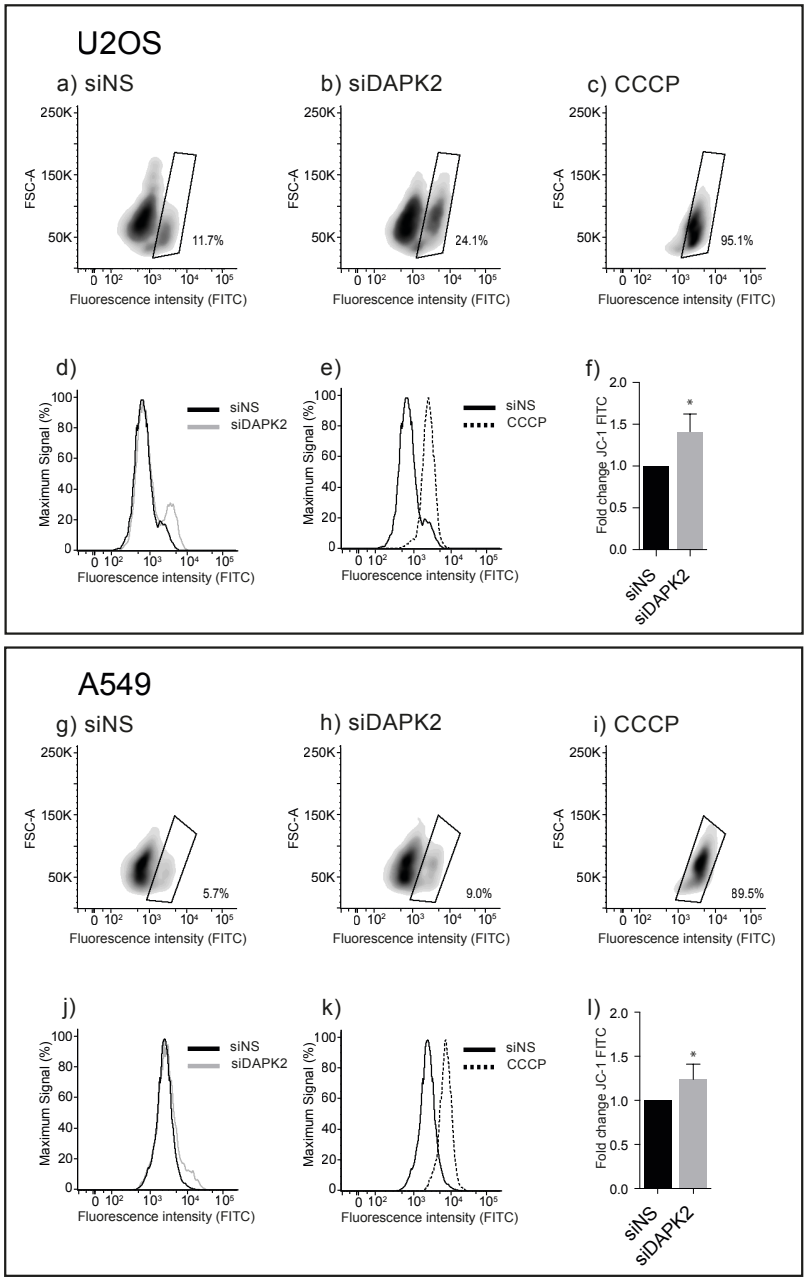

Figure 6-5. RNAi-mediated ablation of DAPK2 increases the rate of spontaneous mitochondrial membrane depolarisation.

U2OS (**a - f**) and A549 (**g - l**) cells were transfected with either siNS, or siDAPK2. Forty-eight h after transfection cells were incubated with JC-1 and the fluorescence of J-aggregates, or monomers was measured in red and green fluorescence channels by flow cytometry. CCCP (50 µM) was used to induce complete mitochondrial depolarisation (**c, i**) and to set appropriate gates in U2OS (**a - c**) and A549 cells (**g - i**) used for the quantification of mitochondrial depolarisation following transfection with siNS (**a**, **g**), or siDAPK2 (**b**, **h**). Overall green fluorescence (FITC) data are also presented in histograms (U2OS: **d, e**; A549: **j, k**). Staining intensity was quantified using geometric means of three independent experiments and plotted as fold change (**f**, **l**). Data represent mean ± SEM of three independent experiments and the statistical analysis was done using Student's *t*-test (paired, one tailed) (* p< 0.05).

Activation of DAPK1 has been linked to a decrease in Δψm upon treatment with mitochondrial complex inhibitors (Shang et al., 2005). As shown in **Figure 6-6**, when compared to cells transfected with the non-targeting control (siNS), A549 cells depleted of DAPK2 had reduced DAPK1 phosphorylated on S308, which is an inactivating phosphorylation event that modulates DAPK1 activity.

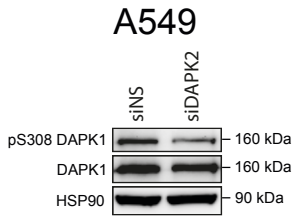

Figure 6-6. Depletion of DAPK2 reduces the phosphorylation of DAPK1.

A549 cells were transfected with either siNS, or DAPK2 siRNA. Forty-eight h later, DAPK1 phosphorylation was assessed by SDS-PAGE/western blotting. When compared to cells transfected with siNS, DAPK2-depleted A549 cells were less phosphorylated on DAPK1 S308, which is an inactivating phosphorylation event that modulates DAPK1 activity. Blots shown are representative of three independent experiments. I am grateful to Ms Maria M. Misterek for her contribution to this experiment.

This suggested that silencing DAPK2 led to the activation of DAPK1. Interestingly, U2OS cells did not express DAPK1 protein or mRNA (as described in **4.2.1**, **Figure 4-1**), which suggested that although the depolarisation of mitochondria in A549 cells might be associated with activation of DAPK1, in U2OS cells the observed reduction in Δψm was likely due to another molecular event.

6.2.3 Altered mitochondrial integrity leads to metabolic changes

The increase in mitochondrial $O_2^{\bullet-}$ production and the increase in spontaneous mitochondrial depolarisation suggested that mitochondria were a likely source of

ROS generated upon DAPK2 knockdown. The data were consistent with a significant impairment of mitochondrial integrity in response to DAPK2 depletion and, in the case of A549 lung cancer cells, activation of DAPK1. The metabolic consequences of these mitochondrial alterations in DAPK2-depleted U2OS and A549 cells were, therefore, investigated next.

Eukaryotic cells use two key metabolic pathways for the generation of ATP (**Figure 1-11**). Both pathways start with glycolysis as the first step of glucose metabolism, converting one glucose molecule into two molecules of pyruvate with gain of two ATP molecules. Aerobic respiration involves the transport of pyruvate into the mitochondria and mitochondrial respiration downstream of glycolysis through the tricarboxylic acid (TCA) /Krebs cycle, which yields another thirty four ATP molecules/molecule of glucose (giving a total of thirty six ATP molecules) (Rich, 2003). Anaerobic respiration includes glycolysis and the fermentation of pyruvate to lactate, a metabolic pathway that bypasses mitochondrial respiration, and is predominantly up-regulated in cancer cells in the so-called Warburg effect, which, somewhat counter intuitively, cancer cells use to produce most of their energy (Warburg, 1956, Bialik and Kimchi, 2006).

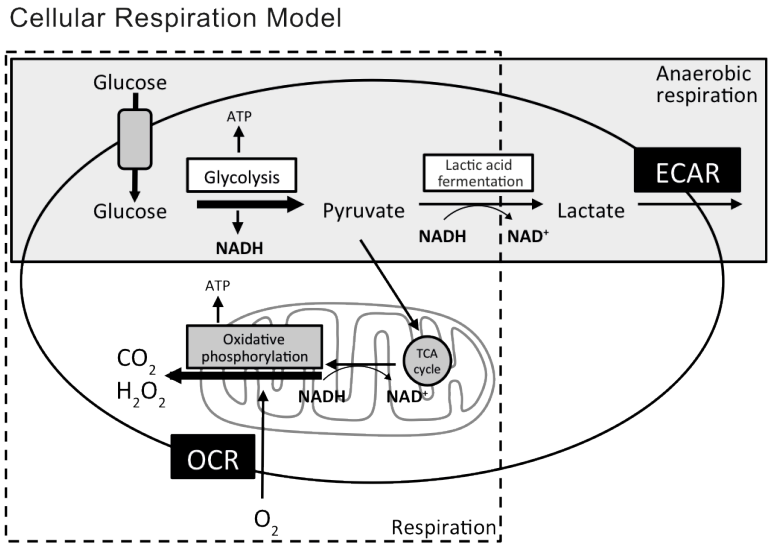

Figure 6-7. Simplified cartoon of cellular metabolism pathways.

Simplified cartoon depicting cellular metabolism pathways with glycolysis as the first step of glucose breakdown, and oxidative phosphorylation and anaerobic respiration as subsequent steps.

A Seahorse was used to determine changes in aerobic and anaerobic respiration. This powerful instrument measures the oxygen consumption rate (OCR), an accurate indicator of mitochondrial respiration, as well as the extracellular acidification rate (ECAR), which is an indirect measurement of lactic acid production (**Figure 1-11**). Cells were transfected as before, and OCR and EACR were determined under basal-conditions in siDAPK2- or siNS-transfected cells. The EACR in siDAPK2-tranfected cells, measured in mpH/min, was normalised to that in siNS-transfected control cells. No statistically significant changes in EACRs were detected between siNS- and siDAPK2-transfected U2OS (**Figure 6-8a**), or A549 (**Figure 6-8g**) cells, suggesting that silencing DAPK2 does not skew metabolism in these cells towards anaerobic respiration. OCR was measured in pMoles/min and normalised as described above for EACR measurements. In contrast to what was seen for EACR, there was a significant decrease in OCRs by mitochondria upon DAPK2 knockdown in both U2OS

(**Figure 6-8b**) and A549 (**Figure 6-8h**) cells, suggesting that DAPK2 modulated mitochondrial respiration but not anaerobic respiration.

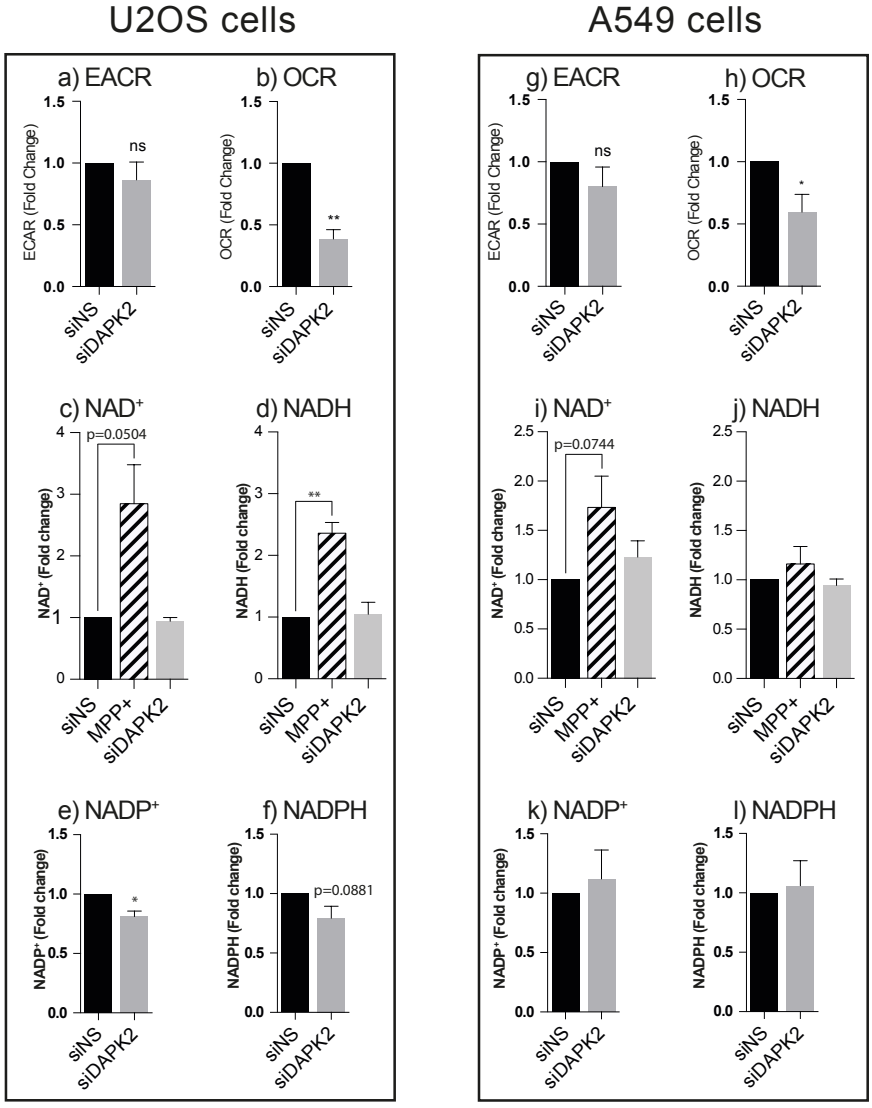

Figure 6-8. The absence of DAPK2 leads to a reduction of oxidative phosphorylation in U2OS and A549 cells.

To quantify cellular metabolic processes, U2OS (**a - f**) and A549 (**g - l**) cells were transfected with either siNS, or DAPK2 siRNA. Forty-eight h after transfection cells were analysed using a Seahorse Analyser. ECAR, an indirect measurement of lactic acid production, is depicted as fold change of mpH/min and normalised to siNS control in U2OS (**a**) and A549 cells (**g**). OCR, which can be used to determine mitochondrial respiration, is shown as fold change of pmol/ min and normalised to siNS control in U2OS (**b**) and A549 cells (**h**). Forty-eight h after siRNA transfection NAD^+, NADH, $NADP^+$ and NADPH levels were analysed using colorimetric assays in U2OS (**c - f**) and A549 cells (**i - l**). Treatment with MPP+ (1 mM, 24 h) served as a positive control. Data represent mean ± SEM of three independent experiments, statistical analyses were done using Student's *t*-test (paired, one tailed) (* $p<0.05$, ** $p<0.01$). I am grateful to Ms Marina L. Georgiou for performing this experiment.

To investigate further the consequences of DAPK2 depletion on cellular metabolism, levels of the coenzymes nicotinamide adenine dinucleotide (NAD^+) and nicotinamide adenine dinucleotide phosphate ($NADP^+$), as well as their corresponding reduced forms (NADH and NADPH, respectively), were analysed. During glycolysis and the TCA cycle, each glucose molecule leads to the reduction of six NAD^+ to NADH, which are then oxidised during oxidative respiration to produce ATP (Rich, 2003). In contrast to NADH, NADPH is not involved in metabolic processes but it has an important role in the regeneration of oxidised glutathione (GSH). GSH is a key antioxidant in cells, thus protecting them against cellular ROS, such as free radicals and peroxides (Kirsch and De Groot, 2001). Colorimetric assays were used to determine the levels of NAD^+ and NADH, as well as $NADP^+$ and NADPH. MPP^+ was used to inhibit oxidative phosphorylation and increase the levels of NAD^+ and NADH, and thus as a control. As shown for U2OS (**Figure 6-8c** + **d**) and A549 cells (**Figure 6-8i** + **j**), MPP^+ treatment increased the levels of NAD^+ and NADH (albeit in A549 cells, the increase in NADH was very small and not statistically significant). However, NAD^+/NADH levels remained unaffected by DAPK2 knockdown. Interestingly, the levels of $NADP^+$ and NADPH in U2OS cells (**Figure 6-8e** + **f**) were slightly decreased upon silencing DAPK2 (only statistically significant for $NADP^+$ where a 20% decrease was consistently measured across experiments), whereas there was no detectable change in A549 cells (**Figure 6-8k** + **l**). It thus appears that RNAi-mediated ablation of DAPK2 affected oxidative phosphorylation without substantially impacting on NAD^+/NADH, or $NADP^+$/NADPH metabolism.

6.2.4 Depletion of DAPK2 leads to decreased glutathione levels and induction of NRF2

Having established that genetic ablation of DAPK2 led to changes in cellular oxidative stress, mitochondrial respiration, activation of stress kinases and up-regulation of SODs in two distinct cancer cell types, we next asked what effect down-regulation of DAPK2 had on the levels of GSH. GSH functions as an electron donor for reducing reactions and it is involved in the reduction of cellular ROS (Pompella et al., 2003, Brigelius-Flohe and Maiorino, 2013). In fact, the generation of oxidised GSH (in the form of GSSG) is tightly linked to mitochondrial oxidative phosphorylation, whereby NADPH reduces GSSG to GSH. To assess total levels of GSH levels by colorimetry, cells were transfected as described earlier. Subtle, but highly statistically significant, down-regulation of GSH levels upon DAPK2 knockdown were detected and this was more prominent in U2OS (**Figure 6-9a**) than in A549 cells (**Figure 6-9d**).

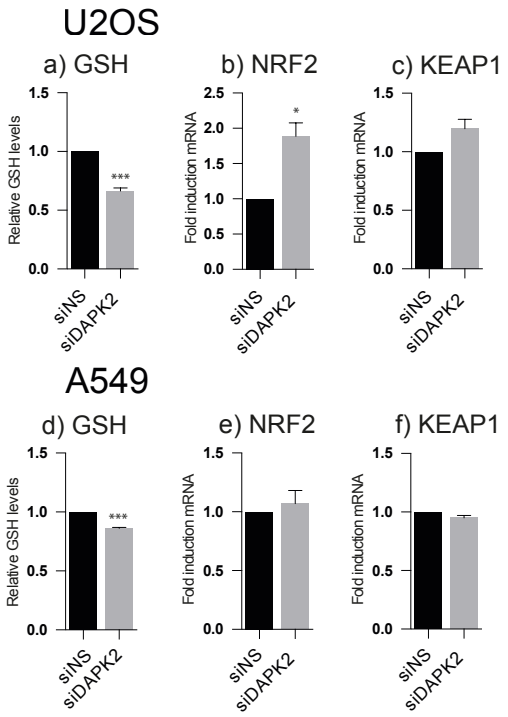

Figure 6-9. Ablation of DAPK2 leads to decreased GSH levels and, in U2OS cells, to the induction of NRF2 mRNA.

U2OS (**a - c**) and A549 (**d - f**) cells were transfected with either siNS, or siDAPK2 the levels of GSH were analysed using a colorimetric assay 24 h later (**a, d**). NRF2 (**b**, **e**) and KEAP1 (**c**, **f**) mRNA levels were assessed by qPCR. Data represent mean ± SEM of at least three independent experiments and the statistical analyses were done using Student's *t*-test (paired, one tailed) (* $p<0.05$, ** $p<0.01$, *** $p< 0.005$). I am grateful to Ms Emily Chater for performing the GSH assay and Ms Sarah Stöcker for performing the qPCR experiments.

The question was whether such small reductions in GSH levels were sufficient to induce nuclear factor (erythroid-derived 2)-like 2 (NFE2L2/NRF2), a latent transcription factor responsible for the transcription of a multitude of key antioxidants that can protect cells from oxidative stress. NRF2 is known to bind to the so-called antioxidant response element (ARE), leading to transcriptional activation of GSH synthesising enzymes and other antioxidant enzymes, such as SOD1 and SOD2, which were up-regulated upon DAPK2 silencing (**Figure 6-2b + d**). After U2OS and A549 cells were transfected with siDAPK2 or siNS, RNA and proteins were extracted and the levels of NRF2 and its key-regulating ubiquitin ligase kelch-like ECH-associated protein 1 (KEAP1) analysed.

Interestingly, NRF2 mRNA levels were significantly elevated in U2OS cells (**Figure 6-9b**), but not in A549 cells (**Figure 6-9e**). KEAP1 was not induced in either U2OS (**Figure 6-9c**), or A549 cells (**Figure 6-9f**).

6.2.5 The mitochondrial-associated function of DAPK2 is likely to be kinase mediated

The data thus far suggested that the increase in intracellular ROS caused by downregulating DAPK2 was due to an impairment of mitochondrial functions. In order to understand how DAPK2 preserved mitochondrial integrity, the relevance of DAPK2's kinase domain was investigated. For that purpose, tetracycline (Tet)-inducible U2OS cell lines (U2OS-TetR) containing HA-tagged DAPK2 constructs that were either wild-type (HA-DAPK2.wt), or kinase-dead (HA-DAPK2.K42A), described earlier (Inbal et al., 2002), were used. The caveat with this approach was that it was impossible to express the constructs at endogenous levels. Indeed, over-expression of wild-type DAPK2 is known to be sufficient to induce apoptotic features, such as membrane blebbing and nuclear fragmentation (Inbal et al., 2002). As such, this approach could not be used as an alternative experimental method to revert the phenotype observed after silencing DAPK2 using RNAi. It did, however, enable the analysis of the role of the kinase domain on the regulation of intracellular oxidative stress.

Expression of the transgene was induced in HA-DAPK2.wt cells **(Figure 6-10a**) and HA-DAPK2.K42A cells (**Figure 6-10c**) using doxycycline (DOX) and ROS levels were measured using the DCFDA probe. Overexpression of wild-type DAPK2, rather than leading to reduced oxidative stress, led to an increase in

general ROS production (**Figure 6-10b**), but importantly this was not observed if cells overexpressed a kinase-dead DAPK2 mutant (**Figure 6-10d**). The overexpressed kinase dead mutant (HA-DAPK2.K42A) did not behave as a dominant negative and did not mimic the phenotype caused by DAPK2 depletion seen after RNAi. This might be due to the fact that, in this cell system, the cells still expressed endogenous wild-type DAPK2.

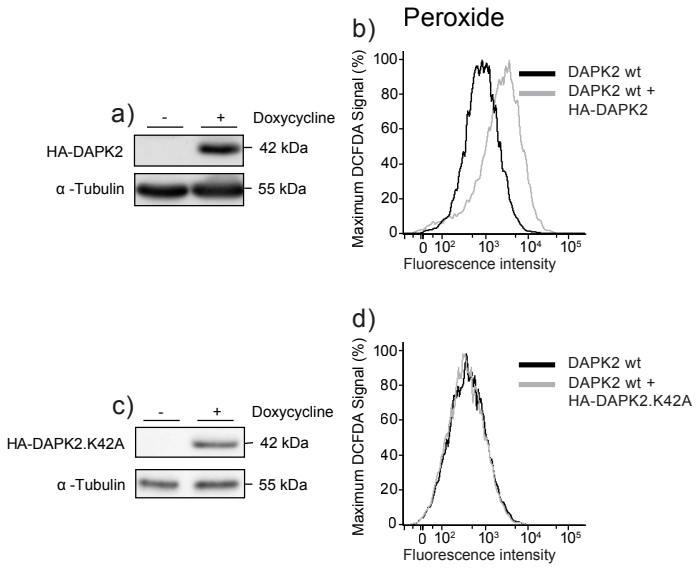

Figure 6-10. Effect of wild-type (wt) and kinase-dead (K42A) DAPK2 overexpression on oxidative stress.

The expression of HA-tagged wild-type (wt), or HA-tagged kinase-dead (K42A) DAPK2 in U2OS-TetR cells was induced using doxycycline (10 ng/ml). HA-DAPK2 (**a**) and HA-DAPK2.K42A (**c**) expression was verified by SDS-PAGE/western blotting. The impact of wild-type **(b)** or kinase-dead **(d)** DAPK2 overexpression have on oxidative stress was analysed as described earlier using the DCFDA probe.

To eliminate the endogenous wild-type DAPK2 in the inducible cell model, 3'UTR-specific siRNAs were used. These molecules target exclusively endogenous DAPK2 (**Figure 6-11**). Cells were transfected with either siNS or custom made Dharmacon DAPK2 siRNA oligonucleotide that specifically targeted the DAPK2 3'UTR (described in 117 and shown in **Figure 4-1**) and, in order to induce the expression of HA-DAPK2.K42A, cells were stimulated with DOX as they were being transfected. As shown in **Figure 6-11a**, siDAPK2-3'UTR specifically targeted endogenous DAPK2 and did not impact on the expression of kinase dead DAPK2, which was detected using an anti-HA antibody. Having established a cell system where it was possible to efficiently down-regulate endogenous DAPK2 and concomitantly overexpress a kinase dead DAPK2 mutant, enabled studying the effect of kinase-dead DAPK2 on the generation of general ROS. Consistent with our previous results (**Figure 6-1a**), depletion of wild-type DAPK2 without (**Figure 6-11c,** grey line) or with overexpression of kinase-dead DAPK2 (**Figure 6-11c**, dotted black line), using siDAPK2-3'UTR, led in both cases to a significant increase in ROS (**Figure 6-11c** and **d**). The overexpression of kinase-dead DAPK2, importantly, actually led to a significantly higher level of oxidative stress in U2OS cells than the wild-type endogenous protein (**Figure 6-11d**). In control cells transfected with siNS, the level of oxidative stress was the same regardless of the presence or absence of HA-DAPK2.K42A (**Figure 6-11c**). Collectively, our data thus suggest that DAPK2 kinase activity is important for preserving mitochondria's integrity and protecting cells from oxidative stress.

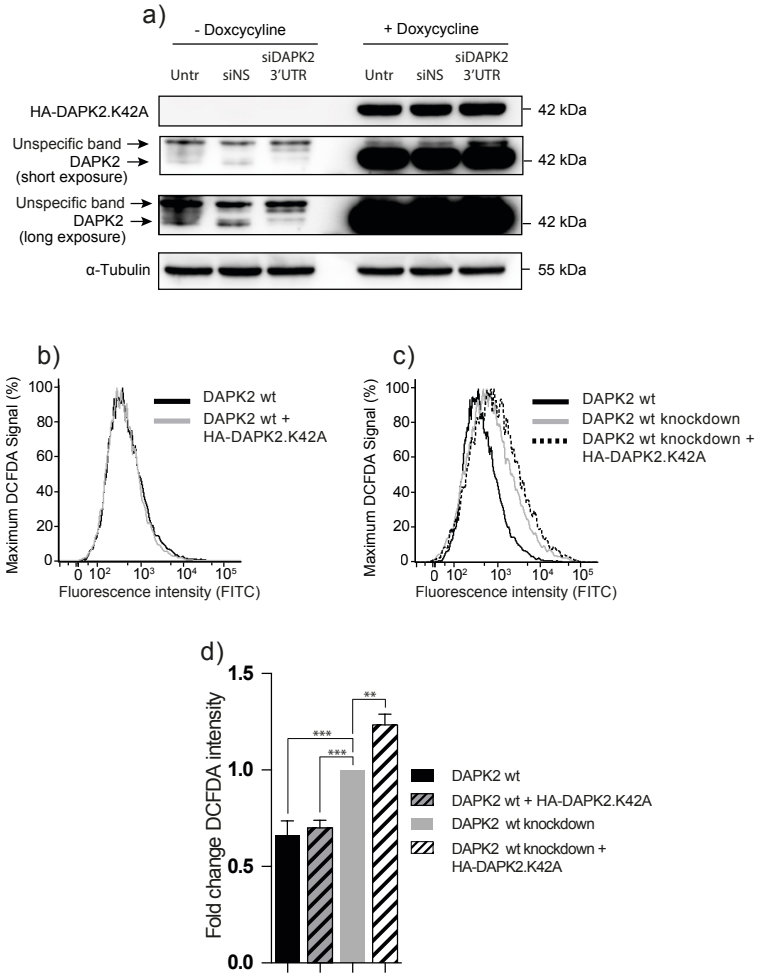

Figure 6-11. Effect of kinase-dead (K42A) DAPK2 overexpression on oxidative stress in cells that are depleted of endogenous DAPK2.

The expression of HA-tagged kinase-dead (K42A) DAPK2 in U2OS-TetR cells was induced using doxycycline (10 ng/ml). To eliminate endogenous DAPK2 and study the effect of the kinase-dead DAPK2 mutant individually, U2OS TetR cells containing the HA-DAPK2.K42A construct were transfected with either siNS, or siDAPK2-3'UTR and concomitantly stimulated with doxycycline (10 ng/ml). Targeted knockdown of endogenous DAPK2 and overexpression of HA-DAPK2.K42A were then assessed by SDS-PAGE/western blotting (**a**). The effect of the kinase dead DAPK2 mutant overexpression, in the presence (**b, grey line**) and absence (**c, dotted black line**) of endogenous DAPK2, on oxidative stress was quantified by flow cytometry with the DCFDA probe (**b**, **c**). Data were plotted as fold change of DCFDA fluorescence of U2OS TetR cell transfected with siDAPK2-3'UTR without doxycycline treatment (**d**). Statistical analysis was done using one-way ANOVA test (** p<0.01, *** p< 0.005).

6.2.6 Discussion

Although DAPK1, DAPK2 and DAPK3 are structurally different, recent analyses have revealed that DAPK2 and DAPK3 evolved from DAPK1 around the development of jawed vertebrates (Shoval et al., 2011). DAPK1 regulates mitochondrial integrity(Shang et al., 2005) and metabolic processes (Mor et al., 2012). Given the common ancestry and sequence homology within DAPKs' kinase domains, common mechanisms of action and functional redundancy have been postulated, which invoke the formation of a so-called 'death-associated multi-protein complex' (Gozuacik and Kimchi, 2006). Indeed, all three have been associated with apoptotic processes and are thought to be potential tumour suppressors (Bialik and Kimchi, 2006).

Here, we showed that depletion of DAPK2 results in ROS generation in U2OS and A549 cells (**Figure 6-1a**, **c**, **e**, **g**) and, phosphorylation/activation of MAPKs (**Figure 6-2a** and **c**), and induction of SODs (**Figure 6-2b** and **d**). Mitochondrial SOD2 was induced more than cytosolic SOD1, suggesting that in the absence of DAPK2 (**Figure 6-2b** and **d**), ROS were produced by mitochondria(Turrens, 2003). Additional experiments support this hypothesis (**Figure 6-3**) and indicate that the ER was an unlikely additional ROS source (**Figure 6-4**). Silencing DAPK2 led to increased spontaneous mitochondrial depolarisation (**Figure 6-5**) and, in A549 cells, to the activation of DAPK1 (**Figure 6-6**), thought to be a Δψm sensor involved in cytoskeletal rearrangements responsible for mitochondrial transport mechanisms (Shang et al., 2005). Apart from the homology on the kinase domain, DAPK1 and DAPK2 have also been reported to heterodimerise (Gozuacik and Kimchi, 2006). It is thus reasonable to assume that they may

operate in a similar fashion with regards to mitochondrial maintenance, sensing the mitochondrial membrane potential and leading to downstream processes of mitophagy and mitochondrial degradation, which result in faulty mitochondria. Interestingly, neither overexpression of DAPK1, nor DAPK2 has been shown to induce mitochondrial depolarisation (Inbal et al., 2002).

DAPK2 knockdown led to significantly reduced oxidative phosphorylation without affecting lactic acid fermentation (**Figure 6-8a** + **g** and **b** + **h)**. This suggested a fundamental role for DAPK2 in the regulation of mitochondrial metabolism and/or maintenance. This, in turn, raises the question of how these cells maintain their energy supply, as without increased lactic acid fermentation (ECAR), DAPK2-depleted cells are unlikely to be compensating the decrease in oxidative phosphorylation *via* anaerobic respiration (**Figure 1-11**). Consistent with this, no significant changes in NAD^+/NADH and/or $NADP^+$/NADPH upon DAPK2 silencing were seen (**Figure 6-8c** - **f** and **i** - **l**). All experiments were performed 48 h post-RNAi. Thus, eventual cellular compensatory mechanisms, such as increased glycolytic rate or lactic acid production, may not yet be detectable. For example, it has been shown that inhibition of the mitochondrial electron transport by low doses of ethidium bromide causes NADH accumulation, halts the TCA cycle and drives cells towards anaerobic glucose metabolism, but these results were obtained after 4 days of mitochondrial electron transport inhibition (Noda et al., 2002).

The ROS increase and mitochondrial depolarisation were accompanied by a small, but statistically significant, GSH decrease (**Figure 6-9a** and **d**) and, in

U2OS cells by the transcriptional induction of the 'master regulator of antioxidant responses' NRF2 (Gorrini et al., 2013) (**Figure 6-9b**). There was no induction of NRF2 in A549 cells (**Figure 6-9e**) and the levels of KEAP1 mRNA, an NRF2 regulator, remained unchanged in both cell lines (**Figure 6-9c** + **f**).

Overexpression of HA-tagged wild-type DAPK2 *per se* increased the levels of intracellular ROS in U2OS cells (with endogenous DAPK2), whereas kinase-dead DAPK2 did not (**Figure 6-10**). The overexpression of the kinase-dead mutant, in the absence of endogenous DAPK2, led to increased oxidative stress in U2OS cells and this was greater than that seen with the wild-type protein (**Figure 6-11**). Collectively, these data indicate that DAPK2 kinase activity is important for preserving mitochondrial integrity and protecting cells from oxidative stress.

DAPK2 is emerging as a tumour suppressor in several types of cancer cells, especially in acute promyelocytic leukaemia (APL), a subtype of acute myelogenous leukaemia (AML), which responds to treatment with all-trans retinoic acid (ATRA) (Rizzi et al., 2007). This is interesting, as ATRA is known to up-regulate DAPK2 expression. Given the role of ROS in the aetiology of AML (Rassool et al., 2007), downregulation and/or loss of DAPK2 is likely to benefit emerging cancer cells, by leading to deregulated mitochondria, increase in cellular ROS and, thus, genomic instability. Indeed, somatic mitochondrial mutations and accumulated mitochondrial damage have been linked to AML development (He et al., 2003). Despite it relatively small size and straightforward structural features, DAPK2 appears to be a double-edge sword, depending on cellular context and, presumably, interaction partners. Indeed, earlier, we have

shown that downregulation of endogenous DAPK2 sensitises multiple cancer cell types to TRAIL-induced apoptosis. This is due to ability to activate NF-κB, which is another multi-faceted protein that, curiously, can also be activated by oxidative stress.

We have thus identified a completely novel role for DAPK2 in the regulation of mitochondrial integrity, as its absence leads to mitochondrial depolarisation and increased oxidative stress. This may be a mechanism by which, depending on the intracellular context, DAPK2 can act as a tumour suppressor gene. Importantly, as the effect of DAPK2 silencing on mitochondrial respiration is conserved between mesenchymal U2OS cells and epithelial A549 cells, it is likely that our findings can be further extended to additional cell lineages and malignancies. Time will tell.

7. General Discussion and Future Perspective

7.1 General Discussion

7.1.1 Overview

TRAIL is a member of the TNF ligand superfamily and has been described to be involved in innate anti-tumour surveillance. By binding to its corresponding receptors DR4 and DR5, TRAIL has been shown to selectively induce cell death in tumours cells without affecting 'normal' tissue. Experimental cancer therapies using TRAIL-receptor agonists (TRAs) have proven promising in preclinical work and have made it into phase II clinical trials. Unfortunately, their success has been hindered for a variety of reasons. In contrast to homotrimeric TRAIL, many TRAs are antibody based and are only capable of clustering two DRs, whereas TRAIL induces clustering of three DRs, leading to a stronger activation of extrinsic apoptosis pathways. Moreover, it was described that many initially TRAIL sensitive cells develop resistance to TRAIL-induced apoptosis and several strategies have been developed to attempt to overcome this resistance, including the concomitant use of chemotherapeutic drugs or proteasome inhibitors. Despite good re-sensitising effects triggered by these agents in an *in vitro* setting, these findings were not reproduced in a clinical environment. To enable the success of TRAIL-based therapies in the clinic more powerful TRAs and more sophisticated and/or novel strategies are currently being developed, as they are clearly needed to overcome TRAIL-resistance in the clinic.

Previous work carried out in Dr. Costa-Pereira's laboratory by Dr. Sutton and Dr. Fonseca revealed that RNAi-mediated depletion of DAPK2 resulted in the sensitisation of TRAIL-resistant U2OS osteosarcoma cells to TRAIL-induced apoptosis (**Figure 2-1C**). The sensitisation was reported to be specific, as

DAPK2 did not sensitise cells to other cytotoxic agents such as taxol and H_2O_2 (**Figure 2-1A** and **B**) or to apoptosis triggered by the death-inducing cytokine TNF-α (**Figure 2-1D**). The aim of my Ph.D. project, therefore, was to elucidate the underlying molecular mechanism(s) leading to the sensitisation of TRAIL-resistant cancer cells to TRAIL-induced cell death.

7.1.2 RNAi-mediated depletion of TRAIL specifically sensitises cancer cells to TRAIL-induced cell death

In **4.2.1** we established that the siRNA oligonucleotides used throughout this work specifically targeted DAPK2 without affecting the protein levels of the other DAPK-family members, namely DAPK1 or DAPK3 (**Figure 4-1**). We further established that U2OS cells did not express detectable amounts of DAPK1. By using a pool of two siRNA oligonucleotides we confirmed the initial observation that DAPK2 depletion sensitised U2OS cells to TRAIL-induced apoptosis (**Figure 4-2a** - **e**). We extended these findings to the NSCLC cell line A549, another solid tumour cell line that has recently been reported as resistant to TRAIL-induced apoptosis (**Figure 4-2f** - **j**). As for U2OS cells, RNAi-mediated depletion of DAPK2 in A549 cells sensitised these to TRAIL-induced apoptosis but not to other cytotoxic agents. To further validate that RNAi-mediated DAPK2 depletion could sensitise cancer cells to TRAIL-induced apoptosis, cells were transfected with additional four siRNA oligonucleotides. As shown in **Figure 4-4**, each individual DAPK2-targeting siRNA oligonucleotide sensitised U2OS and A549 cells to TRAIL-induced apoptosis. These results not only afforded further support to the initial findings but they also excluded the possibility that the sensitisation to

TRAIL-induced apoptosis was caused by a potential RNAi-mediated off-target effect.

7.1.3 Sensitisation to TRAIL-mediated apoptosis requires the upregulation of DRs

Molecular pathways leading to TRAIL-induced apoptosis in DAPK2-depleted U2OS and A549 cells were analysed further using SDS-PAGE/western blotting, which revealed that DAPK2-depleted cells, in response to TRAIL, showed a stronger activation of the executioner caspase, caspase-8 (**Figure 4-5**). We sought to unravel the molecular background leading to this stronger activation. As depicted in **Figure 1-5** a common mechanism of resistance to TRAIL includes the downregulation of its corresponding receptors, or the upregulation of the protease-deficient caspase homolog, c-FLIP. We hypothesised that DAPK2 depletion might revert such processes and thus further analysed the effect of RNAi-mediated DAPK2 depletion on the levels of DR4, DR5 and c-FLIP. While we did not observe any changes in c-FLIP mRNA or protein levels (**Figure 4-6**), we did detect a significant increase in DR4 and DR5 mRNA (**Figure 4-7**) and protein expression (**Figure 4-8**) in response to RNAi-mediated DAPK2 depletion. To further validate that the depletion of DAPK2 specifically upregulated TRAIL's DRs, we performed single knockdowns with four different DAPK2-targeting siRNA oligonucleotides. As expected, each one of these single oligonucleotides induced the expression of these DRs (**Figure 4-9** and **Figure 4-10**).

After establishing that DAPK2 depletion induced the expression of DRs, we asked whether this upregulation *per se* led to re-sensitisation of cells towards

TRAIL-induced apoptosis. For this purpose, we used U2OS cells as they only expressed DR5. By using double knockdowns combining different siRNA oligonucleotides we were able to target DAPK2 and DR5 concomitantly. We initially titrated the amount of DR5 siRNA that reverted the DR5 induction in response to DAPK2 knockdown (**Figure 4-13a**). Remarkably, co-transfection of 1.25 nM siDR5 with 20 nM siDAPK2 was sufficient to rescue U2OS cells from TRAIL-induced apoptosis in response to DAPK2 knockdown (**Figure 4-13c**), suggesting that the induction of DR expression was the main driver for the sensitisation towards TRAIL-induced apoptosis.

Given the fact that activation of TRAIL DRs and the FasR exhibit a high degree of signalling similarities and signalling components, we also assessed the effect of DAPK2 depletion on FasL-triggered apoptosis. Interestingly, we found that silencing DAPK2 sensitised U2OS cells towards FasL, whereas A549 remained resistant (**Figure 4-16**). Curiously, knockdown of DAPK2 resulted in the induction of FasR mRNA and increased protein levels in both cell lines, suggesting that A549 cells may have an additional inhibitory molecule that will need to be targeted before they can succumb to the cytotoxic effects of FasL. We further discovered that U2OS cells, that become sensitive to FasL-induced apoptosis in response to DAPK2 depletion, also showed a reduction of FasL decoy receptor DcR3 mRNA levels (**Figure 4-16b**). Thus, the upregulation of FasR *per se* might not have been the actual cause of the sensitisation to FasL-induced apoptosis, instead it might have been the repression of DcR3, which would the explain why U2OS cells become sensitive to DAPK2-mediated FasL-induced apoptosis.

7.1.4 RNAi-mediated depletion of DAPK2 induces NF-κB

Having established that inhibition of DAPK2 led to the selective sensitisation to TRAIL in U2OS and A459 cells and that this was mediated by the upregulation of its corresponding receptors, we analysed some of the underlining mechanisms causing such an induction. To measure the potential increase of mRNA and/or protein stability, we used classical biochemical assays that revealed that neither mRNA nor protein stability was affected in response to RNAi-mediated DAPK2 depletion (**Figure 5-1**). Given the increased mRNA levels for DR4, DR5 and FasR in response to DAPK2 knockdown, we then focused on potential transcription factors causing such induction. A thorough literature research revealed that the transcription factor p53 and the NF-κB family of transcription factors were likely candidates as both were previously described to be involved in the induction of DR4, DR5 and FasR transcripts. Although we did not detect elevated p53 mRNA levels in response to DAPK2 knockdown, the observed that the transcription of p21, one of it most immediate p53 target genes, was elevated (**Figure 5-2**). The use of p53 mutant T24 bladder carcinoma and p53-null prostate carcinoma PC3 cells (**Figure 5-3**) established that both cell lines were readily sensitised to TRAIL-induced apoptosis after DAPK2 knockdown despite their altered p53 status. Therefore, we concluded that p53 *per se* was dispensable for siDAPK2-mediated sensitisation to TRAIL. As mentioned before, the NF-κB family of transcription factors had also been described to activate the transcription of DRs and FasR. By using NF-κB luciferase reporter assays we showed that NF-κB was transcriptionally active in DAPK2 depleted cells (**Figure 5-4**) and qPCR experiments revealed that NF-κB family members were induced

at the mRNA and/or protein level (**Figure 5-5** and **Figure 5-6**). Further investigation into the transcriptional activation of NF-κB target genes revealed that several were upregulated in response to RNAi-mediated DAPK2 depletion (**Figure 5-7**). Remarkably, the transcription of the TNF-α receptor and NF-κB target gene TNFR2 was elevated in A549 cells, whereas the transcription of the second TNF-α receptor TNFR1 remained unaffected, however this was not observed in U2OS cells (**Figure 5-7**). TNFR2 has been previously described as a NF-κB target gene (Santee and Owen-Schaub, 1996). However, to the best of our knowledge, so far TNFR1 has not been reported to be transcriptionally regulated by NF-κB. As described in **1.6**, TNFR2 does not contain a DD and is therefore incapable of inducing apoptosis. In contrast to TNFR1, which can activate extrinsic apoptotic signalling and pro-survival cues *via* NF-κB. As shown in **Figure 4-2** RNAi-mediated depletion of DAPK2 had no effect on the sensitivity of A549 cells towards TNF-α, which could readily be explained by the unaltered expression of TNFR1 and the elevated expression of the pro-survival receptor, TNFR2.

In 2010, Bai et al. described that RNAi-mediated depletion of the DAPK-family member DAPK1 in endometrial carcinoma cells resulted in their sensitisation to TRAIL-induced apoptosis (Bai et al., 2010). The authors proposed that this was driven by the induced secretion of TRAIL itself and the induction of DR4, DR5 and TRAIL expression. They also reported on an induced expression of FasR and DcR1. Given the great homology of DAPK1 and DAPK2 in their kinase domain (**Figure 1-9**) it is likely that depletion of either kinase could induce similar cellular changes leading to the expression of DR4, DR5 and FasR in a

comparable way. Indeed, as described earlier we found elevated levels of DR4, DR5 and FasR in DAPK2 depleted cells. However, in contrast to these observations, we detected no induction of DcR1 or TRAIL mRNA in either of the studied cell lines (**Figure 4-7** and **Figure 5-7**).

7.1.5 Activation of NF-κB is necessary for the sensitisation to TRAIL

Having established a clear activation of NF-κB in response to DAPK2 knockdown we investigated whether or not this activation was causal for the upregulation of DRs and sensitisation to TRAIL-induced apoptosis. Therefore, double knockdown experiments were carried out, where NF-κB family members and DAPK2 were concomitantly targeted. As depicted in **Figure 5-8**, depletion of NF-κB1, a key molecule of the canonical NF-κB branch, rescued the siDAPK2-induced sensitisation to TRAIL in U2OS and A549 cells. Depletion of NF-κB2, a key molecule of the non-canonical branch in combination with DAPK2 depletion led to a partial rescue only in A549 cells. Knockdown of RELB and DAPK2 resulted in a partial rescue only in A549 cells, whereas knockdown of RELA had no effect on the siDAPK2-mediated sensitisation to TRAIL. These observations clearly suggested that the activation of NF-κB was crucial for the sensitisation of U2OS and A549 cells to TRAIL-induced apoptosis. To verify previous reports stating that NF-κB activation induces the transcription of DR5 (Shetty et al., 2005), we used DR5 promoter luciferase constructs to demonstrate that RNAi-mediated depletion of DAPK2 induced the transcriptional activation of DR5. Furthermore, DR5 promoter luciferase constructs containing a mutated NF-κB-binding site remained inactivated in DAPK2-depleted cells (**Figure 5-10**). Together, these

results provide compelling evidence for a direct requirement of NF-κB for the induction of DR5 in DAPK2-depleted cells and furthermore sensitisation to TRAIL-induced apoptosis.

In 2008, Chuang et al. reported that DAPK1 modulates T cell receptor (TCR) -induced NF-κB signalling in T cells. The authors reported that RNAi-mediated depletion of DAPK1 or overexpression of kinase dead (K42A) DAPK1 resulted in increased TCR activation and basal RELA phosphorylation. They proposed that DAPK1 functions by affecting the translocation of IKK proteins into lipid membrane rafts (Chuang et al., 2008). Moreover, in 2012 Yoo et al. reported that overexpression of DAPK1 in ovarian cancer cells inhibited the expression of NF-κB target genes and proposed that DAPK1 functions as an NF-κB repressor downstream of TNF-α (Yoo et al., 2012). Given the previously described sensitisation of endometrial carcinoma cells to TRAIL-induced apoptosis and their induced expression of NF-κB response genes such as DR4, DR5, TRAIL and DcR1 in response to RNAi-mediated DAPK1 depletion, we explored the possibility that DAPK2 might exhibit similar effects on NF-κB.

By carrying out experiments using TNF-α to induce NF-κB signalling, we discovered that DAPK2-depleted U2OS and A549 cells have decreased basal levels of IκBα, resulting in a delayed activation of NF-κB (RELA S536 phosphorylation) (**Figure 5-11**). In contrast, the overexpression of wild type DAPK2 reduced the levels of IκBα but it also 'dampened' the activation of NF-κB (as assessed by measuring RELA S536 phosphorylation). Interestingly, the

overexpression of a kinase dead DAPK2 (K42A) resulted in elevated levels of basal RELA S536 phosphorylation in both cell lines (**Figure 5-12b**). These results were in agreement with previous work carried out with DAPK1 by Chuang et al. 2008. It is worth while pointing out that the majority of our work was carried out in U2OS cells that as shown in **Figure 4-1a** and **b** do not express detectable amounts of DAPK1 protein. The A549 cells did express detectable levels of DAPK1 and these were unaffected upon RNAi-mediated depletion of DAPK2 (**Figure 4-1c**). However, DAPK2 depletion resulted in an activating de-phosphorylation of DAPK1 S308 in A549 cells (**Figure 6-6**), potentially to compensate for the loss of DAPK2. These findings open the possibility that DAPK2 and DAPK1 may, in fact, exhibit similar effect(s) on the regulation of NF-κB.

The question thus remains as to how downregulating DAPK2 leads to the activation of NF-κB, which is vital to sensitise otherwise resistant cells to TRAIL-mediated death. Clearly, the involvement of NF-κB in TRAIL signalling is complex and highly cell type- and context-dependent and DAPK2 appears to regulate an upstream component of NF-κB signalling. Such a component could be the NF-κB negative regulator, IκB. As described above, silencing DAPK2 led to its disappearance. This then poses the question of why IκB is being degraded with the most immediate hypothesis being its phosphorylation by an IKK complex, coupled to the TRAIL receptor complex. Remarkably, Chuang et al. reported that depletion of DAPK1 or overexpression of kinase dead DAPK1 resulted in a stronger recruitment of IKK-α and IKK-β into lipid rafts. Spatial accumulation of the IKK complex proteins activates the phosphorylation and subsequent

degradation of IκB, which could be enhanced in DAPK2-depleted and kinase dead DAPK2-overexpressing cells. This indicates a potential involvement of DAPK1 and DAPK2s kinase domain in the regulation of IKK proteins. Such regulation may occur *via* RIPK and/or TRADD (Liu et al., 2008a). Interestingly, the increased basal phosphorylation of RELA upon DAPK2 knockdown was more pronounced in U2OS cells, compared to A549 cells (**Figure 5-11**), which could potentially be explained by a compensatory mechanism of activated DAPK1 in A549 cells.

Perhaps the interaction of DAPK2 with DR5 (**Figure 5-14**) enabled it to act as a 'plug' that effectively stops cells from 'inadvertently' succumbing to TRAIL. Removing DAPK2 may free binding sites on the receptor complex necessary to couple the pathway to the initiator caspases and accumulation of the IKK complex which can also be activated downstream of DRs. It is also possible that the interaction between NF-κB signalling components and DAPK2 occurs in the cytoplasm rather than at the membrane level and, again, IKKs and IκB are the most likely interaction partners. Another possibility is that DAPK2 represses NF-κB activation by, for example, protecting the cell from cellular stress, which is known to activate NF-κB. Whichever way DAPK2 silencing leads to NF-κB activation, NF-κB activation seemed to lead to the degradation of DAPK2 in response to a classical NF-κB activator such as TNF-α (**Figure 5-13**). What is intriguing is why the output of the TRAIL stimulus is death considering NF-κB also leads to the activation of key survival genes. The balance must thus rest on the faster caspase activation observed following DAPK2 silencing and on the

NF-κB-mediated induction of DR5 and/or DR4. As mentioned above, overexpression of DAPK2 was able to suppress the TNF-α mediated activation of NF-κB. Overexpression of DAPK2 did not, however, revert the phenotype observed upon DAPK2 knockdown, as IκB also decreased. The latter was consistent with the findings of Yoo et al. who found IκB to be downregulated in response to DAPK1 overexpression (Yoo et al., 2012). A model that shows our understanding of the effect of DAPK2 depletion on the regulation of TRAIL-induced apoptosis is depicted in **Figure 5-15**.

7.1.6 Deregulation of the mitochondria in response to DAPK2 silencing is likely to be independent of the mechanism that sensitises resistant cancer cells to TRAIL

RNAi-mediated depletion of DAPK2 also induced significant metabolic changes in the mitochondrion. By using ROS specific probes, we found that the levels of cellular ROS, particularly superoxide, were elevated in DAPK2 depleted U2OS and A549 cells (**Figure 6-1**). Indeed, a number of stress kinases and anti-oxidative enzymes were elevated in cells upon DAPK2 knockdown (**Figure 6-2**). Further analyses revealed that these cellular changes most likely originated from the mitochondria. By using mitochondria specific probes we showed that DAPK2-depleted cells contained elevated levels of superoxide in their mitochondria (**Figure 6-3**) and that their membranes spontaneously depolarised (**Figure 6-5**). These alterations had further functional consequences on the mitochondria and resulted in a decreased rate of oxidative phosphorylation in DAPK2-depleted cells (**Figure 6-8**). Interestingly, DAPK1 has also been previously shown to regulate mitochondrial integrity and to modulate the mitochondrial membrane

potential. More specifically, inhibition of mitochondrial complex proteins was reported to induce activating de-phosphorylation of DAPK1 S308. It was thus proposed that DAPK1 plays a crucial role in maintaining mitochondria integrity and in the recycling of mitochondria with low Δψm (Shang et al., 2005). The ROS-inducing effect of DAPK2 depletion is further enhanced when kinase dead DAPK2 is overexpressed (**Figure 6-11**), which ultimately suggests that the DAPK2 effect on the mitochondria is kinase mediated. Given the high sequence homology between the kinase domain of DAPK1 and DAPK2 (**Figure 1-9**) it is hardly surprising that their kinase dependent functions may overlap and thus both proteins may affect mitochondrial maintenance *via* their kinase activity.

Remarkably, other scientists have previously reported that challenging cancer cells with several compounds could induce oxidative stress in these cells and sensitise them to TRAIL-induced apoptosis. For example, treatment of different types of cancer cells with compounds such as cardamomin, an experimental anti-inflammatory drug, 20(S)-ginsenoside Rg_3, a steroidal saponin that has been shown to sensitise resistant cells to several chemotherapeutic drugs, or indomethacin, a non-steroidal anti-inflammatory drug, resulted in increased intracellular ROS levels and re-sensitisation to TRAIL-induced apoptosis (Yadav et al., 2012, Lee et al., 2013, Tse et al., 2014). All of these compounds specifically activated the ER stress response gene CHOP which resulted in the transcriptional induction of DRs and thereby re-sensitisation to TRAIL-induced apoptosis. Other authors reported that induction of ROS using andrographolide, a diterpenoid lactone isolated from a traditional herbal medicine *Andrographis paniculata*, or γ-Tocotrienol, a member of the vitamin E family, led to p53-

mediated upregulation of DRs (Zhou et al., 2008, Kannappan et al., 2010). Remarkably, the use of the uncoupler of oxidative phosphorylation CCCP resulted in an increased sensitisation to TRAIL *via* increased intrinsic apoptotic signalling (Izeradjene et al., 2005).

Given the various reports linking ROS generation to sensitisation to TRAIL-induced apoptosis, there was the possibility that depletion of DAPK2 induced ROS through deregulation of mitochondrial maintenance, which then turned U2OS and A549 cells sensitive to the killing effects of TRAIL. However, in contrast to previous reports, under the experimental conditions used throughout my PhD we did not detect induction of the transcription factor CHOP (**Figure 6-4**) and we demonstrated that p53 was not essential for the siDAPK2-mediated sensitisation to TRAIL (**Figure 5-3**). Moreover, in 2014 Tse et al. showed that the re-sensitisation of cancer cells to TRAIL-induced apoptosis in response to ROS induced using indomethacin involved the inhibition of NF-κB (Tse et al., 2014). In contrast, here, we have demonstrated that NF-κB activation plays a crucial role in the sensitisation to TRAIL. The relationship between NF-κB and ROS is rather complex. It has been reported that NF-κB pro-survival cues can be activated in response to ROS induction thereby promoting the transcription of antioxidant genes such as SOD2 (Jones et al., 1997). However, NF-κB has also been shown to induce cellular ROS by upregulating the expression of COX2 or the NADPH oxidase 2 (NOX2) (Deng et al., 2003, Anrather et al., 2006). Therefore, it is possible that increased levels of cellular ROS triggered the induction of NF-κB that was seen in response to RNAi-mediated depletion of DAPK2. In contrast, we found that the overexpression of DAPK2 ‘dampened’ the activation of NF-κB

(**Figure 5-12a**), but it was also accompanied by an increase of cellular ROS (**Figure 6-10a**). Our data thus suggest that the induction of NF-κB in response to DAPK2 knockdown and mitochondrial alterations seen likely represent two independent events.

7.2 Limitations of the work

7.2.1 Are *in vitro* studies 'physiological enough'?

The most concerning limitation of any work carried out with cell lines is that some findings may not translate into the *in vivo* setting. Unfortunately, we were unable to obtain DAPK2-null cells, which would have allowed us to exclude the remote possibility that the observed phenotypes were caused by the methods used to either increase or decrease. The first report of a DAPK2 knockout mouse was only reported this year (Guay et al., 2014), which is why it was not possible to utilise any DAPK2-negative mouse embryonic fibroblasts (MEFs) to help further understand the role of DAPK2 in NF-κB signalling and mitochondrial regulation.

7.2.2 RNAi-mediated depletion: the ideal method?

All experiments carried out during this PhD involved RNAi-mediated depletion of relevant target genes 48 h after siRNA-transfection. This time point allowed the efficient knockdown of targeted genes. However, for some particular experiments a more prolonged downregulation of DAPK2 would potentially have given further insights into DAPK2 molecular roles. Especially the effect of DAPK2 on mitochondrial metabolism would have been easier to analyse with a prolonged

DAPK2 depletion. Unfortunately, several attempts to create inducible small hairpin (sh) DAPK2-expressing cell lines that target DAPK2 and would have allowed a sustained DAPK2 depletion were unsuccessful. Newer methods using the CRISPR/Cas system may help to remedy this and it is certainly something that should be explored as a priority, as it may have a significant impact on the understanding of DAPK2 biology.

7.3 Future perspectives

7.3.1 Understanding the role of DAPK2's kinase domain in TRAIL-induced apoptosis

Throughout this work the majority of observations were made using siRNAs, which target endogenous DAPK2. To understand whether the kinase domain of DAPK2 was involved in the modulation of NF-κB or mitochondria viability, cells were transfected with a kinase dead DAPK2, which is thought to mimic the effect of depleting this enzyme. When analysing the effect of kinase dead DAPK2 on NF-κB, we overexpressed kinase dead DAPK2 in U2OS TetR cells and assessed the effect of overexpressing this molecule on REL phosphorylation (**Figure 5-12**b). Unfortunately, our initial attempts to mimic the effect of DAPK2 depletion on the sensitisation to TRAIL by overexpressing kinase dead DAPK2 were unsuccessful, most likely due to the expression of endogenous DAPK2, as overexpression of kinase dead DAPK2 lead only to a slight induction of RELA phosphorylation. Further experiments, as those shown in **Figure 6-11**, should be carried out, where a 3'UTR specific siRNA oligonucleotide was used to deplete

endogenous DAPK2 and only assess the effects of the exogenously overexpressed protein.

7.3.2 How does DAPK2 regulate NF-κB?

Despite the clear-cut data showing that downregulation of DAPK2 led to the activation of NF-κB, the precise way by which DAPK2 expression regulates the activity of NF-κB remains elusive. It remains a possibility that DAPK2 actually directly interacts with NF-κB family members and, apart from the obvious co-immunoprecipitation experiments; more wide-ranging experiments with tandem affinity purification (TAP) could be used to identify interaction partners, followed by co-immunoprecipitations to verify potential findings. If these experiments reveal direct interactions between DAPK2 and NF-κB family members or their upstream regulators, interaction studies should be carried out to map down the exact interaction domains. These finding could make a significant difference to our current understanding of DAPK2 biology and its potential role as a therapeutic target.

7.3.3 How does DAPK2 regulate the mitochondria?

Experiments carried out during this PhD aimed at analysing the relations of DAPK2 and the mitochondria focused solely on mitochondrial changes upon DAPK2 knockdown. Further experiments analysing the activation status, and indeed cellular localisation, of DAPK2 in response to mitochondrial stress should be carried out to further analyse the potentially protective effect of DAPK2 on the

mitochondria. As DAPK2 must be dephosphorylated on S308 to become active, specific antibodies, raised against this epitope, could provide valuable information about the activation status of DAPK2 in response to mitochondrial stress and greatly facilitate the analyses. Furthermore, future work should include an analysis of the induction and/or stabilisation of DAPK2 in response to mitochondrial changes.

7.3.4 Dynamics of DAPK2: where is the protein located?

To date, the vast majority of reports analysing the function of DAPK2 have been based on overexpression studies. This is the reason why, for most of our experiments, we chose to manipulate endogenous DAPK2 using RNAi methodologies but which are also not without their own intrinsic problems. The exception to this were experiments carried out to ascertain certain properties of a kinase dead DAPK2, in which case, as others, we too made use of overexpressing systems,

To gain further insight into the physiological role of DAPK2, future work should include the analysis of the cellular location(s) of endogenous DAPK2 using high-resolution microscopy. Due to the lack of suitable good quality antibodies, fluorescence tagged versions of DAPK2 might be needed as a strategy to overcome this issue. By using advanced imaging techniques, such as förster resonance energy transfer (FRET), one could analyse the proximity of DAPK2 to members of the NF-κB family, or mitochondrial proteins and monitor their interactions in response to extracellular stimulations.

7.3.5 DAPK2 as a therapeutic target

This work has revealed that DAPK2 is a potential therapeutic clinical target in combination with TRAs. For potential clinical application(s), DAPK2-specific kinase inhibitors should be tested for their ability to mimic the effect of RNAi-mediated DAPK2 depletion. In 2014 Geering et al. published the first research article focusing on leucocyte biology using a DAPK2 specific inhibitor. Atempts should be made to source this inhibitor, which should then be used in further studies to analyse the effect of DAPK2 kinase inhibition on the regulation of NF-κB and mitochondrial maintenance.

7.3.6 Role of siDAPK2-induced ROS in the activation of NF-κB

Unfortunately, attempts to scavenge cellular ROS levels using N-acetylcysteine (NAC) and assessing the effect of reduced cellular ROS levels on the re-sensitisation to TRAIL-induced apoptosis were so far unsuccessful. This was most likely due to the length of the assay required for the RNAi-mediated depletion of DAPK2 (48 h). After 48 h higher doses of NAC exhibited a considerable amount of toxicity, whereas lower doses were unable to prevent the siDAPK2-induced induction of ROS. Further experiments making use of less toxic and more sophisticated ROS scavengers should be carried out to further understand the potential role of ROS in the activation of NF-κB and re-sensitisation of resistant cancer cells to TRAIL-induced apoptosis in response to RNAi-mediated depletion of DAPK2.

7.3.7 Unravelling of the DAPK1-DAPK2 interactome

This thesis provides persuasive evidence for a role of DAPK2 in the regulation of NF-κB and maintenance of mitochondria viability. Previous reports have also suggested the involvement of DAPK1 in the regulation of NF-κB and have postulated that DAPK1 is a potential sensor for the Δψm. As shown in **Figure 4-1**, U2OS cells did not express detectable amounts of DAPK1, whereas A549 did and this was de-phosphorylated, and thus presumably activated, upon DAPK2 knockdown (**Figure 6-6**). This suggests that DAPK1 might have been activated in A549 cells to compensate for the loss of DAPK2. Therefore, further experiments should analyse the possibility of a direct interaction between both kinases and ascertain whether these kinases are capable of cross-phosphorylating each other. For this purpose, co-immunoprecipitation experiments and mapping of interaction domains, together with FRET and other high-resolution imaging techniques, could be carried out to provide an understanding of their complex relationship

7.4 Final conclusion

The kinase domain of DAPK2 and DAPK1 share strong sequence homology, which makes it reasonable to assume that they share substrates. Clearly our understanding of how DAPK2 regulates and interacts with NF-κB, as well as its precise role in mitochondria metabolism, is in its infancy and much remains to be understood. As a regulator of NF-κB, DAPK2 is probably part of a multi-protein complex that is likely to be in relative proximity to membrane receptors, associated with upstream mediators of NF-κB, which may include proteins such as DAPK1. The disappearance of DAPK2 may disturb the balance of signalling components within or associated with this complex, thereby leading to the activation of NF-κB. As a mitochondrial regulator, DAPK2 is also likely to be part of a larger protein network that may be involved in processes such as the recycling of 'faulty' mitochondria. Overall, work carried out during my PhD point towards DAPK2 being an important mitochondrial regulator and potentially a clinical target to overcome TRAIL resistance. Indeed, DAPK2 inhibition in combination with TRAIL or TRAs may provide an alternative, novel, approach to overcome TRAIL-resistance by virtue of activating the pro-apoptotic facet of the NF-κB response. It is encouraging to think that it may ultimately open up new avenues for treatments of certain types of malignancies.

8. References

AGGARWAL, B. B., EESSALU, T. E. & HASS, P. E. 1985a. Characterization of receptors for human tumour necrosis factor and their regulation by gamma-interferon. *Nature,* 318**,** 665-7.

AGGARWAL, B. B., HENZEL, W. J., MOFFAT, B., KOHR, W. J. & HARKINS, R. N. 1985b. Primary structure of human lymphotoxin derived from 1788 lymphoblastoid cell line. *J Biol Chem,* 260**,** 2334-44.

AGGARWAL, B. B., MOFFAT, B. & HARKINS, R. N. 1984. Human lymphotoxin. Production by a lymphoblastoid cell line, purification, and initial characterization. *J Biol Chem,* 259**,** 686-91.

AGGARWAL, B. B., SCHWARZ, L., HOGAN, M. E. & RANDO, R. F. 1996. Triple helix-forming oligodeoxyribonucleotides targeted to the human tumor necrosis factor (TNF) gene inhibit TNF production and block the TNF-dependent growth of human glioblastoma tumor cells. *Cancer Res,* 56**,** 5156-64.

ANRATHER, J., RACCHUMI, G. & IADECOLA, C. 2006. NF-kappaB regulates phagocytic NADPH oxidase by inducing the expression of gp91phox. *J Biol Chem,* 281**,** 5657-67.

ARORA, A. & SCHOLAR, E. M. 2005. Role of tyrosine kinase inhibitors in cancer therapy. *J Pharmacol Exp Ther,* 315**,** 971-9.

ASHKENAZI, A., PAI, R. C., FONG, S., LEUNG, S., LAWRENCE, D. A., MARSTERS, S. A., BLACKIE, C., CHANG, L., MCMURTREY, A. E., HEBERT, A., DEFORGE, L., KOUMENIS, I. L., LEWIS, D., HARRIS, L., BUSSIERE, J., KOEPPEN, H., SHAHROKH, Z. & SCHWALL, R. H. 1999. Safety and antitumor activity of recombinant soluble Apo2 ligand. *J Clin Invest,* 104**,** 155-62.

AZIJLI, K., YUVARAJ, S., VAN ROOSMALEN, I., FLACH, K., GIOVANNETTI, E., PETERS, G. J., DE JONG, S. & KRUYT, F. A. 2013. MAPK p38 and JNK have opposing activities on TRAIL-induced apoptosis activation in NSCLC H460 cells that involves RIP1 and caspase-8 and is mediated by Mcl-1. *Apoptosis,* 18**,** 851-60.

BAETU, T. M., KWON, H., SHARMA, S., GRANDVAUX, N. & HISCOTT, J. 2001. Disruption of NF-kappaB signaling reveals a novel role for NF-kappaB in the regulation of TNF-related apoptosis-inducing ligand expression. *J Immunol,* 167**,** 3164-73.

BAI, T., TANAKA, T. & YUKAWA, K. 2010. Targeted knockdown of death-associated protein kinase expression induces TRAIL-mediated apoptosis in human endometrial adenocarcinoma cells. *Int J Oncol,* 37**,** 203-10.

BALABAN, R. S., NEMOTO, S. & FINKEL, T. 2005. Mitochondria, oxidants, and aging. *Cell,* 120**,** 483-95.

BALKWILL, F. 2006. TNF-alpha in promotion and progression of cancer. *Cancer Metastasis Rev,* 25**,** 409-16.

BARRIOS-RODILES, M., BROWN, K. R., OZDAMAR, B., BOSE, R., LIU, Z., DONOVAN, R. S., SHINJO, F., LIU, Y., DEMBOWY, J., TAYLOR, I. W., LUGA, V., PRZULJ, N., ROBINSON, M., SUZUKI, H., HAYASHIZAKI, Y., JURISICA, I. & WRANA, J. L. 2005. High-throughput mapping of a dynamic signaling network in mammalian cells. *Science,* 307**,** 1621-5.

BASAK, S., KIM, H., KEARNS, J. D., TERGAONKAR, V., O'DEA, E., WERNER, S. L., BENEDICT, C. A., WARE, C. F., GHOSH, G., VERMA, I. M. & HOFFMANN, A. 2007. A fourth IkappaB protein within the NF-kappaB signaling module. *Cell,* 128**,** 369-81.

BASILE, J. R., EICHTEN, A., ZACNY, V. & MUNGER, K. 2003. NF-kappaB-mediated induction of p21(Cip1/Waf1) by tumor necrosis factor alpha induces growth arrest and cytoprotection in normal human keratinocytes. *Mol Cancer Res,* 1**,** 262-70.

BASITH, S., MANAVALAN, B., GOSU, V. & CHOI, S. 2013. Evolutionary, structural and functional interplay of the IkappaB family members. *PLoS One,* 8**,** e54178.

BEG, A. A. & BALDWIN, A. S., JR. 1993. The I kappa B proteins: multifunctional regulators of Rel/NF-kappa B transcription factors. *Genes Dev,* 7**,** 2064-70.

BELYANSKAYA, L. L., MARTI, T. M., HOPKINS-DONALDSON, S., KURTZ, S., FELLEY-BOSCO, E. & STAHEL, R. A. 2007. Human agonistic TRAIL receptor antibodies Mapatumumab and Lexatumumab induce apoptosis in malignant mesothelioma and act synergistically with cisplatin. *Mol Cancer,* 6**,** 66.

BERNARD, D., QUATANNENS, B., VANDENBUNDER, B. & ABBADIE, C. 2001. Rel/NF-kappaB transcription factors protect against tumor necrosis factor (TNF)-related apoptosis-inducing ligand (TRAIL)-induced apoptosis by up-regulating the TRAIL decoy receptor DcR1. *J Biol Chem,* 276**,** 27322-8.

BERTANI, G. 1951. Studies on lysogenesis. I. The mode of phage liberation by lysogenic Escherichia coli. *J Bacteriol,* 62**,** 293-300.

BERTRAND, M. J. & VANDENABEELE, P. 2010. RIP1's function in NF-kappaB activation: from master actor to onlooker. *Cell Death Differ,* 17**,** 379-80.

BEUTLER, B., MILSARK, I. W. & CERAMI, A. C. 1985. Passive immunization against cachectin/tumor necrosis factor protects mice from lethal effect of endotoxin. *Science,* 229**,** 869-71.

BIALIK, S. & KIMCHI, A. 2006. The death-associated protein kinases: structure, function, and beyond. *Annu Rev Biochem,* 75**,** 189-210.

BLACK, R. A., RAUCH, C. T., KOZLOSKY, C. J., PESCHON, J. J., SLACK, J. L., WOLFSON, M. F., CASTNER, B. J., STOCKING, K. L., REDDY, P., SRINIVASAN, S., NELSON, N., BOIANI, N., SCHOOLEY, K. A., GERHART, M., DAVIS, R., FITZNER, J. N., JOHNSON, R. S., PAXTON, R. J., MARCH, C. J. & CERRETTI, D. P. 1997. A metalloproteinase disintegrin that releases tumour-necrosis factor-alpha from cells. *Nature,* 385**,** 729-33.

BONNEKOH, B., WEVERS, A., JUGERT, F., MERK, H. & MAHRLE, G. 1989. Colorimetric growth assay for epidermal cell cultures by their crystal violet binding capacity. *Arch Dermatol Res,* 281**,** 487-90.

BOYCE, B. F. & XING, L. 2007. Biology of RANK, RANKL, and osteoprotegerin. *Arthritis Res Ther,* 9 Suppl 1**,** S1.

BRADFORD, M. M. 1976. A rapid and sensitive method for the quantitation of microgram quantities of protein utilizing the principle of protein-dye binding. *Anal Biochem,* 72**,** 248-54.

BREASTED, J. H. & NEW-YORK HISTORICAL SOCIETY. LIBRARY. 1930. *The Edwin Smith surgical papyrus. Vol. 1, Hieroglyphic transliterations, translation and commentary,* Chicago, Ill., University of Chicago Press.

BRIGELIUS-FLOHE, R. & MAIORINO, M. 2013. Glutathione peroxidases. *Biochim Biophys Acta,* 1830**,** 3289-303.

CABAL-HIERRO, L. & LAZO, P. S. 2012. Signal transduction by tumor necrosis factor receptors. *Cell Signal,* 24**,** 1297-305.

CARSWELL, E. A., OLD, L. J., KASSEL, R. L., GREEN, S., FIORE, N. & WILLIAMSON, B. 1975. An endotoxin-induced serum factor that causes necrosis of tumors. *Proc Natl Acad Sci U S A,* 72**,** 3666-70.

CASTRO, J. E., LISTMAN, J. A., JACOBSON, B. A., WANG, Y., LOPEZ, P. A., JU, S., FINN, P. W. & PERKINS, D. L. 1996. Fas modulation of apoptosis during negative selection of thymocytes. *Immunity,* 5**,** 617-27.

CHAN, H., BARTOS, D. P. & OWEN-SCHAUB, L. B. 1999. Activation-dependent transcriptional regulation of the human Fas promoter requires NF-kappaB p50-p65 recruitment. *Mol Cell Biol,* 19**,** 2098-108.

CHAUDHARY, P. M., EBY, M., JASMIN, A., BOOKWALTER, A., MURRAY, J. & HOOD, L. 1997. Death receptor 5, a new member of the TNFR family, and DR4 induce FADD-dependent apoptosis and activate the NF-kappaB pathway. *Immunity,* 7**,** 821-30.

CHEN, L., PARK, S. M., TUMANOV, A. V., HAU, A., SAWADA, K., FEIG, C., TURNER, J. R., FU, Y. X., ROMERO, I. L., LENGYEL, E. & PETER, M. E. 2010. CD95 promotes tumour growth. *Nature,* 465**,** 492-6.

CHEN, N. J., CHIO, II, LIN, W. J., DUNCAN, G., CHAU, H., KATZ, D., HUANG, H. L., PIKE, K. A., HAO, Z., SU, Y. W., YAMAMOTO, K., DE POOTER, R. F., ZUNIGA-PFLUCKER, J. C., WAKEHAM, A., YEH, W. C. & MAK, T. W. 2008. Beyond tumor necrosis factor receptor: TRADD signaling in toll-like receptors. *Proc Natl Acad Sci U S A,* 105**,** 12429-34.

CHEN, X., CHEN, J., GAN, S., GUAN, H., ZHOU, Y., OUYANG, Q. & SHI, J. 2013. DNA damage strength modulates a bimodal switch of p53 dynamics for cell-fate control. *BMC Biol,* 11**,** 73.

CHEN, X., KANDASAMY, K. & SRIVASTAVA, R. K. 2003. Differential roles of RelA (p65) and c-Rel subunits of nuclear factor kappa B in tumor necrosis factor-related apoptosis-inducing ligand signaling. *Cancer Res,* 63**,** 1059-66.

CHEW, Y. C., ADHIKARY, G., WILSON, G. M., XU, W. & ECKERT, R. L. 2012. Sulforaphane induction of p21(Cip1) cyclin-dependent kinase inhibitor expression requires p53 and Sp1 transcription factors and is p53-dependent. *J Biol Chem,* 287**,** 16168-78.

CHINNAIYAN, A. M., TEPPER, C. G., SELDIN, M. F., O'ROURKE, K., KISCHKEL, F. C., HELLBARDT, S., KRAMMER, P. H., PETER, M. E. & DIXIT, V. M. 1996. FADD/MORT1 is a common mediator of CD95 (Fas/APO-1) and tumor necrosis factor receptor-induced apoptosis. *J Biol Chem,* 271**,** 4961-5.

CHOI, S. J., LEE, K. H., PARK, H. S., KIM, S. K., KOH, C. M. & PARK, J. Y. 2005. Differential expression, shedding, cytokine regulation and function of TNFR1 and TNFR2 in human fetal astrocytes. *Yonsei Med J,* 46**,** 818-26.

CHUANG, Y. T., FANG, L. W., LIN-FENG, M. H., CHEN, R. H. & LAI, M. Z. 2008. The tumor suppressor death-associated protein kinase targets to TCR-stimulated NF-kappa B activation. *J Immunol,* 180**,** 3238-49.

COHEN, O., FEINSTEIN, E. & KIMCHI, A. 1997. DAP-kinase is a Ca2+/calmodulin-dependent, cytoskeletal-associated protein kinase, with cell death-inducing functions that depend on its catalytic activity. *EMBO J,* 16**,** 998-1008.

COOPER, M. J., HALUSCHAK, J. J., JOHNSON, D., SCHWARTZ, S., MORRISON, L. J., LIPPA, M., HATZIVASSILIOU, G. & TAN, J. 1994. p53 mutations in bladder carcinoma cell lines. *Oncol Res,* 6**,** 569-79.

CRETNEY, E., TAKEDA, K., YAGITA, H., GLACCUM, M., PESCHON, J. J. & SMYTH, M. J. 2002. Increased susceptibility to tumor initiation and metastasis in TNF-related apoptosis-inducing ligand-deficient mice. *J Immunol,* 168**,** 1356-61.

CROWDER, R. N. & EL-DEIRY, W. S. 2012. Caspase-8 regulation of TRAIL-mediated cell death. *Exp Oncol,* 34**,** 160-4.

CUI, J., MINER, B. M., ELDREDGE, J. B., WARRENFELTZ, S. W., DAM, P., XU, Y. & PUETT, D. 2011. Regulation of gene expression in ovarian cancer cells by luteinizing hormone receptor expression and activation. *BMC Cancer,* 11**,** 280.

DANIAL, N. N. & KORSMEYER, S. J. 2004. Cell death: critical control points. *Cell,* 116**,** 205-19.

DANIELS, R. A., TURLEY, H., KIMBERLEY, F. C., LIU, X. S., MONGKOLSAPAYA, J., CH'EN, P., XU, X. N., JIN, B. Q., PEZZELLA, F. & SCREATON, G. R. 2005. Expression of TRAIL and TRAIL receptors in normal and malignant tissues. *Cell Res,* 15**,** 430-8.

DASHTY, M. 2013. A quick look at biochemistry: carbohydrate metabolism. *Clin Biochem,* 46**,** 1339-52.

DECHANT, M. J., FELLENBERG, J., SCHEUERPFLUG, C. G., EWERBECK, V. & DEBATIN, K. M. 2004. Mutation analysis of the apoptotic "death-receptors" and the adaptors TRADD and FADD/MORT-1 in osteosarcoma tumor samples and osteosarcoma cell lines. *Int J Cancer,* 109**,** 661-7.

DECOSTER, E., VANHAESEBROECK, B., VANDENABEELE, P., GROOTEN, J. & FIERS, W. 1995. Generation and biological characterization of membrane-bound, uncleavable murine tumor necrosis factor. *J Biol Chem,* 270**,** 18473-8.

DEEPE, G. S., JR. 2007. Tumor necrosis factor-alpha and host resistance to the pathogenic fungus, Histoplasma capsulatum. *J Investig Dermatol Symp Proc,* 12**,** 34-7.

DEFFIE, A., WU, H., REINKE, V. & LOZANO, G. 1993. The tumor suppressor p53 regulates its own transcription. *Mol Cell Biol,* 13**,** 3415-23.

DEGLI-ESPOSTI, M. A., DOUGALL, W. C., SMOLAK, P. J., WAUGH, J. Y., SMITH, C. A. & GOODWIN, R. G. 1997a. The novel receptor TRAIL-R4 induces NF-kappaB and

protects against TRAIL-mediated apoptosis, yet retains an incomplete death domain. *Immunity,* 7**,** 813-20.

DEGLI-ESPOSTI, M. A., SMOLAK, P. J., WALCZAK, H., WAUGH, J., HUANG, C. P., DUBOSE, R. F., GOODWIN, R. G. & SMITH, C. A. 1997b. Cloning and characterization of TRAIL-R3, a novel member of the emerging TRAIL receptor family. *J Exp Med,* 186**,** 1165-70.

DEISS, L. P., FEINSTEIN, E., BERISSI, H., COHEN, O. & KIMCHI, A. 1995. Identification of a novel serine/threonine kinase and a novel 15-kD protein as potential mediators of the gamma interferon-induced cell death. *Genes Dev,* 9**,** 15-30.

DELMAS, D., REBE, C., MICHEAU, O., ATHIAS, A., GAMBERT, P., GRAZIDE, S., LAURENT, G., LATRUFFE, N. & SOLARY, E. 2004. Redistribution of CD95, DR4 and DR5 in rafts accounts for the synergistic toxicity of resveratrol and death receptor ligands in colon carcinoma cells. *Oncogene,* 23**,** 8979-86.

DENG, W. G., ZHU, Y. & WU, K. K. 2003. Up-regulation of p300 binding and p50 acetylation in tumor necrosis factor-alpha-induced cyclooxygenase-2 promoter activation. *J Biol Chem,* 278**,** 4770-7.

DEVIN, A., COOK, A., LIN, Y., RODRIGUEZ, Y., KELLIHER, M. & LIU, Z. 2000. The distinct roles of TRAF2 and RIP in IKK activation by TNF-R1: TRAF2 recruits IKK to TNF-R1 while RIP mediates IKK activation. *Immunity,* 12**,** 419-29.

DEVITA, V. T., JR. & CHU, E. 2008. A history of cancer chemotherapy. *Cancer Res,* 68**,** 8643-53.

DILLER, L., KASSEL, J., NELSON, C. E., GRYKA, M. A., LITWAK, G., GEBHARDT, M., BRESSAC, B., OZTURK, M., BAKER, S. J., VOGELSTEIN, B. & ET AL. 1990. p53 functions as a cell cycle control protein in osteosarcomas. *Mol Cell Biol,* 10**,** 5772-81.

DOMAZET-LOSO, T., KLIMOVICH, A., ANOKHIN, B., ANTON-ERXLEBEN, F., HAMM, M. J., LANGE, C. & BOSCH, T. C. 2014. Naturally occurring tumours in the basal metazoan Hydra. *Nat Commun,* 5**,** 4222.

DOPP, J. M., SARAFIAN, T. A., SPINELLA, F. M., KAHN, M. A., SHAU, H. & DE VELLIS, J. 2002. Expression of the p75 TNF receptor is linked to TNF-induced NFkappaB translocation and oxyradical neutralization in glial cells. *Neurochem Res,* 27**,** 1535-42.

DRAPPA, J., VAISHNAW, A. K., SULLIVAN, K. E., CHU, J. L. & ELKON, K. B. 1996. Fas gene mutations in the Canale-Smith syndrome, an inherited lymphoproliferative disorder associated with autoimmunity. *N Engl J Med,* 335**,** 1643-9.

DROSE, S. 2013. Differential effects of complex II on mitochondrial ROS production and their relation to cardioprotective pre- and postconditioning. *Biochim Biophys Acta,* 1827**,** 578-87.

EA, C. K., DENG, L., XIA, Z. P., PINEDA, G. & CHEN, Z. J. 2006. Activation of IKK by TNFalpha requires site-specific ubiquitination of RIP1 and polyubiquitin binding by NEMO. *Mol Cell,* 22**,** 245-57.

EBBELL, B. B. L. 1937. *The Papyrus Ebers : the greatest Egyptian medical document,* Copenhagen, Levin & Munksgaard.

EHRLICH, S., INFANTE-DUARTE, C., SEEGER, B. & ZIPP, F. 2003. Regulation of soluble and surface-bound TRAIL in human T cells, B cells, and monocytes. *Cytokine,* 24**,** 244-53.

EISENBERG-LERNER, A. & KIMCHI, A. 2007. DAP kinase regulates JNK signaling by binding and activating protein kinase D under oxidative stress. *Cell Death Differ,* 14**,** 1908-15.

EL-DEIRY, W. S. 2005. *Death Receptors in Cancer Therapy*, Humana Press.

ELLIOTT, M. J., MAINI, R. N., FELDMANN, M., KALDEN, J. R., ANTONI, C., SMOLEN, J. S., LEEB, B., BREEDVELD, F. C., MACFARLANE, J. D., BIJL, H. & ET AL. 1994. Randomised double-blind comparison of chimeric monoclonal antibody to tumour necrosis factor alpha (cA2) versus placebo in rheumatoid arthritis. *Lancet,* 344**,** 1105-10.

EMERY, J. G., MCDONNELL, P., BURKE, M. B., DEEN, K. C., LYN, S., SILVERMAN, C., DUL, E., APPELBAUM, E. R., EICHMAN, C., DIPRINZIO, R., DODDS, R. A., JAMES, I. E., ROSENBERG, M., LEE, J. C. & YOUNG, P. R. 1998. Osteoprotegerin is a receptor for the cytotoxic ligand TRAIL. *J Biol Chem,* 273**,** 14363-7.

ESTELLER, M., CORN, P. G., BAYLIN, S. B. & HERMAN, J. G. 2001. A gene hypermethylation profile of human cancer. *Cancer Res,* 61**,** 3225-9.

FANG, J., MENON, M., ZHANG, D., TORBETT, B., OXBURGH, L., TSCHAN, M., HOUDE, E. & WOJCHOWSKI, D. M. 2008. Attenuation of EPO-dependent erythroblast formation by death-associated protein kinase-2. *Blood,* 112**,** 886-90.

FANTIN, V. R., ST-PIERRE, J. & LEDER, P. 2006. Attenuation of LDH-A expression uncovers a link between glycolysis, mitochondrial physiology, and tumor maintenance. *Cancer Cell,* 9**,** 425-34.

FARISS, M. W., CHAN, C. B., PATEL, M., VAN HOUTEN, B. & ORRENIUS, S. 2005. Role of mitochondria in toxic oxidative stress. *Mol Interv,* 5**,** 94-111.

FAUSTMAN, D. & DAVIS, M. 2010. TNF receptor 2 pathway: drug target for autoimmune diseases. *Nat Rev Drug Discov,* 9**,** 482-93.

FENNER, B. J., SCANNELL, M. & PREHN, J. H. 2010. Expanding the substantial interactome of NEMO using protein microarrays. *PLoS One,* 5**,** e8799.

FINNBERG, N., GRUBER, J. J., FEI, P., RUDOLPH, D., BRIC, A., KIM, S. H., BURNS, T. F., AJUHA, H., PAGE, R., WU, G. S., CHEN, Y., MCKENNA, W. G., BERNHARD, E., LOWE, S., MAK, T. & EL-DEIRY, W. S. 2005. DR5 knockout mice are compromised in radiation-induced apoptosis. *Mol Cell Biol,* 25**,** 2000-13.

FINNBERG, N., KLEIN-SZANTO, A. J. & EL-DEIRY, W. S. 2008. TRAIL-R deficiency in mice promotes susceptibility to chronic inflammation and tumorigenesis. *J Clin Invest,* 118**,** 111-23.

FISHER, M. J., VIRMANI, A. K., WU, L., APLENC, R., HARPER, J. C., POWELL, S. M., REBBECK, T. R., SIDRANSKY, D., GAZDAR, A. F. & EL-DEIRY, W. S. 2001. Nucleotide substitution in the ectodomain of trail receptor DR4 is associated with lung cancer and head and neck cancer. *Clin Cancer Res,* 7**,** 1688-97.

FUCHS, Y. & STELLER, H. 2011. Programmed cell death in animal development and disease. *Cell,* 147**,** 742-58.

FULDA, S. 2014. Molecular pathways: targeting inhibitor of apoptosis proteins in cancer--from molecular mechanism to therapeutic application. *Clin Cancer Res,* 20**,** 289-95.

FURUKAWA, F., KANAUCHI, H., WAKITA, H., TOKURA, Y., TACHIBANA, T., HORIGUCHI, Y., IMAMURA, S., OZAKI, S. & TAKIGAWA, M. 1996. Spontaneous autoimmune skin lesions of MRL/n mice: autoimmune disease-prone genetic background in relation to Fas-defect MRL/1pr mice. *J Invest Dermatol,* 107**,** 95-100.

GALLIGAN, L., LONGLEY, D. B., MCEWAN, M., WILSON, T. R., MCLAUGHLIN, K. & JOHNSTON, P. G. 2005. Chemotherapy and TRAIL-mediated colon cancer cell death: the roles of p53, TRAIL receptors, and c-FLIP. *Mol Cancer Ther,* 4**,** 2026-36.

GALLUZZI, L., MAIURI, M. C., VITALE, I., ZISCHKA, H., CASTEDO, M., ZITVOGEL, L. & KROEMER, G. 2007. Cell death modalities: classification and pathophysiological implications. *Cell Death Differ,* 14**,** 1237-43.

GANTEN, T. M., HAAS, T. L., SYKORA, J., STAHL, H., SPRICK, M. R., FAS, S. C., KRUEGER, A., WEIGAND, M. A., GROSSE-WILDE, A., STREMMEL, W., KRAMMER, P. H. & WALCZAK, H. 2004. Enhanced caspase-8 recruitment to and activation at the DISC is critical for sensitisation of human hepatocellular carcinoma cells to TRAIL-induced apoptosis by chemotherapeutic drugs. *Cell Death Differ,* 11 Suppl 1**,** S86-96.

GARDAM, S. & BRINK, R. 2014. Non-Canonical NF-kappaB Signaling Initiated by BAFF Influences B Cell Biology at Multiple Junctures. *Front Immunol,* 4**,** 509.

GEERING, B., STOECKLE, C., ROZMAN, S., OBERSON, K., BENARAFA, C. & SIMON, H. U. 2013. DAPK2 positively regulates motility of neutrophils and eosinophils in response to intermediary chemoattractants. *J Leukoc Biol*.

GHOSH, S. & HAYDEN, M. S. 2008. New regulators of NF-kappaB in inflammation. *Nat Rev Immunol,* 8**,** 837-48.

GHOSH, S. & KARIN, M. 2002. Missing pieces in the NF-kappaB puzzle. *Cell,* 109 Suppl**,** S81-96.

GIARD, D. J., AARONSON, S. A., TODARO, G. J., ARNSTEIN, P., KERSEY, J. H., DOSIK, H. & PARKS, W. P. 1973. In vitro cultivation of human tumors: establishment of cell lines derived from a series of solid tumors. *J Natl Cancer Inst,* 51**,** 1417-23.

GIEFFERS, C., KLUGE, M., MERZ, C., SYKORA, J., THIEMANN, M., SCHAAL, R., FISCHER, C., BRANSCHADEL, M., ABHARI, B. A., HOHENBERGER, P., FULDA, S., FRICKE, H. & HILL, O. 2013. APG350 induces superior clustering of TRAIL receptors and shows therapeutic antitumor efficacy independent of cross-linking via Fcgamma receptors. *Mol Cancer Ther,* 12**,** 2735-47.

GIORDANO, C., STASSI, G., DE MARIA, R., TODARO, M., RICHIUSA, P., PAPOFF, G., RUBERTI, G., BAGNASCO, M., TESTI, R. & GALLUZZO, A. 1997. Potential involvement of Fas and its ligand in the pathogenesis of Hashimoto's thyroiditis. *Science,* 275**,** 960-3.

GIRGIS, H., MASUI, O., WHITE, N. M., SCORILAS, A., ROTONDO, F., SEIVWRIGHT, A., GABRIL, M., FILTER, E. R., GIRGIS, A. H., BJARNASON, G. A., JEWETT, M. A.,

EVANS, A., AL-HADDAD, S., SIU, K. M. & YOUSEF, G. M. 2014. Lactate dehydrogenase A is a potential prognostic marker in clear cell renal cell carcinoma. *Mol Cancer,* 13**,** 101.

GIULIETTI, A., OVERBERGH, L., VALCKX, D., DECALLONNE, B., BOUILLON, R. & MATHIEU, C. 2001. An overview of real-time quantitative PCR: applications to quantify cytokine gene expression. *Methods,* 25**,** 386-401.

GONZALVEZ, F. & ASHKENAZI, A. 2010. New insights into apoptosis signaling by Apo2L/TRAIL. *Oncogene*.

GORRINI, C., HARRIS, I. S. & MAK, T. W. 2013. Modulation of oxidative stress as an anticancer strategy. *Nat Rev Drug Discov,* 12**,** 931-47.

GOTTESMAN, M. M. 2002. Mechanisms of cancer drug resistance. *Annu Rev Med,* 53**,** 615-27.

GOZUACIK, D. & KIMCHI, A. 2006. DAPk protein family and cancer. *Autophagy,* 2**,** 74-9.

GREGORY, M. S., HACKETT, C. G., ABERNATHY, E. F., LEE, K. S., SAFF, R. R., HOHLBAUM, A. M., MOODY, K. S., HOBSON, M. W., JONES, A., KOLOVOU, P., KARRAY, S., GIANI, A., JOHN, S. W., CHEN, D. F., MARSHAK-ROTHSTEIN, A. & KSANDER, B. R. 2011. Opposing roles for membrane bound and soluble Fas ligand in glaucoma-associated retinal ganglion cell death. *PLoS One,* 6**,** e17659.

GRELL, M., BECKE, F. M., WAJANT, H., MANNEL, D. N. & SCHEURICH, P. 1998. TNF receptor type 2 mediates thymocyte proliferation independently of TNF receptor type 1. *Eur J Immunol,* 28**,** 257-63.

GRIFFITH, T. S., BRUNNER, T., FLETCHER, S. M., GREEN, D. R. & FERGUSON, T. A. 1995. Fas ligand-induced apoptosis as a mechanism of immune privilege. *Science,* 270**,** 1189-92.

GRIVENNIKOV, S. I., TUMANOV, A. V., LIEPINSH, D. J., KRUGLOV, A. A., MARAKUSHA, B. I., SHAKHOV, A. N., MURAKAMI, T., DRUTSKAYA, L. N., FORSTER, I., CLAUSEN, B. E., TESSAROLLO, L., RYFFEL, B., KUPRASH, D. V. & NEDOSPASOV, S. A. 2005. Distinct and nonredundant in vivo functions of TNF produced by t cells and macrophages/neutrophils: protective and deleterious effects. *Immunity,* 22**,** 93-104.

GROSSE-WILDE, A., VOLOSHANENKO, O., BAILEY, S. L., LONGTON, G. M., SCHAEFER, U., CSERNOK, A. I., SCHUTZ, G., GREINER, E. F., KEMP, C. J. & WALCZAK, H. 2008. TRAIL-R deficiency in mice enhances lymph node metastasis without affecting primary tumor development. *J Clin Invest,* 118**,** 100-10.

GUAY, J. A., WOJCHOWSKI, D. M., FANG, J. & OXBURGH, L. 2014. Death associated protein kinase 2 is expressed in cortical interstitial cells of the mouse kidney. *BMC Res Notes,* 7**,** 345.

HAAS, T. L., EMMERICH, C. H., GERLACH, B., SCHMUKLE, A. C., CORDIER, S. M., RIESER, E., FELTHAM, R., VINCE, J., WARNKEN, U., WENGER, T., KOSCHNY, R., KOMANDER, D., SILKE, J. & WALCZAK, H. 2009. Recruitment of the linear ubiquitin chain assembly complex stabilizes the TNF-R1 signaling complex and is required for TNF-mediated gene induction. *Mol Cell,* 36**,** 831-44.

HAHNE, M., RIMOLDI, D., SCHROTER, M., ROMERO, P., SCHREIER, M., FRENCH, L. E., SCHNEIDER, P., BORNAND, T., FONTANA, A., LIENARD, D., CEROTTINI, J. & TSCHOPP, J. 1996. Melanoma cell expression of Fas(Apo-1/CD95) ligand: implications for tumor immune escape. *Science,* 274**,** 1363-6.

HAJDU, S. I. 2004. Greco-Roman thought about cancer. *Cancer,* 100**,** 2048-51.

HAJDU, S. I. 2011. A note from history: landmarks in history of cancer, part 1. *Cancer,* 117**,** 1097-102.

HALAAS, O., VIK, R., ASHKENAZI, A. & ESPEVIK, T. 2000. Lipopolysaccharide induces expression of APO2 ligand/TRAIL in human monocytes and macrophages. *Scand J Immunol,* 51**,** 244-50.

HAMILTON, K. E., SIMMONS, J. G., DING, S., VAN LANDEGHEM, L. & LUND, P. K. 2011. Cytokine induction of tumor necrosis factor receptor 2 is mediated by STAT3 in colon cancer cells. *Mol Cancer Res,* 9**,** 1718-31.

HANAHAN, D. 1983. Studies on transformation of Escherichia coli with plasmids. *J Mol Biol,* 166**,** 557-80.

HANAHAN, D. & WEINBERG, R. A. 2000. The hallmarks of cancer. *Cell,* 100**,** 57-70.

HANAHAN, D. & WEINBERG, R. A. 2011. Hallmarks of cancer: the next generation. *Cell,* 144**,** 646-74.

HASHKES, P. J., BECKER, M. L., CABRAL, D. A., LAXER, R. M., PALLER, A. S., RABINOVICH, C. E., TURNER, D. & ZULIAN, F. 2014. Methotrexate: new uses for an old drug. *J Pediatr,* 164**,** 231-6.

HAUER, J., PUSCHNER, S., RAMAKRISHNAN, P., SIMON, U., BONGERS, M., FEDERLE, C. & ENGELMANN, H. 2005. TNF receptor (TNFR)-associated factor (TRAF) 3 serves as an inhibitor of TRAF2/5-mediated activation of the noncanonical NF-kappaB pathway by TRAF-binding TNFRs. *Proc Natl Acad Sci U S A,* 102**,** 2874-9.

HAYDEN, M. S. & GHOSH, S. 2008. Shared principles in NF-kappaB signaling. *Cell,* 132**,** 344-62.

HAYDEN, M. S. & GHOSH, S. 2012. NF-kappaB, the first quarter-century: remarkable progress and outstanding questions. *Genes Dev,* 26**,** 203-34.

HAYNES, N. M., HAWKINS, E. D., LI, M., MCLAUGHLIN, N. M., HAMMERLING, G. J., SCHWENDENER, R., WINOTO, A., WENSKY, A., YAGITA, H., TAKEDA, K., KERSHAW, M. H., DARCY, P. K. & SMYTH, M. J. 2010. CD11c+ dendritic cells and B cells contribute to the tumoricidal activity of anti-DR5 antibody therapy in established tumors. *J Immunol,* 185**,** 532-41.

HE, L., LUO, L., PROCTOR, S. J., MIDDLETON, P. G., BLAKELY, E. L., TAYLOR, R. W. & TURNBULL, D. M. 2003. Somatic mitochondrial DNA mutations in adult-onset leukaemia. *Leukemia,* 17**,** 2487-91.

HEISKANEN, K. M., BHAT, M. B., WANG, H. W., MA, J. & NIEMINEN, A. L. 1999. Mitochondrial depolarization accompanies cytochrome c release during apoptosis in PC6 cells. *J Biol Chem,* 274**,** 5654-8.

HENRY, R. E., ANDRYSIK, Z., PARIS, R., GALBRAITH, M. D. & ESPINOSA, J. M. 2012. A DR4:tBID axis drives the p53 apoptotic response by promoting oligomerization of poised BAX. *EMBO J,* 31**,** 1266-78.

HENSHALL, D. C., ARAKI, T., SCHINDLER, C. K., SHINODA, S., LAN, J. Q. & SIMON, R. P. 2003. Expression of death-associated protein kinase and recruitment to the tumor necrosis factor signaling pathway following brief seizures. *J Neurochem,* 86**,** 1260-70.

HERNANDEZ-SAAVEDRA, D., ZHOU, H. & MCCORD, J. M. 2005. Anti-inflammatory properties of a chimeric recombinant superoxide dismutase: SOD2/3. *Biomed Pharmacother,* 59**,** 204-8.

HIGAI, K., ISHIHARA, S. & MATSUMOTO, K. 2006. NFkappaB-p65 dependent transcriptional regulation of glycosyltransferases in human colon adenocarcinoma HT-29 by stimulation with tumor necrosis factor alpha. *Biol Pharm Bull,* 29**,** 2372-7.

HIRST, J., KING, M. S. & PRYDE, K. R. 2008. The production of reactive oxygen species by complex I. *Biochem Soc Trans,* 36**,** 976-80.

HITOMI, J., CHRISTOFFERSON, D. E., NG, A., YAO, J., DEGTEREV, A., XAVIER, R. J. & YUAN, J. 2008. Identification of a molecular signaling network that regulates a cellular necrotic cell death pathway. *Cell,* 135**,** 1311-23.

HOLOHAN, C., VAN SCHAEYBROECK, S., LONGLEY, D. B. & JOHNSTON, P. G. 2013. Cancer drug resistance: an evolving paradigm. *Nat Rev Cancer,* 13**,** 714-26.

HOPKINS-DONALDSON, S., ZIEGLER, A., KURTZ, S., BIGOSCH, C., KANDIOLER, D., LUDWIG, C., ZANGEMEISTER-WITTKE, U. & STAHEL, R. 2003. Silencing of death receptor and caspase-8 expression in small cell lung carcinoma cell lines and tumors by DNA methylation. *Cell Death Differ,* 10**,** 356-64.

HORAK, P., PILS, D., HALLER, G., PRIBILL, I., ROESSLER, M., TOMEK, S., HORVAT, R., ZEILLINGER, R., ZIELINSKI, C. & KRAINER, M. 2005. Contribution of epigenetic silencing of tumor necrosis factor-related apoptosis inducing ligand receptor 1 (DR4) to TRAIL resistance and ovarian cancer. *Mol Cancer Res,* 3**,** 335-43.

HSU, H., HUANG, J., SHU, H. B., BAICHWAL, V. & GOEDDEL, D. V. 1996a. TNF-dependent recruitment of the protein kinase RIP to the TNF receptor-1 signaling complex. *Immunity,* 4**,** 387-96.

HSU, H., SHU, H. B., PAN, M. G. & GOEDDEL, D. V. 1996b. TRADD-TRAF2 and TRADD-FADD interactions define two distinct TNF receptor 1 signal transduction pathways. *Cell,* 84**,** 299-308.

HSU, H., XIONG, J. & GOEDDEL, D. V. 1995. The TNF receptor 1-associated protein TRADD signals cell death and NF-kappa B activation. *Cell,* 81**,** 495-504.

HUANG, S. & SINICROPE, F. A. 2008. BH3 mimetic ABT-737 potentiates TRAIL-mediated apoptotic signaling by unsequestering Bim and Bak in human pancreatic cancer cells. *Cancer Res,* 68**,** 2944-51.

HUDIS, C. A. 2007. Trastuzumab--mechanism of action and use in clinical practice. *N Engl J Med,* 357**,** 39-51.

HUMBERT, M., FEDERZONI, E. A., BRITSCHGI, A., SCHLAFLI, A. M., VALK, P. J., KAUFMANN, T., HAFERLACH, T., BEHRE, G., SIMON, H. U., TORBETT, B. E., FEY, M. F. & TSCHAN, M. P. 2013. The tumor suppressor gene DAPK2 is induced by the myeloid transcription factors PU.1 and C/EBPalpha during granulocytic differentiation but repressed by PML-RARalpha in APL. *J Leukoc Biol*.

HUMBERT, M., FEDERZONI, E. A., BRITSCHGI, A., SCHLAFLI, A. M., VALK, P. J., KAUFMANN, T., HAFERLACH, T., BEHRE, G., SIMON, H. U., TORBETT, B. E., FEY, M. F. & TSCHAN, M. P. 2014. The tumor suppressor gene DAPK2 is induced by the myeloid transcription factors PU.1 and C/EBPalpha during granulocytic differentiation but repressed by PML-RARalpha in APL. *J Leukoc Biol,* 95**,** 83-93.

INBAL, B., BIALIK, S., SABANAY, I., SHANI, G. & KIMCHI, A. 2002. DAP kinase and DRP-1 mediate membrane blebbing and the formation of autophagic vesicles during programmed cell death. *J Cell Biol,* 157**,** 455-68.

INBAL, B., SHANI, G., COHEN, O., KISSIL, J. L. & KIMCHI, A. 2000. Death-associated protein kinase-related protein 1, a novel serine/threonine kinase involved in apoptosis. *Mol Cell Biol,* 20**,** 1044-54.

IRWIN, M. W., MAK, S., MANN, D. L., QU, R., PENNINGER, J. M., YAN, A., DAWOOD, F., WEN, W. H., SHOU, Z. & LIU, P. 1999. Tissue expression and immunolocalization of tumor necrosis factor-alpha in postinfarction dysfunctional myocardium. *Circulation,* 99**,** 1492-8.

ISAACS, W. B., CARTER, B. S. & EWING, C. M. 1991. Wild-type p53 suppresses growth of human prostate cancer cells containing mutant p53 alleles. *Cancer Res,* 51**,** 4716-20.

ISHIKAWA, E., NAKAZAWA, M., YOSHINARI, M. & MINAMI, M. 2005. Role of tumor necrosis factor-related apoptosis-inducing ligand in immune response to influenza virus infection in mice. *J Virol,* 79**,** 7658-63.

ISRAEL, A. 2010. The IKK complex, a central regulator of NF-kappaB activation. *Cold Spring Harb Perspect Biol,* 2**,** a000158.

IZERADJENE, K., DOUGLAS, L., TILLMAN, D. M., DELANEY, A. B. & HOUGHTON, J. A. 2005. Reactive oxygen species regulate caspase activation in tumor necrosis factor-related apoptosis-inducing ligand-resistant human colon carcinoma cell lines. *Cancer Res,* 65**,** 7436-45.

JANSSENS, S. & TSCHOPP, J. 2006. Signals from within: the DNA-damage-induced NF-kappaB response. *Cell Death Differ,* 13**,** 773-84.

JIN, Y., BLUE, E. K., DIXON, S., HOU, L., WYSOLMERSKI, R. B. & GALLAGHER, P. J. 2001. Identification of a new form of death-associated protein kinase that promotes cell survival. *J Biol Chem,* 276**,** 39667-78.

JIN, Z., MCDONALD, E. R., 3RD, DICKER, D. T. & EL-DEIRY, W. S. 2004. Deficient tumor necrosis factor-related apoptosis-inducing ligand (TRAIL) death receptor transport to the cell surface in human colon cancer cells selected for resistance to TRAIL-induced apoptosis. *J Biol Chem,* 279**,** 35829-39.

JONES, P. L., PING, D. & BOSS, J. M. 1997. Tumor necrosis factor alpha and interleukin-1beta regulate the murine manganese superoxide dismutase gene through a

complex intronic enhancer involving C/EBP-beta and NF-kappaB. *Mol Cell Biol,* 17**,** 6970-81.

JORDAN, V. C. 2006. Tamoxifen (ICI46,474) as a targeted therapy to treat and prevent breast cancer. *Br J Pharmacol,* 147 Suppl 1**,** S269-76.

JOUAN-LANHOUET, S., ARSHAD, M. I., PIQUET-PELLORCE, C., MARTIN-CHOULY, C., LE MOIGNE-MULLER, G., VAN HERREWEGHE, F., TAKAHASHI, N., SERGENT, O., LAGADIC-GOSSMANN, D., VANDENABEELE, P., SAMSON, M. & DIMANCHE-BOITREL, M. T. 2012. TRAIL induces necroptosis involving RIPK1/RIPK3-dependent PARP-1 activation. *Cell Death Differ,* 19**,** 2003-14.

JUNG, Y. H., HEO, J., LEE, Y. J., KWON, T. K. & KIM, Y. H. 2010. Quercetin enhances TRAIL-induced apoptosis in prostate cancer cells via increased protein stability of death receptor 5. *Life Sci,* 86**,** 351-7.

KAIGHN, M. E., NARAYAN, K. S., OHNUKI, Y., LECHNER, J. F. & JONES, L. W. 1979. Establishment and characterization of a human prostatic carcinoma cell line (PC-3). *Invest Urol,* 17**,** 16-23.

KANAREK, N., LONDON, N., SCHUELER-FURMAN, O. & BEN-NERIAH, Y. 2010. Ubiquitination and degradation of the inhibitors of NF-kappaB. *Cold Spring Harb Perspect Biol,* 2**,** a000166.

KANDASAMY, K. & KRAFT, A. S. 2008. Proteasome inhibitor PS-341 (VELCADE) induces stabilization of the TRAIL receptor DR5 mRNA through the 3'-untranslated region. *Mol Cancer Ther,* 7**,** 1091-100.

KANNAPPAN, R., RAVINDRAN, J., PRASAD, S., SUNG, B., YADAV, V. R., REUTER, S., CHATURVEDI, M. M. & AGGARWAL, B. B. 2010. Gamma-tocotrienol promotes TRAIL-induced apoptosis through reactive oxygen species/extracellular signal-regulated kinase/p53-mediated upregulation of death receptors. *Mol Cancer Ther,* 9**,** 2196-207.

KARIN, M. 1999. How NF-kappaB is activated: the role of the IkappaB kinase (IKK) complex. *Oncogene,* 18**,** 6867-74.

KARIN, M., CAO, Y., GRETEN, F. R. & LI, Z. W. 2002. NF-kappaB in cancer: from innocent bystander to major culprit. *Nat Rev Cancer,* 2**,** 301-10.

KATZENELLENBOGEN, R. A., BAYLIN, S. B. & HERMAN, J. G. 1999. Hypermethylation of the DAP-kinase CpG island is a common alteration in B-cell malignancies. *Blood,* 93**,** 4347-53.

KAUFMAN, R. J. 1999. Stress signaling from the lumen of the endoplasmic reticulum: coordination of gene transcriptional and translational controls. *Genes Dev,* 13**,** 1211-33.

KAWAI, T., MATSUMOTO, M., TAKEDA, K., SANJO, H. & AKIRA, S. 1998. ZIP kinase, a novel serine/threonine kinase which mediates apoptosis. *Mol Cell Biol,* 18**,** 1642-51.

KAWAI, T., NOMURA, F., HOSHINO, K., COPELAND, N. G., GILBERT, D. J., JENKINS, N. A. & AKIRA, S. 1999. Death-associated protein kinase 2 is a new calcium/calmodulin-dependent protein kinase that signals apoptosis through its catalytic activity. *Oncogene,* 18**,** 3471-80.

KAYAGAKI, N., YAMAGUCHI, N., NAKAYAMA, M., ETO, H., OKUMURA, K. & YAGITA, H. 1999. Type I interferons (IFNs) regulate tumor necrosis factor-related apoptosis-inducing ligand (TRAIL) expression on human T cells: A novel mechanism for the antitumor effects of type I IFNs. *J Exp Med,* 189**,** 1451-60.

KEFFER, J., PROBERT, L., CAZLARIS, H., GEORGOPOULOS, S., KASLARIS, E., KIOUSSIS, D. & KOLLIAS, G. 1991. Transgenic mice expressing human tumour necrosis factor: a predictive genetic model of arthritis. *EMBO J,* 10**,** 4025-31.

KEMP, T. J., ELZEY, B. D. & GRIFFITH, T. S. 2003. Plasmacytoid dendritic cell-derived IFN-alpha induces TNF-related apoptosis-inducing ligand/Apo-2L-mediated antitumor activity by human monocytes following CpG oligodeoxynucleotide stimulation. *J Immunol,* 171**,** 212-8.

KHARKWAL, G., CHANDRA, V., FATIMA, I. & DWIVEDI, A. 2012. Ormeloxifene inhibits osteoclast differentiation in parallel to downregulating RANKL-induced ROS generation and suppressing the activation of ERK and JNK in murine RAW264.7 cells. *J Mol Endocrinol,* 48**,** 261-70.

KIM, Y. S., SCHWABE, R. F., QIAN, T., LEMASTERS, J. J. & BRENNER, D. A. 2002. TRAIL-mediated apoptosis requires NF-kappaB inhibition and the mitochondrial permeability transition in human hepatoma cells. *Hepatology,* 36**,** 1498-508.

KIMBERLEY, F. C. & SCREATON, G. R. 2004. Following a TRAIL: update on a ligand and its five receptors. *Cell research,* 14**,** 359-72.

KIRIENKO, N. V., MANI, K. & FAY, D. S. 2010. Cancer models in Caenorhabditis elegans. *Dev Dyn,* 239**,** 1413-48.

KIRSCH, M. & DE GROOT, H. 2001. NAD(P)H, a directly operating antioxidant? *FASEB J,* 15**,** 1569-74.

KISCHKEL, F. C., LAWRENCE, D. A., CHUNTHARAPAI, A., SCHOW, P., KIM, K. J. & ASHKENAZI, A. 2000. Apo2L/TRAIL-dependent recruitment of endogenous FADD and caspase-8 to death receptors 4 and 5. *Immunity,* 12**,** 611-20.

KLEBER, S., SANCHO-MARTINEZ, I., WIESTLER, B., BEISEL, A., GIEFFERS, C., HILL, O., THIEMANN, M., MUELLER, W., SYKORA, J., KUHN, A., SCHREGLMANN, N., LETELLIER, E., ZULIANI, C., KLUSSMANN, S., TEODORCZYK, M., GRONE, H. J., GANTEN, T. M., SULTMANN, H., TUTTENBERG, J., VON DEIMLING, A., REGNIER-VIGOUROUX, A., HEROLD-MENDE, C. & MARTIN-VILLALBA, A. 2008. Yes and PI3K bind CD95 to signal invasion of glioblastoma. *Cancer Cell,* 13**,** 235-48.

KNUDSON, A. G., JR. 1971. Mutation and cancer: statistical study of retinoblastoma. *Proc Natl Acad Sci U S A,* 68**,** 820-3.

KOLB, W. P. & GRANGER, G. A. 1968. Lymphocyte in vitro cytotoxicity: characterization of human lymphotoxin. *Proc Natl Acad Sci U S A,* 61**,** 1250-5.

KONSTANTAKOU, E. G., VOUTSINAS, G. E., KARKOULIS, P. K., ARAVANTINOS, G., MARGARITIS, L. H. & STRAVOPODIS, D. J. 2009. Human bladder cancer cells undergo cisplatin-induced apoptosis that is associated with p53-dependent and p53-independent responses. *Int J Oncol,* 35**,** 401-16.

KOVALENKO, A. & WALLACH, D. 2006. If the prophet does not come to the mountain: dynamics of signaling complexes in NF-kappaB activation. *Mol Cell,* 22**,** 433-6.

KRAMMER, P. H. 2000. CD95's deadly mission in the immune system. *Nature,* 407**,** 789-95.

KRATSOVNIK, E., BROMBERG, Y., SPERLING, O. & ZOREF-SHANI, E. 2005. Oxidative stress activates transcription factor NF-kB-mediated protective signaling in primary rat neuronal cultures. *J Mol Neurosci,* 26**,** 27-32.

KRIEGLER, M., PEREZ, C., DEFAY, K., ALBERT, I. & LU, S. D. 1988. A novel form of TNF/cachectin is a cell surface cytotoxic transmembrane protein: ramifications for the complex physiology of TNF. *Cell,* 53**,** 45-53.

KRUGLOV, A. A., KUCHMIY, A., GRIVENNIKOV, S. I., TUMANOV, A. V., KUPRASH, D. V. & NEDOSPASOV, S. A. 2008. Physiological functions of tumor necrosis factor and the consequences of its pathologic overexpression or blockade: mouse models. *Cytokine Growth Factor Rev,* 19**,** 231-44.

LACKNER, M. R., WILSON, T. R. & SETTLEMAN, J. 2012. Mechanisms of acquired resistance to targeted cancer therapies. *Future Oncol,* 8**,** 999-1014.

LAKIN, N. D. & JACKSON, S. P. 1999. Regulation of p53 in response to DNA damage. *Oncogene,* 18**,** 7644-55.

LAMHAMEDI-CHERRADI, S. E., ZHENG, S. J., MAGUSCHAK, K. A., PESCHON, J. & CHEN, Y. H. 2003. Defective thymocyte apoptosis and accelerated autoimmune diseases in TRAIL-/- mice. *Nat Immunol,* 4**,** 255-60.

LANE, D., COTE, M., GRONDIN, R., COUTURE, M. C. & PICHE, A. 2006. Acquired resistance to TRAIL-induced apoptosis in human ovarian cancer cells is conferred by increased turnover of mature caspase-3. *Mol Cancer Ther,* 5**,** 509-21.

LANE, D. P. 1992. Cancer. p53, guardian of the genome. *Nature,* 358**,** 15-6.

LAWRENCE, T. 2009. The nuclear factor NF-kappaB pathway in inflammation. *Cold Spring Harb Perspect Biol,* 1**,** a001651.

LE, A., COOPER, C. R., GOUW, A. M., DINAVAHI, R., MAITRA, A., DECK, L. M., ROYER, R. E., VANDER JAGT, D. L., SEMENZA, G. L. & DANG, C. V. 2010. Inhibition of lactate dehydrogenase A induces oxidative stress and inhibits tumor progression. *Proc Natl Acad Sci U S A,* 107**,** 2037-42.

LEE, J. Y., JUNG, K. H., MORGAN, M. J., KANG, Y. R., LEE, H. S., KOO, G. B., HONG, S. S., KWON, S. W. & KIM, Y. S. 2013. Sensitization of TRAIL-induced cell death by 20(S)-ginsenoside Rg3 via CHOP-mediated DR5 upregulation in human hepatocellular carcinoma cells. *Mol Cancer Ther,* 12**,** 274-85.

LEE, S. H., SHIN, M. S., KIM, H. S., LEE, H. K., PARK, W. S., KIM, S. Y., LEE, J. H., HAN, S. Y., PARK, J. Y., OH, R. R., KANG, C. S., KIM, K. M., JANG, J. J., NAM, S. W., LEE, J. Y. & YOO, N. J. 2001. Somatic mutations of TRAIL-receptor 1 and TRAIL-receptor 2 genes in non-Hodgkin's lymphoma. *Oncogene,* 20**,** 399-403.

LEE, T. H., SHANK, J., CUSSON, N. & KELLIHER, M. A. 2004. The kinase activity of Rip1 is not required for tumor necrosis factor-alpha-induced IkappaB kinase or p38 MAP kinase activation or for the ubiquitination of Rip1 by Traf2. *J Biol Chem,* 279**,** 33185-91.

LEHMAN, T. A., BENNETT, W. P., METCALF, R. A., WELSH, J. A., ECKER, J., MODALI, R. V., ULLRICH, S., ROMANO, J. W., APPELLA, E., TESTA, J. R. & ET AL. 1991. p53 mutations, ras mutations, and p53-heat shock 70 protein complexes in human lung carcinoma cell lines. *Cancer Res,* 51**,** 4090-6.

LEMKE, J., VON KARSTEDT, S., ABD EL HAY, M., CONTI, A., ARCE, F., MONTINARO, A., PAPENFUSS, K., EL-BAHRAWY, M. A. & WALCZAK, H. 2014a. Selective CDK9 inhibition overcomes TRAIL resistance by concomitant suppression of cFlip and Mcl-1. *Cell Death Differ,* 21**,** 491-502.

LEMKE, J., VON KARSTEDT, S., ZINNGREBE, J. & WALCZAK, H. 2014b. Getting TRAIL back on track for cancer therapy. *Cell Death Differ*.

LEVRERO, M., DE LAURENZI, V., COSTANZO, A., GONG, J., WANG, J. Y. & MELINO, G. 2000. The p53/p63/p73 family of transcription factors: overlapping and distinct functions. *J Cell Sci,* 113 (Pt 10)**,** 1661-70.

LI, L., THOMAS, R. M., SUZUKI, H., DE BRABANDER, J. K., WANG, X. & HARRAN, P. G. 2004. A small molecule Smac mimic potentiates TRAIL- and TNFalpha-mediated cell death. *Science,* 305**,** 1471-4.

LI, W., ZHANG, C., CHEN, C. & ZHUANG, G. 2007. Correlation between expression of DcR3 on tumor cells and sensitivity to FasL. *Cell Mol Immunol,* 4**,** 455-60.

LI, X., YANG, Y. & ASHWELL, J. D. 2002. TNF-RII and c-IAP1 mediate ubiquitination and degradation of TRAF2. *Nature,* 416**,** 345-7.

LIABAKK, N. B., SUNDAN, A., TORP, S., AUKRUST, P., FROLAND, S. S. & ESPEVIK, T. 2002. Development, characterization and use of monoclonal antibodies against sTRAIL: measurement of sTRAIL by ELISA. *J Immunol Methods,* 259**,** 119-28.

LIM, S. M., KIM, T. H., JIANG, H. H., PARK, C. W., LEE, S., CHEN, X. & LEE, K. C. 2011. Improved biological half-life and anti-tumor activity of TNF-related apoptosis-inducing ligand (TRAIL) using PEG-exposed nanoparticles. *Biomaterials,* 32**,** 3538-46.

LIN, Y., STEVENS, C. & HUPP, T. 2007. Identification of a dominant negative functional domain on DAPK-1 that degrades DAPK-1 protein and stimulates TNFR-1-mediated apoptosis. *J Biol Chem,* 282**,** 16792-802.

LISTER, A., NEDJADI, T., KITTERINGHAM, N. R., CAMPBELL, F., COSTELLO, E., LLOYD, B., COPPLE, I. M., WILLIAMS, S., OWEN, A., NEOPTOLEMOS, J. P., GOLDRING, C. E. & PARK, B. K. 2011. Nrf2 is overexpressed in pancreatic cancer: implications for cell proliferation and therapy. *Mol Cancer,* 10**,** 37.

LIU, B., CHEN, Y. & ST CLAIR, D. K. 2008a. ROS and p53: a versatile partnership. *Free Radic Biol Med,* 44**,** 1529-35.

LIU, F. T., AGRAWAL, S. G., GRIBBEN, J. G., YE, H., DU, M. Q., NEWLAND, A. C. & JIA, L. 2008b. Bortezomib blocks Bax degradation in malignant B cells during treatment with TRAIL. *Blood,* 111**,** 2797-805.

LIU, S., YU, Y., ZHANG, M., WANG, W. & CAO, X. 2001. The involvement of TNF-alpha-related apoptosis-inducing ligand in the enhanced cytotoxicity of IFN-beta-stimulated human dendritic cells to tumor cells. *J Immunol,* 166**,** 5407-15.

LIU, X., KIM, C. N., YANG, J., JEMMERSON, R. & WANG, X. 1996. Induction of apoptotic program in cell-free extracts: requirement for dATP and cytochrome c. *Cell,* 86**,** 147-57.

LIU, X., YUE, P., CHEN, S., HU, L., LONIAL, S., KHURI, F. R. & SUN, S. Y. 2007. The proteasome inhibitor PS-341 (bortezomib) up-regulates DR5 expression leading to induction of apoptosis and enhancement of TRAIL-induced apoptosis despite up-regulation of c-FLIP and survivin expression in human NSCLC cells. *Cancer Res,* 67**,** 4981-8.

LIU, X., YUE, P., KHURI, F. R. & SUN, S. Y. 2004. p53 upregulates death receptor 4 expression through an intronic p53 binding site. *Cancer Res,* 64**,** 5078-83.

LIU, X., YUE, P., KHURI, F. R. & SUN, S. Y. 2005. Decoy receptor 2 (DcR2) is a p53 target gene and regulates chemosensitivity. *Cancer Res,* 65**,** 9169-75.

LOCKLIN, R. M., FEDERICI, E., ESPINA, B., HULLEY, P. A., RUSSELL, R. G. & EDWARDS, C. M. 2007. Selective targeting of death receptor 5 circumvents resistance of MG-63 osteosarcoma cells to TRAIL-induced apoptosis. *Mol Cancer Ther,* 6**,** 3219-28.

LU, W., MCCALLUM, L. & IRVINE, A. E. 2009. A rapid and sensitive method for measuring cell adhesion. *J Cell Commun Signal,* 3**,** 147-9.

LUM, M. G. & NAGLEY, P. 2003. Two phases of signalling between mitochondria during apoptosis leading to early depolarisation and delayed cytochrome c release. *J Cell Sci,* 116**,** 1437-47.

LUO, W., HU, H., CHANG, R., ZHONG, J., KNABEL, M., O'MEALLY, R., COLE, R. N., PANDEY, A. & SEMENZA, G. L. 2011. Pyruvate kinase M2 is a PHD3-stimulated coactivator for hypoxia-inducible factor 1. *Cell,* 145**,** 732-44.

MACEWAN, D. J. 2002. TNF receptor subtype signalling: differences and cellular consequences. *Cell Signal,* 14**,** 477-92.

MACFARLANE, M., AHMAD, M., SRINIVASULA, S. M., FERNANDES-ALNEMRI, T., COHEN, G. M. & ALNEMRI, E. S. 1997. Identification and molecular cloning of two novel receptors for the cytotoxic ligand TRAIL. *J Biol Chem,* 272**,** 25417-20.

MACLEOD, K. F., SHERRY, N., HANNON, G., BEACH, D., TOKINO, T., KINZLER, K., VOGELSTEIN, B. & JACKS, T. 1995. p53-dependent and independent expression of p21 during cell growth, differentiation, and DNA damage. *Genes Dev,* 9**,** 935-44.

MADGE, L. A., KLUGER, M. S., ORANGE, J. S. & MAY, M. J. 2008. Lymphotoxin-alpha 1 beta 2 and LIGHT induce classical and noncanonical NF-kappa B-dependent proinflammatory gene expression in vascular endothelial cells. *J Immunol,* 180**,** 3467-77.

MAHONEY, D. J., CHEUNG, H. H., MRAD, R. L., PLENCHETTE, S., SIMARD, C., ENWERE, E., ARORA, V., MAK, T. W., LACASSE, E. C., WARING, J. & KORNELUK, R. G. 2008. Both cIAP1 and cIAP2 regulate TNFalpha-mediated NF-kappaB activation. *Proc Natl Acad Sci U S A,* 105**,** 11778-83.

MARSTERS, S. A., SHERIDAN, J. P., PITTI, R. M., HUANG, A., SKUBATCH, M., BALDWIN, D., YUAN, J., GURNEY, A., GODDARD, A. D., GODOWSKI, P. & ASHKENAZI, A. 1997. A novel receptor for Apo2L/TRAIL contains a truncated death domain. *Curr Biol,* 7**,** 1003-6.

MARTINEZ-LORENZO, M. J., ANEL, A., GAMEN, S., MONLE N, I., LASIERRA, P., LARRAD, L., PINEIRO, A., ALAVA, M. A. & NAVAL, J. 1999. Activated human T cells release bioactive Fas ligand and APO2 ligand in microvesicles. *J Immunol,* 163**,** 1274-81.

MATSUDA, A., SUZUKI, Y., HONDA, G., MURAMATSU, S., MATSUZAKI, O., NAGANO, Y., DOI, T., SHIMOTOHNO, K., HARADA, T., NISHIDA, E., HAYASHI, H. & SUGANO, S. 2003. Large-scale identification and characterization of human genes that activate NF-kappaB and MAPK signaling pathways. *Oncogene,* 22**,** 3307-18.

MATSUDA, T., ALMASAN, A., TOMITA, M., UCHIHARA, J. N., MASUDA, M., OHSHIRO, K., TAKASU, N., YAGITA, H., OHTA, T. & MORI, N. 2005. Resistance to Apo2 ligand (Apo2L)/tumor necrosis factor-related apoptosis-inducing ligand (TRAIL)-mediated apoptosis and constitutive expression of Apo2L/TRAIL in human T-cell leukemia virus type 1-infected T-cell lines. *J Virol,* 79**,** 1367-78.

MCCOOL, K. W. & MIYAMOTO, S. 2012. DNA damage-dependent NF-kappaB activation: NEMO turns nuclear signaling inside out. *Immunol Rev,* 246**,** 311-26.

MCDONALD, E. R., 3RD, CHUI, P. C., MARTELLI, P. F., DICKER, D. T. & EL-DEIRY, W. S. 2001. Death domain mutagenesis of KILLER/DR5 reveals residues critical for apoptotic signaling. *J Biol Chem,* 276**,** 14939-45.

MCNALLY, J., YOO, D. H., DRAPPA, J., CHU, J. L., YAGITA, H., FRIEDMAN, S. M. & ELKON, K. B. 1997. Fas ligand expression and function in systemic lupus erythematosus. *J Immunol,* 159**,** 4628-36.

MEDEMA, J. P., TOES, R. E., SCAFFIDI, C., ZHENG, T. S., FLAVELL, R. A., MELIEF, C. J., PETER, M. E., OFFRINGA, R. & KRAMMER, P. H. 1997. Cleavage of FLICE (caspase-8) by granzyme B during cytotoxic T lymphocyte-induced apoptosis. *Eur J Immunol,* 27**,** 3492-8.

MEIJER, A., KRUYT, F. A., VAN DER ZEE, A. G., HOLLEMA, H., LE, P., TEN HOOR, K. A., GROOTHUIS, G. M., QUAX, W. J., DE VRIES, E. G. & DE JONG, S. 2013. Nutlin-3 preferentially sensitises wild-type p53-expressing cancer cells to DR5-selective TRAIL over rhTRAIL. *Br J Cancer,* 109**,** 2685-95.

MELLIER, G., HUANG, S., SHENOY, K. & PERVAIZ, S. 2010. TRAILing death in cancer. *Mol Aspects Med,* 31**,** 93-112.

MELLIER, G. & PERVAIZ, S. 2012. The three Rs along the TRAIL: resistance, re-sensitization and reactive oxygen species (ROS). *Free Radic Res,* 46**,** 996-1003.

MENDOZA, F. J., ISHDORJ, G., HU, X. & GIBSON, S. B. 2008. Death receptor-4 (DR4) expression is regulated by transcription factor NF-kappaB in response to etoposide treatment. *Apoptosis,* 13**,** 756-70.

MERCHANT, M. S., GELLER, J. I., BAIRD, K., CHOU, A. J., GALLI, S., CHARLES, A., AMAOKO, M., RHEE, E. H., PRICE, A., WEXLER, L. H., MEYERS, P. A., WIDEMANN,

B. C., TSOKOS, M. & MACKALL, C. L. 2012. Phase I trial and pharmacokinetic study of lexatumumab in pediatric patients with solid tumors. *J Clin Oncol,* 30**,** 4141-7.

MERINO, D., LALAOUI, N., MORIZOT, A., SCHNEIDER, P., SOLARY, E. & MICHEAU, O. 2006. Differential inhibition of TRAIL-mediated DR5-DISC formation by decoy receptors 1 and 2. *Mol Cell Biol,* 26**,** 7046-55.

MERLO, L. M., PEPPER, J. W., REID, B. J. & MALEY, C. C. 2006. Cancer as an evolutionary and ecological process. *Nat Rev Cancer,* 6**,** 924-35.

MIAO, P., SHENG, S., SUN, X., LIU, J. & HUANG, G. 2013. Lactate dehydrogenase A in cancer: a promising target for diagnosis and therapy. *IUBMB Life,* 65**,** 904-10.

MICHEAU, O. & TSCHOPP, J. 2003. Induction of TNF receptor I-mediated apoptosis via two sequential signaling complexes. *Cell,* 114**,** 181-90.

MICHOR, F., NOWAK, M. A. & IWASA, Y. 2006. Evolution of resistance to cancer therapy. *Curr Pharm Des,* 12**,** 261-71.

MIRANDOLA, P., SPONZILLI, I., GOBBI, G., MARMIROLI, S., RINALDI, L., BINAZZI, R., PICCARI, G. G., RAMAZZOTTI, G., GABOARDI, G. C., COCCO, L. & VITALE, M. 2006. Anticancer agents sensitize osteosarcoma cells to TNF-related apoptosis-inducing ligand downmodulating IAP family proteins. *Int J Oncol,* 28**,** 127-33.

MITCHELL, P. & MOYLE, J. 1967. Chemiosmotic hypothesis of oxidative phosphorylation. *Nature,* 213**,** 137-9.

MOLOGNI, L., BRUSSOLO, S., CECCON, M. & GAMBACORTI-PASSERINI, C. 2012. Synergistic effects of combined Wnt/KRAS inhibition in colorectal cancer cells. *PLoS One,* 7**,** e51449.

MONROE, D. G., GETZ, B. J., JOHNSEN, S. A., RIGGS, B. L., KHOSLA, S. & SPELSBERG, T. C. 2003. Estrogen receptor isoform-specific regulation of endogenous gene expression in human osteoblastic cell lines expressing either ERalpha or ERbeta. *J Cell Biochem,* 90**,** 315-26.

MOR, I., CARLESSI, R., AST, T., FEINSTEIN, E. & KIMCHI, A. 2012. Death-associated protein kinase increases glycolytic rate through binding and activation of pyruvate kinase. *Oncogene,* 31**,** 683-93.

MULLER, C. W., REY, F. A., SODEOKA, M., VERDINE, G. L. & HARRISON, S. C. 1995. Structure of the NF-kappa B p50 homodimer bound to DNA. *Nature,* 373**,** 311-7.

MULLER, F. L., LIU, Y. & VAN REMMEN, H. 2004. Complex III releases superoxide to both sides of the inner mitochondrial membrane. *J Biol Chem,* 279**,** 49064-73.

MULLER, M., WILDER, S., BANNASCH, D., ISRAELI, D., LEHLBACH, K., LI-WEBER, M., FRIEDMAN, S. L., GALLE, P. R., STREMMEL, W., OREN, M. & KRAMMER, P. H. 1998. p53 activates the CD95 (APO-1/Fas) gene in response to DNA damage by anticancer drugs. *J Exp Med,* 188**,** 2033-45.

MULLER, P. A. & VOUSDEN, K. H. 2013. p53 mutations in cancer. *Nat Cell Biol,* 15**,** 2-8.

MUNGER, K. & HOWLEY, P. M. 2002. Human papillomavirus immortalization and transformation functions. *Virus Res,* 89**,** 213-28.

MURCHISON, E. P., TOVAR, C., HSU, A., BENDER, H. S., KHERADPOUR, P., REBBECK, C. A., OBENDORF, D., CONLAN, C., BAHLO, M., BLIZZARD, C. A., PYECROFT, S., KREISS, A., KELLIS, M., STARK, A., HARKINS, T. T., MARSHALL GRAVES, J. A., WOODS, G. M., HANNON, G. J. & PAPENFUSS, A. T. 2010. The Tasmanian devil transcriptome reveals Schwann cell origins of a clonally transmissible cancer. *Science,* 327**,** 84-7.

MUSCOLI, C., CUZZOCREA, S., RILEY, D. P., ZWEIER, J. L., THIEMERMANN, C., WANG, Z. Q. & SALVEMINI, D. 2003. On the selectivity of superoxide dismutase mimetics and its importance in pharmacological studies. *Br J Pharmacol,* 140**,** 445-60.

NAGATA, S. 1997. Apoptosis by death factor. *Cell,* 88**,** 355-65.

NAKA, T., SUGAMURA, K., HYLANDER, B. L., WIDMER, M. B., RUSTUM, Y. M. & REPASKY, E. A. 2002. Effects of tumor necrosis factor-related apoptosis-inducing ligand alone and in combination with chemotherapeutic agents on patients' colon tumors grown in SCID mice. *Cancer Res,* 62**,** 5800-6.

NAKAGAWA, Y. 2004. Role of mitochondrial phospholipid hydroperoxide glutathione peroxidase (PHGPx) as an antiapoptotic factor. *Biol Pharm Bull,* 27**,** 956-60.

NECKERS, L. & WORKMAN, P. 2012. Hsp90 molecular chaperone inhibitors: are we there yet? *Clin Cancer Res,* 18**,** 64-76.

NG, C. P. & BONAVIDA, B. 2002. X-linked inhibitor of apoptosis (XIAP) blocks Apo2 ligand/tumor necrosis factor-related apoptosis-inducing ligand-mediated apoptosis of prostate cancer cells in the presence of mitochondrial activation: sensitization by overexpression of second mitochondria-derived activator of caspase/direct IAP-binding protein with low pl (Smac/DIABLO). *Mol Cancer Ther,* 1**,** 1051-8.

NICULESCU-DUVAZ, I. 2010. Trastuzumab emtansine, an antibody-drug conjugate for the treatment of HER2+ metastatic breast cancer. *Curr Opin Mol Ther,* 12**,** 350-60.

NISHITOH, H. 2012. CHOP is a multifunctional transcription factor in the ER stress response. *J Biochem,* 151**,** 217-9.

NODA, M., YAMASHITA, S., TAKAHASHI, N., ETO, K., SHEN, L. M., IZUMI, K., DANIEL, S., TSUBAMOTO, Y., NEMOTO, T., IINO, M., KASAI, H., SHARP, G. W. & KADOWAKI, T. 2002. Switch to anaerobic glucose metabolism with NADH accumulation in the beta-cell model of mitochondrial diabetes. Characteristics of betaHC9 cells deficient in mitochondrial DNA transcription. *J Biol Chem,* 277**,** 41817-26.

O'BRIEN, S. G., GUILHOT, F., LARSON, R. A., GATHMANN, I., BACCARANI, M., CERVANTES, F., CORNELISSEN, J. J., FISCHER, T., HOCHHAUS, A., HUGHES, T., LECHNER, K., NIELSEN, J. L., ROUSSELOT, P., REIFFERS, J., SAGLIO, G., SHEPHERD, J., SIMONSSON, B., GRATWOHL, A., GOLDMAN, J. M., KANTARJIAN, H., TAYLOR, K., VERHOEF, G., BOLTON, A. E., CAPDEVILLE, R., DRUKER, B. J. & INVESTIGATORS, I. 2003. Imatinib compared with interferon and low-dose cytarabine for newly diagnosed chronic-phase chronic myeloid leukemia. *N Engl J Med,* 348**,** 994-1004.

O'CONNELL, J., O'SULLIVAN, G. C., COLLINS, J. K. & SHANAHAN, F. 1996. The Fas counterattack: Fas-mediated T cell killing by colon cancer cells expressing Fas ligand. *J Exp Med,* 184**,** 1075-82.

O'DONNELL, M. A., LEGARDA-ADDISON, D., SKOUNTZOS, P., YEH, W. C. & TING, A. T. 2007. Ubiquitination of RIP1 regulates an NF-kappaB-independent cell-death switch in TNF signaling. *Curr Biol,* 17**,** 418-24.

O'TOOLE, C., PERLMANN, P., UNSGAARD, B., MOBERGER, G. & EDSMYR, F. 1972. Cellular immunity to human urinary bladder carcinoma. I. Correlation to clinical stage and radiotherapy. *Int J Cancer,* 10**,** 77-91.

OBRIG, T. G., CULP, W. J., MCKEEHAN, W. L. & HARDESTY, B. 1971. The mechanism by which cycloheximide and related glutarimide antibiotics inhibit peptide synthesis on reticulocyte ribosomes. *J Biol Chem,* 246**,** 174-81.

OYARZO, M. P., MEDEIROS, L. J., ATWELL, C., FERETZAKI, M., LEVENTAKI, V., DRAKOS, E., AMIN, H. M. & RASSIDAKIS, G. Z. 2006. c-FLIP confers resistance to FAS-mediated apoptosis in anaplastic large-cell lymphoma. *Blood,* 107**,** 2544-7.

OZOREN, N. & EL-DEIRY, W. S. 2002. Defining characteristics of Types I and II apoptotic cells in response to TRAIL. *Neoplasia,* 4**,** 551-7.

PAHL, H. L. 1999. Activators and target genes of Rel/NF-kappaB transcription factors. *Oncogene,* 18**,** 6853-66.

PAI, S. I., WU, G. S., OZOREN, N., WU, L., JEN, J., SIDRANSKY, D. & EL-DEIRY, W. S. 1998. Rare loss-of-function mutation of a death receptor gene in head and neck cancer. *Cancer Res,* 58**,** 3513-8.

PAN, G., NI, J., WEI, Y. F., YU, G., GENTZ, R. & DIXIT, V. M. 1997a. An antagonist decoy receptor and a death domain-containing receptor for TRAIL. *Science,* 277**,** 815-8.

PAN, G., O'ROURKE, K., CHINNAIYAN, A. M., GENTZ, R., EBNER, R., NI, J. & DIXIT, V. M. 1997b. The receptor for the cytotoxic ligand TRAIL. *Science,* 276**,** 111-3.

PARSONS, B. D., SCHINDLER, A., EVANS, D. H. & FOLEY, E. 2009. A direct phenotypic comparison of siRNA pools and multiple individual duplexes in a functional assay. *PLoS One,* 4**,** e8471.

PATEL, A. K., YADAV, R. P., MAJAVA, V., KURSULA, I. & KURSULA, P. 2011. Structure of the dimeric autoinhibited conformation of DAPK2, a pro-apoptotic protein kinase. *J Mol Biol,* 409**,** 369-83.

PELLERITO, O., CALVARUSO, G., PORTANOVA, P., DE BLASIO, A., SANTULLI, A., VENTO, R., TESORIERE, G. & GIULIANO, M. 2010. The synthetic cannabinoid WIN 55,212-2 sensitizes hepatocellular carcinoma cells to tumor necrosis factor-related apoptosis-inducing ligand (TRAIL)-induced apoptosis by activating p8/CCAAT/enhancer binding protein homologous protein (CHOP)/death receptor 5 (DR5) axis. *Mol Pharmacol,* 77**,** 854-63.

PERKINS, N. D. 2000. The Rel/NF-kappa B family: friend and foe. *Trends Biochem Sci,* 25**,** 434-40.

PERROT-APPLANAT, M., VACHER, S., TOULLEC, A., PELAEZ, I., VELASCO, G., CORMIER, F., SAAD HEL, S., LIDEREAU, R., BAUD, V. & BIECHE, I. 2011. Similar NF-kappaB gene signatures in TNF-alpha treated human endothelial cells and breast tumor biopsies. *PLoS One,* 6**,** e21589.

PETER, M. E. & KRAMMER, P. H. 2003. The CD95(APO-1/Fas) DISC and beyond. *Cell Death Differ,* 10**,** 26-35.

PETITJEAN, A., RUPTIER, C., TRIBOLLET, V., HAUTEFEUILLE, A., CHARDON, F., CAVARD, C., PUISIEUX, A., HAINAUT, P. & CARON DE FROMENTEL, C. 2008. Properties of the six isoforms of p63: p53-like regulation in response to genotoxic stress and cross talk with DeltaNp73. *Carcinogenesis,* 29**,** 273-81.

PETROSILLO, G., RUGGIERO, F. M., PISTOLESE, M. & PARADIES, G. 2004. Ca2+-induced reactive oxygen species production promotes cytochrome c release from rat liver mitochondria via mitochondrial permeability transition (MPT)-dependent and MPT-independent mechanisms: role of cardiolipin. *J Biol Chem,* 279**,** 53103-8.

PITTI, R. M., MARSTERS, S. A., RUPPERT, S., DONAHUE, C. J., MOORE, A. & ASHKENAZI, A. 1996. Induction of apoptosis by Apo-2 ligand, a new member of the tumor necrosis factor cytokine family. *J Biol Chem,* 271**,** 12687-90.

POMPELLA, A., VISVIKIS, A., PAOLICCHI, A., DE TATA, V. & CASINI, A. F. 2003. The changing faces of glutathione, a cellular protagonist. *Biochem Pharmacol,* 66**,** 1499-503.

PONTEN, J. & SAKSELA, E. 1967. Two established in vitro cell lines from human mesenchymal tumours. *Int J Cancer,* 2**,** 434-47.

POTTER, V. R. 1958. The biochemical approach to the cancer problem. *Fed Proc,* 17**,** 691-7.

PRASAD, S., YADAV, V. R., RAVINDRAN, J. & AGGARWAL, B. B. 2011. ROS and CHOP are critical for dibenzylideneacetone to sensitize tumor cells to TRAIL through induction of death receptors and downregulation of cell survival proteins. *Cancer Res,* 71**,** 538-49.

PSAHOULIA, F. H., DROSOPOULOS, K. G., DOUBRAVSKA, L., ANDERA, L. & PINTZAS, A. 2007. Quercetin enhances TRAIL-mediated apoptosis in colon cancer cells by inducing the accumulation of death receptors in lipid rafts. *Mol Cancer Ther,* 6**,** 2591-9.

PUENTE, X. S., VELASCO, G., GUTIERREZ-FERNANDEZ, A., BERTRANPETIT, J., KING, M. C. & LOPEZ-OTIN, C. 2006. Comparative analysis of cancer genes in the human and chimpanzee genomes. *BMC Genomics,* 7**,** 15.

PUZIO-KUTER, A. M. 2011. The Role of p53 in Metabolic Regulation. *Genes Cancer,* 2**,** 385-91.

QUINLAN, C. L., ORR, A. L., PEREVOSHCHIKOVA, I. V., TREBERG, J. R., ACKRELL, B. A. & BRAND, M. D. 2012. Mitochondrial complex II can generate reactive oxygen species at high rates in both the forward and reverse reactions. *J Biol Chem,* 287**,** 27255-64.

RAMADAN, S., TERRINONI, A., CATANI, M. V., SAYAN, A. E., KNIGHT, R. A., MUELLER, M., KRAMMER, P. H., MELINO, G. & CANDI, E. 2005. p73 induces apoptosis by different mechanisms. *Biochem Biophys Res Commun,* 331**,** 713-7.

RASSOOL, F. V., GAYMES, T. J., OMIDVAR, N., BRADY, N., BEURLET, S., PLA, M., REBOUL, M., LEA, N., CHOMIENNE, C., THOMAS, N. S., MUFTI, G. J. & PADUA, R. A. 2007. Reactive oxygen species, DNA damage, and error-prone repair: a model for genomic instability with progression in myeloid leukemia? *Cancer Res,* 67**,** 8762-71.

RATCLIFF, W. C., DENISON, R. F., BORRELLO, M. & TRAVISANO, M. 2012. Experimental evolution of multicellularity. *Proc Natl Acad Sci U S A,* 109**,** 1595-600.

RAVAL, A., TANNER, S. M., BYRD, J. C., ANGERMAN, E. B., PERKO, J. D., CHEN, S. S., HACKANSON, B., GREVER, M. R., LUCAS, D. M., MATKOVIC, J. J., LIN, T. S., KIPPS, T. J., MURRAY, F., WEISENBURGER, D., SANGER, W., LYNCH, J., WATSON, P., JANSEN, M., YOSHINAGA, Y., ROSENQUIST, R., DE JONG, P. J., COGGILL, P., BECK, S., LYNCH, H., DE LA CHAPELLE, A. & PLASS, C. 2007. Downregulation of death-associated protein kinase 1 (DAPK1) in chronic lymphocytic leukemia. *Cell,* 129**,** 879-90.

REBBECK, C. A., THOMAS, R., BREEN, M., LEROI, A. M. & BURT, A. 2009. Origins and evolution of a transmissible cancer. *Evolution,* 63**,** 2340-9.

RICH, P. R. 2003. The molecular machinery of Keilin's respiratory chain. *Biochem Soc Trans,* 31**,** 1095-105.

RIZZI, M., TSCHAN, M. P., BRITSCHGI, C., BRITSCHGI, A., HUGLI, B., GROB, T. J., LEUPIN, N., MUELLER, B. U., SIMON, H. U., ZIEMIECKI, A., TORBETT, B. E., FEY, M. F. & TOBLER, A. 2007. The death-associated protein kinase 2 is up-regulated during normal myeloid differentiation and enhances neutrophil maturation in myeloid leukemic cells. *J Leukoc Biol,* 81**,** 1599-608.

RODRIGUEZ, M., CABAL-HIERRO, L., CARCEDO, M. T., IGLESIAS, J. M., ARTIME, N., DARNAY, B. G. & LAZO, P. S. 2011. NF-kappaB signal triggering and termination by tumor necrosis factor receptor 2. *J Biol Chem,* 286**,** 22814-24.

ROTHE, M., PAN, M. G., HENZEL, W. J., AYRES, T. M. & GOEDDEL, D. V. 1995a. The TNFR2-TRAF signaling complex contains two novel proteins related to baculoviral inhibitor of apoptosis proteins. *Cell,* 83**,** 1243-52.

ROTHE, M., SARMA, V., DIXIT, V. M. & GOEDDEL, D. V. 1995b. TRAF2-mediated activation of NF-kappa B by TNF receptor 2 and CD40. *Science,* 269**,** 1424-7.

ROTHE, M., WONG, S. C., HENZEL, W. J. & GOEDDEL, D. V. 1994. A novel family of putative signal transducers associated with the cytoplasmic domain of the 75 kDa tumor necrosis factor receptor. *Cell,* 78**,** 681-92.

RUDDLE, N. H. & WAKSMAN, B. H. 1968. Cytotoxicity mediated by soluble antigen and lymphocytes in delayed hypersensitivity. I. Characterization of the phenomenon. *J Exp Med,* 128**,** 1237-54.

RUEFLI-BRASSE, A. A., LEE, W. P., HURST, S. & DIXIT, V. M. 2004. Rip2 participates in Bcl10 signaling and T-cell receptor-mediated NF-kappaB activation. *J Biol Chem,* 279**,** 1570-4.

RUPEC, R. A. & BAEUERLE, P. A. 1995. The genomic response of tumor cells to hypoxia and reoxygenation. Differential activation of transcription factors AP-1 and NF-kappa B. *Eur J Biochem,* 234**,** 632-40.

SANCHEZ-PEREZ, I., BENITAH, S. A., MARTINEZ-GOMARIZ, M., LACAL, J. C. & PERONA, R. 2002. Cell stress and MEKK1-mediated c-Jun activation modulate NFkappaB activity and cell viability. *Mol Biol Cell,* 13**,** 2933-45.

SANTEE, S. M. & OWEN-SCHAUB, L. B. 1996. Human tumor necrosis factor receptor p75/80 (CD120b) gene structure and promoter characterization. *J Biol Chem,* 271**,** 21151-9.

SAWYERS, C. 2004. Targeted cancer therapy. *Nature,* 432**,** 294-7.

SCAFFIDI, C., SCHMITZ, I., KRAMMER, P. H. & PETER, M. E. 1999. The role of c-FLIP in modulation of CD95-induced apoptosis. *J Biol Chem,* 274**,** 1541-8.

SCHLEGEL, C. R., FONSECA, A. V., STOCKER, S., GEORGIOU, M. L., MISTEREK, M. B., MUNRO, C. E., CARMO, C. R., SECKL, M. J. & COSTA-PEREIRA, A. P. 2014. DAPK2 is a novel modulator of TRAIL-induced apoptosis. *Cell Death Differ*.

SCHNEIDER, P., OLSON, D., TARDIVEL, A., BROWNING, B., LUGOVSKOY, A., GONG, D., DOBLES, M., HERTIG, S., HOFMANN, K., VAN VLIJMEN, H., HSU, Y. M., BURKLY, L. C., TSCHOPP, J. & ZHENG, T. S. 2003. Identification of a new murine tumor necrosis factor receptor locus that contains two novel murine receptors for tumor necrosis factor-related apoptosis-inducing ligand (TRAIL). *J Biol Chem,* 278**,** 5444-54.

SCHNEIDER-POETSCH, T., JU, J., EYLER, D. E., DANG, Y., BHAT, S., MERRICK, W. C., GREEN, R., SHEN, B. & LIU, J. O. 2010. Inhibition of eukaryotic translation elongation by cycloheximide and lactimidomycin. *Nat Chem Biol,* 6**,** 209-217.

SCHRECK, R., RIEBER, P. & BAEUERLE, P. A. 1991. Reactive oxygen intermediates as apparently widely used messengers in the activation of the NF-kappa B transcription factor and HIV-1. *EMBO J,* 10**,** 2247-58.

SCHULZE-OSTHOFF, K., FERRARI, D., LOS, M., WESSELBORG, S. & PETER, M. E. 1998. Apoptosis signaling by death receptors. *Eur J Biochem,* 254**,** 439-59.

SCREATON, G. R., MONGKOLSAPAYA, J., XU, X. N., COWPER, A. E., MCMICHAEL, A. J. & BELL, J. I. 1997. TRICK2, a new alternatively spliced receptor that transduces the cytotoxic signal from TRAIL. *Current biology : CB,* 7**,** 693-6.

SEDGER, L. M., GLACCUM, M. B., SCHUH, J. C., KANALY, S. T., WILLIAMSON, E., KAYAGAKI, N., YUN, T., SMOLAK, P., LE, T., GOODWIN, R. & GLINIAK, B. 2002. Characterization of the in vivo function of TNF-alpha-related apoptosis-inducing ligand, TRAIL/Apo2L, using TRAIL/Apo2L gene-deficient mice. *Eur J Immunol,* 32**,** 2246-54.

SEN, R. & BALTIMORE, D. 1986. Multiple nuclear factors interact with the immunoglobulin enhancer sequences. *Cell,* 46**,** 705-16.

SHANG, T., JOSEPH, J., HILLARD, C. J. & KALYANARAMAN, B. 2005. Death-associated protein kinase as a sensor of mitochondrial membrane potential: role of lysosome in mitochondrial toxin-induced cell death. *J Biol Chem,* 280**,** 34644-53.

SHANI, G., HENIS-KORENBLIT, S., JONA, G., GILEADI, O., EISENSTEIN, M., ZIV, T., ADMON, A. & KIMCHI, A. 2001. Autophosphorylation restrains the apoptotic activity of DRP-1 kinase by controlling dimerization and calmodulin binding. *EMBO J,* 20**,** 1099-113.

SHANI, G., MARASH, L., GOZUACIK, D., BIALIK, S., TEITELBAUM, L., SHOHAT, G. & KIMCHI, A. 2004. Death-associated protein kinase phosphorylates ZIP kinase, forming a unique kinase hierarchy to activate its cell death functions. *Mol Cell Biol,* 24**,** 8611-26.

SHERIDAN, J. P., MARSTERS, S. A., PITTI, R. M., GURNEY, A., SKUBATCH, M., BALDWIN, D., RAMAKRISHNAN, L., GRAY, C. L., BAKER, K., WOOD, W. I., GODDARD, A. D., GODOWSKI, P. & ASHKENAZI, A. 1997. Control of TRAIL-induced apoptosis by a family of signaling and decoy receptors. *Science,* 277**,** 818-21.

SHETTY, S., GLADDEN, J. B., HENSON, E. S., HU, X., VILLANUEVA, J., HANEY, N. & GIBSON, S. B. 2002. Tumor necrosis factor-related apoptosis inducing ligand (TRAIL) up-regulates death receptor 5 (DR5) mediated by NFkappaB activation in epithelial derived cell lines. *Apoptosis,* 7**,** 413-20.

SHETTY, S., GRAHAM, B. A., BROWN, J. G., HU, X., VEGH-YAREMA, N., HARDING, G., PAUL, J. T. & GIBSON, S. B. 2005. Transcription factor NF-kappaB differentially regulates death receptor 5 expression involving histone deacetylase 1. *Mol Cell Biol,* 25**,** 5404-16.

SHILOH, R., BIALIK, S. & KIMCHI, A. 2013. The DAPK family: a structure-function analysis. *Apoptosis : an international journal on programmed cell death*.

SHIN, M. S., KIM, H. S., LEE, S. H., PARK, W. S., KIM, S. Y., PARK, J. Y., LEE, J. H., LEE, S. K., LEE, S. N., JUNG, S. S., HAN, J. Y., KIM, H., LEE, J. Y. & YOO, N. J. 2001. Mutations of tumor necrosis factor-related apoptosis-inducing ligand receptor 1 (TRAIL-R1) and receptor 2 (TRAIL-R2) genes in metastatic breast cancers. *Cancer Res,* 61**,** 4942-6.

SHOHAT, G., SPIVAK-KROIZMAN, T., COHEN, O., BIALIK, S., SHANI, G., BERRISI, H., EISENSTEIN, M. & KIMCHI, A. 2001. The pro-apoptotic function of death-associated protein kinase is controlled by a unique inhibitory autophosphorylation-based mechanism. *J Biol Chem,* 276**,** 47460-7.

SHOVAL, Y., BERISSI, H., KIMCHI, A. & PIETROKOVSKI, S. 2011. New modularity of DAP-kinases: alternative splicing of the DRP-1 gene produces a ZIPk-like isoform. *PLoS One,* 6**,** e17344.

SIMPSON, A. J. & CAMARGO, A. A. 1998. Evolution and the inevitability of human cancer. *Semin Cancer Biol,* 8**,** 439-45.

SINGH, H., SEN, R., BALTIMORE, D. & SHARP, P. A. 1986. A nuclear factor that binds to a conserved sequence motif in transcriptional control elements of immunoglobulin genes. *Nature,* 319**,** 154-8.

SINGH, N. P., NAGARKATTI, M. & NAGARKATTI, P. S. 2007. Role of dioxin response element and nuclear factor-kappaB motifs in 2,3,7,8-tetrachlorodibenzo-p-dioxin-mediated regulation of Fas and Fas ligand expression. *Mol Pharmacol,* 71**,** 145-57.

SINICROPE, F. A., PENINGTON, R. C. & TANG, X. M. 2004. Tumor necrosis factor-related apoptosis-inducing ligand-induced apoptosis is inhibited by Bcl-2 but restored by

the small molecule Bcl-2 inhibitor, HA 14-1, in human colon cancer cells. *Clin Cancer Res,* 10**,** 8284-92.

SLATER, J. 2012. From X-Rays to Ion Beams: A Short History of Radiation Therapy. *In:* LINZ, U. (ed.) *Ion Beam Therapy.* Springer Berlin Heidelberg.

SMITH, C. A., FARRAH, T. & GOODWIN, R. G. 1994. The TNF receptor superfamily of cellular and viral proteins: activation, costimulation, and death. *Cell,* 76**,** 959-62.

SMYTH, M. J., TAKEDA, K., HAYAKAWA, Y., PESCHON, J. J., VAN DEN BRINK, M. R. & YAGITA, H. 2003. Nature's TRAIL--on a path to cancer immunotherapy. *Immunity,* 18**,** 1-6.

SOBELL, H. M. 1985. Actinomycin and DNA transcription. *Proc Natl Acad Sci U S A,* 82**,** 5328-31.

SON, Y., KIM, S., CHUNG, H. T. & PAE, H. O. 2013. Reactive oxygen species in the activation of MAP kinases. *Methods Enzymol,* 528**,** 27-48.

SORIA, J. C., MARK, Z., ZATLOUKAL, P., SZIMA, B., ALBERT, I., JUHASZ, E., PUJOL, J. L., KOZIELSKI, J., BAKER, N., SMETHURST, D., HEI, Y. J., ASHKENAZI, A., STERN, H., AMLER, L., PAN, Y. & BLACKHALL, F. 2011. Randomized phase II study of dulanermin in combination with paclitaxel, carboplatin, and bevacizumab in advanced non-small-cell lung cancer. *J Clin Oncol,* 29**,** 4442-51.

SRINIVASAN, A., LI, F., WONG, A., KODANDAPANI, L., SMIDT, R., JR., KREBS, J. F., FRITZ, L. C., WU, J. C. & TOMASELLI, K. J. 1998. Bcl-xL functions downstream of caspase-8 to inhibit Fas- and tumor necrosis factor receptor 1-induced apoptosis of MCF7 breast carcinoma cells. *J Biol Chem,* 273**,** 4523-9.

STAUDT, L. M., SINGH, H., SEN, R., WIRTH, T., SHARP, P. A. & BALTIMORE, D. 1986. A lymphoid-specific protein binding to the octamer motif of immunoglobulin genes. *Nature,* 323**,** 640-3.

STEIN, B., BALDWIN, A. S., JR., BALLARD, D. W., GREENE, W. C., ANGEL, P. & HERRLICH, P. 1993. Cross-coupling of the NF-kappa B p65 and Fos/Jun transcription factors produces potentiated biological function. *EMBO J,* 12**,** 3879-91.

STEWART, S. A. & WEINBERG, R. A. 2006. Telomeres: cancer to human aging. *Annu Rev Cell Dev Biol,* 22**,** 531-57.

STIEFEL, M., SHANER, A. & SCHAEFER, S. D. 2006. The Edwin Smith Papyrus: the birth of analytical thinking in medicine and otolaryngology. *Laryngoscope,* 116**,** 182-8.

STRACHAN, T., READ, A. P. & NATIONAL CENTER FOR BIOTECHNOLOGY INFORMATION. 1999. Human molecular genetics 2. 2nd ed. New York ; London: Garland Science/National Center for Biotechnology Information (NCBI).

STRAND, S., HOFMANN, W. J., HUG, H., MULLER, M., OTTO, G., STRAND, D., MARIANI, S. M., STREMMEL, W., KRAMMER, P. H. & GALLE, P. R. 1996. Lymphocyte apoptosis induced by CD95 (APO-1/Fas) ligand-expressing tumor cells--a mechanism of immune evasion? *Nat Med,* 2**,** 1361-6.

SUN, S. C. 2011. Non-canonical NF-kappaB signaling pathway. *Cell Res,* 21**,** 71-85.

SYROVETS, T., BUCHELE, B., KRAUSS, C., LAUMONNIER, Y. & SIMMET, T. 2005. Acetyl-boswellic acids inhibit lipopolysaccharide-mediated TNF-alpha induction in monocytes by direct interaction with IkappaB kinases. *J Immunol,* 174**,** 498-506.

TAN, K. B., HARROP, J., REDDY, M., YOUNG, P., TERRETT, J., EMERY, J., MOORE, G. & TRUNEH, A. 1997. Characterization of a novel TNF-like ligand and recently described TNF ligand and TNF receptor superfamily genes and their constitutive and inducible expression in hematopoietic and non-hematopoietic cells. *Gene,* 204**,** 35-46.

TANG, P., HUNG, M. C. & KLOSTERGAARD, J. 1996. Human pro-tumor necrosis factor is a homotrimer. *Biochemistry,* 35**,** 8216-25.

TERGAONKAR, V. 2006. NFkappaB pathway: a good signaling paradigm and therapeutic target. *Int J Biochem Cell Biol,* 38**,** 1647-53.

TIAN, T., OLSON, S., WHITACRE, J. M. & HARDING, A. 2011. The origins of cancer robustness and evolvability. *Integr Biol (Camb),* 3**,** 17-30.

TOKUNAGA, F., SAKATA, S., SAEKI, Y., SATOMI, Y., KIRISAKO, T., KAMEI, K., NAKAGAWA, T., KATO, M., MURATA, S., YAMAOKA, S., YAMAMOTO, M., AKIRA, S., TAKAO, T., TANAKA, K. & IWAI, K. 2009. Involvement of linear polyubiquitylation of NEMO in NF-kappaB activation. *Nat Cell Biol,* 11**,** 123-32.

TOSCANO, F., FAJOUI, Z. E., GAY, F., LALAOUI, N., PARMENTIER, B., CHAYVIALLE, J. A., SCOAZEC, J. Y., MICHEAU, O., ABELLO, J. & SAURIN, J. C. 2008. P53-mediated upregulation of DcR1 impairs oxaliplatin/TRAIL-induced synergistic anti-tumour potential in colon cancer cells. *Oncogene,* 27**,** 4161-71.

TRUNEH, A., SHARMA, S., SILVERMAN, C., KHANDEKAR, S., REDDY, M. P., DEEN, K. C., MCLAUGHLIN, M. M., SRINIVASULA, S. M., LIVI, G. P., MARSHALL, L. A., ALNEMRI, E. S., WILLIAMS, W. V. & DOYLE, M. L. 2000. Temperature-sensitive differential affinity of TRAIL for its receptors. DR5 is the highest affinity receptor. *J Biol Chem,* 275**,** 23319-25.

TSE, A. K., CAO, H. H., CHENG, C. Y., KWAN, H. Y., YU, H., FONG, W. F. & YU, Z. L. 2014. Indomethacin sensitizes TRAIL-resistant melanoma cells to TRAIL-induced apoptosis through ROS-mediated upregulation of death receptor 5 and downregulation of survivin. *J Invest Dermatol,* 134**,** 1397-407.

TUETTENBERG, J., SEIZ, M., DEBATIN, K. M., HOLLBURG, W., VON STADEN, M., THIEMANN, M., HARENG, B., FRICKE, H. & KUNZ, C. 2012. Pharmacokinetics, pharmacodynamics, safety and tolerability of APG101, a CD95-Fc fusion protein, in healthy volunteers and two glioma patients. *Int Immunopharmacol,* 13**,** 93-100.

TUR, M. K., NEEF, I., JOST, E., GALM, O., JAGER, G., STOCKER, M., RIBBERT, M., OSIEKA, R., KLINGE, U. & BARTH, S. 2009. Targeted restoration of down-regulated DAPK2 tumor suppressor activity induces apoptosis in Hodgkin lymphoma cells. *J Immunother,* 32**,** 431-41.

TURRENS, J. F. 2003. Mitochondrial formation of reactive oxygen species. *J Physiol,* 552**,** 335-44.

ULIVI, V., GIANNONI, P., GENTILI, C., CANCEDDA, R. & DESCALZI, F. 2008. p38/NF-kB-dependent expression of COX-2 during differentiation and inflammatory response of chondrocytes. *J Cell Biochem,* 104**,** 1393-406.

USUI, T., OKADA, M. & YAMAWAKI, H. 2014. Zipper interacting protein kinase (ZIPK): function and signaling. *Apoptosis,* 19**,** 387-91.

VAN DIJK, M., HALPIN-MCCORMICK, A., SESSLER, T., SAMALI, A. & SZEGEZDI, E. 2013. Resistance to TRAIL in non-transformed cells is due to multiple redundant pathways. *Cell Death Dis,* 4**,** e702.

VAN GEELEN, C. M., PENNARUN, B., EK, W. B., LE, P. T., SPIERINGS, D. C., DE VRIES, E. G. & DE JONG, S. 2010. Downregulation of active caspase 8 as a mechanism of acquired TRAIL resistance in mismatch repair-proficient colon carcinoma cell lines. *Int J Oncol,* 37**,** 1031-41.

VANDER HEIDEN, M. G., CANTLEY, L. C. & THOMPSON, C. B. 2009. Understanding the Warburg effect: the metabolic requirements of cell proliferation. *Science,* 324**,** 1029-33.

VARMUS, H. E. 1985. Viruses, genes, and cancer. I. The discovery of cellular oncogenes and their role in neoplasia. *Cancer,* 55**,** 2324-8.

VASSILEV, L. T., VU, B. T., GRAVES, B., CARVAJAL, D., PODLASKI, F., FILIPOVIC, Z., KONG, N., KAMMLOTT, U., LUKACS, C., KLEIN, C., FOTOUHI, N. & LIU, E. A. 2004. In vivo activation of the p53 pathway by small-molecule antagonists of MDM2. *Science,* 303**,** 844-8.

VELARDE, M. C., FLYNN, J. M., DAY, N. U., MELOV, S. & CAMPISI, J. 2012. Mitochondrial oxidative stress caused by Sod2 deficiency promotes cellular senescence and aging phenotypes in the skin. *Aging (Albany NY),* 4**,** 3-12.

VIDAL, M. & CAGAN, R. L. 2006. Drosophila models for cancer research. *Curr Opin Genet Dev,* 16**,** 10-6.

VON EYBEN, F. E. 2001. A systematic review of lactate dehydrogenase isoenzyme 1 and germ cell tumors. *Clin Biochem,* 34**,** 441-54.

VOORTMAN, J., RESENDE, T. P., ABOU EL HASSAN, M. A., GIACCONE, G. & KRUYT, F. A. 2007. TRAIL therapy in non-small cell lung cancer cells: sensitization to death receptor-mediated apoptosis by proteasome inhibitor bortezomib. *Mol Cancer Ther,* 6**,** 2103-12.

WAJANT, H., PFIZENMAIER, K. & SCHEURICH, P. 2003. Tumor necrosis factor signaling. *Cell Death Differ,* 10**,** 45-65.

WAJANT, H. & SCHEURICH, P. 2011. TNFR1-induced activation of the classical NF-kappaB pathway. *FEBS J,* 278**,** 862-76.

WAKSMAN, S. A., GEIGER, W. B. & REYNOLDS, D. M. 1946. Strain Specificity and Production of Antibiotic Substances: VII. Production of Actinomycin by Different Actinomycetes. *Proc Natl Acad Sci U S A,* 32**,** 117-20.

WALCZAK, H., DEGLI-ESPOSTI, M. A., JOHNSON, R. S., SMOLAK, P. J., WAUGH, J. Y., BOIANI, N., TIMOUR, M. S., GERHART, M. J., SCHOOLEY, K. A., SMITH, C. A., GOODWIN, R. G. & RAUCH, C. T. 1997. TRAIL-R2: a novel apoptosis-mediating receptor for TRAIL. *EMBO J,* 16**,** 5386-97.

WANG, S. & EL-DEIRY, W. S. 2004. Inducible silencing of KILLER/DR5 in vivo promotes bioluminescent colon tumor xenograft growth and confers resistance to chemotherapeutic agent 5-fluorouracil. *Cancer Res,* 64**,** 6666-72.

WANG, V. Y., HUANG, W., ASAGIRI, M., SPANN, N., HOFFMANN, A., GLASS, C. & GHOSH, G. 2012a. The transcriptional specificity of NF-kappaB dimers is coded within the kappaB DNA response elements. *Cell Rep,* 2**,** 824-39.

WANG, Y., NARTISS, Y., STEIPE, B., MCQUIBBAN, G. A. & KIM, P. K. 2012b. ROS-induced mitochondrial depolarization initiates PARK2/PARKIN-dependent mitochondrial degradation by autophagy. *Autophagy,* 8**,** 1462-76.

WARBURG, O. 1956. On the origin of cancer cells. *Science,* 123**,** 309-14.

WARE, C. F., CROWE, P. D., VANARSDALE, T. L., ANDREWS, J. L., GRAYSON, M. H., JERZY, R., SMITH, C. A. & GOODWIN, R. G. 1991. Tumor necrosis factor (TNF) receptor expression in T lymphocytes. Differential regulation of the type I TNF receptor during activation of resting and effector T cells. *J Immunol,* 147**,** 4229-38.

WATERHOUSE, N. J., RICCI, J. E. & GREEN, D. R. 2002. And all of a sudden it's over: mitochondrial outer-membrane permeabilization in apoptosis. *Biochimie,* 84**,** 113-21.

WATLING, D., CARMO, C. R., KERR, I. M. & COSTA-PEREIRA, A. P. 2008. Multiple kinases in the interferon-gamma response. *Proc Natl Acad Sci U S A,* 105**,** 6051-6.

WEINBERG, R. A. 2007. *The biology of cancer,* New York, Garland Science.

WEINBERGER, J., BALTIMORE, D. & SHARP, P. A. 1986. Distinct factors bind to apparently homologous sequences in the immunoglobulin heavy-chain enhancer. *Nature,* 322**,** 846-8.

WEISS, L. 2000. Early concepts of cancer. *Cancer and Metastasis Reviews,* 19**,** 205-217.

WERNER, A. B., DE VRIES, E., TAIT, S. W., BONTJER, I. & BORST, J. 2002. TRAIL receptor and CD95 signal to mitochondria via FADD, caspase-8/10, Bid, and Bax but differentially regulate events downstream from truncated Bid. *J Biol Chem,* 277**,** 40760-7.

WICK, W., WELLER, M., WEILER, M., BATCHELOR, T., YUNG, A. W. & PLATTEN, M. 2011. Pathway inhibition: emerging molecular targets for treating glioblastoma. *Neuro Oncol,* 13**,** 566-79.

WILEY, S. R., SCHOOLEY, K., SMOLAK, P. J., DIN, W. S., HUANG, C. P., NICHOLL, J. K., SUTHERLAND, G. R., SMITH, T. D., RAUCH, C., SMITH, C. A. & ET AL. 1995. Identification and characterization of a new member of the TNF family that induces apoptosis. *Immunity,* 3**,** 673-82.

WILSON, N. S., YANG, B., YANG, A., LOESER, S., MARSTERS, S., LAWRENCE, D., LI, Y., PITTI, R., TOTPAL, K., YEE, S., ROSS, S., VERNES, J. M., LU, Y., ADAMS, C., OFFRINGA, R., KELLEY, B., HYMOWITZ, S., DANIEL, D., MENG, G. & ASHKENAZI, A. 2011. An Fcgamma receptor-dependent mechanism drives antibody-mediated target-receptor signaling in cancer cells. *Cancer Cell,* 19**,** 101-13.

WOLBERGER, C. 1998. Combinatorial transcription factors. *Curr Opin Genet Dev,* 8**,** 552-9.

WOLFF, A. C., HAMMOND, M. E., SCHWARTZ, J. N., HAGERTY, K. L., ALLRED, D. C., COTE, R. J., DOWSETT, M., FITZGIBBONS, P. L., HANNA, W. M., LANGER, A., MCSHANE, L. M., PAIK, S., PEGRAM, M. D., PEREZ, E. A., PRESS, M. F., RHODES, A., STURGEON, C., TAUBE, S. E., TUBBS, R., VANCE, G. H., VAN DE VIJVER, M., WHEELER, T. M., HAYES, D. F. & AMERICAN SOCIETY OF CLINICAL ONCOLOGY/COLLEGE OF AMERICAN, P. 2007. American Society of Clinical Oncology/College of American Pathologists guideline recommendations for human epidermal growth factor receptor 2 testing in breast cancer. *Arch Pathol Lab Med,* 131**,** 18-43.

WOLTER, S., DOERRIE, A., WEBER, A., SCHNEIDER, H., HOFFMANN, E., VON DER OHE, J., BAKIRI, L., WAGNER, E. F., RESCH, K. & KRACHT, M. 2008. c-Jun controls histone modifications, NF-kappaB recruitment, and RNA polymerase II function to activate the ccl2 gene. *Mol Cell Biol,* 28**,** 4407-23.

WU, G. S., BURNS, T. F., MCDONALD, E. R., 3RD, JIANG, W., MENG, R., KRANTZ, I. D., KAO, G., GAN, D. D., ZHOU, J. Y., MUSCHEL, R., HAMILTON, S. R., SPINNER, N. B., MARKOWITZ, S., WU, G. & EL-DEIRY, W. S. 1997. KILLER/DR5 is a DNA damage-inducible p53-regulated death receptor gene. *Nat Genet,* 17**,** 141-3.

WU, G. S., BURNS, T. F., ZHAN, Y., ALNEMRI, E. S. & EL-DEIRY, W. S. 1999. Molecular cloning and functional analysis of the mouse homologue of the KILLER/DR5 tumor necrosis factor-related apoptosis-inducing ligand (TRAIL) death receptor. *Cancer Res,* 59**,** 2770-5.

XU, G., LO, Y. C., LI, Q., NAPOLITANO, G., WU, X., JIANG, X., DREANO, M., KARIN, M. & WU, H. 2011. Crystal structure of inhibitor of kappaB kinase beta. *Nature,* 472**,** 325-30.

XU, Y., KRISHNAN, A., WAN, X. S., MAJIMA, H., YEH, C. C., LUDEWIG, G., KASARSKIS, E. J. & ST CLAIR, D. K. 1999. Mutations in the promoter reveal a cause for the reduced expression of the human manganese superoxide dismutase gene in cancer cells. *Oncogene,* 18**,** 93-102.

YADAV, V. R., PRASAD, S. & AGGARWAL, B. B. 2012. Cardamonin sensitizes tumour cells to TRAIL through ROS- and CHOP-mediated up-regulation of death receptors and down-regulation of survival proteins. *Br J Pharmacol,* 165**,** 741-53.

YAMAMOTO, K., ARAKAWA, T., UEDA, N. & YAMAMOTO, S. 1995. Transcriptional roles of nuclear factor kappa B and nuclear factor-interleukin-6 in the tumor necrosis factor alpha-dependent induction of cyclooxygenase-2 in MC3T3-E1 cells. *J Biol Chem,* 270**,** 31315-20.

YANG, Y., JUNG, D. W., BAI, D. G., YOO, G. S. & CHOI, J. K. 2001. Counterion-dye staining method for DNA in agarose gels using crystal violet and methyl orange. *Electrophoresis,* 22**,** 855-9.

YOBOUA, F., MARTEL, A., DUVAL, A., MUKAWERA, E. & GRANDVAUX, N. 2010. Respiratory syncytial virus-mediated NF-kappa B p65 phosphorylation at serine 536 is dependent on RIG-I, TRAF6, and IKK beta. *J Virol,* 84**,** 7267-77.

YONEHARA, S., ISHII, A. & YONEHARA, M. 1989. A cell-killing monoclonal antibody (anti-Fas) to a cell surface antigen co-downregulated with the receptor of tumor necrosis factor. *J Exp Med,* 169**,** 1747-56.

YOO, H. J., BYUN, H. J., KIM, B. R., LEE, K. H., PARK, S. Y. & RHO, S. B. 2012. DAPk1 inhibits NF-kappaB activation through TNF-alpha and INF-gamma-induced apoptosis. *Cell Signal,* 24**,** 1471-7.

YUAN, K., SUN, Y., ZHOU, T., MCDONALD, J. & CHEN, Y. 2013. PARP-1 regulates resistance of pancreatic cancer to TRAIL therapy. *Clin Cancer Res,* 19**,** 4750-9.

YUE, H. H., DIEHL, G. E. & WINOTO, A. 2005. Loss of TRAIL-R does not affect thymic or intestinal tumor development in p53 and adenomatous polyposis coli mutant mice. *Cell Death Differ,* 12**,** 94-7.

ZELKO, I. N., MARIANI, T. J. & FOLZ, R. J. 2002. Superoxide dismutase multigene family: a comparison of the CuZn-SOD (SOD1), Mn-SOD (SOD2), and EC-SOD (SOD3) gene structures, evolution, and expression. *Free Radic Biol Med,* 33**,** 337-49.

ZENDER, L., HUTKER, S., MUNDT, B., WALTEMATHE, M., KLEIN, C., TRAUTWEIN, C., MALEK, N. P., MANNS, M. P., KUHNEL, F. & KUBICKA, S. 2005. NFkappaB-mediated upregulation of bcl-xl restrains TRAIL-mediated apoptosis in murine viral hepatitis. *Hepatology,* 41**,** 280-8.

ZERAFA, N., WESTWOOD, J. A., CRETNEY, E., MITCHELL, S., WARING, P., IEZZI, M. & SMYTH, M. J. 2005. Cutting edge: TRAIL deficiency accelerates hematological malignancies. *J Immunol,* 175**,** 5586-90.

ZHANG, J., YANG, P. L. & GRAY, N. S. 2009. Targeting cancer with small molecule kinase inhibitors. *Nat Rev Cancer,* 9**,** 28-39.

ZHANG, L. & FANG, B. 2005. Mechanisms of resistance to TRAIL-induced apoptosis in cancer. *Cancer Gene Ther,* 12**,** 228-37.

ZHANG, X., JIN, T. G., YANG, H., DEWOLF, W. C., KHOSRAVI-FAR, R. & OLUMI, A. F. 2004. Persistent c-FLIP(L) expression is necessary and sufficient to maintain resistance to tumor necrosis factor-related apoptosis-inducing ligand-mediated apoptosis in prostate cancer. *Cancer Res,* 64**,** 7086-91.

ZHANG, Y. & ZHANG, B. 2008. TRAIL resistance of breast cancer cells is associated with constitutive endocytosis of death receptors 4 and 5. *Mol Cancer Res,* 6**,** 1861-71.

ZHENG, J. 2012. Energy metabolism of cancer: Glycolysis versus oxidative phosphorylation (Review). *Oncol Lett,* 4**,** 1151-1157.

ZHENG, S. J., JIANG, J., SHEN, H. & CHEN, Y. H. 2004. Reduced apoptosis and ameliorated listeriosis in TRAIL-null mice. *J Immunol,* 173**,** 5652-8.

ZHONG, H., MAY, M. J., JIMI, E. & GHOSH, S. 2002. The phosphorylation status of nuclear NF-kappa B determines its association with CBP/p300 or HDAC-1. *Mol Cell,* 9**,** 625-36.

ZHOU, J., LU, G. D., ONG, C. S., ONG, C. N. & SHEN, H. M. 2008. Andrographolide sensitizes cancer cells to TRAIL-induced apoptosis via p53-mediated death receptor 4 up-regulation. *Mol Cancer Ther,* 7**,** 2170-80.

ZHOU, M., ZHAO, Y., DING, Y., LIU, H., LIU, Z., FODSTAD, O., RIKER, A. I., KAMARAJUGADDA, S., LU, J., OWEN, L. B., LEDOUX, S. P. & TAN, M. 2010. Warburg

effect in chemosensitivity: targeting lactate dehydrogenase-A re-sensitizes taxol-resistant cancer cells to taxol. *Mol Cancer,* 9**,** 33.

ZHUANG, H., JIANG, W., CHENG, W., QIAN, K., DONG, W., CAO, L., HUANG, Q., LI, S., DOU, F., CHIU, J. F., FANG, X. X., LU, M. & HUA, Z. C. 2010. Down-regulation of HSP27 sensitizes TRAIL-resistant tumor cell to TRAIL-induced apoptosis. *Lung Cancer,* 68**,** 27-38.

ZOU, H., HENZEL, W. J., LIU, X., LUTSCHG, A. & WANG, X. 1997. Apaf-1, a human protein homologous to C. elegans CED-4, participates in cytochrome c-dependent activation of caspase-3. *Cell,* 90**,** 405-13.

9. Publications

Cell Death and Differentiation (2014) 21, 1780–1791

www.nature.com/cdd

DAPK2 is a novel modulator of TRAIL-induced apoptosis

CR Schlegel[1], A-V Fonseca[1,2], S Stöcker[1,3], ML Georgiou[1], MB Misterek[1,4], CE Munro[1], CR Carmo[1,5], MJ Seckl[1] and AP Costa-Pereira*[,1]

Targeting molecules involved in TRAIL-mediated signalling has been hailed by many as a potential magic bullet to kill cancer cells efficiently, with little side effects on normal cells. Indeed, initial clinical trials showed that antibodies against TRAIL receptors, death receptor (DR)4 and DR5, are well tolerated by cancer patients. Despite efficacy issues in the clinical setting, novel approaches to trigger TRAIL-mediated apoptosis are being developed and its clinical potential is being reappraised. Unfortunately, as observed with other cancer therapies, many patients develop resistance to TRAIL-induced apoptosis and there is thus impetuous for identifying additional resistance mechanisms that may be targetable and usable in combination therapies. Here, we show that the death-associated protein kinase 2 (DAPK2) is a modulator of TRAIL signalling. Genetic ablation of DAPK2 using RNA interference causes phosphorylation of NF-κB and its transcriptional activity in several cancer cell lines. This then leads to the induction of a variety of NF-κB target genes, which include proapoptotic DR4 and DR5. DR4 and DR5 protein expression is correspondingly increased on the cell surface and this leads to the sensitisation of resistant cells to TRAIL-induced killing, in a p53-independent manner. As DAPK2 is a kinase, it is imminently druggable, and our data thus offer a novel avenue to overcome TRAIL resistance in the clinic.
Cell Death and Differentiation (2014) **21,** 1780–1791; doi:10.1038/cdd.2014.93; published online 11 July 2014

Despite the effort and resources invested in cancer research, cancer remains a serious public health problem. Most patients are treated surgically, with chemotherapeutic drugs and/or antibodies and small molecule inhibitors. Patients generally respond well to the initial therapy but frequently develop resistance to it. This poses a challenge to their treatment and calls for alternative approaches to be developed. Indeed, much excitement was generated in the mid-1990s when tumour necrosis factor (TNF)-related apoptosis-inducing ligand (TRAIL) was identified.[1–4]

TRAIL is a death receptor (DR) ligand that signals through DR4 and DR5, two members of the TNF receptor family.[5–7] DR5 has two isoforms that differ by 29 amino acids and which are functionally indistinguishable.[5,8] TRAIL ligation activates primarily the extrinsic apoptotic pathway. The formation of ligand/receptor complexes leads to the assembly of a multi-protein death-inducing signalling complex (DISC), which in the case of TRAIL is typically composed of the adaptor Fas-associated death domain, caspase-8, caspase-10 and/or c-FLIP. These initiator caspases proteolytically cleave effector caspases such as caspase-3, caspase-6 and/or caspase-7 thereby activating them. This leads to the destruction of key cellular components and the appearance of typical features of apoptosis. TRAIL can also activate intrinsic apoptotic pathways via BID and thus involve mitochondria. By virtue of preferentially killing tumour cells, TRAIL is seen by many as a 'magic bullet' against cancer cells. Some cancer cells, however, are resistant, or develop resistance, to TRAIL-induced apoptosis. Several resistance mechanisms have been described but they do not account for all cases of resistant cells,[9] suggesting that additional as yet unidentified mechanisms exist. Deregulation at receptor, DISC and mitochondria levels have all been described, and the involvement of mitogen-activated protein kinases and poly-(ADP-ribose) polymerase 1 (PARP1) have also been suggested. Here we show that death-associated protein kinase 2 (DAPK2) can be used as a target to overcome resistance to TRAIL-induced apoptosis.

[1]Department of Surgery and Cancer, Imperial College London, Faculty of Medicine, Hammersmith Hospital, Hammersmith Hospital Campus, ICTEM, Du Cane Road, London W12 0NN, UK
*Corresponding author: AP Costa-Pereira, Department of Surgery and Cancer, Imperial College London, Faculty of Medicine, Hammersmith Hospital, Hammersmith Hospital Campus, ICTEM, Du Cane Road, London W12 0NN, UK. Tel: +44 20 7594 2815; Fax: +44 20 3313 5830; E-mail: a.costa-pereira@imperial.ac.uk
[2]Current address: Medical Research Council National Institute for Medical Research, The Ridgeway, London, UK
[3]Current address: German Cancer Research Center, Im Neuenheimer Feld 280, Heidelberg, Germany
[4]Current address: Otto-von-Guericke-University Magdeburg, Faculty of Process and Systems Engineering, Universitätsplatz 2, Magdeburg, Germany
[5]Current address: Instituto Gulbenkian de Ciência, Oeiras, Portugal

Abbreviations: BID, BH3 interacting-domain death agonist; DAPK, death-associated protein kinase; DcR, decoy receptor; DISC, death-inducing signalling complex; DR, death receptor; FADD, Fas-associated death domain; FLIP, Fas-associated death domain-like interleukin-1β-converting enzyme-like inhibitory protein; FITC, fluorescein isothiocyanide; H_2O_2, hydrogen peroxide; MAPK, mitogen-activated protein kinase; NF-κB, nuclear factor-κB; PARP, poly-(ADP-ribose) polymerase; PE, phycoerythrin; qPCR, quantitative (real-time) polymerase chain reaction; qWB, quantitative western blot; REL, v-rel avian reticuloendotheliosis viral oncogene homolog; RIP, receptor interacting protein; RNAi, RNA interference; ROS, reactive oxygen species; SDS-PAGE, sodium dodecyl sulphate polyacrylamide gel electrophoresis; SEM, standard error of the mean; si, short interfering; siNS, non-targeting siRNA molecule; TNF, tumour necrosis factor; TRADD, tumor necrosis factor receptor type 1-associated DEATH domain protein; TRAIL, tumour necrosis factor-related apoptosis-inducing ligand; WB, western blot

Received 20.12.13; revised 27.5.14; accepted 28.5.14; Edited by A Villunger; published online 11.7.14

DAPK2 (also known as DRP-1) belongs to the DAPK family, which comprises a number of serine/threonine kinases regulated by calcium/calmodulin that are involved in death-inducing pathways. The three main members (DAPK1–3) share a high degree of homology in the kinase domain but vary greatly outside this key region. The most studied protein is the founder molecule DAPK1, which has been implicated in interferon-γ, FAS ligand, TNF-α and ceramide-induced cell death, among others.[10] The gene is often methylated in tumour cells and it is thought to be a tumour suppressor.[11] DAPK2 is a much smaller protein than DAPK1 (42 *versus* 120 kDa), it lacks ankyrin repeats and, critically, the death domain (Supplementary Figure S1). Accordingly, evidence for a proapoptotic role is largely based on its ability to induce apoptosis-like cell morphology upon overexpression.[12–14] We thus hypothesised that endogenous DAPK2 may under some circumstances have antiapoptotic properties and provide cancer cells with prosurvival cues.

Results

DAPK2 depletion sensitises resistant cells to TRAIL-mediated apoptosis. As DAPK2 lacks a recognisable death motif, we asked what the contribution of endogenous DAPK2 to cell death induced by different apoptotic triggers was. We used U2OS osteosarcoma cells and A549 non-small-cell lung cancer cells as examples of two cancer cell lines with different mutational backgrounds and which have been extensively characterised in our laboratory.[15,16] RNA interference (RNAi) was used to modulate the levels of DAPK2 in these cells. A pool of short interfering (si) oligonucleotides targeting different regions of DAPK2 (henceforth, siDAPK2), which were validated by deconvolution (Supplementary Figure S2), efficiently reduced DAPK2 mRNA and protein levels in U2OS (Figure 1a) and A549 (Figure 1g) cells. Cells were transfected with siDAPK2, challenged with TRAIL (Figures 1b and h), cisplatin (Figures 1c and i), hydrogen peroxide (H_2O_2) (Figures 1d and j), TNF-α (Figures 1e and k), taxol or etoposide (not shown), and cell death levels assessed using crystal violet viability assays. Cells transfected with a non-targeting siRNA pool (siNS) were used as controls in all experiments. The susceptibility of cells with near-to-none DAPK2 expression was compared with that of control cells. Data from three independent experiments (each with triplicate samples) are shown as the mean percentage of live cells $\pm$ S.E.M. (Figure 1). U2OS were readily killed by cisplatin (Figure 1c), oxidative stress (Figure 1d), etoposide and taxol (not shown), and this was not dependent on DAPK2. A549 were less susceptible than U2OS to the killing effects of cisplatin (Figure 1i) or H_2O_2 (Figure 1j), but, as for U2OS cells, the induction of apoptosis was also independent of DAPK2 expression levels. As many other tumour cells, U2OS and A549, were resistant to DR-mediated cell death induced by TRAIL (Figures 1b and h, black bars) or TNF-α (Figures 1e and k). Both cell types could be sensitised to TNF-α-induced death by inhibiting protein synthesis using cycloheximide (CHX) (not shown), but sensitisation to TNF-α was not achieved by silencing DAPK2 (Figures 1e and k). In contrast, reducing the levels of DAPK2 significantly sensitised U2OS and A549 cells to TRAIL-induced cell death (Figures 1b and h, green bars), suggesting that DAPK2 functioned as an inhibitory molecule that modulated TRAIL signalling. Cell death was also assessed by measuring DNA hypoploidy (Supplementary Figure S3), which yielded similar results to those shown in Figures 1b and h.

Downregulation of DAPK2 leads to sensitisation to TRAIL-induced apoptosis via increased apoptotic signalling. Having observed that U2OS and A549 cells were more susceptible to TRAIL-induced cell death after DAPK2 knockdown, we asked what the molecular consequences of DAPK2 silencing were. Cells were transfected as before, treated with TRAIL for varying periods of time, and proteins extracted and separated by sodium dodecyl sulphate (SDS)-polyacrylamide gel electrophoresis (PAGE) (Figures 1f and l). Western blot (WB) membranes were subsequently probed with antibodies specific to molecules activated downstream of TRAIL. TRAIL-induced apoptosis was studied over a period of 1–24 h and we chose to focus on earlier time points as caspase activation is generally a rapid event in cells sensitive to TRAIL. Caspase-8 and -10 are two initiator caspases downstream of DRs and were thus analysed first. Caspase activation was faster and stronger in siDAPK2-transfected cells than in control cells (siNS) (Figures 1f and l), as seen by both the emergence of smaller caspase fragments (43, 41 and 18 kDa) and also by the reduction in the full-length 55 kDa protein. Indeed, caspase-8 cleavage 1 h after TRAIL treatment was much weaker in siNS-transfected cells than in cells transfected with siDAPK2. The same was observed for caspase-10 (not shown). Activation of caspase-8 leads to activation of the effector caspase-3 and subsequent degradation of molecules such as PARP, which ultimately results in cellular demise. Accordingly, DAPK2 silencing also resulted in increased caspase-3 and PARP cleavage (Figures 1f and l). In addition, the reduction of BID expression and increased caspase-9 cleavage after DAPK2 silencing indicated the recruitment of the intrinsic apoptotic pathway (Figures 1f and l). Collectively, these data suggest that DAPK2 inhibited caspase activation downstream of TRAIL by interfering both with the extrinsic and intrinsic apoptosis pathways.

DAPK2 silencing leads to the upregulation of DR5, a key receptor for TRAIL-induced apoptosis. The evidence for the involvement of both these pathways suggested that DAPK2 affected an upstream event common to both arms of TRAIL apoptotic pathways. Accordingly, transfection of U2OS and A549 cells with siDAPK2 led to the upregulation of DR5 (Figures 2a–d), one of the receptors through which TRAIL can signal to kill. DR4 was not expressed in U2OS cells (not shown) but it was expressed in A549 and its expression was also increased after silencing DAPK2 (Figure 2e). The greatly enhanced expression of DR4 and DR5 was analysed both by SDS-PAGE/quantitative WB (qWB) (Figures 2a and c) and by flow cytometry (Figures 2b, d and e). Silencing DAPK2 had no effect on the mRNA levels of any of the three TRAIL decoy receptors: DcR1 (TRAIL-R3/TRID/TNFRSF10C),[17] DcR2 (TRAIL-R4/TRUNDD/TNFRSF10D)[17] and osteoprotegerin (OPG/TNFSF11)[18] (not shown). Interestingly, it also

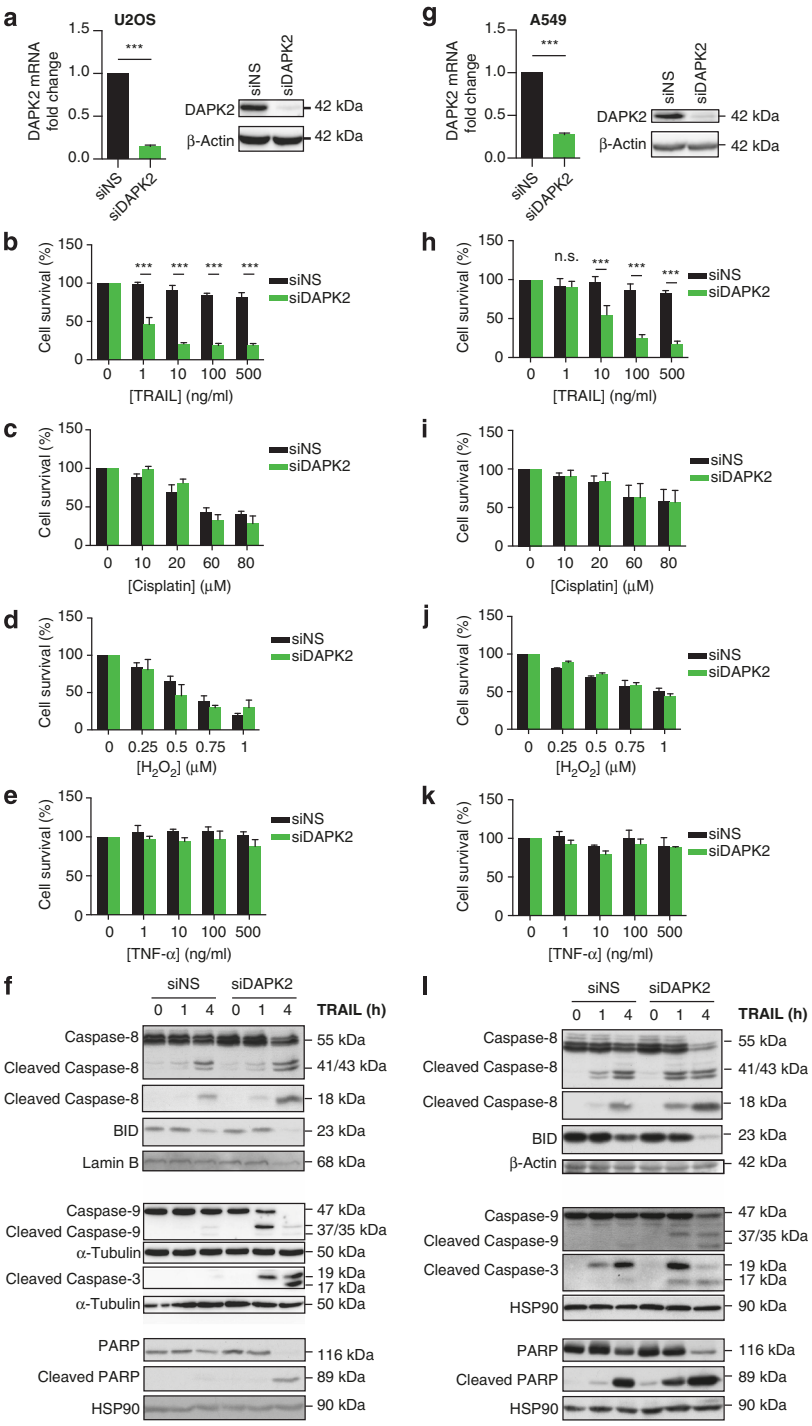

Figure 1 Knockdown of DAPK2 increases apoptotic signalling and sensitises resistant cancer cell lines to TRAIL-induced cell death. U2OS (**a**–**e**) and A549 (**g**–**k**) cells were transfected with either siNS or DAPK2 siRNA. Forty-eight hours after transfection knockdown efficiency was determined by SDS-PAGE/WB and qPCR (**a** and **g**). Data represent mean ± S.E.M. of three independent experiments. Statistical analyses were carried out using Student's *t*-test (paired, one-tailed) (***$P<0.005$). For cell survival assays (U2OS in **b**–**e** and A549 in **h**–**k**), cells were replated into 96-well plates at a density of 2×10^4 cells per well 24 h after siRNA transfection. The following day, cells were treated with the indicated concentrations of TRAIL (**b** and **h**), cisplatin (**c** and **i**), H_2O_2 (**d** and **j**) and TNF-α (**e** and **k**) for 24 h. Cells were then fixed using methanol and stained with crystal violet. Crystals were dissolved in 10% (v/v) acetic acid and quantified by measuring the absorbance at 595 nm. Values were normalised to the untreated samples. Data represent mean ± S.E.M. of three independent experiments performed in triplicate. Statistical analyses were carried out using two-way ANOVA test (***$P<0.005$). Molecular events of TRAIL-induced apoptosis (**f** and **l**) were assessed by SDS-PAGE/WB. Forty-eight hours after A549 and U2OS cells were transfected with siNS and siDAPK2, cells were treated with TRAIL (100 ng/ml) for the indicated time points. Activation of the extrinsic and intrinsic pathways were assessed by WB using cleavage of BID, caspase-8, caspase-9, caspase-3 and PARP as read-outs. Lamin B, α-tubulin and HSP90 served as loading controls

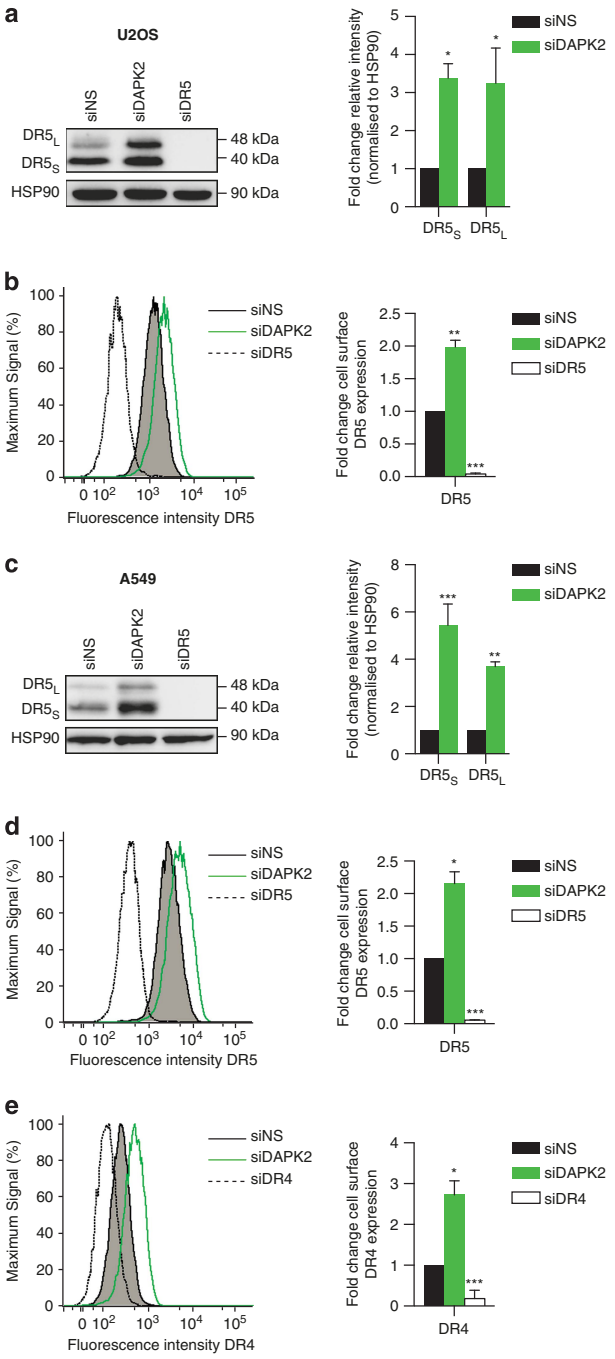

Figure 2 DAPK2 silencing leads to the upregulation of DR5 and DR4, key receptors for TRAIL. U2OS (**a** and **b**) and A549 (**c**–**e**) cells were transfected with either siNS or siDAPK2 for 48 h. Proteins were isolated and the level of DR expression was assessed by WB (**a** and **c**) or flow cytometry (**b**, **d** and **e**). Densitometric analyses of WBs were plotted as fold change of DR expression relative to the siNS control. Data represent mean ± S.E.M. of three independent experiments. Statistical analyses were carried out using one-way ANOVA test (*$P<0.05$, **$P<0.01$ and ***$P<0.005$). Cell surface expression quantification was carried out using geometric means of three independent experiments and plotted as fold change of surface expression. Statistical analysis was carried out using Student's *t*-test (paired, one-tailed) (*$P<0.05$ and **$P<0.01$)

had no impact on the induction or expression of c-FLIP (Supplementary Figure S4), effectively ruling out the induction of FLIP in the upregulation of DR5 and DR4, and, therefore, in the sensitisation process.

In the absence of DR5, DAPK2 can neither sensitise U2OS nor A549 cancer cells to TRAIL-induced apoptosis. The upregulation of DR5 may have been necessary but not sufficient for the sensitisation to TRAIL-induced apoptosis observed after silencing DAPK2 (Figure 1). To determine its relevance, knockdowns targeting concomitantly DAPK2 and DR5 were performed. As controls, cells were transfected with siNS, siDR5 or siBID. BID is part of a well-known amplification loop downstream of TRAIL, which in some cells is required to induce death. Cells were transfected with all permutations of siRNA, as indicated. Downregulation of DR5 *per se* did not impact on the susceptibility of U2OS or A549 to TRAIL-induced death (Figures 3a and c). In contrast, the downregulation of DAPK2-sensitised cells, as shown previously, provided that the expression of DR5 was not downregulated (compare cells transfected with siDAPK2/siNS *versus* siDAPK2/siDR5). However, silencing DR5 would almost certainly revert the phenotype observed when DAPK2 was silenced, as this is a key receptor for TRAIL. We, therefore, titrated siDR5 (Figure 3f), measured its impact on DR5 protein expression (Figures 3f and g) and established the concentration at which only the DAPK2 RNAi effect was reverted (1.25 nM). Co-transfection of U2OS cells with siDAPK2 (20 nM) and siDR5 (1.25 nM) impaired siDAPK2-mediated TRAIL sensitisation (Figure 3h), thus backing up the data shown in Figures 3a and c. This suggested that the upregulation of DR5 following silencing of DAPK2 was critical to sensitise resistant cells to apoptosis. A549 cells also express DR4 and double knockouts of DR4 and DAPK2 suggested that DR4 was partially required to sensitise them to TRAIL-induced apoptosis. The effect does not seem to be as pronounced as that seen when DR5 was silenced and, despite the trend shown, it was not statistically significant (Figure 3d). At higher concentrations of TRAIL, DR5 knockdown did not fully revert the phenotype, suggesting that in these cells DR4 might be engaged to overcome impaired DR5 expression (Figures 3c and d). Interestingly, double knockdown of DAPK2 and BID (Supplementary Figure S8) demonstrated that A549 cells required a BID amplification loop for sensitisation (Figure 3e), whereas U2OS cells did not (Figure 3b). Overexpression of BCL-X_L in U2OS cells further indicated that BID was not involved in the sensitisation to TRAIL achieved in U2OS cells after RNAi against DAPK2 (Supplementary Figure S5).

Increased DR5 expression following DAPK2 knockdown is transcriptionally regulated and not due to altered mRNA or protein stability. Having established that DR5 upregulation was a key event during DAPK2-mediated sensitisation to TRAIL-induced death in A549 and U2OS, we sought to establish within this context how DR5 expression was regulated. Using qPCR, we observed that silencing DAPK2 upregulated the levels of DR5 mRNA in both cell lines (Figures 4a and b). We then conducted classic

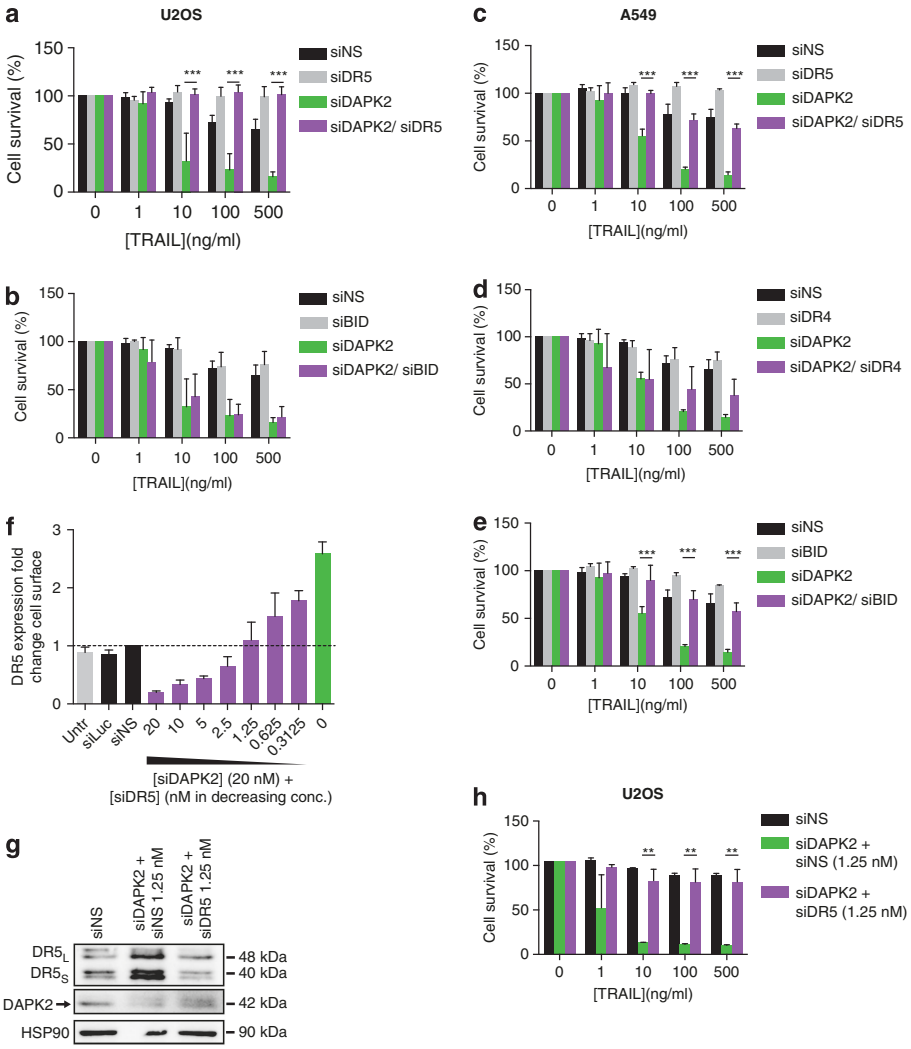

Figure 3 In the absence of DR5, siDAPK2 can neither sensitise U2OS nor A549 to TRAIL-induced apoptosis. Double knockdowns were carried out in U2OS (**a** and **b**) and A549 (**c**–**e**) cells. For this purpose, cells were transfected with 40 nM of the following siRNA mixtures: (**a** and **c**) siNS + siNS, siDR5 + siNS, siDAPK2 + siNS and siDR5 + siDAPK2 and (**b** and **e**) siNS + siBID and siBID + siDAPK2. A549 cells were also transfected with siNS + siDR4 and siDR4 + siDAPK2 (**d**). Twenty-four hours after transfection, cells were replated into 96-well plates at a density of 2×10^4 cells per well. The following day cells were treated with TRAIL for 24 h at the indicated final concentrations. Cells were methanol-fixed and stained with crystal violet. Staining was dissolved in acetic acid and quantified by measuring the absorbance at 595 nm. Values were normalised to the untreated samples. Data represent mean ± S.E.M. of three independent experiments performed in triplicate. Statistical analysis was carried out using two-way ANOVA test (*$P<0.05$, **$P<0.01$ and ***$P<0.005$). (**f**) U2OS cells were transfected with either siNS, siLuc (both controls for RNAi off-target effects), siDAPK2 or with siDAPK2 (20 nM) concomitantly with siDR5 (0.31–20 nM) for 48 h. DR5 expression was measured by flow cytometry and cell surface expression quantification carried out as before. Co-transfection of U2OS cells with 1.25 nM siDR5 and 20 nM siDAPK2 abolished siDAPK2-mediated DR5 induction. (**g**) The effect of co-transfection was also assessed using quantitative WB, which confirmed the results obtained by flow cytometry. (The shadow bands seen in the DAPK2 panel correspond to DR5, as the membrane was probed for with this antibody after being stripped from the anti-DR5 antibody.) (**h**) To assess the impact of reverting the siDAPK2-mediated effects on DR5 protein levels on cell survival after TRAIL, U2OS cells were transfected with either siDAPK2 (20 nM) and siNS (1.25 nM), or siDAPK2 (20 nM) and siDR5 (1.25 nM). Cells were replated into 96-well plates at a density of 2×10^4 cells per well 24 h after siRNA transfection and treated the following day with the indicated concentrations of TRAIL for another 24 h. Cell viability was assessed as in (**a**–**e**)

experiments with actinomycin D (Figure 4c), which blocks transcription or CHX (Figure 4f), which blocks translation and thus *de novo* protein synthesis. Neither DR5 mRNA stability (Figures 4d and e) nor the protein's half-life (Figures 4g and h) were significantly altered by reducing the expression levels of DAPK2. The data are therefore consistent with a transcriptional effect.

NF-κB is phosphorylated and transcriptionally active when DAPK2 is downregulated. DR5 is transcriptionally regulated by the tumour suppressor p53 and by NF-κB.[19] Upon silencing DAPK2, there was no change in p53 mRNA levels and both prostate cancer PC3 cells, which are p53 null, and bladder cancer T24 cells, which have an inactivating mutation in p53, can be sensitised to TRAIL by downregulating

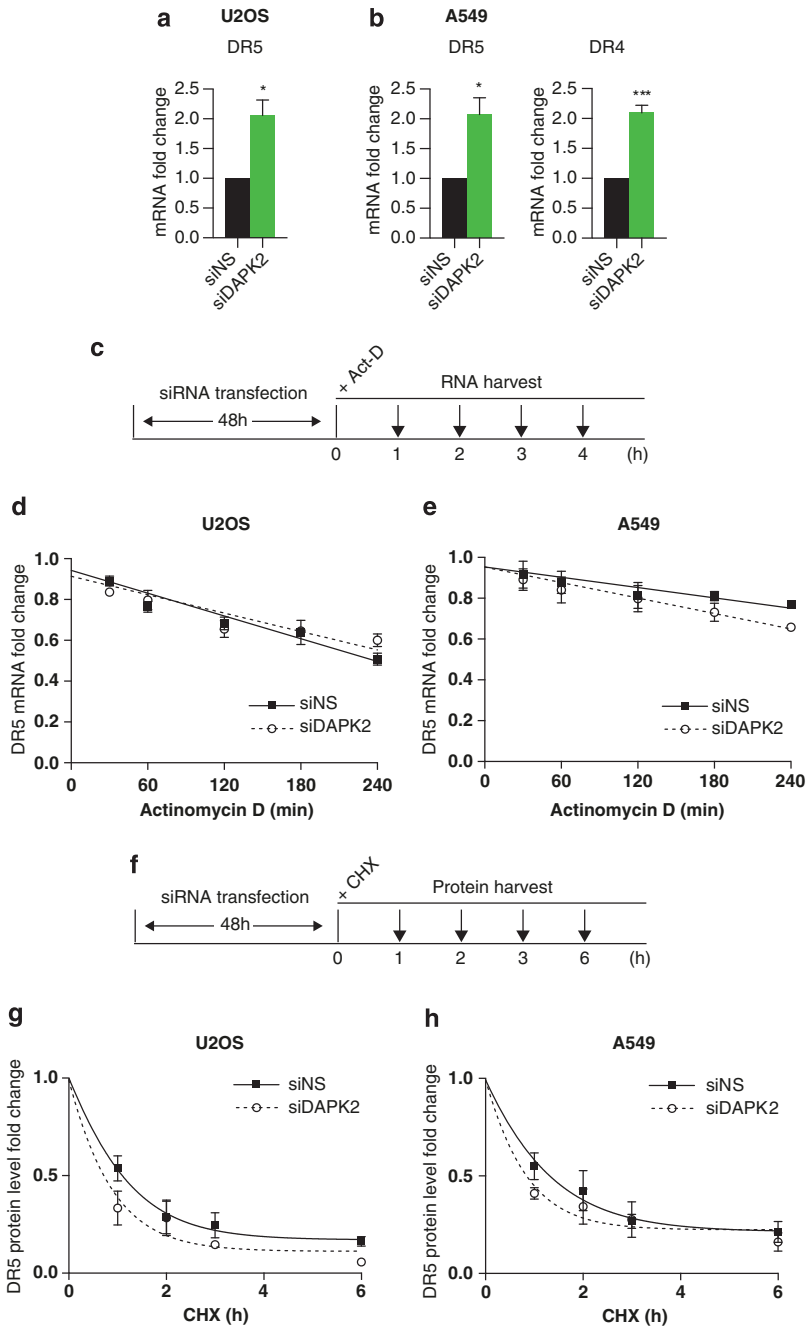

Figure 4 DR5 increased expression following the knockdown of DAPK2 is transcriptionally regulated and not due to alterations on mRNA or protein stability. U2OS (**a**, **d** and **g**) and A549 (**b**, **e** and **h**) cells were transfected with either siNS or siDAPK2. Forty-eight hours after transfection, RNA was harvested and DR5 (U2OS, A549) and DR4 mRNA (A549) levels were analysed by qPCR (**a** and **b**). The experimental procedure for analysing DR5 mRNA stability is represented schematically in (**c**). RNA stability was determined after RNAi against DAPK2 by inhibiting RNA synthesis with actinomycin D (Act-D) over the time periods indicated in the figure (**d** and **e**). Experimental procedures used to analyse DR5 protein stability are represented in (**f**). Protein synthesis was inhibited using cycloheximide (CHX) after 48 h transfection with siNS and siDAPK2 (**g** and **h**). DR5 protein levels were measured over time using quantitative WB followed by densitometric analysis, where each value was normalised to the corresponding HSP90 loading control. For these analyses, the DR5l isoform was used. The data represent the mean of three independent experiments ± S.E.M. and no significant changes were detected using a two-way ANOVA test

DAPK2 (Supplementary Figure S6). These data suggested that p53 was not necessary to sensitise TRAIL-resistant cells to TRAIL-induced apoptosis and we thus focused on NF-κB.

Protein expression analysis of NF-κB components by SDS-PAGE/qWB demonstrated that p100 and p52 (NF-κB2) were induced (Figures 5c and d), whereas p105 (NF-κB1) levels

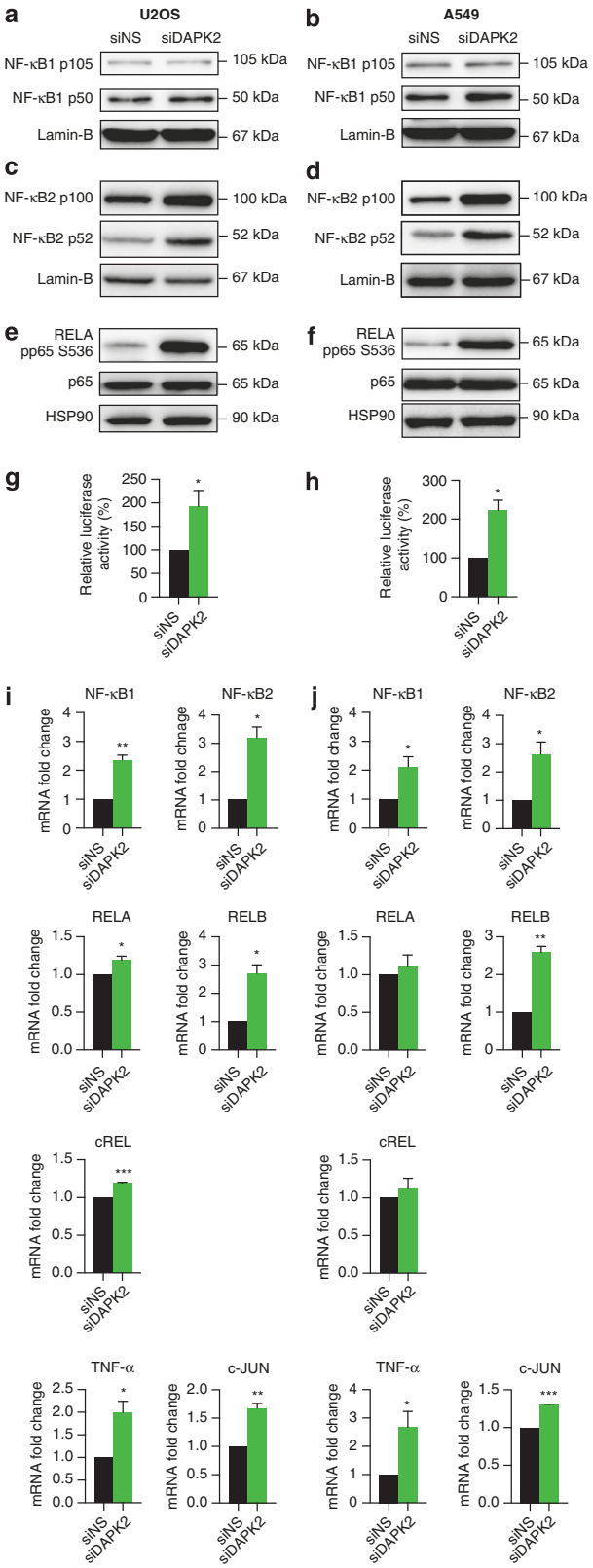

remained unchanged, with a slight increase in its proteolytic cleavage as demonstrated by a 1.5- and 2-fold increase in p50 expression in U2OS and A549 cells, respectively (Figures 5a and b). Importantly, RELA (p65/NF-κB3) was robustly phosphorylated on S536 in both cell lines (Figures 5e and f). This suggested that NF-κB was transcriptionally active when DAPK2 was downregulated, which was confirmed using luciferase reporter assays (Figures 5g and h). Further analysis of NF-κB target genes by qPCR, which also included induction of NF-κB components, further corroborated that NF-κB was activated following RNAi against DAPK2. Indeed, silencing DAPK2 led to robust induction of TNF-α, c-JUN, NF-κB1, NF-κB2 and RELB, and, although modest, to an increase in RELA and c-REL mRNA levels (Figures 5i and j). The data are thus consistent with NF-κB having a critical role in the aforementioned sensitisation.

NF-κB transcriptionally regulates DR5 expression and leads to sensitisation of osteosarcoma and non-small-cell lung cancer cells to TRAIL-induced apoptosis. The absence of DAPK2 in U2OS and A549 cells sensitised these otherwise resistant cells to TRAIL-induced cell death in what appeared to be an NF-κB-dependent manner. We hypothesised that if NF-κB activation was critical for the sensitisation, then knocking down its components should lead to a reversal of this phenotype. We, therefore, performed RNAi against NF-κB1, NF-κB2 or RELA with or without targeting DAPK2 concomitantly (Figure 6 and Supplementary Figure S8) and observed that U2OS cells with silenced DAPK2 became resistant to TRAIL again only when NF-κB1 was absent (Figures 6a and c–e). In contrast, A549 cells became resistant when either NF-κB1 or NF-κB2 was silenced (Figures 6f and h–j). Despite its strong phosphorylation, RELA was redundant and its absence *per se* did not prevent DAPK2 silencing from sensitising U2OS or A549 cells to TRAIL-induced apoptosis. Interestingly, silencing RELB was also without an effect on the sensitisation of U2OS cells to TRAIL-mediated death but it partially blocked sensitisation of A549 cells (Supplementary Figures S7 and S8). Taken together, these data indicate that DAPK2 may be a core, upstream, modulator of TRAIL signalling and that targeting it may affect multiple resistance pathways. We further

Figure 5 NF-κB is transcriptionally active upon knockdown of DAPK2. U2OS (**a**, **c**, **e**, **g** and **i**) and A549 (**b**, **d**, **f**, **h** and **j**) cells were transfected with either siNS or DAPK2 siRNA. Forty-eight hours after transfection, the expression levels of NF-κB1 (**a** and **b**), NF-κB2 (**c** and **d**), RELA pp65-S536 and RELA (**e** and **f**) was evaluated by qWB. Lamin-B and HSP90 served as loading controls. Blots shown are representative of three independent experiments yielding identical data. Luciferase assays were performed to assess the transcriptional activity of NF-κB in response to DAPK2 knockdown in U2OS (**g**) and A549 (**h**). RNAi-mediated DAPK2 depletion was induced 24 h before co-transfection with a pNF-κB-Luc reporter *Firefly* luciferase and a CMV promoter/*Renilla*-luciferase constructs. Twenty-four hours later, both *Firefly- and Renilla*-luciferase activities were measured. Data were analysed by normalising the *Firefly* luciferase to the luminescence obtained for the *Renilla*-luciferase construct. Data represent mean ± S.E.M. of three independent experiments performed in triplicate. Statistical analysis was carried out using Student's *t*-test (paired, two-tailed) (*$P<0.05$). The effect of DAPK2 depletion on the transcription of NF-κB target genes in U2OS (**i**) and A549 (**j**) cells was assessed by qPCR after RNAi against DAPK2, which was carried out as described previously. Statistical analysis was carried out using Student's *t*-test (paired, one-tailed) (*$P<0.05$, **$P<0.01$ and ***$P<0.005$)

analysed the importance of NF-κB activation in DR5 transcription using luciferase reporter assays (Figure 6k). The DR5 promoter was engaged upon cell transfection with siDAPK2 (Figures 6l and n), and this engagement was abrogated if the NF-κB binding site on this promoter was abolished (Figures 6k, m and o), indicating an absolute requirement for NF-κB in siDAPK2-mediated DR5 upregulation.

Discussion

As DAPK2 shares ~80% of homology to DAPK1 in the kinase domain but has no discernible death domain[12] (Supplementary Figure S1), we hypothesised that depending on the cellular content and expression levels of DAPK2 this kinase would work either as a pro- or antiapoptotic protein. Here, we have shown that RNAi-mediated depletion of DAPK2 (Figures 1a and g) specifically sensitises U2OS and A549 cells to TRAIL-induced apoptosis (Figures 1b and h), but not to a wide range of other apoptotic stimuli (Figures 1c–e and i–k).

Downregulation of DAPK2 leads to TRAIL-mediated activation of both extrinsic and intrinsic death pathways (Figure 7), and this is quicker in A549 cells than in U2OS cells (Figures 1f and l). Interestingly, activation of the intrinsic signalling appears dispensable in U2OS cells (Figure 3b and Supplementary Figure S5) but represents a crucial part of TRAIL-induced apoptosis upon DAPK2 depletion in A549 cells (Figure 3e). Many mechanisms of TRAIL resistance and strategies to overcome these involve the DISC complex, including downregulation of c-FLIP.[20] Inhibition of BCL-2/BCL-X_L has also been shown to resensitise cells to TRAIL-induced apoptosis.[21,22] There was no change on FLIP upon siDAPK2 (Supplementary Figure S4) and overexpressing BCL-X_L had no impact on DAPK2-mediated sensitisation of U2OS to TRAIL (Supplementary Figure S5), suggesting that these molecules are factors of TRAIL resistance that are unlikely to be surpassed by silencing DAPK2. Perhaps, the most prominent mechanism to overcome TRAIL resistance is the upregulation of its receptors, DR4 and/or DR5. DAPK2 depletion leads to a significant increase of DR5 protein in U2OS and A549 cells (Figures 2a–d). In A549 cells, it also increases the expression of DR4 (Figure 2e). Such receptor upregulation is essential for the sensitisation of U2OS and A549 cells to TRAIL-induced apoptosis following downregulation of DAPK2 (Figure 3).

DR expression can be induced by several chemicals, which can cause either their mRNA stabilisation[23] or transcriptional upregulation by various transcription factors.[19,24] DR induction leads to an increase in the number of receptor molecules on the cell surface, thus overcoming the threshold required to sensitise cells to TRAIL cytotoxicity. As U2OS cells do not express DR4 and silencing DAPK2 leads to the upregulation of DR5 in both U2OS and A549 cells (Figure 2), we focused on the regulation of DR5 induction/expression upon DAPK2 depletion. We showed that depletion of DAPK2 does not increase the mRNA (Figures 4c–e) or protein (Figures 4f–h) stability of DR5. However, DR5 and DR4 mRNAs are elevated after silencing DAPK2 (Figures 4a and b), suggesting that inhibition of DAPK2 leads to the transcriptional regulation of DRs.

DR5 is regulated by a variety of transcription factors such as p53 and NF-κB.[19] The fact that DAPK2 silencing can also sensitise p53-mutated (mt) T24 colon cancer cells and p53-null prostate cancer PC3 cells rules out the absolute requirement for p53 (Supplementary Figure S6). In contrast, activation of NF-κB (Figure 5) is absolutely essential (Figure 6 and Supplementary Figures S7 and S8). This is interesting as NF-κB has an ambiguous role in TRAIL signalling. For example, there are reports suggesting an antiapoptotic role for NF-κB, involving the upregulation of DcR1[25] or of antiapoptotic BCL-X_L,[26] whereas other reports suggest a proapoptotic role due to the induction of DR4 or DR5.[19,24] Interestingly, binding of TRAIL to DcR2 has been shown to activate NF-κB, which then initiates a negative feedback loop protecting cells from TRAIL-induced apoptosis.[27] Using an NF-κB reporter plasmid, we were able to show that NF-κB is transcriptionally active in both U2OS and A549 cells following DAPK2 knockdown (Figures 5g and h). RELA is phosphorylated on S536 (Figures 5e and f), and NF-κB1 and NF-κB2 are upregulated (Figures 5a–d) in response to DAPK2 knockdown. NF-κB signalling is highly complex and different members assemble in different dimmers, which then participate in canonical and non-canonical signalling pathways. Canonical pathways tend to involve NF-κB1 and RELA, whereas the non-canonical pathway is thought to involve primarily NF-κB2 and RELB. This distinction is not absolute and a great deal of signalling specificity is determined by the cell type and cellular environment.[28] Indeed, NF-κB1, NF-κB2 and RELB were robustly induced in response to RNAi against DAPK2 both in U2OS and A549 cells, and there was a hint of an induction of RELA and c-REL (Figures 5i and j). To unravel the complex role of NF-κB in TRAIL signalling, we performed double-knockdown experiments (Figure 6). By analysing the effect of TRAIL on U2OS and A549 cells transfected with siDAPK2 concomitantly with siRNAs directed against NF-κB family members, we identified NF-κB1 as key molecules responsible for sensitisation to TRAIL-induced apoptosis in response to DAPK2 depletion. Interestingly, in A549 cells, knockdown of NF-κB2 and RELB in combination with DAPK2 also resulted in a partial rescue (Figure 6i and Supplementary Figure S7b). It thus appears that U2OS cells require mainly the activation of the NF-κB canonical pathway, whereas A549 cells require activation of both the canonical and non-canonical pathways. It is still unclear why this is but it is fair to assume that, due to distinct cellular environments in these two cell lines, silencing DAPK2 leads to the formation of different NF-κB dimers, which are nevertheless capable of resulting in an identical biologic response, namely upregulation of DR5. The fact that A549 seem to also require BID to be fully sensitised to TRAIL after DAPK2 silencing may be related to the partial requirement for NF-κB2/RELB. It is also possible that NF-κB2 and/or RELB are required to induce DR4, which is not expressed in U2OS cells. Using DR5 promoter luciferase constructs with either wild-type (wt) or NF-κB-mt consensus sites, we established the necessity of NF-κB as a transcription factor required for the induction of DR5 in response to DAPK2 depletion. Recently, Yoo *et al*.[29] suggested that DAPK1 could function as a repressor for NF-κB activation.[29] Additionally, NF-κB activation

downstream of T-cell receptor signalling is increased in DAPK1-knockout cells.[30] As all DAPKs are thought to form multiprotein complexes,[31] the activation of NF-κB proteins upon DAPK2 knockdown is likely to be caused by at least some of the same molecular events described for DAPK1. Different NF-κB family members can thus differentially regulate TRAIL receptors, which is reflected by sensitisation to TRAIL following DAPK2 silencing being dependent on NF-κB1 in U2OS and A549 cells and by the additional requirement of NF-κB2 and RELB in A549 cells.

The question thus remains how downregulating DAPK2 leads to the activation of NF-κB (Figure 5), vital to sensitising resistant cells to TRAIL-mediated death (Figure 6). The

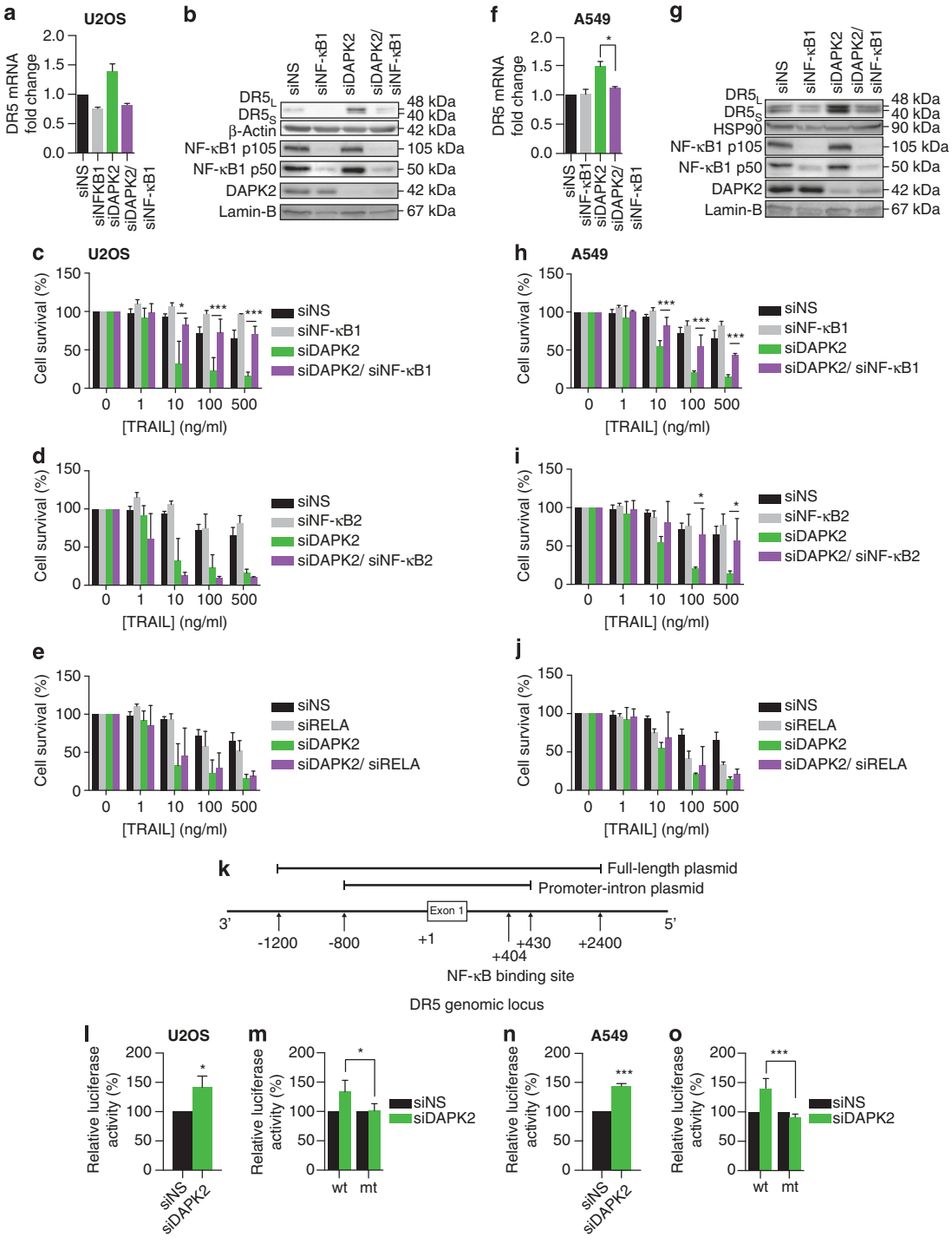

involvement of NF-κB in TRAIL signalling is highly cell context-dependent and DAPK2 likely regulates an upstream component of NF-κB signalling. Such a component may be the NF-κB-negative regulator, IκB. Indeed, silencing DAPK2 leads to its disappearance (not shown), which is probably the main cause for the activation of NF-κB. This then poses the question of why IκB is being degraded and the most immediate hypothesis is that it is being phosphorylated by IKKs, coupled to the TRAIL receptor complex. Such coupling may occur via RIP and/or TRADD.[32] Perhaps, DAPK2

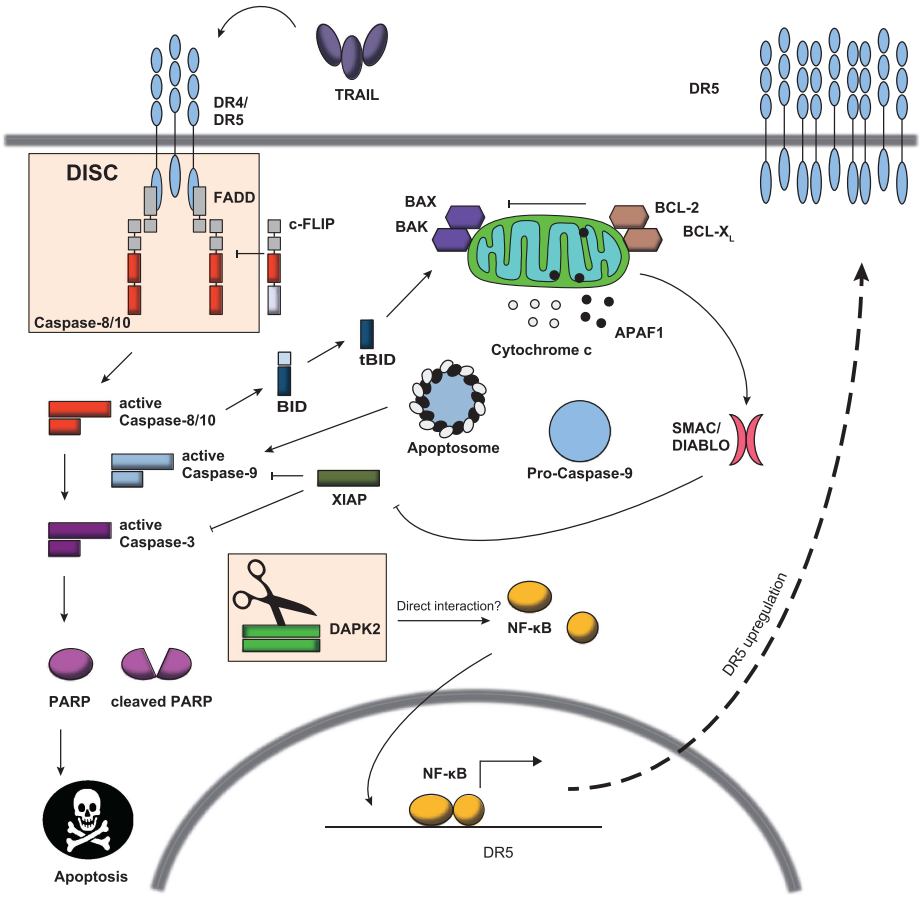

Figure 7 DAPK2 is a novel modulator of TRAIL-induced apoptosis. Death receptor ligation by TRAIL primarily activates the extrinsic apoptotic pathway. TRAIL binding induces DISC formation. Activation of the initiator caspases-8/10 leads to proteolytic cleavage and activation of downstream effector caspases such as caspase-3, which eventually culminates in apoptosis. TRAIL can also activate the intrinsic apoptotic pathway via BID. This involves depolarisation of the mitochondrial membrane potential via BAK and BAX, followed by cytochrome *c* release and downstream activation of caspase-9. Resistance mechanisms can occur at many different stages of the cascade. c-FLIP can inhibit the activation of initiator caspases within the extrinsic pathway, XIAP can block the action of effector caspases and antiapoptotic members of the BCL-2 family, such as BCL-X_L and BCL-2, which are known inhibitors of the intrinsic apoptosis pathway. Depletion of DAPK2 triggers the activation of NF-κB and leads to NF-κB-mediated induction of DR5 mRNA and to an increase in DR5 protein levels. The increase in the number of DR5 molecules presumably overcomes the inhibition threshold and lead to the resensitisation of cancer cells to TRAIL-induced apoptosis

Figure 6 The transcription factor NF-κB is a critical component of DR5 expression and is necessary for the sensitisation to TRAIL-induced cell death seen after DAPK2 silencing. U2OS (**a**–**e**, **l** and **m**) and A549 (**f**–**j**, **n** and **o**) cells were transfected with either siNS or the following siRNA 1 : 1 mixes: siNF-κB1 + siNS, siDAPK2 + siNS and siDAPK2 + NF-κB1 (40 nM in total). Forty-eight hours after transfection, RNA and proteins were isolated and levels of DR5 mRNA (**a** and **f**) and protein were measured (**b** and **g**). For mRNA, data represent mean ± S.E.M. of two independent experiments in U2OS cells (**a**) and three independent experiments in A549 (**f**). Statistical analyses were carried out using Student's *t*-test (paired, two-tailed) (*$P<0.05$). For protein, DR5 levels and knockdown verification were achieved with qWB, using lamin B as a loading control. Cell survival analyses in response to TRAIL after the double knockdowns were carried out in U2OS and A549 cells that were transfected with either siNS or the following siRNA 1:1 mixes: siNF-κB1 + siNS, siDAPK2 + siNS, siDAPK2 + NF-κB1 (**c** and **h**), siNS + siNF-κB2, siDAPK2 + siNF-κB2 (**d** and **i**) and siNS + siRELA, siDAPK2 + siRELA (**e** and **j**). Twenty-four hours after transfection, cells were replated into 96-well plates at a density of 2×10^4 cells per well and treated with TRAIL for 24 h at the indicated final concentrations the day after. Crystal violet viability assays were carried out as described previously. Values were normalised to the untreated samples. Data represent mean ± S.E.M. of three independent experiments performed in triplicate. Statistical analysis was carried out using two-way ANOVA test (*$P<0.05$, **$P<0.01$ and ***$P<0.005$). Plasmids used for DR5 promoter analyses are represented in (**k**). As before, DAPK2 depletion was initiated 24 h before co-transfection with the DR5 full-length promoter (**l** and **n**), DR5 promoter-intron wt or NF-κB-mt (**m** and **o**) plasmid *Firefly*-luciferase pGL3 construct and a CMV promoter/*Renilla*-luciferase construct. Twenty-four hours later, both *Firefly- and Renilla*-luciferase activities were measured. Data were analysed by normalising the *Firefly* luciferase to the luminescence obtained for the *Renilla*-luciferase activity. Data represent mean ± S.E.M. of three independent experiments. Statistical analysis was carried out using Student's *t*-test (paired, two-tailed) (*$P<0.05$ and ***$P<0.005$)

interacts with the TRAIL receptor complex and it acts as a 'plug' that stops cells from 'inadvertently' succumbing to TRAIL. Removing DAPK2 may free binding sites necessary to couple the pathway to the initiator caspases and to NF-κB. It is also possible that the interaction between NF-κB signalling components and DAPK2 occurs in the cytoplasm rather than at the membrane with IKKs and IκB being the most likely interactors. DAPK2 may alternatively repress NF-κB by, for example, protecting the cell from cellular stress, known to activate NF-κB. Whichever way DAPK2 silencing leads to NF-κB activation, NF-κB activation *per se*, in response to a classic NF-κB activator such as TNF-α, leads to the degradation of DAPK2 (not shown). What is intriguing is why the output of the TRAIL stimulus is death, as NF-κB also leads to the activation of key survival genes. The balance must thus rest on the faster caspase activation observed following DAPK2 silencing and on the NF-κB-mediated induction of DR5 and/or DR4. Clearly, our understanding of how DAPK2 and NF-κB interact is in its infancy and much remains to be understood.

Overall, our work suggests that inhibition of DAPK2 in combination with TRAIL or TRAIL mimics may provide an alternative, novel, approach to overcome TRAIL resistance via activating proapoptotic functions of the NF-κB response, and may ultimately open new avenues for treatments of certain types of malignancies.

Materials and Methods

Cell culture. U2OS and A549 cells were grown in Dulbecco's modified Eagle's medium supplemented with 10% (v/v) foetal calf serum (FirstLink, Wolverhampton, UK), 2 mM L-glutamine, 50 U/ml penicillin and 50 μg/ml streptomycin (Sigma-Aldrich, St. Louis, MO, USA) in a humidified atmosphere of 10% CO_2 at 37 °C. TRAIL and TNF-α were from PeproTech (London, UK) and all other chemicals were from Sigma-Aldrich.

Antibodies. Anti-DAPK2 was purchased from Epitomics (Burlingame, CA, USA). Antibodies against DR5, NF-κB1 (p50, p105), NF-κB2 (p52, p100), RELA (p65), phosphorylated RELA (pp65-S536), BID, PARP, BCL-X_L, caspase-3, caspase-8 and caspase-9 were bought from Cell Signaling Technology (Cambridge, UK). The antibodies against β-actin, α-tubulin and Flag were obtained from Sigma-Aldrich and the one against HSP90 was from NeoMarkers (Fremont, CA, USA). The antibody against lamin B was from Santa Cruz Biotechnology (Santa Cruz, CA, USA). Secondary antibodies were from Dako (Glostrup, Denmark). For flow cytometry, the antibody against DR5 was from eBioscience (Hatfield, UK) and the one against DR4 was from Abcam (Cambridge, UK).

RNAi. RNAi was performed as described before[16] using Lipofectamine RNAiMax (Invitrogen, Paisley, UK). Briefly, cells plated at 2.5×10^5 in 6-well plates were left untransfected or were transfected with either 20 nM AllStars negative control siRNA (Qiagen, Hilden, Germany) or 20 nM siGENOME pooled siRNA (Dharmacon, Lafayette, CO, USA) to DAPK2 (oligonucleotides 3 and 4), DR4, DR5, BID, NF-κB1, NF-κB2 and RELA (pool of four oligonucleotides) (Supplementary Table SI). A custom-made siDAPK-3′-UTR oligonucleotide from Dharmacon and another 3′-UTR-targeting siDAPK2 oligonucleotide from Qiagen (Hs_DAPK2_11 FlexiTube siRNA) were also used. For double knockdowns, equal amounts of AllStars negative control and/or targeting siRNA were mixed to a final concentration of 40 nM. To avoid variability in cell numbers, 24 h after transfection, cells were counted and replated at identical numbers. Cells were then treated and analysed as described in the figures using the methods described below.

Cell survival assays. Cells were plated in triplicate in 96-well plates (2×10^4 cells per well) and treated the next day with different concentrations of TRAIL, cisplatin, H_2O_2 or TNF-α for 24 h, as indicated in the figures. Cell survival was assessed using crystal violet staining. For that purpose, cells were washed in phosphate-buffered saline (PBS), and fixed and stained with 0.5% (w/v) crystal violet in 25% (v/v) methanol for 30 min. The plates were then thoroughly washed with water, dried and the dried dye dissolved in 10% (v/v) acetic acid. The absorbance was measured at 595 nm in a spectrophotometer. Apoptosis was also determined by studying cell cycle profiles: cells were washed two times with PBS and fixed with ice-cold 70% (v/v) ethanol for 30 min. After two additional washing steps, cells were incubated with 20 μg/ml ribonuclease A (Qiagen) and stained with 50 μg/ml PI for 15 min in the dark. Cells were processed using a flow cytometer and the data were analysed using FlowJo version 8.8.7 (Tree Star Inc., Ashland, OR, USA).

Western blotting. Proteins were extracted using radioimmunoprecipitation assay buffer (RIPA; 50 mM Tris-HCl (pH 7.4), 0.5% (v/v) NP-40, 150 mM NaCl, 1 mM EDTA, 1 mM Na_3VO_4 and 'cOmplete and Mini, EDTA-free protease inhibitor cocktail', the latter used as instructed by the manufacturer; Roche, Mannheim, Germany). Concentrations were determined using a Bradford assay according to the manufacturer's instructions. They were then analysed by SDS-PAGE/qWB. Membranes were blocked and secondary antibodies diluted in 5% (w/v) non-fat milk/TBS-Tween-20 and primary antibodies were dissolved in 5% (w/v) BSA/TBS-Tween-20. WBs were analysed using the quantitative luminescence system Fusion SOLO (Analis, Ghent, Belgium). Densitometric analysis was performed using Image Studio Lite software (LI-COR Biosciences, Lincoln, NE, USA) (http: //www.licor.com/islite).

Flow cytometry. Cells were incubated with anti-DR4-FITC or anti-DR5-PE for 1 h at 4 °C, washed five times with cold PBS and fixed with 1% (w/v) *p*-formaldehyde. Cells were analysed using a FACS Canto (Becton Dickinson, Franklin Lakes, NJ, USA) and data were analysed with FlowJo Version 8.8.7. Geometric means were used for the analyses.[16]

Real-time PCR. Gene expression analysis was carried out by quantitative two-step reverse transcription PCR. Reverse transcription was performed using total RNA and the High Capacity cDNA Reverse Transcription kit (Life Technologies, Carlsbad, CA, USA), using random hexamers. qPCR was carried out using the Fast SYBR Green Master Mix (Applied Biosystems, Foster City, CA, USA) with specific primer pairs (Supplementary Table SII). For each target mRNA analysed, 2.5 μl of Fast SYBR Green Master Mix, 0.5 μM of each primer pair and 2 μl of cDNA in deionised water (5 ng/μl) were mixed in 384-well plates in duplicates using Matrix Equalizer Electronic Multichannel Pipetters (Thermo Fisher Scientific, Waltham, MA, USA). qPCR was carried out on an ABI PRISM 7900HT (Applied Biosystems) using the following settings: initial activation of 20 s at 95 °C, 40 cycles; denaturation for 1 min at 95 °C; annealing/extension for 20 s at 60 °C; final melting curve was carried out for 15 s at 95 °C and then 15 s at 60 °C. Quantification of target messages was performed using qbasePLUS software (Biogazelle, Ghent, Belgium). *HPRT* and *GAPDH* were the reference genes used for normalisation.

Co-transfection of adherent cells with siRNA and DNA. Co-transfection was performed using Attractene transfection reagent (Qiagen). Briefly, cells plated at density of 4×10^5 in 6-well plates were transfected with either 40 nM AllStars negative control siRNA or 40 nM siDAPK2 and 1.2 μg DNA of empty vector control, or pCDNA3.BCL-X_L plasmid, which was kindly provided by Dr. Ingram Iaccarino (Institute of Human Genetics, University Hospital Schleswig-Holstein, Kiel, Germany). Protein expression was analysed by qWB and cell death using crystal violet assays.

Plasmids. The DR5 full-length promoter pGL3 construct and DR5 promoter-intron wt and NF-κB-mt pGL3 constructs were kindly provided by Professor Spencer Gibson (University of Manitoba, Winnipeg, MB, Canada). pNF-κB-Luc reporter vector was from Clontech (Saint-Germain-en-Laye, France). The BCL-X_L expression plasmid was a gift from Dr. Ingram Iaccarino (Institute of Human Genetics, University Hospital Schleswig-Holstein, Kiel, Germany).

Luciferase assays. Cells were transfected with siRNA oligonucleotides as described above. Twenty-four hours later, cells were co-transfected with 100 ng of pNF-κB-Luc, DR5 full-length promoter *Firefly*-luciferase pGL3, DR5 promoter-intron wt *Firefly*-luciferase pGL3 or DR5 promoter-intron NF-κB-mt *Firefly*-luciferase pGL3 constructs and 10 ng of CMV promoter *Renilla*-luciferase

pRL construct using Attractene transfection reagent (Qiagen). The day after, both *Firefly*- and *Renilla*-luciferase activities were quantified using the Dual-Glo Luciferase Assay System (Promega, Madison, WI, USA) according to the manufacturer's instructions. Luminescence was detected using a PHERAstar Plus plate reader (BMG Labtech, Ortenberg, Germany). The measured luminescence for *Firefly*-luciferase activity was normalised to that of *Renilla* luciferase.

mRNA and protein stability. Cells were transfected with siRNA oligonucleotides as before. Forty-eight hours after transfection cells were treated with 5 μg/ml actinomycin D for 1–4 h. Subsequently, RNA was isolated using an RNeasy Mini Kit (Qiagen) following the manufacturer's instructions. Gene expression analysis was performed by qPCR as described before, using *HPRT* and *GAPDH* as housekeeping genes. For protein stability, cells were incubated with CHX for 2, 4 or 6 h and protein measured by SDS-PAGE/qWB using the Fusion SOLO quantitative luminescence system (PEQLAB, Erlangen, Germany).

Statistical analysis. Mean ± S.E.M. of three independent experiments were calculated. Statistical tests were carried out as indicated in each figure legend using GraphPad Prism (GraphPad Software Inc., San Diego, CA, USA).

Conflict of Interest

The authors declare no conflict of interest.

Acknowledgements. We are grateful to Dr. Spencer Gibson (University of Manitoba, USA) for wild-type and NF-κB-mt DR5-luciferase constructs, Dr. Ingram Iaccarino (Institute of Human Genetics, University Hospital Schleswig-Holstein, Kiel, Germany) for the BCL-X_L expression vector and to Andrew M. Smart for many very fruitful discussions. Within Imperial College London, we are indebted to Dr. Charlotte Bevan, her research team and Dr. Olivier Pardo for helpful discussions, and Dr. Anna Maria Tommasi for technical help. Cancer Research UK funded CRS and APC-P (C37990/A12991) at the Imperial Cancer Research UK Centre, and also AVF and APC-P (CA5775); CEM was funded by MRC and Johnson & Johnson (CASE studentship G1000390); MBM was funded by the ERASMUS programme through a student mobility placement studentship (DE-2013-ERA/MOB-KonsZuV01-CP6); CRS, AVF, CRC, MJS and APC-P were additionally funded by Cancer Treatment and Research Trust (CTRT) and APC-P is the recipient of an Elsie Widdowson Fellowship. The funders had no role in study design, data collection and analysis, decision to publish or preparation of the manuscript.

Author contributions

APC-P and CRS designed the study and wrote the manuscript; CRS, AVF, SST, MLG, MBM and CEM conducted the experiments; all authors analysed the data and commented on the manuscript.

1. Wiley SR, Schooley K, Smolak PJ, Din WS, Huang CP, Nicholl JK *et al.* Identification and characterization of a new member of the TNF family that induces apoptosis. *Immunity* 1995; **3**: 673–682.
2. Pitti RM, Marsters SA, Ruppert S, Donahue CJ, Moore A, Ashkenazi A. Induction of apoptosis by Apo-2 ligand, a new member of the tumor necrosis factor cytokine family. *J Biol Chem* 1996; **271**: 12687–12690.
3. Falschlehner C, Ganten TM, Koschny R, Schaefer U, Walczak H. TRAIL and other TRAIL receptor agonists as novel cancer therapeutics. *Adv Exp Med Biol* 2009; **647**: 195–206.
4. Walczak H, Miller RE, Ariail K, Gliniak B, Griffith TS, Kubin M *et al.* Tumoricidal activity of tumor necrosis factor-related apoptosis-inducing ligand in vivo. *Nat Med* 1999; **5**: 157–163.
5. Walczak H, Degli-Esposti MA, Johnson RS, Smolak PJ, Waugh JY, Boiani N *et al.* TRAIL-R2: a novel apoptosis-mediating receptor for TRAIL. *EMBO J* 1997; **16**: 5386–5397.
6. Pan G, O'Rourke K, Chinnaiyan AM, Gentz R, Ebner R, Ni J *et al.* The receptor for the cytotoxic ligand TRAIL. *Science* 1997; **276**: 111–113.
7. Gonzalvez F, Ashkenazi A. New insights into apoptosis signaling by Apo2L/TRAIL. *Oncogene* 2010; **29**: 4752–4765.
8. Screaton GR, Mongkolsapaya J, Xu XN, Cowper AE, McMichael AJ, JI Bell. TRICK2 a new alternatively spliced receptor that transduces the cytotoxic signal from TRAIL. *Curr Biol* 1997; **7**: 693–696.
9. Mellier G, Huang S, Shenoy K, Pervaiz S. TRAILing death in cancer. *Mol Aspects Med* 2010; **31**: 93–112.
10. Bialik S, Kimchi A. The death-associated protein kinases: structure, function, and beyond. *Annu Rev Biochemis* 2006; **75**: 189–210.
11. Raval A, Tanner SM, Byrd JC, Angerman EB, Perko JD, Chen SS *et al.* Downregulation of death-associated protein kinase 1 (DAPK1) in chronic lymphocytic leukemia. *Cell* 2007; **129**: 879–890.
12. Kawai T, Nomura F, Hoshino K, Copeland NG, Gilbert DJ, Jenkins NA *et al.* Death-associated protein kinase 2 is a new calcium/calmodulin-dependent protein kinase that signals apoptosis through its catalytic activity. *Oncogene* 1999; **18**: 3471–3480.
13. Inbal B, Shani G, Cohen O, Kissil JL, Kimchi A. Death-associated protein kinase-related protein 1, a novel serine/threonine kinase involved in apoptosis. *Mol Cell Biol* 2000; **20**: 1044–1054.
14. Inbal B, Bialik S, Sabanay I, Shani G, Kimchi A. DAP kinase and DRP-1 mediate membrane blebbing and the formation of autophagic vesicles during programmed cell death. *J Cell Biol* 2002; **157**: 455–468.
15. Bonito NA, Drechsler J, Stoecker S, Carmo CR, Seckl MJ, Hermanns HM *et al.* Control of gp130 expression by the mitogen-activated protein kinase ERK2. *Oncogene* 2014; **33**: 2255–2263.
16. Watling D, Carmo CR, Kerr IM, Costa-Pereira AP. Multiple kinases in the interferon-gamma response. *Proc Natl Acad Sci USA* 2008; **105**: 6051–6056.
17. Degli-Esposti MA, Smolak PJ, Walczak H, Waugh J, Huang CP, DuBose RF *et al.* Cloning and characterization of TRAIL-R3, a novel member of the emerging TRAIL receptor family. *J Exp Med* 1997; **186**: 1165–1170.
18. Emery JG, McDonnell P, Burke MB, Deen KC, Lyn S, Silverman C *et al.* Osteoprotegerin is a receptor for the cytotoxic ligand TRAIL. *J Biol Chem* 1998; **273**: 14363–14367.
19. Shetty S, Graham BA, Brown JG, Hu X, Vegh-Yarema N, Harding G *et al.* Transcription factor NF-kappaB differentially regulates death receptor 5 expression involving histone deacetylase 1. *Mol Cell Biol* 2005; **25**: 5404–5416.
20. Ganten TM, Haas TL, Sykora J, Stahl H, Sprick MR, Fas SC *et al.* Enhanced caspase-8 recruitment to and activation at the DISC is critical for sensitisation of human hepatocellular carcinoma cells to TRAIL-induced apoptosis by chemotherapeutic drugs. *Cell Death Differen* 2004; **11**(Suppl 1): S86–S96.
21. Sinicrope FA, Penington RC, Tang XM. Tumor necrosis factor-related apoptosis-inducing ligand-induced apoptosis is inhibited by Bcl-2 but restored by the small molecule Bcl-2 inhibitor, HA 14-1, in human colon cancer cells. *Clin Cancer Res* 2004; **10**: 8284–8292.
22. Huang S, Sinicrope FA. BH3 mimetic ABT-737 potentiates TRAIL-mediated apoptotic signaling by unsequestering Bim and Bak in human pancreatic cancer cells. *Cancer Res* 2008; **68**: 2944–2951.
23. Kandasamy K, Kraft AS. Proteasome inhibitor PS-341 (VELCADE) induces stabilization of the TRAIL receptor DR5 mRNA through the 3'-untranslated region. *Mol Cancer Therap* 2008; **7**: 1091–1100.
24. Mendoza FJ, Ishdorj G, Hu X, Gibson SB. Death receptor-4 (DR4) expression is regulated by transcription factor NF-kappaB in response to etoposide treatment. *Apoptosis* 2008; **13**: 756–770.
25. Bernard D, Quatannens B, Vandenbunder B, Abbadie C. Rel/NF-kappaB transcription factors protect against tumor necrosis factor (TNF)-related apoptosis-inducing ligand (TRAIL)-induced apoptosis by up-regulating the TRAIL decoy receptor DcR1. *J Biol Chem* 2001; **276**: 27322–27328.
26. Zender L, Hutker S, Mundt B, Waltemathe M, Klein C, Trautwein C *et al.* NFkappaB-mediated upregulation of bcl-xl restrains TRAIL-mediated apoptosis in murine viral hepatitis. *Hepatology* 2005; **41**: 280–288.
27. Degli-Esposti MA, Dougall WC, Smolak PJ, Waugh JY, Smith CA, Goodwin RG. The novel receptor TRAIL-R4 induces NF-kappaB and protects against TRAIL-mediated apoptosis, yet retains an incomplete death domain. *Immunity* 1997; **7**: 813–820.
28. Tergaonkar V. NFkappaB pathway: a good signaling paradigm and therapeutic target. *Int J Bioch Cell Biol* 2006; **38**: 1647–1653.
29. Yoo HJ, Byun HJ, Kim BR, Lee KH, Park SY, Rho SB. DAPk1 inhibits NF-kappaB activation through TNF-alpha and INF-gamma-induced apoptosis. *Cell Signal* 2012; **24**: 1471–1477.
30. Chuang YT, Fang LW, Lin-Feng MH, Chen RH, Lai MZ. The tumor suppressor death-associated protein kinase targets to TCR-stimulated NF-kappa B activation. *J Immunol* 2008; **180**: 3238–3249.
31. Gozuacik D, Kimchi A. DAPk protein family and cancer. *Autophagy* 2006; **2**: 74–79.
32. Sprick MR, Weigand MA, Rieser E, Rauch CT, Juo P, Blenis J *et al.* FADD/MORT1 and caspase-8 are recruited to TRAIL receptors 1 and 2 and are essential for apoptosis mediated by TRAIL receptor 2. *Immunity* 2000; **12**: 599–609.

Supplementary Information accompanies this paper on Cell Death and Differentiation website (http://www.nature.com/cdd)

OPEN

Citation: Cell Death and Disease (2015) 6, e●; doi:10.1038/cddis.2015.31

www.nature.com/cddis

DAPK2 regulates oxidative stress in cancer cells by preserving mitochondrial function

CR Schlegel[1], ML Georgiou[1], MB Misterek[2], S Stöcker[3], ER Chater[1], CE Munro[1], OE Pardo[1], MJ Seckl[1] and AP Costa-Pereira*[1]

Death-associated protein kinase (DAPK) 2 is a serine/threonine kinase that belongs to the DAPK family. Although it shows significant structural differences from DAPK1, the founding member of this protein family, DAPK2 is also thought to be a putative tumour suppressor. Like DAPK1, it has been implicated in programmed cell death, the regulation of autophagy and diverse developmental processes. In contrast to DAPK1, however, few mechanistic studies have been carried out on DAPK2 and the majority of these have made use of tagged DAPK2, which almost invariably leads to overexpression of the protein. As a consequence, physiological roles of this kinase are still poorly understood. Using two genetically distinct cancer cell lines as models, we have identified a new role for DAPK2 in the regulation of mitochondrial integrity. RNA interference-mediated depletion of DAPK2 leads to fundamental metabolic changes, including significantly decreased rate of oxidative phosphorylation in combination with overall destabilised mitochondrial membrane potential. This phenotype is further corroborated by an increase in the production of mitochondrial superoxide anions and increased oxidative stress. This then leads to the activation of classical stress-activated kinases such as ERK, JNK and p38, which is observed on DAPK2 genetic ablation. Interestingly, the generation of oxidative stress is further enhanced on overexpression of a kinase-dead DAPK2 mutant indicating that it is the kinase domain of DAPK2 that is important to maintain mitochondrial integrity and, by inference, for cellular metabolism.
Cell Death and Disease (2015) **6,** e●; doi:10.1038/cddis.2015.31; published online xx xxx 2015

Death-associated protein kinase (DAPK) 2 shares a high level of homology within its kinase domain with the other two DAPK family members, DAPK1 (DAPk) and DAPK3 (ZIPK/DLK). Since the identification of DAPK1 by the Kimchi and co-workers[1] numerous studies have shown that DAPK1 functions as a tumour suppressor, is linked to key events in autophagy and is involved in mitochondrial maintenance[2] and metabolism.[3] DAPK2, which was characterised in 1999,[4] is significantly smaller than DAPK1, and it lacks ankyrin repeats, the cytoskeletal binding domain and the death domain, all of which are part of DAPK1's unique structure.[1] Several functions have been ascribed to DAPK2 and they often coincide with those of DAPK1. Like DAPK1, DAPK2 is also involved in the formation of autophagic vesicles,[5,6] modulation of receptor induced cell death[7–9] and several modes of intrinsic apoptotic cell death.[6] While epigenetic silencing of DAPK1 has been reported in many different human cancers,[10,11] DAPK2 appears to be silenced mainly in haematological disorders,[12] although it has been shown to modulate TRAIL-induced apoptosis in several cancer cell lines of non-haematological origin.[9] Most approaches used for studying the role of DAPK2 used tagged DAPK2 and it is, therefore, still unclear whether these functions are also carried out by the native protein, expressed at much lower, endogenous, levels.

DAPK1 has been shown to regulate mitochondrial integrity and to modulate the mitochondrial membrane potential[2] but, to the best of our knowledge, no work has been carried out in this respect with regard to DAPK2. Since DAPK1 and DAPK2 appear to share many functions and both are thought to reside, at least partially, in the mitochondria, we hypothesised that DAPK2 depletion regulated mitochondrial metabolism. Mitochondrial dysfunction is characterised by the induction of reactive oxygen species (ROS) in the cell.[13] Ultimately, dysfunctional mitochondria can no longer be powerhouses of use to the cell and are, therefore, targeted for degradation. Alternatively, their membranes can depolarise leading to the release of cytochrome *c*, an early apoptotic process.[14] Using two distinct cancer cell types, namely U2OS osteosarcoma and A549 non-small cell lung cancer cells,[9,15] we show that DAPK2 depletion increases the levels of intracellular ROS, leads to mitochondrial depolarisation and impairs

[1]Department of Surgery and Cancer, Imperial College London, Faculty of Medicine, Hammersmith Hospital Campus, ICTEM, Du Cane Road, London W12 0NN, UK
*Corresponding author: AP Costa-Pereira, Department of Surgery and Cancer, Imperial College London, Faculty of Medicine, Hammersmith Hospital Campus, ICTEM, Du Cane Road, London W12 0NN, UK. Tel: +44 20 7594 2815; Fax: +44 20 3313 5830; E-mail: a.costa-pereira@imperial.ac.uk
[2]Current address: Otto von Guericke University Magdeburg, Faculty of Process and Systems Engineering, Universitätsplatz 2, 39106 Magdeburg, Germany.
[3]Current address: German Cancer Research Center, Im Neuenheimer Feld 280, 69121 Heidelberg, Germany.

Q1

Abbreviations: ATRA, all-trans retinoic acid; CCCP, carbonyl cyanide 3-chlorophenylhydrazone; CHOP, CCAAT-enhancer-binding protein homologous protein; CM-H2DCFDA, chloromethyl 2′,7′-dichlorodihydrofluorescein diacetate; DAPK, death-associated protein kinase; DHE, dihydroethidium; DMEM, Dulbecco's Modified Eagle's medium; Dox, doxycycline; ECAR, extracellular acidification rate; ER, endoplasmic reticulum; GSH, glutathione; GSSG, oxidised GSH; KEAP1, kelch-like ECH-associated protein 1; MAPK, mitogen-activated protein kinase; MPP^+, mitochondrial complex I inhibitor 1-methyl-4-phenylpyridinium; NAD^+, nicotinamide adenine dinucleotide ; $NADP^+$, nicotinamide adenine dinucleotide phosphate; NFE2L2/NRF2, nuclear factor (erythroid-derived 2)-like 2; OCR, oxygen consumption rate; qWB, quantitative western blots; RNAi, RNA interference; ROS, reactive oxygen species; SDS-PAGE, sodium dodecyl sulphate-PAGE; siNS, non-targeting siRNA oligonucleotide; siRNA, short interfering RNA; SOD, superoxide dismutase; TCA, tricarboxylic acid; Tet, tetracycline; TMRE, tetramethylrhodamine ethyl ester; $\Delta\psi m$, mitochondrial membrane potential

Received 11.6.14; revised 12.12.14; accepted 15.12.14; Edited by C Munoz-Pinedo

mitochondrial metabolism. DAPK2 thus exerts metabolic and mitochondria-regulating functions, which have not been described to date and that can explain why it is downregulated in haematological malignancies,[12,16,17] and involved in modulating death-inducing signalling in solid tumours.[9]

Results

RNAi-mediated ablation of DAPK2 induces oxidative stress and activates mitogen-activated protein kinases. Although DAPK2 is structurally significantly different from DAPK1, their kinase domains are highly homologous.[18] As DAPK1 has been shown to be involved in mitochondrial regulation,[2] we asked whether DAPK2 could also modulate the level of cellular oxidative stress. For that purpose, DAPK2 was targeted with a pool of short interfering (si) RNA oligonucleotides (henceforth referred to as siDAPK2), previously validated in our laboratory (Supplementary Figure S1)[9]. U2OS osteosarcoma and A549 lung cancer cells were transfected with either a control non-targeting siRNA oligonucleotide (siNS) or with siDAPK2 and proteins were analysed by sodium dodecyl sulphate-PAGE electrophoresis (SDS-PAGE). Quantitative western blots (qWB) in Figure 1 show the efficiency of the knockdown of DAPK2 in U2OS (Figure 1a) and A549 (Figure 1e) cells, when compared with the control siNS-transfected cells.

Oxidative stress was studied by flow cytometry in cells transfected with siNS, siDAPK2 or challenged with H_2O_2 (positive control for the production of ROS). General oxidative stress was analysed using the chloromethyl 2′,7′-dichlorodihydrofluorescein diacetate (CM-H_2DCFDA, henceforth referred to as DCFDA) probe (Figures 1c and g) and superoxide production was assessed using the dihydroethidium (DHE) probe (Figures 1d and h). The fluorescence of cells transfected with siDAPK2 or treated with H_2O_2 was compared to that of control cells (siNS). The histograms depict typical cell profiles obtained in each experiment and the bar charts on the right conglomerate mean percentage of fluorescence normalised to control cells ± S.E.M. from three independent experiments. Both DAPK2 depletion and H_2O_2 treatment resulted in an increase in general oxidative stress in U2OS (Figure 1c) and A549 (Figure 1g) cells. The same was observed with regard to the generation of superoxides, which was elevated on siDAPK2 depletion and on treatment with H_2O_2 in both U2OS (Figure 1d) and A549 cells (Figure 1h).

Having observed a clear induction of ROS (H_2O_2 and $O_2^{\bullet -}$) on silencing DAPK2, we asked whether this led to the activation of mitogen-activated protein kinases (MAPKs), which are known to be activated by oxidative stress as part of a pro-survival response.[19] Hence, WB membranes (Figures 1a and e) were probed with antibodies raised against the phosphorylated forms of ERK1/2, p38 and JNK. Depletion of DAPK2, when compared with the siNS control, led to clear phosphorylation/activation of ERK1/2$^{Thr202/Tyr204}$ and JNK$^{Thr183/Tyr185}$ in U2OS and A549 cells, whereas phosphorylation of p38$^{Thr180/Tyr182}$ was only observed in U2OS cells but not in A549 lung cancer cells (Figure 1a *versus* Figure 1e).

Superoxide anion ($O_2^{\bullet -}$) is a potentially damaging free radical, which is converted into less reactive hydrogen peroxide (H_2O_2) by enzymes of the superoxide dismutase (SOD) family. To analyse the effect of DAPK2 depletion on the expression of SOD1, the predominant cytoplasmic SOD, and mitochondrial SOD2, cells were transfected as before and RNA was subsequently extracted. There was significant, *albeit* small (<1.5-fold), upregulation of both SOD1 and SOD2 mRNA in U2OS cells (Figure 1b). In contrast, in A549 cells, SOD1 mRNA was not induced but SOD2 mRNA was greatly increased (greater than fourfold; Figure 1f).

DAPK2 knockdown increases the levels of mitochondrial $O_2^{\bullet -}$ and leads to spontaneous mitochondrial membrane depolarisation. Silencing DAPK2 in two different cell lines led to upregulation of cellular ROS, downstream activation of MAPKs and upregulation of mitochondrial SOD2, whereas SOD1 was only slightly upregulated in one of the cell lines (U2OS). We, therefore, asked whether the source of oxidative stress were mitochondria. Indeed, the production of ATP by oxidative phosphorylation is a major source for mitochondrial ROS, and mitochondrial proton and electron leaks can impact on mitochondrial coupling efficiency and lead to increased production of mitochondrial ROS.[20] MitoSOX Red (Molecular Probes) was used to assess mitochondrial $O_2^{\bullet -}$ levels since it selectively targets mitochondria and is exclusively oxidised by $O_2^{\bullet -}$ (Figure 2). Cells were transfected as before and treatments with H_2O_2 or the mitochondrial complex I inhibitor 1-methyl-4-phenylpyridinium (MPP^+) iodide served as positive controls for the experiment. Unsurprisingly, both treatments increased the levels of mitochondrial $O_2^{\bullet -}$ (Figures 2a and e). As hypothesised, RNA interference (RNAi)-mediated depletion of DAPK2 resulted in a small but statistically significant increase of mitochondrial $O_2^{\bullet -}$ in U2OS (Figures 2b and c) and A549 cells (Figures 2f and g) compared with siNS-transfected cells.

Another potential source for cellular ROS is the endoplasmic reticulum (ER) where the transcription factor CCAAT-enhancer-binding protein homologous protein (CHOP) is specifically activated on ER stress.[21] To induce ER stress we used tunicamycin,[22] which induced the expression of CHOP in both U2OS (Figure 2d) and A549 cells (Figure 2h). In contrast, DAPK2 knockdown did not increase CHOP expression in either cell line (Figures 2d and h).

Elevated levels of mitochondrial $O_2^{\bullet -}$ can be both a cause and a consequence of mitochondrial depolarisation,[23] which is involved in apoptosis and inflammation.[24,25] To study the effect of DAPK2 depletion on mitochondrial membrane potential ($\Delta\psi$m), the JC-1 probe was used. U2OS and A549 cells were transfected with either siNS, or siDAPK2 and, as a control for $\Delta\psi$m depolarisation, cells were treated with carbonyl cyanide 3-chlorophenylhydrazone (CCCP), and then analysed by flow cytometry. Two distinct cell populations were identified after gating the depolarised population that resulted from CCCP treatment: one with intact mitochondria and another that harboured cells with depolarised mitochondria. Depletion of DAPK2 led to ~50% more depolarised mitochondria in both U2OS (Figures 3a–c) and A549 cells (Figures 3g–i), when compared with control cells. This pattern can also be seen in the histograms in Figures 3d, e, j and k. After normalising the absolute fluorescence of cells on DAPK2 knockdown to that of siNS-transfected cells,

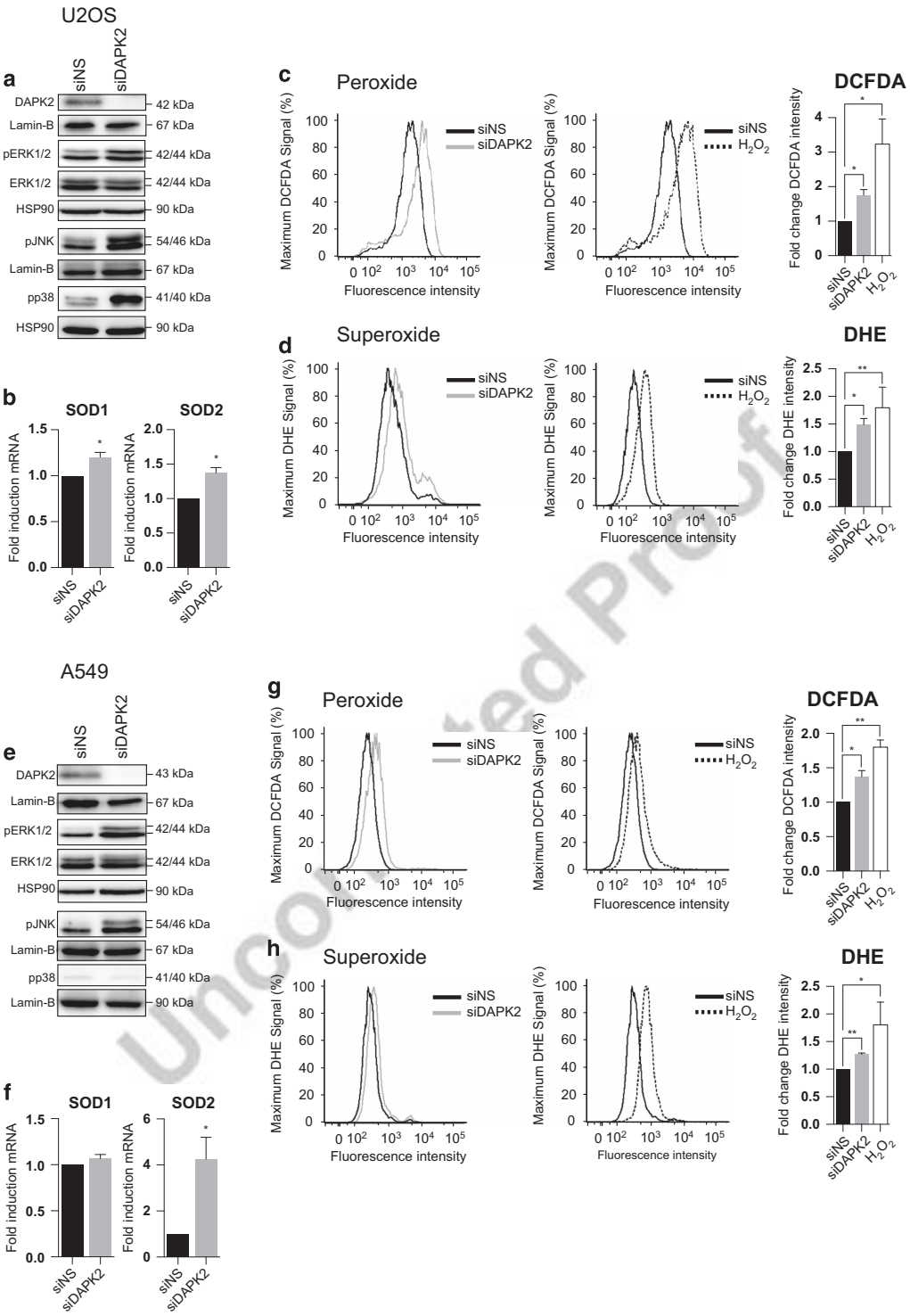

Figure 1 DAPK2 depletion induces oxidative stress, phosphorylation of MAPKs and transcription of SODs. U2OS (**a**–**d**) and A549 (**e**–**h**) cells were transfected with either siNS or DAPK2 siRNA. Forty-eight hours after transfection, the efficacy of DAPK2 silencing and phosphorylation of ERK1/2, JNK and p38 were assessed by SDS-PAGE/qWB using Lamin B and HSP90 as loading controls (**a** and **e**), and the induction of SOD1 and SOD2 mRNA was measured by qPCR (**b** and **f**). Data represent mean ± S.E.M. of three independent experiments. Statistical analyses were done using Student's *t*-test (paired, one tailed) ($P<0.05$). Oxidative stress was detected by flow cytometry. Cells were transfected with siNS or siDAPK2 for 48 h, and H_2O_2 treatment (0.5 mM, 24 h) was used as a positive control for ROS production. The DCFDA probe was used to detect general ROS in U2OS (**c**) and A549 cells (**g**), whereas $O_2^{\bullet -}$ anions were detected in U2OS (**d**) and A549 cells (**h**) using the DHE probe. Staining intensity was quantified using geometric means of three independent experiments and plotted as fold change in relation to the siNS-transfected cells. Statistical analysis was done using Student's *t*-test (paired, one tailed) (*$P<0.05$, **$P<0.01$)

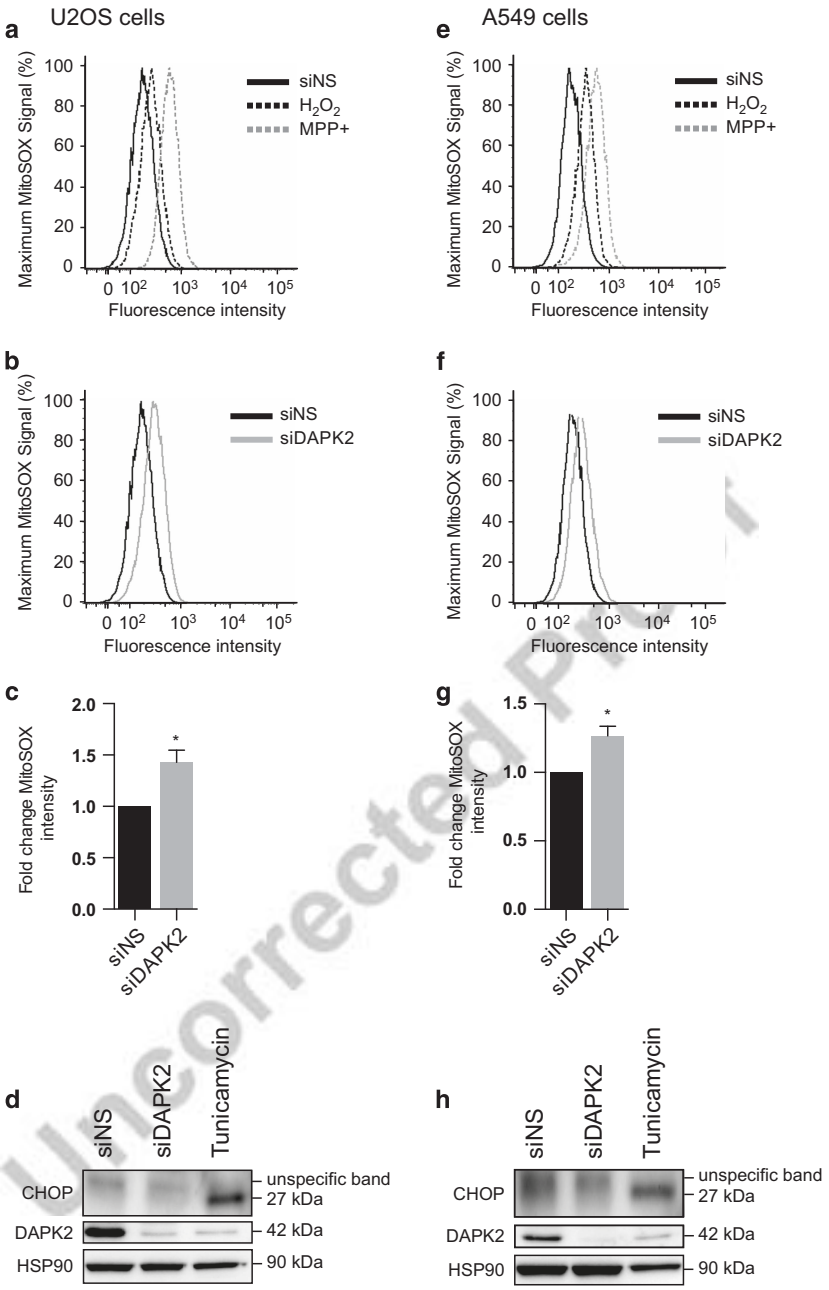

Figure 2 DAPK2 knockdown triggers mitochondrial $O_2^{\bullet -}$ production. U2OS (**a**–**d**) and A549 (**d**–**h**) cells were transfected with either siNS or DAPK2 siRNA. Forty-eight hours later, mitochondrial $O_2^{\bullet -}$ levels were assessed using the MitoSOX Red probe. U2OS (**a** and **b**) and A549 (**e** and **f**) cells were also treated with H_2O_2 (0.5 mM) or MPP^+ (1 mM), which were used as positive controls, for 24 h. The average of geometric means of four independent experiments was plotted as fold change (siNS *versus* siDAPK2) (**c** and **g**). Statistical analysis was done using Student's *t*-test (paired, two tailed) (*$P<0.05$). ER stress was assessed 48 h after siRNA transfection by SDS-PAGE/qWB using CHOP expression as a read-out (**d** and **h**). The induction of CHOP protein following treatment with tunicamycin (0.5 μg/ml) served as positive control and HSP90 expression was used as a loading control

a significant overall increase in green fluorescence, a read-out for decreased $\Delta\psi$m, was measured in both cell lines (Figures 3f and l), suggesting that DAPK2 ablation increased spontaneous mitochondria depolarisation. This was confirmed using tetramethylrhodamine ethyl ester (TMRE), another mitochondrial probe (Figure 4).

Treatment with mitochondrial complex inhibitors leads to the activation of DAPK1 and a decrease in $\Delta\psi m^2$. As shown in Figure 3m A549 cells depleted of DAPK2 have reduced DAPK1 phosphorylated on S308, which is an inactivating phosphorylation event that modulates DAPK1 activity. This suggested that silencing DAPK2 led to the activation of

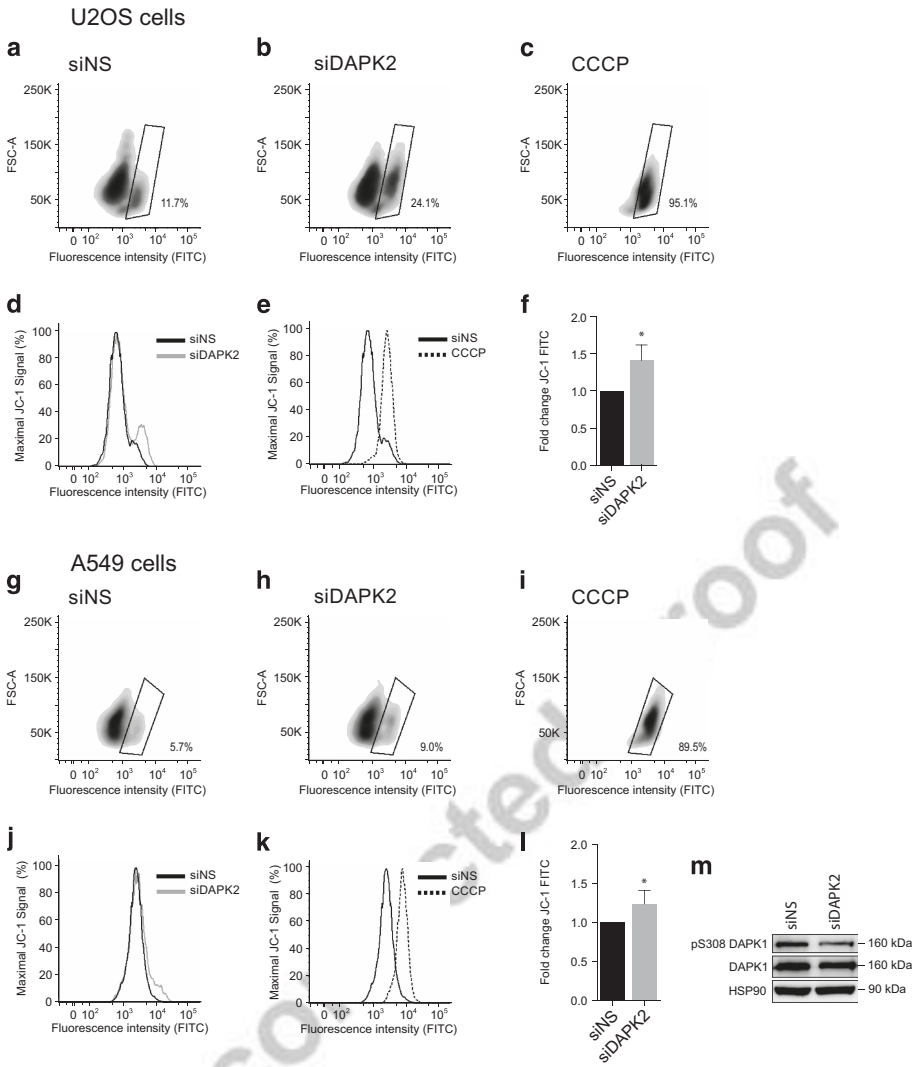

Figure 3 Genetic ablation of DAPK2 increases the rate of spontaneous mitochondrial membrane depolarisation using the JC-1 probe. U2OS (**a**–**f**) and A549 (**g**–**m**) cells were transfected with either siNS or siDAPK2. Forty-eight hours after transfection cells were incubated with JC-1 and the fluorescence of J-aggregates or monomers was measured in red and green fluorescence channels by flow cytometry. CCCP (50 μM) was used to induce complete mitochondrial depolarisation (**c** and **i**) and to set appropriate gates in U2OS (**a**–**c**) and A549 cells (**g**–**i**) used for the quantification of mitochondrial depolarisation following transfection with siNS (**a** and **g**), or siDAPK2 (**b** and **h**). Overall green fluorescence (FITC) data is also presented in histograms (U2OS: **d** and **e**; A549: **j** and **k**). Staining intensity was quantified using geometric means of three independent experiments and plotted as fold change (**f** and **l**). Data represent mean $\pm$ S.E.M. of three independent experiments and the statistical analysis was done using Student's *t*-test (paired, one tailed) (*$P<0.05$). The phosphorylation of DAPK1 on Ser308 and DAPK1 expression levels were analysed in A549 lung cancer cells by SDS-PAGE/qWB, using HSP90 as a loading control (**m**)

DAPK1. Interestingly, U2OS cells did not express DAPK1 protein or mRNA (data not shown). Thus, although mitochondrial depolarisation in A549 cells might be associated with activation of DAPK1, in U2OS cells this is unlikely.

Altered mitochondrial integrity leads to metabolic changes. The increase in mitochondrial $O_2^{\bullet -}$ production and spontaneous mitochondrial depolarisation after DAPK2 silencing suggested that mitochondria were the likely source of ROS. The data were consistent with a significant impairment of mitochondrial integrity in response to DAPK2 depletion and, in the case of A549 lung cancer cells, activation of DAPK1. The metabolic consequences of these mitochondrial alterations in DAPK2-depleted cells were, therefore, investigated next.

Eukaryotic cells use two key metabolic pathways for ATP generation (Figure 5a). Both pathways start with glycolysis as the first step of glucose metabolism, converting one glucose molecule into two molecules of pyruvate with gain of two ATP molecules. Aerobic respiration involves the transport of pyruvate into the mitochondria and mitochondrial respiration downstream of glycolysis through the tricarboxylic acid (TCA)/Krebs cycle, which yields another thirty four ATP molecules/molecule of glucose.[26] Anaerobic respiration includes glycolysis and the fermentation of pyruvate to lactate, a metabolic pathway that bypasses mitochondrial

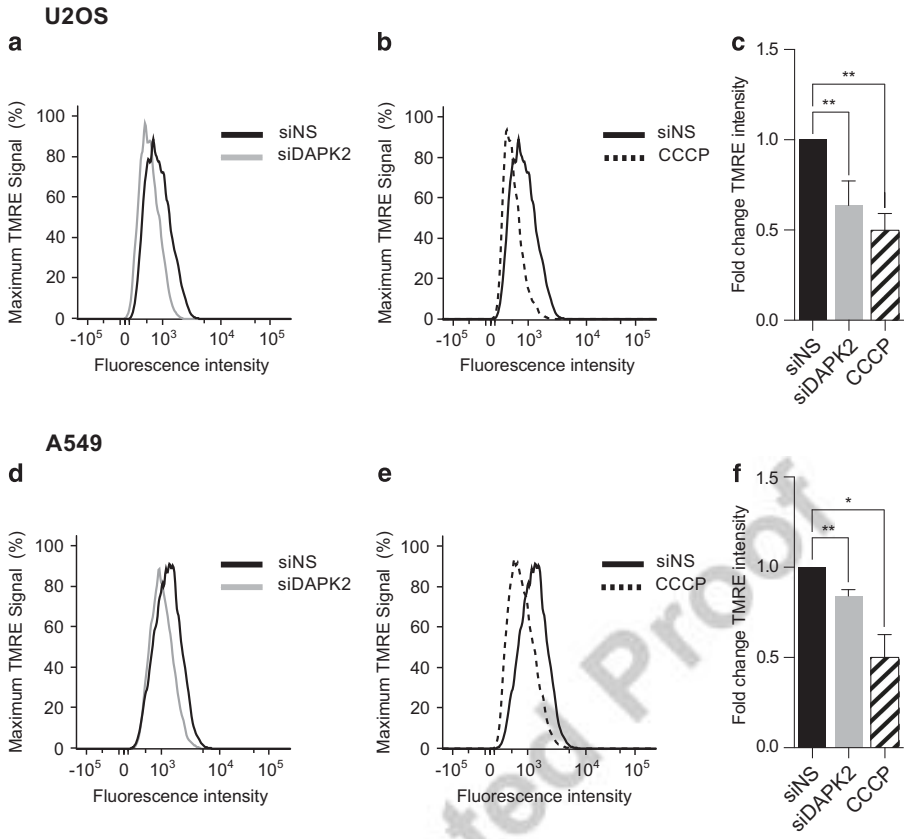

Figure 4 Measurement of spontaneous mitochondrial membrane depolarisation after transfection with siDAPK2 using the TMRE probe. U2OS (**a**–**c**) and A549 (**d** and **e**) cells were transfected with either siNS or siDAPK2. Forty-eight hours after transfection cells were incubated with TMRE and the fluorescence intensity in the red fluorescence channel (PE) was measured by flow cytometry. CCCP (50 μM) was used to induce mitochondrial depolarisation (**b** and **e**). Staining intensity was quantified using geometric means of three independent experiments and plotted as fold change (**c** and **e**). Data represent mean ± S.E.M. of three independent experiments and the statistical analysis was done using Student's *t*-test (paired, one tailed) (*$P<0.05$, **$P<0.01$)

respiration, and is predominantly upregulated in cancer cells (Warburg effect), which cancer cells use to produce most of their energy.[18,27]

Changes in aerobic and anaerobic respiration were analysed by measuring the oxygen consumption rate (OCR), an accurate indicator of mitochondrial respiration, and the extracellular acidification rate (ECAR), an indirect measurement of lactic acid production, with a Seahorse XF96 analyser (Seahorse Bioscience, North Billerica, MA, USA; Figure 5). OCR and EACR were determined under basal conditions in siDAPK2- or siNS-transfected cells. The EACR in siDAPK2-tranfected cells, measured in mpH/min, was normalised to that in siNS-transfected control cells. No statistically significant changes in EACRs were detected between siNS- and siDAPK2-transfected U2OS (Figure 5b), or A549 (Figure 5h) cells, suggesting that silencing DAPK2 did not skew metabolism in these cells towards anaerobic respiration. OCR was measured in pMoles/min and normalised as described above for EACR measurements. In contrast to what was seen for EACR, there was a significant decrease in OCRs by mitochondria on DAPK2 knockdown in both U2OS (Figure 5c) and A549 (Figure 5i) cells, suggesting that DAPK2 modulated mitochondrial respiration but not anaerobic respiration.

To investigate further the consequences of DAPK2 depletion on cellular metabolism, levels of the coenzymes nicotinamide adenine dinucleotide (NAD^+) and nicotinamide adenine dinucleotide phosphate ($NADP^+$), as well as their corresponding reduced forms (NADH and NADPH, respectively), were analysed. During glycolysis and the TCA cycle, each glucose molecule leads to the reduction of six NAD^+ to NADH, which are then oxidised during oxidative respiration to produce ATP.[26] In contrast to NADH, NADPH is not involved in metabolic processes but it has an important role in the regeneration of oxidised glutathione (GSH), a key antioxidant in cells.[28] Colorimetric assays were used to determine the levels of NAD^+ and NADH, as well as $NADP^+$ and NADPH. MPP^+ was used to inhibit oxidative phosphorylation and increase the levels of NAD^+ and NADH. As shown for U2OS (Figures 5d and e) and A549 cells (Figures 5j and k), the control MPP^+ treatment increased the levels of NAD^+ and NADH (*albeit* in A549 cells the increase in NADH was small and not statistically significant). However, NAD^+/NADH levels remained unaffected by DAPK2 knockdown. Interestingly, the levels of $NADP^+$ and NADPH in U2OS cells (Figures 5f and g) appeared slightly decreased on silencing DAPK2, whereas there was no detectable change in A549 cells (Figures 5l and m). The data thus suggested that RNAi-

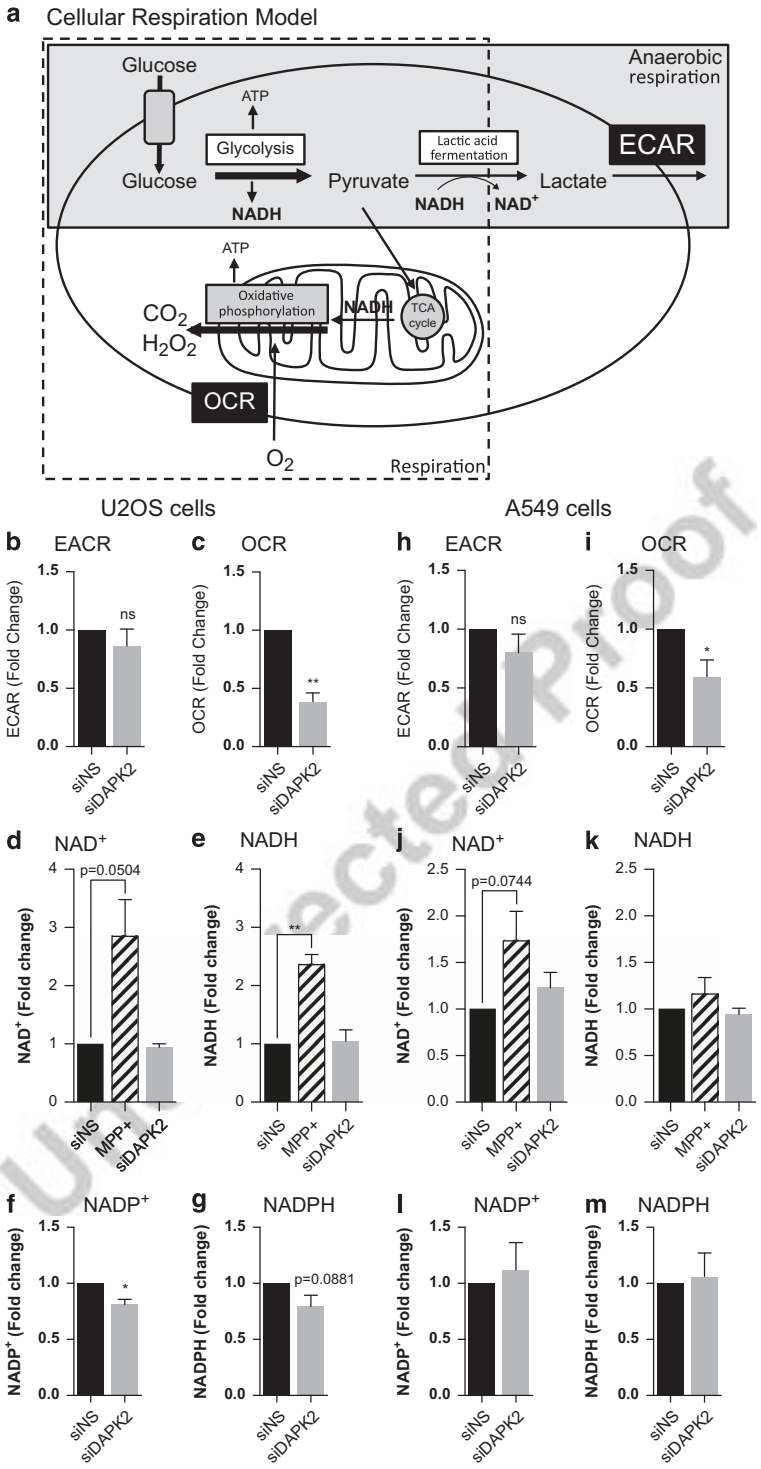

Figure 5 The absence of DAPK2 leads to reduced oxidative phosphorylation in U2OS and A549 cells. (**a**) Simplified cartoon depicting cellular metabolism pathways with glycolysis as the first step of glucose breakdown, and oxidative phosphorylation and anaerobic respiration as subsequent steps. To quantify cellular metabolic processes, U2OS (**b**–**g**) and A549 (**h**–**m**) cells were transfected with either siNS or DAPK2 siRNA. Forty-eight hours after transfection cells were analysed using a Seahorse Analyser. ECAR, an indirect measurement of lactic acid production, is depicted as fold change of mpH/min and normalised to siNS control in U2OS (**b**) and A549 cells (**h**). OCR, which can be used to determine mitochondrial respiration, is shown as fold change of pmol/min and normalised to siNS control in U2OS (**c**) and A549 cells (**i**). Forty-eight hours after siRNA transfection, NAD^+, NADH, $NADP^+$ and NADPH levels were analysed using colorimetric assays in U2OS (**d**–**g**) and A549 cells (**j**–**m**). Treatment with MPP+ (1 mM, 24 h) served as a positive control. Data represent mean ± S.E.M. of three independent experiments, statistical analyses were done using Student's *t*-test (paired, one tailed) ($^*P<0.05$, $^{**}P<0.01$)

mediated ablation of DAPK2 affected oxidative phosphorylation without substantially impacting on NAD^+/NADH or $NADP^+$/NADPH metabolism.

Depletion of DAPK2 leads to decreased GSH levels and induction of NRF2. Having established that genetic ablation of DAPK2 led to changes in cellular oxidative stress, mitochondrial respiration, activation of stress kinases and upregulation of SODs in two distinct cancer cell types, we next asked what effect downregulation of DAPK2 had on the levels of GSH, which functions as an electron donor and is involved in the reduction of cellular ROS.[29,30] In fact, the generation of oxidised GSH (GSSG) is tightly linked to mitochondrial oxidative phosphorylation, whereby NADPH reduces GSSG to GSH. To assess total GSH level, cells were transfected as described earlier and a subtle, but statistically significant, downregulation of GSH levels on DAPK2 knockdown was detected, which was more prominent in U2OS (Figure 6a) than in A549 cells (Figure 6e).

The question was whether such small reductions in GSH levels were sufficient to induce nuclear factor (erythroid-derived 2)-like 2 (NFE2L2/NRF2), which is responsible for the transcription of a multitude of antioxidants that protect cells from oxidative stress. NRF2 binds to the antioxidant response element, leading to transcriptional activation of GSH synthesising enzymes and other antioxidant enzymes, such as SOD1 and SOD2, which were upregulated on DAPK2 silencing (Figures 1b and f). After U2OS and A549 cells were transfected with siDAPK2 or siNS, RNA and proteins were extracted and the levels of NRF2 and its ubiquitin ligase kelch-like ECH-associated protein 1 (KEAP1) analysed. Interestingly, NRF2 mRNA levels were significantly elevated in U2OS cells (Figure 6b), but not in A549 cells (Figure 6f). KEAP1 was not induced in either U2OS (Figure 6c) or A549 cells (Figure 6g).

The mitochondrial-associated function of DAPK2 is likely to be kinase mediated. The data thus far suggested that the increase in intracellular ROS caused by downregulating DAPK2 was due to an impairment of mitochondrial functions. To understand how DAPK2 preserved mitochondrial integrity, the relevance of DAPK2's kinase domain was investigated. For that purpose, tetracycline (Tet)-inducible U2OS cell lines (U2OS-TetR) containing HA-tagged DAPK2 constructs that were either wild-type (HA-DAPK2.wt) or kinase-dead (HA-DAPK2.K42A)[6] were used. The caveat with this approach is that it was impossible to express the constructs at endogenous levels and overexpression of DAPK2 is sufficient to induce apoptotic features.[6] This approach could not thus be used experimentally to rescue the phenotype observed after RNAi targeting DAPK2. It did, however, enable analysis of the role of the kinase domain on the regulation of intracellular oxidative stress.

Transgene expression was induced in HA-DAPK2.wt (Figure 7a) and HA-DAPK2.K42A cells (Figure 7c) using doxycycline (Dox) and ROS levels were measured using DCFDA. As expected from previously published work, overexpression of wild-type DAPK2, rather than leading to reduced oxidative stress, led to an increase in general ROS production

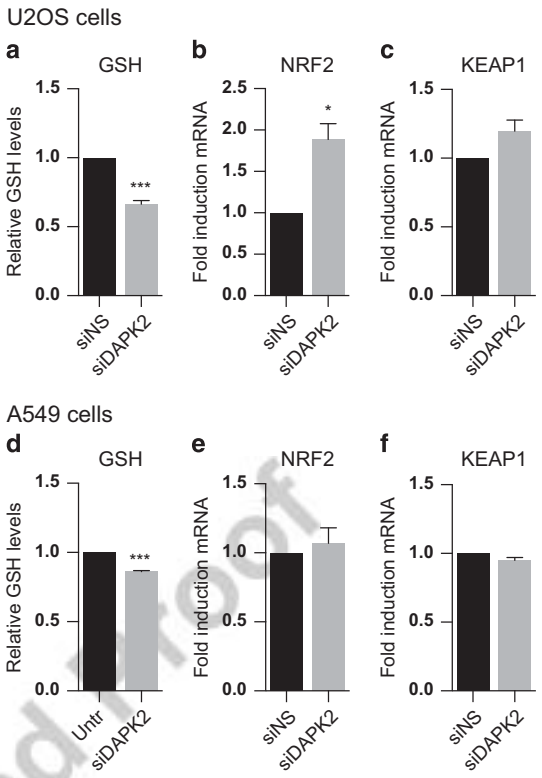

Figure 6 Ablation of DAPK2 leads to decreased GSH levels, and in U2OS cells to the induction of NRF2 mRNA. U2OS (**a**–**c**) and A549 (**d**–**f**) cells were transfected with either siNS or siDAPK2, and the levels of GSH were analysed using a colorimetric assay 24 h later (**a** and **d**). NRF2 (**b** and **e**) and KEAP1 (**c** and **f**) mRNA levels were assessed by qPCR. Data represent mean ± S.E.M. of at least three independent experiments and the statistical analyses were done using Student's *t*-test (paired, one tailed) (*$P<0.05$, **$P<0.01$, ***$P<0.005$)

(Figure 7b), but importantly this was not observed if cells overexpressed a kinase-dead DAPK2 mutant (Figure 7d).

The overexpressed kinase-dead mutant (HA-DAPK2.K42A) did not behave as a dominant-negative and did not mimic the phenotype caused by DAPK2 silencing (Figure 7d). This might be due to the cells still expressing endogenous wild-type DAPK2. To eliminate the endogenous wild-type DAPK2 in the inducible cell model, 3′UTR-specific siRNAs were used. These molecules exclusively target endogenous DAPK2 (Figures 7e–h).[9] Cells were transfected with either siNS or 3′ UTR-specific DAPK2 siRNA (henceforth siDAPK2–3′UTR) and to induce HA-DAPK2.K42A expression cells were stimulated with Dox as they were being transfected. As shown in Figure 7e, siDAPK2–3′UTR specifically targeted endogenous DAPK2 and did not impact on the expression of kinase-dead DAPK2, which was detected using an anti-HA antibody.

Having established a cell system where it was possible to efficiently downregulate endogenous DAPK2 and concomitantly overexpress a kinase-dead DAPK2 mutant enabled studying the effect of kinase-dead DAPK2 on the generation of general ROS. Consistent with our previous results (Figure 1c), depletion of wild-type DAPK2 without (Figure 7g, grey line) or with overexpression of kinase-dead DAPK2 (Figure 7g, dotted line), using siDAPK2–3′UTR, led in both cases to a significant

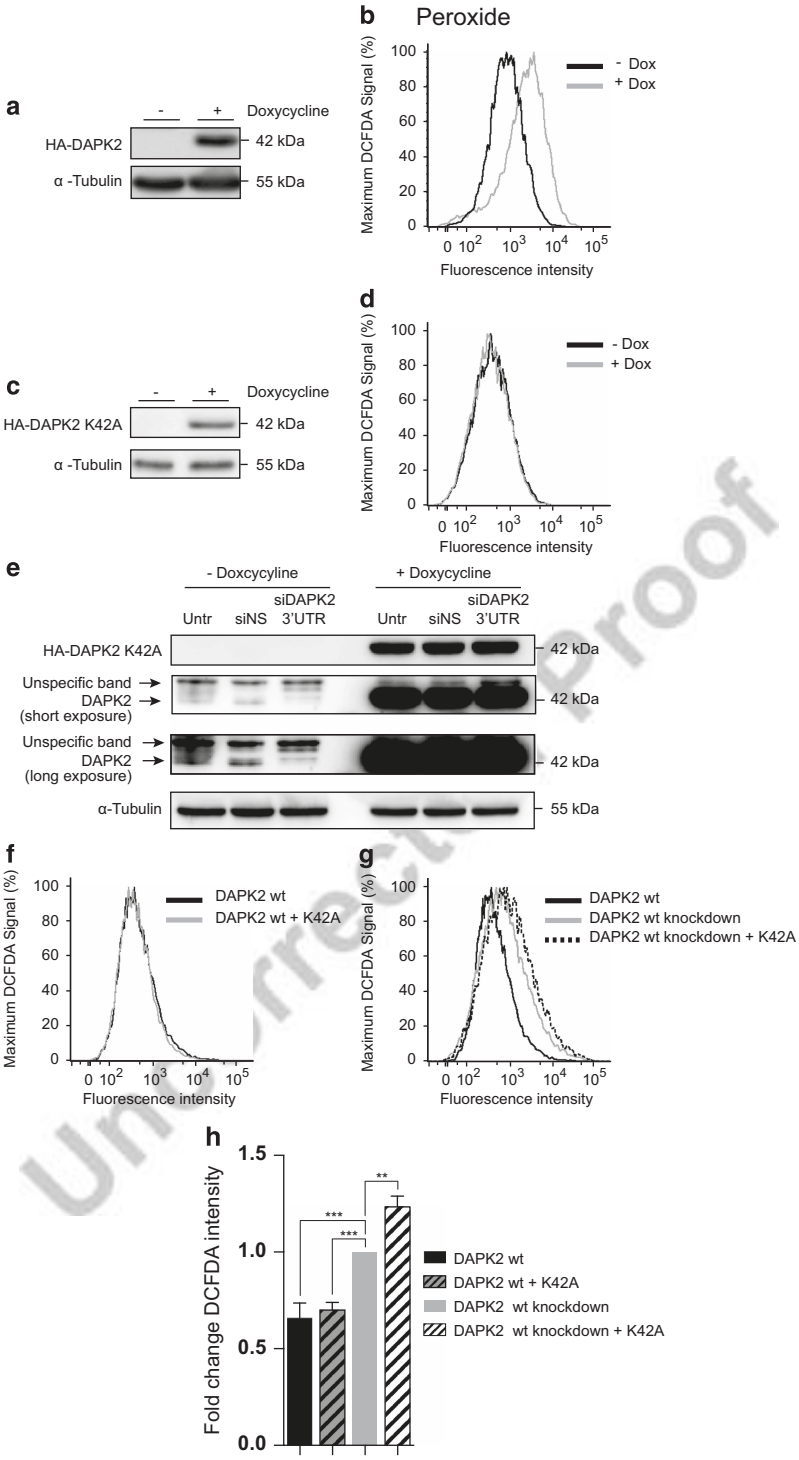

Figure 7 Effect of wild-type (wt) and kinase-dead (K42A) DAPK2 overexpression on oxidative stress. The expression of HA-tagged wild-type (wt) or HA-tagged kinase-dead (K42A) DAPK2 in U2OS-TetR cells was induced using doxycycline (10 ng/ml). HA-DAPK2 (**a**) and HA-DAPK2.K42A (**c**) expression was verified by SDS-PAGE/qWB. The impact of wild-type (**b**) or kinase-dead (**d** and **f**) DAPK2 overexpression on oxidative stress was analysed as described earlier using the DCFDA probe. To eliminate endogenous DAPK2 and study the effect of the kinase-dead DAPK2 mutant individually, U2OS-TetR cells containing the HA-DAPK2.K42A construct were transfected with either siNS or siDAPK2–3′ UTR and concomitantly stimulated with doxycycline (10 ng/ml). Targeted knockdown of endogenous DAPK2 and overexpression of HA-DAPK2.K42A were then assessed by SDS-PAGE/qWB (**e**). The effect of the kinase-dead DAPK2 mutant overexpression, in the presence (**f,** grey line) and absence (**g,** dotted black line) of endogenous DAPK2, on oxidative stress was quantified by flow cytometry with the DCFDA probe (**f** and **g**). Data were plotted as fold change of DCFDA fluorescence of U2OS-TetR cell transfected with siDAPK2–3′UTR without doxycycline treatment (**h**). Statistical analysis was done using one-way ANOVA test (**$P<0.01$, ***$P<0.005$)

increase in ROS (Figures 7g and h). The overexpression of kinase-dead DAPK2, importantly, actually led to a significantly higher level of oxidative stress in U2OS cells than the wild-type endogenous protein (Figure 7h). In control cells transfected with siNS, the level of oxidative stress was the same regardless of the presence or absence of HA-DAPK2.K42A (Figure 7f). Collectively, our data suggested that DAPK2 kinase activity was important for preserving mitochondria's integrity and protecting cells from oxidative stress.

Discussion

Although DAPK1–3 are structurally different, both DAPK2 and DAPK3 evolved from DAPK1,[31] which regulates mitochondrial integrity[2] and metabolic processes.[3] Given the common ancestry and sequence homology within DAPKs' kinase domains, common mechanisms of action and functional redundancy have been postulated.[32] Indeed, all three have been associated with apoptotic processes and thought to be potential tumour suppressors.[18]

Here we show that depletion of DAPK2 results in ROS generation (Figures 1c, d, g and h), induction of SODs (Figures 1b and f) and phosphorylation/activation of MAPKs (Figures 1a and e). Mitochondrial SOD2 was induced more than cytosolic SOD1 (Figures 1b and f), suggesting that in the absence of DAPK2, increased levels of ROS were produced by mitochondria.[13] Additional experiments support this hypothesis (Figures 2a–c and e–g) and indicate that the ER is an unlikely additional ROS source (Figures 2d and h). Silencing DAPK2 leads to increased spontaneous mitochondrial depolarisation (Figures 3a–l and Figure 4), and in A549 cells to the activation of DAPK1 (Figure 3m), thought to be a $\Delta\psi$m sensor involved in cytoskeletal rearrangements responsible for mitochondrial transport mechanisms.[2] DAPK1 and DAPK2 have also been reported to heterodimerise.[32] It is thus reasonable to assume that they may operate similarly with regard to mitochondrial maintenance, sensing the mitochondrial membrane potential and leading to downstream processes of mitophagy and mitochondrial degradation, which result in faulty mitochondria. Interestingly, neither overexpression of DAPK1 nor DAPK2 has been shown to induce mitochondrial depolarisation.[6] Immunofluorescence analyses using MitoTracker Red did not suggest any obvious mitochondrial morphological changes in cells devoid of DAPK2 (data not shown).

DAPK2 knockdown leads to significantly reduced oxidative phosphorylation without affecting lactic acid fermentation (Figures 5b, c, h and i). This suggests a fundamental role for DAPK2 in the regulation of mitochondrial metabolism and/or maintenance. This, in turn, raises the question of how these cells maintain their energy supply, without increased lactic acid fermentation, DAPK2-depleted cells are unlikely to be compensating the decrease in oxidative phosphorylation via anaerobic respiration (Figure 5a). Consistent with this, no significant changes in NAD^+/NADH and/or $NADP^+$/NADPH on DAPK2 silencing are seen (Figures 5d–g and j–m). All experiments were performed 48 h post RNAi. Thus, eventual cellular compensatory mechanisms, such as increased glycolytic rate or lactic acid production, may not yet be detectable. For example, it has been shown that inhibition of the mitochondrial electron transport by low doses of ethidium bromide for 4 days causes NADH accumulation, halts the TCA cycle and drives cells towards anaerobic glucose metabolism.[33]

The ROS increase and mitochondrial depolarisation were accompanied by a small, statistically significant, GSH decrease (Figures 6a and e), and in U2OS cells by the induction of NRF2 (Figure 6b). There was no induction of NRF2 in A549 cells (Figure 6f) and the levels of KEAP1, a NRF2 regulator,[34] remained unchanged in both cell lines (Figures 6c and g). SOD2 protein expression levels, unlike what was observed at the mRNA level, did not vary with the downregulation of DAPK2 expression. In fact, the expression of GCLC, GPX1, GSTpi and GSS, enzymes involved in GSH metabolism, did not change significantly either on RNAi against DAPK2 (data not shown). These data thus suggest that it is their enzymatic activity that matters, which is corroborated by the GSH quantification shown in Figures 6a and e, used as an indirect read-out for these enzymes.

Overexpression of HA-tagged wild-type DAPK2 *per se* increases the levels of intracellular ROS in U2OS cells (with endogenous DAPK2), whereas kinase-dead DAPK2 does not (Figures 7a–d). In contrast, as previously shown,[6] overexpression of wild-type DAPK2 does not induce mitochondrial ROS (data not shown). Interestingly, overexpression of the kinase-dead mutant, in the absence of endogenous DAPK2, leads to increased oxidative stress and this is greater than that seen with the wild-type protein (Figures 7e–h). Collectively, these data indicate that DAPK2 kinase activity is important for preserving mitochondrial integrity and protecting cells from oxidative stress.

DAPK2 is emerging as a tumour suppressor in several types of cancer cells, especially in acute promyelocytic leukaemia, which responds to treatment with all-trans retinoic acid (ATRA).[12] This is interesting as ATRA leads to increased DAPK2 expression. Given the role of ROS in the aetiology of AML,[35] downregulation and/or loss of DAPK2 likely benefits cancer cells by leading to deregulated mitochondria, increased cellular ROS and, thus, genomic instability. Indeed, somatic mitochondrial mutations and accumulated mitochondrial damage have been linked to AML development.[36] Despite its relatively small size and straightforward structural features, DAPK2 appears to be a double-edge sword, depending on cellular context and interaction partners. Indeed, recently, we have shown that downregulation of endogenous DAPK2 activates NF-κB and sensitises multiple cancer cell types to TRAIL-induced apoptosis but not to other cytotoxic stimuli.[9] NF-κB, another multi-faceted protein, can also be activated by oxidative stress but TRAIL-induced apoptosis appears to be independent of oxidative stress since it can be blocked by caspase inhibitors (Supplementary Figure S2), but these inhibitors do not impair the production of ROS (Supplementary Figure S3) or mitochondrial depolarisation (Supplementary Figure S4) seen after DAPK2 depletion. Experiments using U2OS cells that express LC3–GFP (an autophagy readout) suggest that depletion of DAPK2 also affects autophagy, as in these cells nutrient starvation leads to an increase in the expression of LC3I (data not shown). It is still unclear if this directly impairs mitochondrial recycling, leading to the accumulation of 'faulty' mitochondria, and if it

contributes for the oxidative stress measured here. This is entirely consistent with a novel report by Kimchi and co-workers,[37] where it is shown that DAPK2 is a novel mTORC1 kinase and therefore a novel regulator of autophagic processes. How this relates to the regulation of NF-κB[9] remains under scrutiny.

We have thus identified a novel role for DAPK2 in the regulation of mitochondrial integrity, as its absence leads to mitochondrial depolarisation and increased oxidative stress. This may be a mechanism by which, depending on the intracellular context, DAPK2 can act as a tumour suppressor gene. Importantly, as the effect of DAPK2 silencing on mitochondrial respiration is conserved between mesenchymal U2OS cells and epithelial A549 cells, it is likely that our findings can be further extended to additional cell lineages and malignancies.

Materials and Methods

Cell culture. U2OS and A549 cells were grown in Dulbecco's Modified Eagle's medium (DMEM) supplemented with 10% (v/v) foetal calf serum (FCS) (FirstLink, Wolverhampton, UK), 2 mM L-glutamine, 50 U/ml penicillin and 50 μg/ml streptomycin (henceforth referred to as 'complete DMEM'), in a humidified atmosphere of 10% CO_2 at 37 °C. The U2OS-TetR cell line was provided by Johnsen and co-workers[38] and cultured in full DMEM media supplemented with 5 μg/ml blasticidine S hydrochloride. All chemicals were from Sigma-Aldrich, unless otherwise specified.

Plasmids. N-terminal HA-tagged wild-type and kinase-dead (K42A) DAPK2 pcDNA3 plasmids were kindly provided by Kimchi and co-workers.[6] Both constructs were sub-cloned using Bam*HI* and Xho*I* restriction sites into a pcDNA4/TO vector, which is part of the Tet-inducible mammalian expression system, T-REx System (Life Technologies, Paisley, UK).

Generation of stable inducible cell lines. HA-tagged DAPK2 wild-type and kinase-dead (K42A) constructs, cloned into the pcDNA4/TO vector, were linearised using the restriction enzyme *PvuI* (New England Biolabs, Hitchin, UK) and transfected into U2OS-TetR cells using Lipofectamine 2000 (Life Technologies), as instructed by the manufacturer. Forty-eight hours later, cells were re-plated and incubated with complete DMEM supplemented with 5 μg/ml blasticidine S hydrochloride and 500 μg/ml Zeocin (Life Technologies). Individual clones were isolated using cloning cylinders and tested for induction of the transgene and background expression by SDS-PAGE/qWB. For each construct, at least five inducible clones were generated and tested.

Antibodies. The anti-DAPK2 antibody was purchased from Epitomics (Burlingame, CA, USA); anti-phospho-DAPK1 (Ser308) and DAPK1 from Abcam (Cambridge, UK); antibodies against phospho-ERK1/2 (Thr202/Tyr204), phospho-p38 MAPK (Thr180/Tyr182), phospho-JNK (Thr183/Tyr185) and CHOP from Cell Signaling Technology (Cambridge, UK); antibodies against HA, β-actin and α-tubulin from Sigma-Aldrich; anti- HSP90 (HSP86) from NeoMarkers (Fremont, CA, USA); antibodies against ERK1/2 and Lamin B were from Santa Cruz Biotechnology (Santa Cruz, CA, USA). Anti-mouse and anti-rabbit secondary antibodies were from DAKO (Glostrup, Denmark) and the anti-goat antibody was from Sigma-Aldrich.

RNA interference. RNAi was performed using Lipofectamine RNAiMax (Life Technologies), essentially as described in ref. 39. For forward siRNA transfection cells, plated at a density of 2.5×10^5 in six-well plates, were left untransfected, or were transfected with either 20 nM AllStars non-targeting control siRNA (siNS) (Qiagen, Hilden, Germany), 20 nM of a siDAPK2 pool (siRNA oligonucleotides 3 and 4 from Dharmacon, Lafayette, CO, USA) or with either of two different 3′UTR-specific siRNAs (from Dharmacon or Qiagen). Cells were then treated and analysed as described in the figures using methods described below. Reverse siRNA transfections were carried out in 10 cm dishes using 5×10^5 cells in suspension (8 ml). Cells were left untransfected or were mixed with transfection reagent and either 20 nM siNS or siDAPK2. All siRNA oligonucleotide sequences are listed on Supplementary Table SI.

Protein expression analysis. Proteins were extracted using radioimmunoprecipitation assay buffer (50 mM Tris-HCl pH 7.4; 0.5% (v/v) NP-40, 150 mM NaCl, 1 mM EDTA, 1 mM Na_3VO_4 and cOmplete and Mini, EDTA-free protease inhibitor cocktail, the latter used as instructed by the manufacturer (Roche, Mannheim, Germany)). Concentrations were determined using a Bradford assay according to the manufacturer's instructions (BioRad, Hercules, CA, USA). They were then analysed by SDS-PAGE/ qWB. Membranes were blocked using 5% (w/v) non-fat milk/TBS-Tween 20, which was the buffer also used to dilute secondary antibodies. Primary antibodies were diluted in 5% (w/v) BSA/ TBS-Tween 20. WBs were analysed using the quantitative luminescence system FUSION Solo (PEQLAB, Sarisbury Green, UK). Images were analysed using Image Studio Lite software (LI-COR Biosciences, Lincoln, NE, USA) (www.licor.com/islite). The WB images have been cropped for clarity purposes: that has in no way altered the essence of the data obtained in three independent experiments.

Detection of oxidative stress by flow cytometry. Cells were cultured in six-well plates and transfected with siRNA oligonucleotides as described before, or treated with 0.5 mM H_2O_2 for 24 h, which was used as a positive control for ROS production. General ROS were detected using CM-H_2DCFDA (Molecular Probes, Life Technologies; referred throughout the text as DCFDA). For that purpose, cells were incubated with 10 μM DCFDA dissolved in pre-warmed PBS for 30 min at 37 °C. Cells were then trypsinised, resuspended in complete DMEM, washed twice with PBS and analysed by flow cytometry. Cellular superoxide anions were detected using DHE (Molecular Probes) 48 h after transfection. Essentially, cells were trypsinised, resuspended in complete DMEM, washed twice with PBS, incubated in 10 μM DHE dissolved in pre-warmed PBS for 15 min and analysed by flow cytometry. Mitochondrial superoxide anions were measured using the MitoSOX Red mitochondrial superoxide indicator. Briefly, cells were transfected as described earlier, or they were treated for 24 h with 1 mM MPP^+, or with 0.5 mM H_2O_2, the latter two used as positive controls. Forty-eight hours later, cells were washed with PBS and incubated for 10 min at 37 °C in the dark with 5 μM MitoSOX Red reagent diluted in pre-warmed PBS. Samples were subsequently washed twice with PBS before being analysed. Depolarised mitochondria were quantified using the MitoProbe 5′,6,6′-tetrachloro-1,1′,3,3′-tetraethylbenzimidazolylcarbocyanine iodide (JC-1) Assay Kit and Tetramethylrhodamine, ethyl Ester, perchlorate (TMRE; Molecular Probes). For JC-1 staining, 48 h after transfection, cells were trypsinised, resuspended in complete DMEM, washed twice with PBS and incubated with 2 μM JC-1 dissolved in pre-warmed PBS at 37 °C, 10% CO_2 for 15 min and analysed by flow cytometry. TMRE staining was performed as follows: 48 h after transfection cells were incubated with 100 nM TMRE dissolved in pre-warmed complete DMEM at 37 °C, 10% CO_2 for 10 min and analysed by flow cytometry. To induce complete mitochondrial depolarisation, the protonophore CCCP (50 mM) was used for 5 min prior to the incubation of cells with JC-1 and TMRE.

All flow cytometry analyses were performed using a FACS Canto (Becton Dickinson, Franklin Lakes, NJ, USA) and data mining was done using FlowJo (Tree Star, Inc., Ashland, OR, USA). Fluorescence geometric means were used for the analyses and samples were normalised to siNS-transfected control cells, essentially as described earlier.[39]

Induction of ER stress. ER stress was induced using the glycosylation inhibitor tunicamycin (0.5 μg/ml, 24 h) and monitored by SDS-PAGE/qWB using CHOP expression as a read-out.

Real-time quantitative PCR. Gene expression analysis was done by quantitative two-step reverse transcription PCR. Reverse transcription was performed using total RNA and a High Capacity cDNA Reverse Transcription kit (Life Technologies), using random hexamers. Quantitative PCR (qPCR) was done using the Fast SYBR Green Master Mix (Life Technologies) with specific primer pairs (Supplementary Table SII). For each target mRNA analysed, 2.5 μl of Fast SYBR Green Master Mix, 0.5 μM of each primer pair and 2 μl of cDNA in deionised water (5 ng/μl) were mixed in 384-well plates in duplicates using Matrix Equalizer Electronic Multichannel Pipetters (Thermo Fisher Scientific, Loughborough, UK). qPCR was carried out on an ABI PRISM 7900HT (Applied Biosystems, Foster City, CA, USA) using the following settings: initial activation of 20″ at 95 °C, 40 cycles; denaturation for 1′ at 95 °C; annealing/extension for 20″ at 60 °C; final melting curve was carried out for 15″ at 95 °C and then for 15″ at 60 °C. Quantification of target messages was performed using qbasePLUS software (Biogazelle, Ghent, Belgium). HPRT and GAPDH were the reference genes used for normalisation.

Metabolic analyses. Metabolic measurements were done in real-time, non-invasively, using a Seahorse XF96 analyser, which measured the OCR and the ECAR under basal conditions in siDAPK2- or siNS-transfected cells. A cell titration assay was used to determine a suitable cell plating density for both A549 and U2OS cells. For the experiment proper, 0.5×10^6 cells were plated per 10 cm dish and reverse transfected on day 1 as previously described. Forty-eight hours post transfection, cells were re-plated into the XF96 microplates (Seahorse Bioscience; 4×10^4 cells per 100 μl per well) and incubated overnight at 37 °C. The XF calibration solution was added into the XF sensor cartridge and was also incubated at 37 °C overnight but without CO_2. The next day, prior to the assay, complete DMEM was replaced with an XF Assay Medium Modified DMEM (1 g/ml glucose, pH 7.4) and cells were incubated at 37 °C for 1 h without CO_2. Analyses were performed according to the manufacturer's instructions using eight measurements that the instrument recorded for OCR (nmoles/min) and ECAR (mpH/min) pertaining to each well. Results were analysed using the provided XFe Wave software (Seahorse Bioscience).

GSH colorimetric assay. Cells (2.5×10^5 per well in 6-well plates) were transfected with siRNA oligonucleotides as described earlier. Cell lysates were collected and sonicated in 50 mM PBS per 1 mM EDTA. Protein concentrations were determined using a Bradford assay, according to the manufacturer's instructions, which enabled subsequent normalisation of each sample so that the final protein concentration was 1 μg/μl. GSH levels in each sample were quantified using the Glutathione Assay Kit from BioAssay Systems (Hayward, CA, USA), as per the manufacturer's protocol.

NADH and NADPH assay. Reverse siRNA transfections were carried out in 10-cm dishes using 5×10^5 cells in suspension. As positive control, cells were treated for 24 h with 1 mM of MPP^+. Forty-eight hours after transfection, NADP/NADPH levels for each sample were quantified using the NADP/NADPH assay kit (Abcam) and NAD/NADH levels using the NAD/NADH assay kit (BioVision, San Francisco, CA, USA), according to the two manufacturers' protocols.

Statistical analysis. Mean ± S.E.M. of at least three independent experiments were used throughout. ANOVA or *t*-test statistical analyses were carried out as indicated in each figure legend using GraphPad Prism (GraphPad Software Inc., San Diego, CA, USA).

Conflict of Interest

The authors declare no conflict of interest.

Acknowledgements. We are grateful to Prof. Adi Kimchi (Weizmann Institute of Science, Rehovot, Israel) for the HA-tagged wild-type and kinase-dead (K42A) DAPK2 pcDNA3 plasmids, and to Prof. Steven A. Johnsen (the University Medical Center Hamburg-Eppendorf, Hamburg, Germany) for providing us with U2OS-TetR cells. Within Imperial College London, we are indebted to Dr Charlotte Bevan and her research team for many helpful discussions and Dr Anna Maria Tommasi for excellent technical help. Cancer Research UK funded CRS and APC-P (C37990/A12991) at the Imperial Cancer Research UK Centre; and APC-P (CA5775); CEM was funded by MRC and Johnson & Johnson (CASE studentship G1000390); MBM was funded by the ERASMUS programme through a student mobility placement studentship (DE-2013-ERA/MOB-KonsZuV01-CP6); CRS, CEM, OEP, MJS and APC-P were additionally funded by Cancer Treatment and Research Trust (CTRT) and APC-P is the recipient of an Elsie Widdowson Fellowship.

Author contributions

CRS and APC-P designed the study and wrote the manuscript; CRS, MLG, MBM, SS, ERC and CEM conducted the experiments; all authors analysed the data and commented on the manuscript.

Disclaimer

The funders had no role in study design, data collection and analysis, decision to publish or preparation of the manuscript.

1. Deiss LP, Feinstein E, Berissi H, Cohen O, Kimchi A. Identification of a novel serine/threonine kinase and a novel 15-kD protein as potential mediators of the gamma interferon-induced cell death. *Genes Dev* 1995; **9**: 15–30.
2. Shang T, Joseph J, Hillard CJ, Kalyanaraman B. Death-associated protein kinase as a sensor of mitochondrial membrane potential: role of lysosome in mitochondrial toxin-induced cell death. *J Biol Chem* 2005; **280**: 34644–34653.
3. Mor I, Carlessi R, Ast T, Feinstein E, Kimchi A. Death-associated protein kinase increases glycolytic rate through binding and activation of pyruvate kinase. *Oncogene* 2012; **31**: 683–693.
4. Kawai T, Nomura F, Hoshino K, Copeland NG, Gilbert DJ, Jenkins NA *et al.* Death-associated protein kinase 2 is a new calcium/calmodulin-dependent protein kinase that signals apoptosis through its catalytic activity. *Oncogene* 1999; **18**: 3471–3480.
5. Cohen O, Feinstein E, Kimchi A. DAP-kinase is a Ca2+/calmodulin-dependent, cytoskeletal-associated protein kinase, with cell death-inducing functions that depend on its catalytic activity. *The EMBO J* 1997; **16**: 998–1008.
6. Inbal B, Bialik S, Sabanay I, Shani G, Kimchi A. DAP kinase and DRP-1 mediate membrane blebbing and the formation of autophagic vesicles during programmed cell death. *J Cell Biol* 2002; **157**: 455–468.
7. Inbal B, Shani G, Cohen O, Kissil JL, Kimchi A. Death-associated protein kinase-related protein 1, a novel serine/threonine kinase involved in apoptosis. *Mol Cell Biol* 2000; **20**: 1044–1054.
8. Lin Y, Stevens C, Hupp T. Identification of a dominant negative functional domain on DAPK-1 that degrades DAPK-1 protein and stimulates TNFR-1-mediated apoptosis. *J Biol Chem* 2007; **282**: 16792–16802.
9. Schlegel CR, Fonseca AV, Stocker S, Georgiou ML, Misterek MB, Munro CE *et al.* DAPK2 is a novel modulator of TRAIL-induced apoptosis. *Cell Death Differ* 2014; **21**: 1780–1791.
10. Esteller M, Corn PG, Baylin SB, Herman JG. A gene hypermethylation profile of human cancer. *Cancer Res* 2001; **61**: 3225–3229.
11. Katzenellenbogen RA, Baylin SB, Herman JG. Hypermethylation of the DAP-kinase CpG island is a common alteration in B-cell malignancies. *Blood* 1999; **93**: 4347–4353.
12. Rizzi M, Tschan MP, Britschgi C, Britschgi A, Hugli B, Grob TJ *et al.* The death-associated protein kinase 2 is up-regulated during normal myeloid differentiation and enhances neutrophil maturation in myeloid leukemic cells. *J Leukoc Biol* 2007; **81**: 1599–1608.
13. Turrens JF. Mitochondrial formation of reactive oxygen species. *J Physiol* 2003; **552**: 335–344.
14. Liu X, Kim CN, Yang J, Jemmerson R, Wang X. Induction of apoptotic program in cell-free extracts: requirement for dATP and cytochrome c. *Cell* 1996; **86**: 147–157.
15. Bonito NA, Drechsler J, Stoecker S, Carmo CR, Seckl MJ, Hermanns HM *et al.* Control of gp130 expression by the mitogen-activated protein kinase ERK2. *Oncogene* 2013; **33**: 2255–2263.
16. Humbert M, Federzoni EA, Britschgi A, Schlafli AM, Valk PJ, Kaufmann T *et al.* The tumor suppressor gene DAPK2 is induced by the myeloid transcription factors PU.1 and C/EBPalpha during granulocytic differentiation but repressed by PML-RARalpha in APL. *J Leukoc Biol* 2014; **95**: 83–93.
17. Tur MK, Neef I, Jost E, Galm O, Jager G, Stocker M *et al.* Targeted restoration of down-regulated DAPK2 tumor suppressor activity induces apoptosis in Hodgkin lymphoma cells. *J Immunother* 2009; **32**: 431–441.
18. Bialik S, Kimchi A. The death-associated protein kinases: structure, function, and beyond. *Annu Rev Biochem* 2006; **75**: 189–210.
19. Son Y, Kim S, Chung HT, Pae HO. Reactive oxygen species in the activation of MAP kinases. *Methods Enzymol* 2013; **528**: 27–48.
20. Balaban RS, Nemoto S, Finkel T. Mitochondria, oxidants, and aging. *Cell* 2005; **120**: 483–495.
21. Nishitoh H. CHOP is a multifunctional transcription factor in the ER stress response. *J Biochem* 2012; **151**: 217–219.
22. Kaufman RJ. Stress signaling from the lumen of the endoplasmic reticulum: coordination of gene transcriptional and translational controls. *Genes Dev* 1999; **13**: 1211–1233.
23. Wang Y, Nartiss Y, Steipe B, McQuibban GA, Kim PK. ROS-induced mitochondrial depolarization initiates PARK2/PARKIN-dependent mitochondrial degradation by autophagy. *Autophagy* 2012; **8**: 1462–1476.
24. Lum MG, Nagley P. Two phases of signalling between mitochondria during apoptosis leading to early depolarisation and delayed cytochrome c release. *J Cell Sci* 2003; **116**: 1437–1447.
25. Heiskanen KM, Bhat MB, Wang HW, Ma J, Nieminen AL. Mitochondrial depolarization accompanies cytochrome c release during apoptosis in PC6 cells. *J Biol Chem* 1999; **274**: 5654–5658.
26. Rich PR. The molecular machinery of Keilin's respiratory chain. *Biochem Soc Trans* 2003; **31**: 1095–1105.
27. Warburg O. On the origin of cancer cells. *Science* 1956; **123**: 309–314.
28. Kirsch M, De Groot H. NAD(P)H, a directly operating antioxidant? *FASEB J* 2001; **15**: 1569–1574.
29. Pompella A, Visvikis A, Paolicchi A, De Tata V, Casini AF. The changing faces of glutathione, a cellular protagonist. *Biochemical Pharmacol* 2003; **66**: 1499–1503.
30. Brigelius-Flohe R, Maiorino M. Glutathione peroxidases. *Biochim Biophys Acta* 2013; **1830**: 3289–3303.
31. Shoval Y, Berissi H, Kimchi A, Pietrokovski S. New modularity of DAP-kinases: alternative splicing of the DRP-1 gene produces a ZIPk-like isoform. *PLoS One* 2011; **6**: e17344.
32. Gozuacik D, Kimchi A. DAPk protein family and cancer. *Autophagy* 2006; **2**: 74–79.
33. Noda M, Yamashita S, Takahashi N, Eto K, Shen LM, Izumi K *et al.* Switch to anaerobic glucose metabolism with NADH accumulation in the beta-cell model of mitochondrial diabetes. Characteristics of betaHC9 cells deficient in mitochondrial DNA transcription. *J Biol Chem* 2002; **277**: 41817–41826.
34. Gorrini C, Harris IS, Mak TW. Modulation of oxidative stress as an anticancer strategy. *Nature reviews. Drug Discov* 2013; **12**: 931–947.
35. Rassool FV, Gaymes TJ, Omidvar N, Brady N, Beurlet S, Pla M *et al.* Reactive oxygen species, DNA damage, and error-prone repair: a model for genomic instability with progression in myeloid leukemia? *Cancer Res* 2007; **67**: 8762–8771.

36. He L, Luo L, Proctor SJ, Middleton PG, Blakely EL, Taylor RW *et al.* Somatic mitochondrial DNA mutations in adult-onset leukaemia. *Leukemia* 2003; **17**: 2487–2491.
37. Ber Y, Shiloh R, Gilad Y, Degani N, Bialik S, Kimchi A. DAPK2 is a novel regulator of mTORC1 activity and autophagy. *Cell Death Differ* 2014; **22**: 465–475.
38. Monroe DG, Getz BJ, Johnsen SA, Riggs BL, Khosla S, Spelsberg TC. Estrogen receptor isoform-specific regulation of endogenous gene expression in human osteoblastic cell lines expressing either ERalpha or ERbeta. *J Cell Biochem* 2003; **90**: 315–326.
39. Watling D, Carmo CR, Kerr IM, Costa-Pereira AP. Multiple kinases in the interferon-gamma response. *Proc Natl Acad Sci USA* 2008; **105**: 6051–6056.

Supplementary Information accompanies this paper on Cell Death and Disease website (http://www.nature.com/cddis)